Investigating Childhood Health in the Central Zagros Mountains During the Chalcolithic: A Visual Assessment of Subadult Human Remains from Seh Gabi

A Thesis Submitted to the
Faculty of Graduate Studies
In Partial Fulfillment of the Requirements for
The Degree of Master of Science
In the Department of Anthropology
Lakehead University
Thunder Bay, Ontario

By
CLAIRE ELIZABETH WOODLEY

Abstract

This thesis explores the relationship between subsistence strategies in a marginal environment and how it can impact human health. It includes a comparison of all the types of metabolic bone disease (MBD) and their associated lesions and how this informs different possible diagnoses. The residents of the Chalcolithic site of Seh Gabi, Iran (about 6850 to 5100 cal BP) lived in a marginal environment which, when coupled with the intensification of agricultural practices and the use of animal husbandry, could have left the population susceptible to the type of stressors associated with both vitamin C (VCD) and D deficiencies (VDD). This thesis was designed to determine whether the subadult population at Seh Gabi, represented by 32 individuals, experienced VCD and VDD throughout its period of occupancy. The radiographs and excavated skeletal remains of these individuals were macroscopically assessed for any morphology beyond the range of normal. Probable and possible diagnoses of VCD and VDD were made based on the number of diagnostic and suggestive lesions that individuals demonstrated. Probable VCD was evident in 10.7% of the subadult population; all these probable scurvy cases occurred in individuals less than six months old. While there were no probable cases of VDD, two individuals had a possible comorbid case of rickets and scurvy but there was insufficient skeletal evidence to make a probable diagnosis. Extrapolations of maternal health were made based on these subadult health findings given that those under the age of six months were still likely being breastfed. The environmental context and subsistence strategy used by this population, along with these diagnoses, suggest that vitamin C deficiency was likely experienced by this population.

Acknowledgements

This project would not have been possible without the access provided by Dr. Deborah Merrett to the skeletal population of Seh Gabi, which granted me the opportunity of assessing juvenile human skeletal remains. This thesis would also not have been possible without the continued support and guidance of both Dr. Tamara Varney and Dr. Deborah Merrett, who made themselves available for my numerous questions, and gave encouragement throughout the process. Their feedback helped shape me into a better writer, and researcher. Thanks also to Dr. Tim Kaiser, my third committee member, for his interest in the project and his feedback. Additionally, thanks go to Dr. Andrea Waters-Rist, my external reviewer, for their feedback on my thesis. I also want to extend thanks to my peers who were always available to brainstorm ideas and give advice on all things whether that be graduate school, friendship or life in general! It always helped to know that everyone went through a similar process throughout our time as master's students. A huge thank you also goes to my family who were a massive support for me during this time. Anytime I needed, my mom (Rebecca Southern) and dad (Philip Woodley) were always there to listen and help me however they could. My sister (Kate Woodley), who is also going through graduate school, was a big help during this process as well. The focus of both of our research is bioarchaeology, so we would frequently come to each other with bone questions! Finally, I would like to extend thanks to Chris Moore, as his constant and unwavering support helped get me to this point.

Table of Contents

List of Tables

List of Figures

Chapter 1: Introduction

Prior to the late 1970s, there was extensive archaeological research on Neolithic and Chalcolithic period sites throughout the Middle East, including Iran. However, with the Iranian Revolution in 1979, archaeological research in Iran came to a halt for close to 30 years. As a result, much less is known about the transition from Epipalaeolithic through Neolithic to the Chalcolithic in the Eastern Fertile Cresent than in the Levant and Anatolia. But, there was a publication boom in the 1980s on notable sites such as Ganj Dareh and its associated zooarchaeology and paleobotany (e.g., Hesse 1982; van Zeist et al. 1984). Since this time, scant research was published on Iranian sites until another research resurgence starting in 2009. This more recent work is mostly based on materials which had been excavated and collected prior to the Revolution, although there is starting to be more research on more recent excavations as well (e.g., Anderson et al. 2014; Darabi et al. 2019; Matthews et al. 2013; Meiklejohn et al. 2017; Merrett et al. 2021; Richter et al. 2021) and has effectively started to fill the gap in archaeological research and understanding. Given the types of sites being explored, we are gaining insight into what life might have been like in this region during the transition from pastoralism and early agriculture to intensive agriculture[1], however more research is needed to further our understanding of this time period.

One site which has promise to provide further understanding is Seh Gabi, located in the Central Zagros Mountains of Iran. This Chalcolithic period site was excavated in the 1970s by Louis Levine of the Royal Ontario Museum. The Chalcolithic refers to a cultural period which takes place at different times around the world, but is defined by small, dispersed villages becoming a network of urban societies (Renette and Ghasrian 2020) along with metallurgy (Rowan and Lovell 2011) and the continued presence of rich mortuary offerings (Rowan and Lovell 2011; Walsh and Matthews 2018). In the Zagros Mountains, there are multiple chronologies available for dating the Chalcolithic period. One such chronology says the Chalcolithic occurred around 6950 cal B.P.[2] through 4950 cal B.P. (Renette and Ghasrian 2020;

[1] Intensive agriculture in Chalcolithic Iran refers to the usage of irrigation with dryland farming, and watercourses running alongside sites is considered evidence for this (Henrickson 1991b). At Seh Gabi, there was a river which is thought to have possibly ran between the mounds present (Hamlin 1974).

[2] Date was converted to cal B.P. by adding 1950 to BC date, as is the standardized conversion method (University of Oxford n.d.). Throughout this thesis this was done for all dates which were originally given in BC, bc, or bp.

Rowan and Golden 2009) while another indicates the date range of 7450 to 5150 cal B.P. (Matthews and Fazeli Nashli 2022).

Seh Gabi is located within a mountain rain shadow (Zohary 1973) which is a dry area on the downwind side of a mountain (Ghazala 2022). This dryland due to a rain shadow means that there is less moisture available for crops and reduces the number of micronutrients available within the soils for the crops (Moreno-Jiménez et al. 2019). Climate during the Chalcolithic was broadly similar to modern climate (Peasnall 2002), thus it could be postulated that the rain shadow effect would have been the same during the Chalcolithic period at Seh Gabi. Not only was Seh Gabi located in a rain shadow, but this area also has an increased rain shadow effect (Henrickson 1983; Kramer 1982; McDonald 1979) which directly contributes to Seh Gabi being part of a marginal location (Zohary 1973). In a marginal zone agriculture is carried out in less-than-ideal conditions and locations (Binford 1968; Flannery 1971; Merrett 2004; Redding 1988). The lower levels of moisture associated with being in a rain shadow limits the micronutrients available in soil for crops which in turn renders the area around Seh Gabi a marginal zone.

Increasing reliance on food production during the Early Neolithic resulted in resource abundance and sedentism that heighted regional carrying capacity which in turn resulted in population growth (Merrett 2004; Smith and Young 1972). As population density grew, groups were pushed into areas of lower carrying capacity, or marginal zones, to support the expanding population (Binford 1968; Flannery 1971; Merrett 2004; Redding 1988). In this context, marginal locations exist in comparison to more optimal zones, such as that of the Neolithic site of Ganj Dareh (Merrett 2004; Smith and Young 1972).

Considering both the environment and intensive agriculture as factors in daily life at Seh Gabi, this population may have been susceptible to dietary stressors such as vitamin deficiencies (Flannery 1971; McDonald 1979; Melville 1984). The inhabitants of Seh Gabi used a subsistence strategy of intensive cultivation coupled with limited pastoralism, and foraging to supplement their diet (Henrickson 1985b; Kramer 1982; McDonald 1979). These methods of subsistence, the location in a marginal zone, and the increasing population could have had a direct impact on people's susceptibility to dietary stressors and illness (Flannery 1971; Larsen 1995; McDonald 1979; Melville 1984; Rowan and Golden 2009; Şener et al. 2026).

Given these factors, the question remains then why people would stay in such marginal locations. It is thought to be a result of high settlement densities present in the region that limited

re-location options during the Chalcolithic, just as is the case in the region today (Kramer 1982). We are then left with the question of how living in this marginal location impacted the health of Seh Gabi's population during the Chalcolithic.

This question will be addressed through examination of the thirty-two subadult human skeletons (most under the age of one year) that were recovered from the excavations done in the 1970s at Seh Gabi. The hypothesis for this thesis is that some individuals would have experienced metabolic bone disease (MBD), specifically vitamin deficiencies, due to the potential for restricted dietary resources in a marginal environment. The skeletons will be assessed for the presence of evidence that could be indicative of dietary stress in order to:

1) provide insight into the health of these individuals during a period of intensive agriculture in a marginal zone
2) infer from findings a better understanding of health of the overall past population during this time period
3) gain further understanding of the site and the Chalcolithic period by comparing findings to both contemporaneous populations and to modern Iranians, located in rural areas comparable to Seh Gabi.

For this thesis, it was important to look at not only any lesions themselves, but also all lesions that were present on an individual. Given that the marginal zone location of Seh Gabi could have led to inhabitants being exposed to dietary pressures and resulting deficiencies, how dietary deficiencies are identified in human skeletal remains needed to be considered. The study of dietary deficiencies and how they appear on human skeletal remains is ever evolving. In recent years, lesions associated with scurvy and rickets (both dietary deficiencies) have been identified as either diagnostic, non-diagnostic, or suggestive for each disease. This framework of categorizing lesions directly lends itself to potential diagnosis. However, there needs to be a certain number of each category of lesion to provide a probable diagnosis of either deficiency. The categorization of lesions as diagnostic, non-diagnostic, or suggestive within this thesis is based upon the work by Eggington et al. (2024), Schattmann (2014), and Snoddy et al. (2018).

This thesis first provides information regarding the archaeological context for Seh Gabi. Following this an overview of metabolic bone diseases framed within a bioarchaeological context is presented, exploring the associated skeletal changes and symptoms. A discussion of

vitamin deficiencies in modern Iran is given to inform interpretations about modern groups and how it relates to this Chalcolithic population. Once all the relevant background and contextual information is covered, the materials and methods of this thesis are presented. The results are presented in a chapter covering the general prevalence of lesions providing a basis for the discussion and interpretations about the children in this population, the whole population in terms of maternal health, and cultural practices. Lesions are placed within the context of the metabolic bone diseases. Finally, there is a brief discussion on how this compares to modern Iranian groups, especially those living in locations like that of Seh Gabi, followed by suggestions for further research.

Chapter 2: Archaeological Context

Interpretations of health of the inhabitants of Seh Gabi can only be made within the archaeological context of the site. Towards this end, this chapter examines the geography and climate of western Iran and the Zagros Mountains during the Chalcolithic period. Due to research occurring over a long period of time, a substantial research hiatus resulting from the Iranian Revolution, and the transition to calibrated AMS dating there are several chronologies available for the Chalcolithic in the Zagros Mountains. One such chronology provides a date range of around 6950 to 4950 cal B.P. (Renette and Ghasrian 2020; Rowan and Golden 2009) while another alternatively provides the range of around 7450 to 5150 cal B.P. (Matthews and Fazeli Nashli 2022). However, some skeletal remains from Seh Gabi have been radiocarbon dated, and as such, occupation of the site can be directly tied to 6850±50 cal B.P. to 5070±30 cal B.P. (Lazaridis et al. 2016; Narasimhan et al. 2019) (early through late Chalcolithic).

A discussion of the Chalcolithic will lead into the excavation of Seh Gabi, cultural materials recovered (e.g., ceramics), and subsistence, followed by a discussion of the site history to provide insight into the lives of its inhabitants. Relevant ancient DNA (aDNA) research from the spatially related earlier site of Ganj Dareh and aDNA research on Seh Gabi itself (Gallego-Llorente et al. 2016; Lazaridis et al. 2016; Narasimhan et al. 2019) will be discussed to help understand the genetics of the Seh Gabi group and how the relationships between groups in the region changed through time.

2.1 Geography of the Western Zagros Mountains

Seh Gabi is located within the Kangavar valley in the Central Zagros mountains (Hole 1987). The location of Seh Gabi in context of modern borders and rivers can be seen in Figure 2.1 The Kangavar region consists of a series of valleys which have high elevations to the northeast of Kuh-i Sefind, a wall-like mountain range (Hole 1987). The Central Zagros are composed of a series of parallel mountain ridges running northwest to southeast (Henrickson and Vitali 1987) that act as a barrier to travel, communication, and migration routes (Henrickson 1985b; Henrickson and Vitali 1987). The region consists of geographical zones including low plateaus, foothills, and highlands, resulting in differing environments and climates (Zohary 1973). There is variation within the mountain range, with the lower elevation valleys to the east being narrower and steeper than their western counterparts (Henrickson 1985b). The eastern regions of the Zagros are not suitable for large-scale agriculture but are well suited for various forms of pastoralism and small-scale intensive agriculture (Abdi 2003).

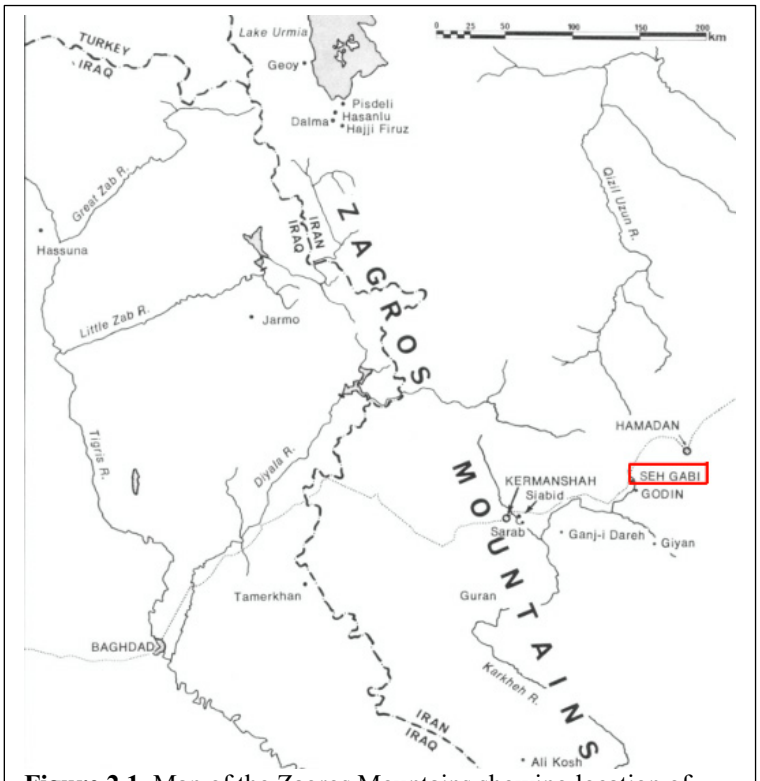

Figure 2.1. Map of the Zagros Mountains showing location of Seh Gabi, modern borders, and rivers (Adapted from Hamlin 1973: 224).

2.2 Climate of the Central Zagros During the Chalcolithic

The modern climate of the Central Zagros consists of hot summer droughts and cold winter rains (Alijani 2008; Arsalani et al. 2015; Henrickson 1983; McDonald 1979). During the Chalcolithic, the Zagros highland valleys were wetter and warmer than today; however, after about 5950 cal B.P. the region became cooler and wetter (Henrickson 1983; McDonald 1979; van Zeist and Wright 1963; van Zeist 1967; Wright et al. 1967). In addition, there is an increased

rain shadow effect or a dry area on the downwind (northeastern) side of the mountain ranges (Ghazala 2022), that extend from southeast to northwest across the Central Zagros (Henrickson 1983; Kramer 1982; McDonald 1979).

Pollen sequencing on sediment cores has been used to approximate past climatic conditions in the Zagros Mountains (van Zeist 1967). It should be noted however, that most sediment cores are not directly associated with archaeological sites but rather from nearby areas in which there are bodies of water within the western Central Zagros Mountains (e.g., Lake Zeribar and Lake Mirabad) (van Zeist 1967), and findings are then extrapolated to nearby archaeological sites (Merrett 2004). Results indicate that as climate became more temperate and precipitation increased during the Neolithic, trees became more common in this region (van Zeist and Wright 1963; van Zeist 1967). After 10,450 cal B.P., pollen cores indicate that the oak-pistachio forest was expanding within the Central Zagros (El-Moslimany 1987; Freitag 1977; van Zeist and Bottema 1977), reaffirming that after 6000 cal B.P. oak, pistachio, and almond trees were dominant in highland valleys (Rothman 2011; van Zeist and Wright 1963; van Zeist 1967).

The Central Zagros were the habitat of the wild ancestors of domestic caprines (goats) and ovines (sheep) (Abdi 2003). Morphologically wild goats have been found at archaeological sites which predate the Chalcolithic, i.e. in the Early Neolithic 10,000 cal B.P. (Hesse 1982, 1984; Zeder and Hesse 2000; Zeder 2001). From the excavations at Seh Gabi, occupied three to four thousand years later, both morphologically wild as well as domesticated caprines and ovines were recovered (Hamlin 1973, 1974). The climate during this time made the area productive for small-ungulate pastoralism (Henrickson 1985b). The inhabitants of Seh Gabi were situated to engage in intensive agriculture and the use of domesticated animals, supplemented with pastoralism, foraging from pistachio and almond trees, and hunting (Henrickson 1985b; Kramer 1982; McDonald 1979).

2.3 The Chalcolithic Period

The Chalcolithic period does not take place during the same time frame everywhere around the globe. In the Zagros the Chalcolithic period started around 7450 cal B.P. and continued until around 5150 cal B.P., based on the most recent available chronologies (Matthews and Fazeli Nashli 2022). The Chalcolithic is defined by a long process in which dispersed small

villages became networks of urban societies (Renette and Ghasrian 2020). This was also the first period in which metallurgy and larger villages appeared. During this period rich mortuary offerings were present (Rowan and Lovell 2011) which were also seen in Neolithic burials within the Eastern Fertile Crescent (Walsh and Matthews 2018).

There was cultural homogeneity across the Iranian plateau during the middle Chalcolithic (Zeynivand et al. 2013) as seen through the widespread use of similar ceramics (Dadaneh et al. 2021; Henrickson and Vitali 1987; Nekouei and Yousefi Zoshk 2021). Different types of ceramics are identified due to stylistic differences, and associated time periods are based on seriation within the Chalcolithic (Hamlin 1973; Henrickson 1985b, 1985a). Much of the early research in this area is based on this way of identifying ceramics and the associated time periods. The Shahnabad period represented the earliest period of occupation within the Kangavar Valley in which Seh Gabi is located (Henrickson 1985a). Ceramics associated with the Shahnabad period are only found in the Kangavar Valley and Malayer region of Iran (McDonald 1979), which are just under 100 kilometers apart. The Shahnabad ceramics found at Seh Gabi, and throughout the aforementioned regions, are typically buff wares which can be painted (Henrickson 1991a; McDonald 1979).

The following Dalma period refers to cultural materials dating from about 6750 cal B.P. to 6350 cal B.P., at which time Dalma-type cultural materials were in widespread use in the Near East (Henrickson 1988). The Dalma tradition was based in Northwestern Iran, which demonstrates long range contacts associated with Seh Gabi (Henrickson and Vitali 1987). This widespread use of Dalma pottery is thought to reflect a specific group with a unique language and distributed lineage system, as well as a possible system of belief (Zeynivand et al. 2013). Alternatively, the knowledge regarding Dalma-ware production could have been spread throughout the region rather than the wares themselves, as the ceramics were made locally (Mardi 2025).

After the Dalma period, the Godin IX, VII, and VI periods are represented. Godin IX, otherwise known as the Seh Gabi period, is associated with the Middle Chalcolithic (Henrickson 1985a) which corresponds to around 6450 cal B.P. at the Seh Gabi site (Hamlin 1974). Godin IX ceramics are tan-buff with black paint, plain red-slipped, or impressed red-slipped (Henrickson 1985a). These ceramics are somewhat similar in appearance to those seen throughout Middle Chalcolithic assemblages in the Zagros (Henrickson 1985a). The Godin VII period corresponds

to around 5950 cal B.P. and Godin VI is associated with 5450 cal B.P. at Seh Gabi (Hamlin 1974). These latter two periods are thought to correspond with the Late Middle and Late Chalcolithic, respectively. Plain and painted ceramics are seen in assemblages from these periods at Seh Gabi and other sites in the Kangavar Valley (Henrickson 1985a). The table below (Table 2.1) lists the period names and associated dates at Seh Gabi, along with cultural periods at other sites during the same time.

Table 2.1. *Cultural Periods at Chalcolithic Sites and their Associated Time Based on Cultural Materials.*

General Chronology [b]		**Seh Gabi**	**Godin**	**NW Iran**
Early	7450 cal B.P. [a]	Shahnabad [a]	XI (Kucheh) [a]	Hajji Firuz [a]
	6950 cal B.P. [a]	Dalma (Godin X) [a]	X (Dalma) [a]	Dalma [a]
Middle	6450 cal B.P. [a]	Seh Gabi (Godin IX) [a]	VIII (Taherabad) [a]	
	5950 cal B.P. [a]	Godin VII [a]	VII (Hosseniabad) [a]	Pisdeli [a]
Late	5450 cal B.P. [a]	Godin VI [a]	VI (Chesmeh Nush) [a]	

[a]Hamlin 1974

[b]Matthews and Fazeli Nashli 2022.

2.4 Seh Gabi: The Archaeological Site

The Seh Gabi site has many archaeological findings, including ceramics, architectural structures, as well as human remains. It is located 350 kilometers east from Baghdad in the Central Zagros Mountains (Hamlin 1973) and was first excavated in 1971 and 1973 (Hamlin 1973, 1974). The precise location of the site is shown in Figure 2.2. It is made up of seven mounds which are the result of continual habitation through time (Fig. 2.3). The first dig season focused on the excavation of Mound B; the second dig season opened Mounds A, B, C, E, F, and

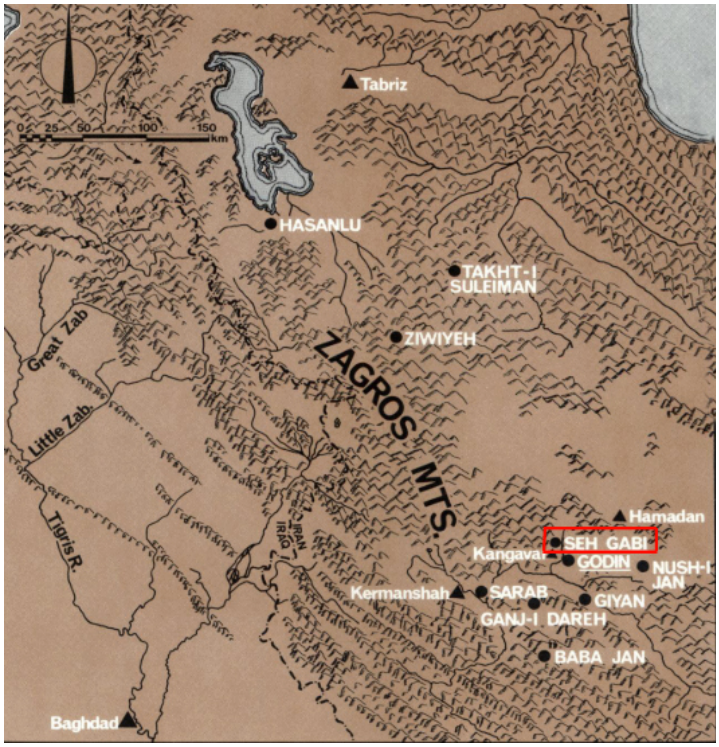

Figure 2.2. Map of the Zagros Mountains showing location of Seh Gabi (Adapted from Hamlin 1974: 274).

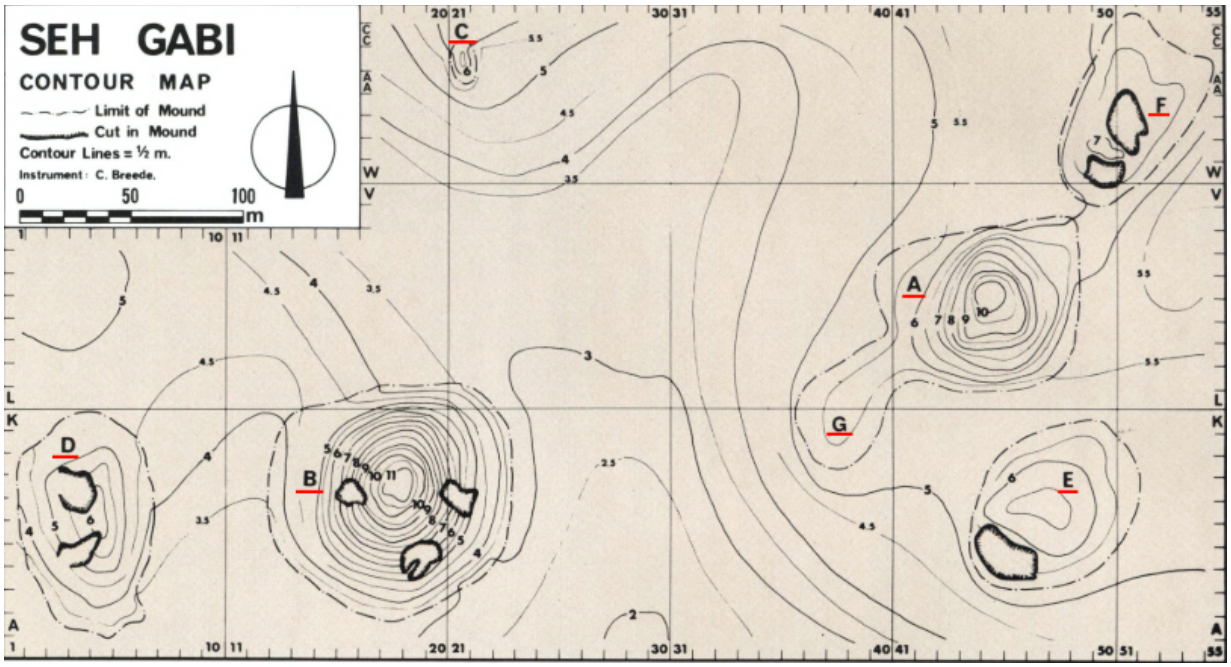

Figure 2.3. Contour Map of Seh Gabi showing the relative locations of the mounds (Adapted from Hamlin 1974: 274).

G. The remnants of windowless architectural structures were found in Mounds A, B (Figs 2.4A and 2.4B, below), C, and E (Hamlin 1973, 1974). The mounds will be discussed in the order they were occupied (i.e., Mounds C, B, A, E, F, and D&G).

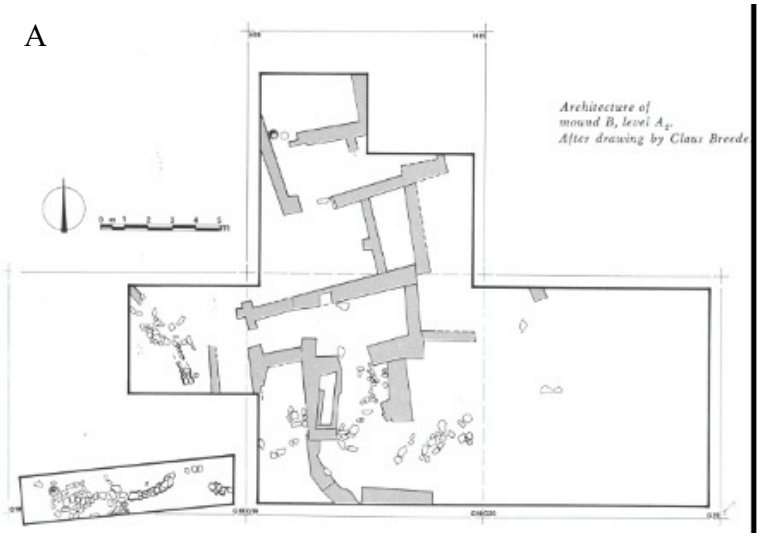

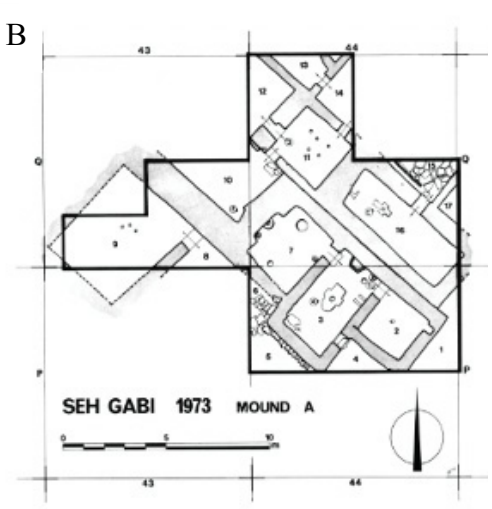

Figure 2.4A. Diagram of Architecture Housed Within Mound B (Adapted from Hamlin 1973: 225).

Figure 2.4B. Diagram of Architecture Found Within Mound A (Adapted from Hamlin 1974: 275).

The date ranges for the mounds are based on all layers within the mounds as the provenience of both cultural materials and skeletal remains is not available within the excavation reports. Ceramics were dated using older methods such as ceramic seriation while some skeletal remains have been radiocarbon dated. As this thesis is focused on the skeletal remains, moving forward radiocarbon dates associated with skeletal material will be preferentially used for the mounds where applicable.

2.4.1 Mound C

Due to the presence of pre-Dalma ceramic-wares Mound C is associated with the earliest occupation at Seh Gabi and has been dated to about 7450 cal B.P. corresponding to the Shahnabad period (Hamlin 1974). One individual of the four excavated from Mound C was radiocarbon dated and places human skeletal material from Mound C at 6850±50 cal B.P. (Lazaridis et al. 2016).

2.4.2 Mound B

Structures within Mound B demonstrated evidence of rebuilding (Hamlin 1973). Based on ceramic seriation, some layers of Mound B are associated with both the Godin X and Dalma period which corresponds to about 6950 cal B.P. Other layers of Mound B are from the Godin IX and Seh Gabi period which date to about 6450 cal B.P. (Hamlin 1974). However, radiocarbon dating of human skeletal materials from Mound B (three of the thirteen individuals were dated) provides a date range of 5870±40 to 5740±40 cal B.P. (Lazaridis et al. 2016).

2.4.3 Mound A

Mound A had multiple periods of occupation and a multi-storied structure (Hamlin 1974) (see the architectural layout of Mound A in Figure 2.4B, p. 11). Mound A had rooms containing central hearth holes, smoothed pits, and grinding stones (Hamlin 1973, 1974). Due to the ceramics and cultural materials found within the mound, Mound A is associated with the Godin VII period, which dates to about 5950 cal B.P. (Hamlin 1974). However, radiocarbon dating on some of Mound A's skeletal material (two of the six individuals were dated) provides a date range of 5105±35 to 5070±30 cal B.P. (Lazaridis et al. 2016).

2.4.4 Mound E

Mound E also had rooms containing central hearths holes, smoothed pits, and grinding stones (Hamlin 1973, 1974). Mound E dates from the Godin VII and Godin VI period, or about 5950 cal B.P. and 5450 cal B.P. respectively (Hamlin 1974). Seven individuals were found and excavated from this mound.

2.4.5 Mound F

Mound F also comes from the Godin VI period, about 5450 cal B.P. (Hamlin 1974). Two individuals were excavated from this mound.

2.4.6 Mounds D & G

The architectural remains which were sometimes reused and rebuilt demonstrate that there were multiple continuous periods of occupation in Mounds D and G, but they have not yet been dated (Hamlin 1974).

2.4.7 Cultural materials

Along with architecture, there is also a variety of cultural materials uncovered at Seh Gabi. The archaeological assemblage contains reed matting, charred wood, faunal remains, plant remains, ceramics, flakes, flint, chert, obsidian, ground stone artifacts, bone implements, shell artifacts, baked clay artifacts, and copper artifacts (Hamlin 1973, 1974). Mound B, for example, contained artifacts which are representative of the entire assemblage listed, including ceramic vessels associated with the Godin VI-VIII periods, flakes, flint, chert, obsidian, ground stone, shell, and implements fashioned from either goat or sheep bone (Hamlin 1973). The ceramics found within the layers of Mound B contained a large range of Dalma wares (Hamlin 1973), along with some black on buff Seh Gabi wares (Henrickson 1985a).

Stone and baked clay artifacts were recovered from all the mounds which consisted of animal figurines, spindle whorls, pot sherds, a stamp seal impression, beads, and geometric shaped pieces (Hamlin 1973, 1974). These geometric shaped pieces resemble those found at Neolithic sites of Jarmo, Sarab, and Ganj Dareh (Hamlin 1973).

Analysis of the faunal remains indicated that inhabitants subsisted off a large variety of small game and a few domesticated animals (Hamlin 1974). Later inhabitants of the site continued hunting but the number of identified domesticates increased with time (Hamlin 1974). The increased number of domesticates through time could indicate a higher reliance on the domesticated animals rather than wild ones.

2.5 Burial Practices

In addition to cultural materials, human skeletal remains of 32 individuals were recovered from Seh Gabi. No adult remains were recovered, however subadult skeletal material was found in Mounds C, B, A, E, and F (Hamlin 1973, 1974). These subadults, generally under the age of five years old, were interred within ceramic vessels or in subfloor inhumations (Hamlin 1973). For example, within Mound B there are subadults who were interred within ceramic vessels associated with the Godin VI-VIII periods, about 5950 to 5450 cal B.P. (Hamlin 1973, 1974). Mound C contained subadults in subfloor inhumation burials, of which one had a bead necklace (Hamlin 1974). Within Mound E the remains of an adolescent were found in a midden (Hamlin 1974).

Burial types may provide insight into specific time periods and places. Regional mortuary practices are hard to detect from Chalcolithic sites but broadly speaking storage jars were used as "coffins" for infant burials (Rowan 2014). There were more distinct mortuary practices seen in the later occupied mounds than what was seen in Mound C. Overall, it seems that the people of Seh Gabi aligned with the cultural practice of interring subadults in ceramic vessels. At Dalman sites, for example Dalma Tepe, burials are characterized by ceramic vessel and sub-floor internment in which only infants are represented in the skeletal record (Henrickson and Vitali 1987). At Seh Gabi, this patterning is more commonly represented within temporally later burials. While infants from temporally later contexts were recovered within vessels (i.e., Mounds A, B, and E), those from earlier temporal contexts (Mound C) were interred in subfloor inhumations (McDonald 1979). The occupation of Mound C is associated temporally with the Late Neolithic (Hamlin 1973, 1974), and this pattern of subfloor inhumations is similar to other Neolithic sites in the region like Ganj Dareh (Merrett 2004), and Sheik-e Abad (Walsh and Matthews 2018).

A summary of burial practices along with the burials themselves can be seen in Table 2.2, below. The associated dates for the mounds are also presented. Radiocarbon dates, when available, are used preferentially for the chronological organization of mounds within this table.

Table 2.2. *Burial Location and Type at Seh Gabi.*

Burial	Mound C 6850±50 cal B.P.[a] (7450 cal B.P.[b])	Mound E 5950 to 5450 cal B.P.[b]	Mound B 5870±40 to 5740±40 cal B.P.[a] (6950–6450 cal B.P.[b])	Mound F 5450 cal B.P.[b]	Mound A 5105±35 to 5070±30 cal B.P.[a]
1	SG 1: SF	SG 22: PB	SG 5: PB	SG 24: UNK.	SG 18: PB
2	*SG 2: SF	SG 23: PB	SG 6: SF	SG 29: SF	*SG 19: PB
3	SG 3: SF	SG 25: SF	*SG 7: SF		SG 20: PB
4	SG 4: SF	SG 26: SF	SG 8: PB		*SG 21: PB
5		SG 27: PB	SG 9: PB		SG 30: UNK.
6		SG 28: PB	SG 10: PB		SG 31: UNK.
7		SG 32: UNK.	*SG 11: PB		
8			SG 12: PB		
9			SG 13: PB		
10			SG 14: PB		
11			SG 15: PB		
12			*SG 16: PB		
13			SG 17: UNK.		

Table 2.2 Legend
SF = subfloor inhumation
PB = pot burial
UNK. = unknown
*= radiocarbon dated

[a] Lazaridis et al. 2016; Narasimhan et al. 2019
[b] Hamlin 1974.

2.6 The Culture of Seh Gabi

One of the most prominent artifact types uncovered at Seh Gabi was ceramics that consisted of three categories: Shahnabad, Dalma, and Seh Gabi (Hamlin 1973; Henrickson 1985b, 1985a). The Seh Gabi wares are distinguishable because their motifs are made from black paint which crystallized during the firing process (Motarjem and Sharifi 2014). This is technologically and stylistically distinct from other kinds of pottery found at other Chalcolithic

sites in the Near East (Renette and Ghasrian 2020). A variety of over-fired ceramic sherds were also found at Seh Gabi, suggesting that pottery was locally made (Hamlin 1973). Despite potentially being geographically isolated, the inhabitants of Seh Gabi created ceramics which followed the tradition and style of the rest of the Iranian plateau to the northwest at the time. This could mean that information and style was disseminated to and/or from Seh Gabi. Genetic analyses suggest that people started to move to both the north and northeast during the middle Chalcolithic, so it is possible that as groups of people moved, they disseminated knowledge associated with ceramics making and styles with them (Lazaridis et al. 2016, Narasimhan et al. 2019).

Other cultural materials found at Seh Gabi were seals and sealings which can indicate an early form of centralized administration (Rothman and Badler 2011). Within Mound B, one Dalma period seal and sealing was found that bears imagery of a schematic bird in flight, while the sealing had a quartered circle upon it. This type of imagery was used across the northern and central Zagros. Other seals and sealings reflect other cultural periods within the Chalcolithic (Henrickson 1988). Based on typology, seals and sealings found within Mounds A and E are dated to the Hosseniabad period, from about 5750–5550 cal B.P. Most of the seals and sealings found at Seh Gabi are from this period. One of these sealings has anthropomorphic features which could suggest a thematic connection to those found at Tepe Gawra, northern Iraq. As well, Mound E had a sealing which reflected the Chesmeh Nush period of around 5550–5050 cal B.P. This sealing had stylistic similarities to a middle Uruk assemblage from the site of Susa and could represent an early version of an archer motif from other Chalcolithic archaeological sites in Iran, such as Susa and Godin Tepe (Henrickson 1988). These stylistic similarities to seals and sealings found at other sites could be representative of knowledge dissemination and ties to surrounding areas. Additionally, the geometric shaped pieces were initially thought to be gaming pieces (Hamlin 1973) but alternatively they may have been tokens related to trading and contact with other areas (Schmandt-Besserat and Moghimi 2017). It has also been suggested that those who lived at Seh Gabi could have conducted metallurgy based on the recovery of a fragmentary crucible and several pieces of molds with molten metal inside (Hamlin 1974; Rothman and Badler 2011). This underlines the idea that cultural practices were disseminated into and out of Seh Gabi, as indicated by the uniformity of some of the imagery found at the site.

There seems to have been regional variation in terms of subsistence methods within the Zagros Mountains and access to cereals, legumes, and various nuts (Hole 1984). In the middle and late Chalcolithic, inhabitants of the Kangavar region were sedentary agriculturalists who engaged in dry land farming supplemented with hunting and gathering (Flannery 1983; Heathcote in Hamlin 1974; Heathcote 1974). In the central Zagros, the density of sites associated with the middle and late Chalcolithic increases (Smith and Young 1983). It has been argued that the presumed associated population density increase would decrease the amount of area available to forage and construct villages (Flannery 1971; McDonald 1979; Melville 1984; Smith and Young 1972). This in turn would force an increased reliance on domesticates and cultivated products, leaving populations open to periodic dietary stress (Flannery 1971; McDonald 1979; Melville 1984).

Specialized nomadic pastoralism increased in the middle and late Chalcolithic and came to characterize the subsistence method employed in the western Central Zagros (Henrickson 1985b, 1985a). This was the result of population growth and dispersal, subsistence specialization, and maintaining social ties between villages and herders (Henrickson 1985b). Transhumant pastoralism is a form of mobile pastoralism which is based out of a sedentary settlement (Abdi et al. 2002). The Zagros was an early center of goat domestication (Hole 1984) as initial domestication occurred in the mountains ca 10,000 cal B.P. (Zeder and Hesse 2000). At the geographically related Early Neolithic site Ganj Dareh, there were the remains of wild goats but also indicators of human control over them (Hesse 1978). It has also been suggested that an individual at Ganj Dareh engaged in transhumant pastoralism due to sulfur isotope analysis (Merrett et al. 2021). However, unlike Seh Gabi, Ganj Dareh was not in a rain shadow (i.e. Ganj Dareh is located in an optimal region for goat herding) as it is located more westerly (Hesse 1982; Merrett 2004; Zohary 1973). The climate of Ganj Dareh would have differed from Seh Gabi given that it was occupied during the Neolithic, closer to the last glacial maximum and just recovering from the Younger Dryas cold period with more steppe-like vegetation, while the Chalcolithic climate was closer to that of the present-day (Henrickson 1983, 1985a; McDonald 1979).

Seh Gabi appears to have been occupied year-round (Levine 1974). Excavation revealed the presence of morphologically wild faunal remains in all the mounds at Seh Gabi, indicating that hunting was a persistent activity (Hamlin 1973, 1974). The faunal remains indicated that

there was also an increased reliance on domesticates throughout time (Heathcote in Hamlin 1974) including a higher prevalence of sheep and goat skeletal remains than cattle and pigs (Heathcote 1974). While many of the caprines (goats) and ovines (sheep) present were young individuals, some were neonate or old. These caprine and ovine remains showed morphological indicators of domestication while the cattle and pigs did not (Heathcote 1974). Caprines and ovines could have been used for meat, wool, and milk (Hole 1984). Residue analysis of ceramics from Late Neolithic sites (Abdul Hosein, Ali Kosh, Chogah Mish, Qale Rostam, Mar Suchar, Sang-e Chakhmaq, Tepe Sohz, Tepe Tula'i, and Wezmeh) in the Zagros Mountains indicate that exploitation of caprine dairy products was occurring in the region though the degree of utilization depended on the site (Casanova et al. 2026). Thus, it is possible that the inhabitants of Seh Gabi were also engaging in dairying, but this is hypothetical. Other animals like wild boar, gazelle, red deer, hare, and turtle have also been identified in the faunal assemblage (Heathcote 1974). However, it is not apparent which animals were used preferentially for meat during Seh Gabi's occupation.

There is also some evidence of subsistence farming at the site (Levine 1990), due to the presence of grinding stones and sickles in the assemblage as well as built-in storage facilities (Kramer 1982). Additionally, it is thought that a river could have wound through the mounds during the period of occupation (Hamlin 1974). Specific evidence of crops at Seh Gabi has not yet been assessed, however looking to nearby sites could provide insight. The Zagros Mountains have been identified as a region which would have supported the growth of cereals and legumes (Henrickson 1985b) which can be see through the presence of domesticated characteristics on cereals which were associated with later phases of occupation at Ganj Dareh (Rothman and Badler 2011) (see Merrett (2004) for a differing opinion on cereal domestication at Ganj Dareh). Additionally, at Godin Tepe (Chalcolithic) multiple types of wheat along with barley, lentils, chickpeas, and coriander have all been identified through archaeobotanical analysis (Miller 1990). Further support is provided by isotopic analysis of the human bone from Seh Gabi has indicated a terrestrial diet (Scott 2018). It is possible then that cultivated crops like wheat and barley were used at Seh Gabi. But the understanding of subsistence strategy at Seh Gabi is more hypothetical at this point without a botanical analysis available.

However, within the earliest mound, Mound C, it is suggested that the method of subsistence would not have incorporated animal husbandry along with processed plant products

(McDonald 1979) as there were few domesticates recovered (Heathcote 1974). The architecture of Mound C suggests that there might have been periodic site abandonment which may reflect unsuccessful initial attempts to occupy an otherwise marginal location (McDonald 1979). From the temporally later Mounds A, E, and F, artifacts like sickles and grinding stones, and faunal remains suggests sedentary agriculturalists who engaged in dry land farming and animal husbandry, which was supplemented by hunting and fowling (McDonald 1979; Kramer 1982). This animal husbandry could have involved the nomadic pastoralism of both caprines and ovines (Henrickson 1985b).

2.6 aDNA, Genetics and Seh Gabi

aDNA analysis has been performed on some of the skeletal remains from Seh Gabi, as well as those from Ganj Dareh, a geographically related Early Neolithic site (Lazaridis et al. 2016; Narasimhan et al 2019). The results indicate that Western Iran was populated by those who were most genetically like hunter-gatherers from the Caucasus during the Neolithic. However, they were distinct from Neolithic Anatolian peoples who brought food production to Europe. Those who lived within the Central Zagros were isolated from other genetic groups in the region, for example in the Levant and Anatolia (Gallego-Llorente et al. 2016). This genetic distinctiveness and isolation of the people from Ganj Dareh is somewhat replicated at Seh Gabi. The Chalcolithic population of Seh Gabi appears to be related to the Neolithic individuals from Ganj Dareh but does not form a strict clade with them (Lazaridis et al. 2016). Populations outside of Iran share more alleles with the Chalcolithic than Neolithic Iranian population which suggests that those from Seh Gabi may have had mixed ancestry (Lazaridis et al. 2016). Genetic admixture with peoples from Anatolia did not occur until after the period associated with Seh Gabi (Lazaridis et al. 2016; Narasimhan et al. 2019). Despite there appearing to be cultural transmission throughout the region, due to the widespread usage of the same ceramic styles, gene flow does not appear to have followed this trend.

2.7 Summary

The areas of geography and climate, excavation, culture, and aDNA analysis have all been explored to gain a fuller picture of life at Seh Gabi. The excavations provided evidence of cultural materials, architecture, as well as skeletal remains (the focus of this thesis). Cultural

materials have also shown evidence of daily life and mortuary practices while aDNA indicates that this population was genetically distinct from contemporary groups in other regions. The geography of the region indicates that there were topographic characteristics which could have presented barriers to those who made the area their home while climate at the time of occupation, along with the cultural materials represented within the assemblage suggest that mixed subsistence methods were the most effective form of living for those who occupied Seh Gabi. However, to gain a full understanding of what a lived experience of potential dietary stress might have looked like for the population at Seh Gabi, the modern clinical symptoms and resulting effects on skeletal remains must be examined.

Chapter 3: Metabolic Bone Disease

3.1 Introduction

Palaeopathology is the study of disease in the past (Roberts and Manchester 2007). When applied to the archaeological record and skeletal remains, skeletal lesions represent a variety of lived conditions for people in the past. Changes resulting from fractures, repetitive motion, and disease, infectious or otherwise, which can be evident in bone or in soft tissues, are encompassed under the palaeopathology umbrella (Roberts and Manchester 2007). It is important to note that as some diseases take longer to appear in bone than in other tissues, it is possible that there are undiagnosed cases in the archaeological record as a person could have died prior to the formation of bony indicators (DeWitte and Stojanowski 2015; Wood et al. 1992). Quite often, diseases do not cause bony changes at all and of those that can, only a small fraction do so prior to death. It is also possible for osseous lesions to be unrelated to the cause of death. Further, a skeleton which shows many lesions may represent an individual who was healthier in life with stronger or more effective immune responses than one without lesions. This is what is known as the osteological paradox (DeWitte and Stojanowski 2015; Wood et al. 1992). An archaeological case of disease will not necessarily present with all possible lesions — it depends on the preservation of remains, how much of the skeleton is present, the stage of disease progression, and the individual's immune system (e.g., Cope and Dupras 2011; Gresky et al. 2020; Nord et al. 2005).

One category of lived conditions within palaeopathology are metabolic bone diseases (MBD). Metabolic bone diseases cause changes in normal bone formation, resorption, mineralization, or a combination of all three (Brickley and Mays 2019). These diseases can arise through a variety of causes, for example dietary deficiencies such as vitamins C and D deficiencies. They can cause bony changes at any point during the life course. Many bone lesions which are a result of metabolic bone disease are similar. A differential diagnosis for any individual skeleton with lesions is necessary to determine the possible options as to which conditions could have resulted in the lesions. To provide a thorough differential diagnosis, any archaeological, temporal, historical, climatic, geographic, and cultural information available must be considered along with the lesions (Buikstra et al. 2017). In a differential diagnosis the main features of lesions are summarized and then compared to all diseases which can exhibit the same array of lesions, until the closest match(es) possible is (are) found (Klaus 2017; Mays 2020). This comparison will include the lesions themselves, the distribution of lesions across

skeletal elements and the entire skeleton, and the sex and age of the individual (Klaus 2017; Mays 2020). Information from both social and medical sciences should be used to inform interpretations about lifeways from this differential diagnosis (Buikstra et al. 2017).

Today, metabolic disease can be common (Albahri et al. 2021), and as such, could theoretically have been as, if not more, common in the past. For example, cases of rickets in the United States were common in the early 20th century, then decreased to almost non-existent levels in the mid-20th century, but in the present-day there is a resurgence being experienced amongst the non-white juvenile population due to breastfeeding practices (Rajakumar and Thomas 2005). By understanding which metabolic diseases could be present today and what they look like in skeletal remains, a deeper understanding of the past can be had.

Within this chapter, an overview of Vitamin C and D deficiencies, then other metabolic diseases such as anaemia, fluorosis, hyperostosis, and osteogenesis imperfecta is given. These diseases could have been present at Seh Gabi given the site's archaeological context and because these diseases have been seen in subadult remains from antiquity. This overview will include what each metabolic disease is, and possible lesions in human remains. Additionally, what these lesions could mean in an archaeological context will be discussed. While there are other metabolic bone diseases (pellagra, osteoporosis and osteopenia, Paget's Disease, hyperparathyroidism, hypophosphatasia, osteopetrosis), these are rarer in subadults, and as such are not discussed here (Arumugam et al. 2015; Cleveland Clinic 2024; Genetic and Rare Diseases Information Center; Naveen et al. 2013; National Institute of Arthritis and Musculoskeletal and Skin Diseases; Walczyk et al. 2011). Despite how rare these metabolic bone diseases are they should still be included in broader differential diagnoses where applicable (see Chapter 6).

3.2 Vitamin Deficiencies

The first metabolic bone diseases discussed are vitamin deficiencies. Vitamin C and D deficiencies are frequently mentioned in archaeological literature and new research is often emerging on their manifestation in skeletal remains (e.g., Brown and Ortner 2011; Ortner and Ericksen 1997; Geber and Murphy 2012). These two deficiencies are perhaps more well-known by their colloquial names of scurvy and rickets, respectively.

3.2.1 Vitamin C deficiency

Vitamin C deficiency (VCD) occurs when an individual does not ingest an adequate amount of vitamin C (ascorbic acid), and as a result suffers both clinical symptoms and bony changes with prolonged deficiency (Brickley and Ives 2006; Fain 2005; Mays 2008; Mimasaka et al. 2000; Ortner and Ericksen 1997; Tamura et al. 2000). Vitamin C is a systemic antioxidant and is used in the development, function, maintenance, and regulation of different cell and tissue types throughout the body including bone cells (e.g., osteoblasts) and other connective tissue forming cells (Aghajanian et al. 2015). While most other animals can synthesize their own vitamin C, humans cannot (Aghajanian et al. 2015; Brickley and Mays 2019; Ortner and Ericksen 1997) and are completely reliant on dietary intake to provide sufficient vitamin C for biological processes (Brickley and Mays 2019; Brown and Ortner 2011; Fain 2005). Additionally, the human body has minimal storage capacity for vitamin C, so regular consumption is required (Brown and Ortner 2011; Fain 2005). Scurvy stems from an inadequate intake of fruits and vegetables, as well as other foods which contain vitamin C (Brickley and Mays 2019; Fain 2005; Ortner and Ericksen 1997) such as liver and cow's milk (World Health Organization 1999). It is interesting to note that goat milk contains higher levels of vitamin C than cow milk (Holmes et al. 1943; Kondyli et al. 2007), meaning that the inhabitants of Seh Gabi could have been ingesting some vitamin C if they were consuming goat dairy products.

Other stressors on the body such as pregnancy, lactation, and growth can also drain the body of vitamin C (Fain 2005). VCD is defined as <11.4 umol/L of serum ascorbic acid (Aghajanian et al. 2015), whereas normal levels are >28 umol/L (Jacob 1990; Loria et al. 1998). In adults, symptoms of VCD will manifest after complete deprivation of ascorbic acid after about 22–28 weeks (Hodges et al. 1971). In children, clinical symptoms can appear within 8–12 weeks of insufficient vitamin C intake (Algahtani et al. 2010). For complete recovery to occur all that is needed is a return to normal vitamin C intake (Hodges et al. 1971).

Scurvy is not commonly found in individuals prior to the age of four months, unless their mother is also deficient in vitamin C; it is more frequently seen during later infancy and childhood (Brickley and Mays 2019), although it can occur at any age (Gulko et al. 2015). Neonatal levels of vitamin C are related to maternal levels and the amount of vitamin C present in breast milk (Aghajanian et al. 2015). It is also possible that if a mother is scorbutic (has scurvy or changes related to scurvy) and is nursing her child, the child may not receive enough vitamin

C in their diet and thus become scorbutic themselves (Popovich et al. 2009). This may have been the case for some of the infants present at Seh Gabi.

Children are more susceptible to being scorbutic due to the extensive synthesis of collagen during the growth process (Zuckerman et al. 2014). The reduced quantity and stability of collagen induced by VCD alters the growth process, resulting in pathological changes. Vitamin C is crucial for the hydroxylation of key amino acids (e.g., proline, lysine) which provide stability to the collagen molecules (Fain 2005; Koon 2010; Travis 2008) (Fig. 3.1). This creates more opportunities for fragile blood vessels to be formed, weakness in connective tissues, and impaired wound healing (Aghajanian et al. 2015; Armelagos et al. 2014; Brickley and Ives 2006; Brickley et al. 2020a; Fain 2005; Marini et al. 2007; Ortner et al. 2001; Ortner and Ericksen 1997; Tiesler et al. 2016; Walmsley et al. 1999; Zuckerman et al. 2014). With prolonged deficiency, synthesis of collagen is impaired, and there is abnormal bleeding due to connective tissue defects (Tiesler et al. 2016).

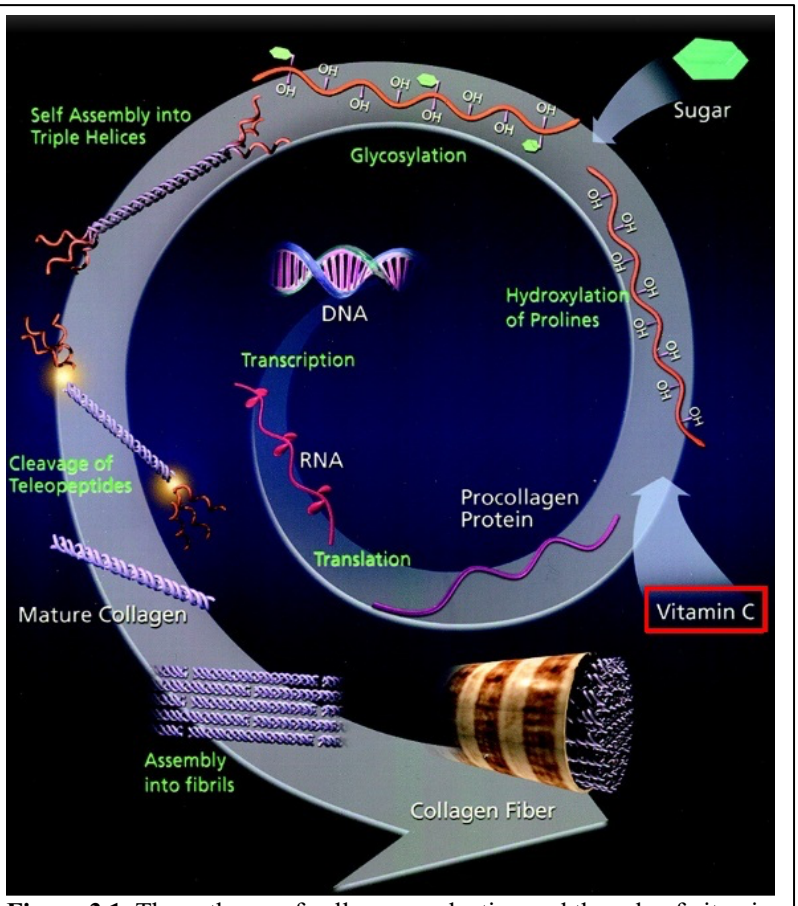

Figure 3.1. The pathway of collagen production and the role of vitamin C within that (Adapted from Libby and Aikawa 2002: 1397).

Collagen is a primary component of bones, teeth, and blood vessel walls (Brickley and Ives 2006). Blood vessel walls are weak such that hemorrhaging is commonplace (Brickley and Mays 2019; Ortner and Ericksen 1997) especially in response to minor trauma (Jaffe 1972). The periosteum, which encapsulates bone, is impaired by defective collagen as well, which leads to weakened Sharpey's fibres and subsequent subperiosteal hemorrhage (Tiesler et al. 2016). Hemorrhage can easily occur between the periosteum and bone as it is less firmly attached;

especially in children and in the eye orbits, making these areas more susceptible to bleeding (Ma'luf et al. 2002; Ortner and Ericksen 1997). Subperiosteal hemorrhage lifts the periosteum away from the underlying bone disrupting blood vessel walls and stimulating new bone formation due to either subsequent inflammation or mechanical pressure (Ortner and Ericksen 1997; Weston 2012). These changes to internal body structures, along with the clinical experience of chronic bleeding, lead directly to skeletal changes as indicated by subperiosteal new bone formation. This directly relates to how this lived experience translates into repeated episodes of capillary damage and bony changes observed in skeletal samples of past populations.

3.2.1.1 Skeletal indicators of VCD.

Inadequate collagen production changes the way bones model and remodel, and as such may be visible macroscopically. Children experience more rapid bone growth and modelling than adults, so the skeletal changes associated with scurvy are more readily visible upon their remains (Fain 2005). Scurvy is one of the more well-researched and more visible metabolic diseases recognized in the archaeological record. It has been described in many archaeological cases, beginning in the 1990s and increasingly since then (e.g., Eggington et al. 2024; Geber and Murphy 2012; Ortner and Ericksen 1997; Ortner et al. 1999; Schattmann et al. 2016; Snoddy et al. 2018).

In general, porosity is associated with scurvy. In response to the bleeding outside of the circulatory system, the body creates new vessels for the blood to go through in the bones, thus dealing with the hemorrhage, and leaving porosity on the bone surface (Brickley and Mays 2019; Brown and Ortner 2011; Ortner and Ericksen 1997; Ortner et al. 1999; Ortner 2003). One of the most likely skeletal indicators of scurvy is porosity on the greater wing of the sphenoid (Ortner et al. 2001), however, this skeletal element is not often present in the archaeological record (Brickley and Ives 2006). Other bony indicators of scurvy are porosity on the cranial bones (facial bones, palate, basiocciput [see below for more recent exclusion], orbits), and scapulae, irregular and spongy new bone formation and porosity on the metaphyses of long bones (Brickley and Ives 2006; Mays 2008; Moore and Koon 2017; Ortner et al. 2001; Ortner and Ericksen 1997). This long bone metaphyseal porosity can be confused with normal growth patterning seen on the cut-back zones of long bones (Carter et al. 1996). The porosity associated with scurvy seen on the cortical surface of the bones infiltrates the cortex but does not connect to

the diploë or medullary cavity (Ortner et al. 2001). Porosity, in the context of scurvy, comes from either chronic inflammation (Ortner and Ericksen 1997) or from stress on the soft tissues surrounding the bone, which results in haemorrhage (Brickley and Ives 2006). This porosity within the osteons of cortical bone results in a widening of the Haversian canal space since there is reduced deposition of new osteoid and thus reduced infilling of the Haversian canal during remodelling in an individual with scurvy. Scurvy-related porosity is common in areas of the skeleton which are attachment sites for muscles (Ortner et al. 2001). For example, attachment sites for muscles of mastication (e.g., the coronoid process of the mandible) are commonly impacted (Ortner et al. 2001).

Subperiosteal new bone formation occurs on skeletal remains as a response to haemorrhaging associated with scurvy (Brickley et al. 2020a). An example of both porosity and new bone formation associated with scurvy is shown in Figure 3.2. However, it should be noted that the use of a porotic basiocciput as a diagnostic feature of scurvy has been debated due to the muscle attachment patterning on that area (e.g., Eggington et al. 2024; González Martín et al. 2018; Moore and Koon 2017). Given the uncertain nature of this feature, and that the research surrounding it is ever evolving, it will not be used as a diagnostic feature within this thesis' analysis but will still be noted when present.

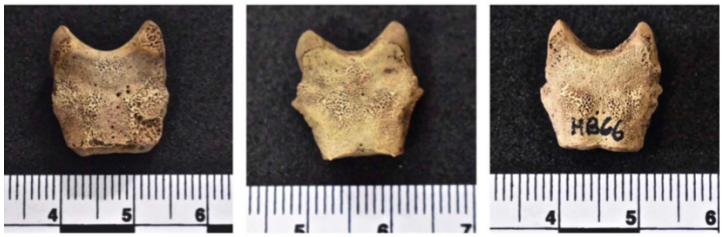

Figure 3.2. Porosity and new bone formation on inferior view of basiocciputs of individuals (<12 years old) with infantile scurvy, 1 cm scale bar (Adapted from Moore and Koon 2017: 96).

There are also radiological indicators which can be used to identify scurvy when x-rays are available for remains. These include a white line of Fraenkel, Wimberger's ring, Pelkan spurs, metaphyseal fractures, generalized osteopenia, and cortical thinning in the long bones (Fig. 3.3A) (Schattmann et al. 2016). The white line of Fraenkel is a dense area of calcification that occurs in a growing metaphysis whereas a Wimberger's ring is an epiphysis surrounded by a sclerotic ring with a more radiolucent center. Pelkan's spurs (Fig. 3.3B) are bony protrusions which occur at the metaphyseal margins and extend at right angles to the shaft of the bone (Schattmann et al. 2016). Fractures can occur in these areas (i.e. metaphyseal fractures) (Brickley et al. 2020a). Using the multiple skeletal indicators described above in a differential diagnosis can theoretically provide a more accurate diagnosis.

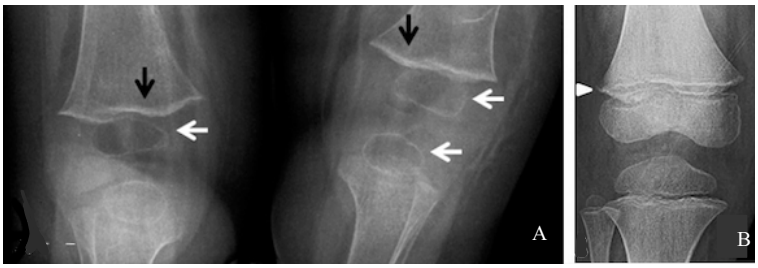

Figure 3.3A. Wimberger's rings (white arrows), and white lines of Fraenkel (black arrows) on the distal femora and unfused epiphyses of the femora and tibiae (Adapted from Vitoria et al. 2016: e3).

Figure 3.3B. A Pelkan spur indicated by the (arrowhead) (Gulko et al. 2015: 293).

3.2.1.2 Archaeological examples of VCD.

In archaeology, the presence of scorbutic lesions on skeletal remains can inform researchers about the diet of a past population. An archaeological case (Ortner et al. 2001) of subadults from Indigenous populations (1000 to 150 cal B.P.) from the Mid-Atlantic, Southwest, Southeast (Florida), and Plains regions of the United States, were assessed for any lesions associated with VCD. Prevalence of scurvy ranged from 0% within Plains groups to 38% in groups in Florida. Different reasons suggested for this variability in prevalence included regional and seasonal variation in food types, cultural patterns of storage and utilization, and periodic food shortages. However, it is thought that the most plausible explanation for the low scurvy prevalence in Plains groups was the consumption of pemmican. Pemmican would have ensured adequate vitamin C levels for people throughout the winter on the Plains (Ortner et al. 2001). This case shows that different diets impacted the levels of VCD experienced between cultural

groups within North America. Understanding what VCD is and its physiology, as well as possible past diets informs interpretations about lifeways in the past.

Another notable archaeological case of scurvy was found upon examination of the remains of a Bronze age 2-year-old child from England, dated to 4150–3920 cal B.P. (Mays 2008). Most of the pathological indicators were in the cranial bones. It was suggested that breastfeeding probably stopped some time prior to this individual's death as breast milk is a source of vitamin C, and the presence of scorbutic lesions indicates that the individual was deprived of vitamin C for at least 8–12 weeks. It is also postulated that what the child was eating may have been heated to the point where the vitamin C content was destroyed (Mays 2008) which provides insight into life practices of this group.

3.2.2 Vitamin D deficiency

Vitamin D deficiency (VDD), rickets, is one of the most common health conditions which has been ever present in human populations (Brickley et al. 2017). A prolonged lack of vitamin D leads to deficiency (Brickley and Ives 2008b; Roberts and Manchester 2007). The majority of the body's vitamin D requirement is filled from UV exposure and is produced in the skin (Pitt 1995). Healthy humans can produce all the vitamin D needed through adequate skin exposure to sunlight and UVB radiation (Brickley et al. 2014, 2017; Brickley and Mays 2019; Holick 1996, 1999). Vitamin D may also be ingested, either from food sources, such as eggs and salmon, which contain vitamin D or through dietary supplementation (Brickley et al. 2014, 2020a). Vitamin D serum levels below 25 nmol/L are indicative of deficiency (Mithal et al. 2009). Anything less than 10–15 minutes of sun exposure 2–3 times a week can lead to lower serum levels, and deficiency (Holick 2004).

Vitamin D is a prohormone necessary for the absorption of calcium and phosphorus from the gut (Roberts and Manchester 2007). A deficiency limits the body's ability to absorb calcium and phosphorus from the intestines (Brickley et al. 2014). The pathway of vitamin D metabolism can be seen in Figure 3.4 and also shows interactions between various tissues and metabolic functions.

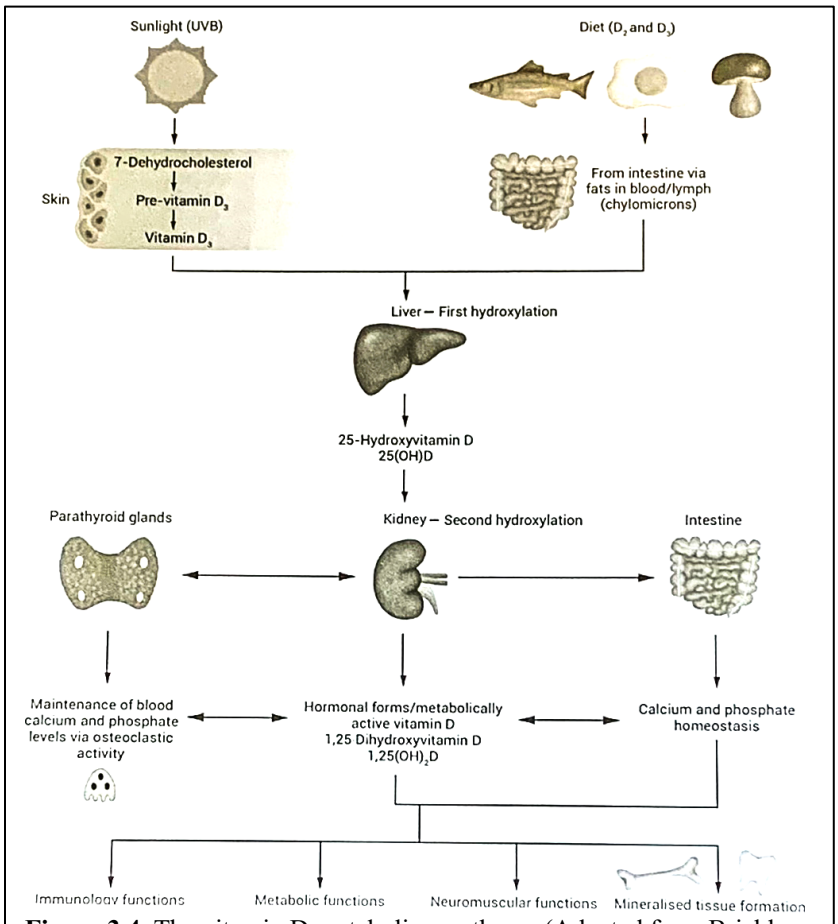

Figure 3.4. The vitamin D metabolism pathway (Adapted from Brickley et al. 2020a:78).

Calcium homeostasis is the main function of vitamin D in the human body, and this homeostasis requires vitamin D to enter systemic circulation as a pro-hormone precursor and undergo conversion steps in the liver and then in the kidneys, to become an active hormone and affect the target tissues (Fig. 3.5A, p. 30) (Holick 2006). Calcium homeostasis is vital for the functioning of metabolic processes and neuromuscular activities (Mithal et al. 2009; Holick 2006). Failure at any step during this process may result in vitamin D deficiency (VDD) (Brickley et al. 2014). The release of parathyroid hormone is also impacted by the levels of calcium absorbed (see Fig. 3.4) (Holick 2002; Parfitt et al. 1982). Additionally, vitamin D is essential for the metabolism of phosphorus, and phosphorus is necessary for osteoid mineralization (Brickley and Mays 2019). When vitamin D levels are too low, minerals, phosphorus, and calcium have decreased absorption in the gut (Fig. 3.5B) (Brickley & Mays, 2019).

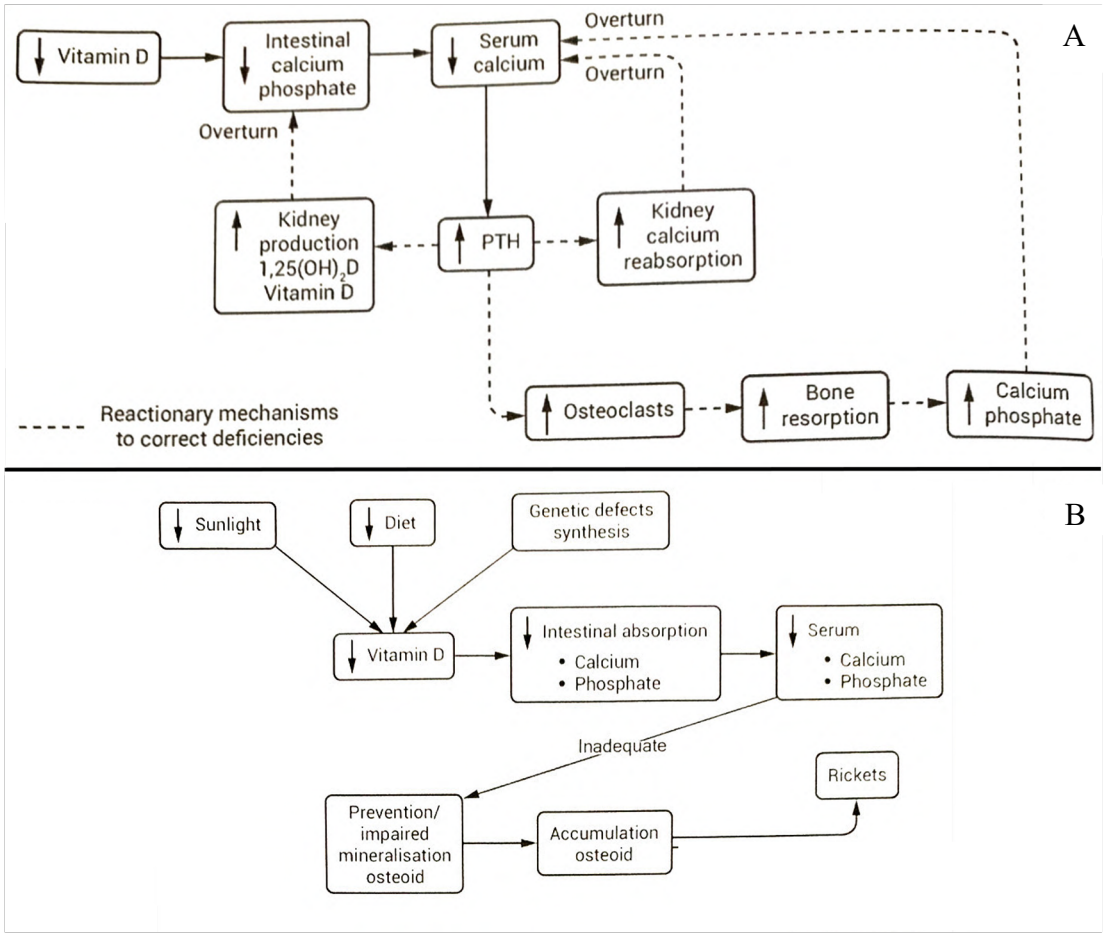

Figure 3.5A. The biological effects of low vitamin D (Adapted from Brickley et al. 2020a: 86).

Figure 3.5B. Low vitamin D and the development of rickets (Adapted from Brickley et al. 2020a: 77).

There are many factors which can result in VDD. These causes include insufficient dietary acquired vitamin D (Dent and Smith 1969), and diet is sensitive to socio-cultural factors (Brickley et al. 2014). Other causes include inherited disorders (Glorieux and St-Arnaud 2005; Holick 2006; Malloy and Feldman 2003), autosomal dominant hypophosphatemic rickets (Econs and McEnery 1997), X-linked hypophosphatemic rickets (HYP Consortium 1995), malabsorption disorders which affect uptake of vitamin D or calcium (Hanly et al. 1985), renal or metabolic disorders (Dusso et al. 2005), and liver failure (Melvin et al. 1970) which results in the loss of conversion enzymes needed for the production of active vitamin D (Brickley et al. 2014). Increased rates of urbanization contribute to higher rates of VDD (Roberts and Manchester 2007) due to air pollution, which can block sunlight (Oberhelman and Thacher 2013). A cultural factor which may increase the rates of VDD are the ways of dressing in areas where there is a lot of sunlight. For example, swaddling and staying indoors reduces the amount

of sunlight to which a subadult would be exposed (Roberts and Manchester 2007; Shin et al. 2008). If skeletal remains come from a location in which structures had no windows, for example at Seh Gabi, this could further reduce sunlight exposure. Cultural practices or religious beliefs which keep girls and women indoors and/or covered with clothing increases rates of VDD among them (Hatun et al. 2005; Hovsepian et al. 2011; Mithal et al. 2009). Other factors include a higher latitude, the winter season, darker skin pigmentation, angle of the sun, and the absence of vitamin D fortification (Brickley et al. 2014; Holick 2008; Mithal et al. 2009). At the present time VDD is commonly found in regions like South Asia and the Middle East due to these factors (Mithal et al. 2009).

A cultural practice which can influence VDD is the extent of breast-feeding and timing of weaning. The vitamin D status of an infant must be considered with that of their mother as the maternal status will directly impact the infant through the time *in utero* and the vehicle of breast milk (Brickley et al. 2014). Rickets rarely appears prior to the age of 4 months due to fetal supply and breast-feeding unless the infant's mother is also vitamin D deficient (Dawodu and Tsang 2012; Maiyegun et al. 2002). Rickets is common in neonates whose mothers have low levels of vitamin D, and their sole source of nutrition is breast milk (Mithal et al. 2009). However, the amount of vitamin D from breastmilk without supplementation is limited (Streym et al. 2016). Adequate vitamin D concentrations are also necessary during pregnancy for neonatal calcium homeostasis, bone maturation, and mineralization (Maghbooli et al. 2007). Neonates who are born to mothers with low vitamin D have a lower cord blood level of vitamin D and may be at risk for developing rickets (Biale et al. 1979; Kimball et al. 2008). In women with low vitamin D serum levels, the fetus is unable to gain sufficient vitamin D for a normal mineralization process *in utero* (Morley et al. 2006). Additionally, when a mother is vitamin D deficient in late-term pregnancy, this can lead to a slightly shorter gestation period which could result in a growth deficit (Morley et al. 2006). VDD can be passed from mother to child during pregnancy and through breastfeeding once the child is born (Maghbooli et al. 2007; Roberts and Manchester 2007). In modern-day Iran, it has been found that many pregnant women have VDD and as such there is also a high prevalence of deficiency amongst their newborns, nine out of ten newborns in the study had lower than normal vitamin D levels (Maghbooli et al. 2007). It is possible that there could have been high rates of MBD amongst mothers at Seh Gabi, leading to notable rates of it amongst the infant remains present.

Vitamin D is essential in the skeleton (Brickley and Ives 2008b) for the mineralization of osteoid and cartilage (Roberts and Manchester 2007). Rickets stems from reduced availability of calcium or phosphates for incorporation into the hydroxyapatite of bone (Jokar et al. 2008). VDD also disrupts the process of bone formation by causing failed mineralization of osteoid during linear growth and remodelling as well as appositional growth of cortical bone in a subadult individual (Pitt 1988, 1995; Schattmann et al. 2016) which leads to lower-than-expected levels of bone across the skeleton (Priemel et al. 2010). This results in accumulation of unmineralized osteoid and reduced skeletal rigidity (Brickley et al. 2014; Schattmann et al. 2016). Bone mineralization during growth and remodelling (Brickley and Mays 2019) stems from the release of parathyroid hormone which mobilizes calcium stores and in turn triggers phosphorus loss through urine (Fig. 3.5B, p. 30) (Holick 2006, 2007). It is important to note that once vitamin D is obtained and levels become normal again skeletal turnover will return to its normal process and function (D'Ortenzio et al. 2016). With treatment, vitamin D levels take at least eight weeks to normalize (Bordelon et al. 2009).

3.2.2.1 Skeletal indicators of VDD.

The pathway of how skeletal changes can occur in rickets is shown in Figure 3.5B (p. 30). Reported early clinical signs of enlarged epiphyses, beading of the ribs, and thickening of the frontal bone (Barlow 1883) have the potential to be seen on archaeological skeletal remains. Rib flaring at the sternal end (Figure 3.6A), long bone metaphyseal flaring, general porosity, a thickening of the long bones, a deep ilium concavity, a deformed mandibular ramus, and frontal bone bossing may all be present in the remains of someone who had VDD (Schattmann et al. 2016). One such indicator is that bone shape is altered in response to mechanical stressors (Brickley and Ives 2008b). VDD leads to a softening of the bones, and as such any weight bearing on long bones will result in bowing, often bowing outwardly (Brickley and Ives 2008b; Brickley et al. 2014; D'Ortenzio et al. 2016; Roberts and Manchester 2007) as seen in Figure 3.6B. Given the young age-at-death of most of the Seh Gabi subadults (on average, birth to 1 year), this bowing is not expected to be very common as most of these individuals were not old enough to move on their own. Additionally, abnormal growth plates have been associated with active cases of VDD whereas the presence of porosity in the concave curvature of long bones has been associated with healing cases. In children with rickets, cortical bone is thinner and more porous whereas there will be sparse trabeculae (Jaffe 1972). Additionally, fractures which are linked to bone loss can occur in various locations throughout the skeleton because of the changes in osteoid from VDD (Priemel et al. 2010). Since VDD leads to deteriorated bone structure, those who lived with VDD are less likely to leave a well-preserved skeleton in the archaeological record (Brickley et al. 2014).

Figure 3.6A. Sternal rib flaring and porosity indicated by arrows (Adapted from Schatmann et al. 2016: 70).

Figure 3.6B. Humeral bowing associated with rickets, with proximal end at right side of image (Adapted from Schattmann et al. 2016: 70).

There are also radiographic features which may be present including metaphyseal fractures, generalized osteopenia, long bone cortical thinning, metaphyseal trabecular coarsening (Fig. 3.7A), loss of integrity in sternal rib ends, fraying of epiphyses (Fig. 3.7B), thick cortical

bone, a sharp cortical outline, and distinction at the end of a growth plate (Schattmann et al. 2016). Metaphyseal trabecular coarsening and thinning are changes that could be confused with taphonomic changes. Cupping at epiphyseal ends of long bones could also be seen radiographically and is due to the altered bone modelling process in rickets (Özkan 2010b). Another possible indicator is the presence of interglobular dentin spaces within teeth (D'Ortenzio et al. 2016) which requires microscopic investigation of teeth. As with any disease in the archaeological record, it is important to note that all these features may not be present based on the timing of the disease relative to growth and development.

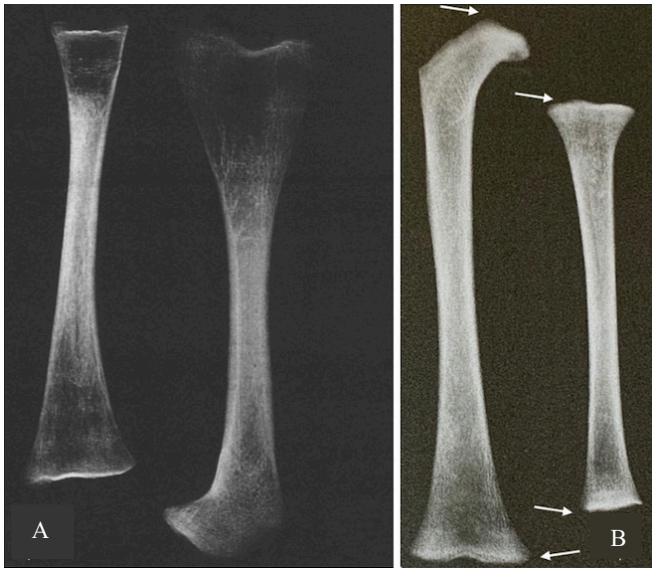

Figure 3.7A. Radiograph showing metaphyseal trabecular coarsening and thinning associated with rickets on a femur and tibia, proximal ends are at the bottom of the image (Adapted from Mays et al. 2006: 369).
Figure 3.7B. Radiograph showing epiphyseal roughening/fraying, indicated by arrows (Adapted from Brickley et al. 2020a: 107).

3.2.2.2 Archaeological examples of VDD.

Understanding VDD can provide insight into dietary and life practices of groups in the past. One example comes from a study of 48 subadult individuals from the Saint-Amé collection from Douai, France which dates to around 450 to 150 cal B.P. (Schattmann et al. 2016). Twelve of these 48 subadults were determined to have rickets. While the researchers concluded that rickets is present in this population, the observed indicators were subtle. They suggest that these children may have been kept inside more, which could have resulted in the presence of rickets. One possible reason for being indoors more could have been that these children were nursed and looked after by hired help, or they did not accompany their mothers on errands. Other factors discussed were clothing choices, a cramped urban environment, and pollution (Schattmann et al. 2016). It was also common at this time for infants to be swaddled which reduces skin exposure to light (Senoir 1983). All these possibilities would have prevented or diminished the UV exposure required for the vitamin D metabolism pathway to begin. In this case, the socioeconomic status

of the individual was not associated with the osseus evidence for rickets, which led researchers to deduce that external pressures, such as climate, were to blame (Schattmann et al. 2016). This conclusion was supported by the date range associated with these remains which coincides with the Little Ice Age, 360–200 cal B.P. (Schattmann et al. 2016).

3.2.3 Comorbidity of VCD & VDD

While discussing Vitamin C and D deficiencies, it should be recognized that these two metabolic diseases can frequently be present at the same time (comorbid) within one individual. For example, the Schattmann and colleagues study discussed above found that the 12 rickets cases were comorbid with scurvy (2016). There are also clinical reports discussing such comorbidity within one individual (e.g., Barlow 1883; Roy et al. 2020). The interaction between the two conditions can be inhibitory in that rickets can interrupt the skeletal changes associated with scurvy and vice versa, depending on time of onset (Schattmann et al. 2016). Scurvy reduces osteoblastic activity which slows the accumulation of unmineralized osteoid. This may inhibit some skeletal manifestations of rickets such as the softening and bowing of the arms or legs (Follis et al. 1940). In their study, Schattmann et al. (2016) suggest that scurvy inhibited rickets, resulting in subtle rickety changes. On the other hand, rickets can inhibit scurvy. Rickets inhibits bone mineralization, which in turn will stop the accumulation of calcified bone matrix and the formation of new bone (Follis et al. 1940; Fouron and Chicoine 1962). In a case of comorbidity, there may be superficially similar lesions resulting from both rickets and scurvy despite having different underlying causes (Brickley et al. 2020a). Vitamin deficiencies are important metabolic bone diseases to be aware of, as their related bony changes can be subtle and concurrent.

There are other metabolic bone diseases which can be unrelated to diet and have been identified in skeletal remains from antiquity. Moving forward, anaemia, fluorosis, hyperostosis, and osteogenesis imperfecta will be discussed for this reason. Other metabolic bone diseases (pellagra, Paget’s disease, osteoporosis and osteopenia, hyperparathyroidism, hypophosphatasia, osteopetrosis) are not discussed as they are known to be rare in children (Arumugam et al. 2015; Cleveland Clinic 2024; Genetic and Rare Diseases Information Center; Naveen et al. 2013; National Institute of Arthritis and Musculoskeletal and Skin Diseases; Walczyk et al. 2011).

3.3 Anaemia

When an individual has a disease like scurvy or rickets it can make them more susceptible to living with another nutritional deficiency condition such as anaemia (Reid and Graham 2024; Tembunde et al. 2022). For example, vitamin C aids in the absorption of iron in the intestinal tract (Cotran et al. 1999; Fain 2005). Thus, if one is deficient in vitamin C, then they may also not be absorbing enough iron, possibly resulting in iron deficiency anemia (Fain 2005). It is possible then that if the individuals of Seh Gabi were vulnerable to vitamin C deficiency that they would have also been susceptible to anaemia.

Anaemia occurs when the number of red blood cells (RBCs) or haemoglobin concentrations in the body are lower than normal causing oxygen deficiency (Brickley et al. 2020b) which can have many causes. Reduced oxygen levels result in less oxygen being transported to tissues and when this occurs at a level which is insufficient for physiological need, results in anaemia (Brickley et al. 2020b). The four root causes are: blood loss, insufficient production of red blood cells, the destruction of red blood cells (Maakaron et al. 2016), and inadequate iron (Sullivan 2005). Additionally, anaemia causes a disruption in blood cell production within the trabecular bone of the skull (the diplöe) (Rinaldo et al. 2019) making the cranial vault bones an important site of observation for signs of anaemia.

3.3.1 Skeletal indicators of anaemia

In archaeological cases, differential diagnosis involving anaemia is usually given as a general anaemia diagnosis rather than indicating the root cause. There are many potential skeletal indicators, but individually they are non-specific. Anaemic skeletal lesions are more easily seen within and on the cranium (Brickley et al. 2020b). Porosity on the orbital roof, labelled as ‘cribra orbitalia’, is one of the common signs of anaemia (Brickley et al. 2020b; Lewis 2012; Rinaldo et al. 2019; Schats 2021; Sullivan 2005). *Cribra* are small holes (pores), of various sizes, which appear mostly on the orbital roofs and other bones of the cranial vault (Rinaldo et al. 2019). However, this skeletal indicator is also common in other illnesses such as Vitamin C deficiency and is associated with all anaemias (Brickley et al. 2020b; Lewis 2012; Rinaldo et al. 2019). There are some features which separate cribra orbitalia in anaemia from other conditions. Cranial porous lesions are due to the perforation of external cortical bone via resorption, which is triggered by marrow expansion in anaemia (Brickley et al. 2020b). Only when there is evidence

of this marrow hyperplasia, can anaemia be inferred. Additionally, these pores must connect to a thickened diploë. There are other indicators within the orbits as well: thinning of trabecular elements and cortical bone (Brickley et al. 2020b). Porosity in general is a theme with anaemic skeletal lesions. Other key areas of the skeleton which may show porosity are the cranial vault and the long bones (Brickley et al. 2020b; Lewis 2012; Rinaldo et al. 2019; Sullivan 2005). Cribra orbitalia and other porous lesions on adult remains can be seen in Figure 3.8. While this thesis is focused on the assessment of subadult remains, this image is a good example of cribrous lesions. *Cribra humeri* typically occur on humeral neck while *cribra femora* typically occur on the femoral neck (Schats 2021).

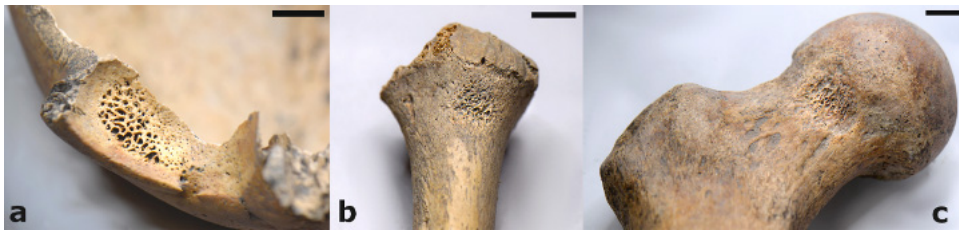

Figure 3.8. Cribrous lesions associated with anaemia. "a" shows cribra orbitalia, "b" *cribra humeri*, and "c" *cribra femora*; 1 cm scale bar (Adapted from Schats 2021: 84).

Changes within long bones are generally macroscopic rather than microscopic (Brickley et al. 2020b). For example, there may be thinning of the cortical and trabecular bone within long bones, which can be seen in radiographs and macroscopically on a cross-section. There can also be perforations in the cortical bone of vertebrae and a slight expansion of the ribs for those who lived with anaemia due to marrow hyperplasia (expansion of cells). In sickle cell anaemia (a genetic form of anaemia) specifically, there may be necrosis of the humeral and/or femoral head (Brickley et al. 2020b).

Thalassemia, another genetic form of anaemia, results in the non-specific bony changes seen in other forms of anemia, as well as some unique changes (Lewis 2012). In addition to the general indicators, there may also be thickening of the sphenoid, maxillae and zygomatics, obliterated cranial sutures and widening of the interorbital space along with protruding upper incisors and an overbite. Other skeletal indicators of thalassemia include hypertrophic metacarpals and phalanges, exaggerated sulci on femora and tibiae, large bony masses on the ribs, osteopenia, and linear striations on the ribs (Lewis 2012).

Aside from macroscopic changes, radiological indicators of anaemia include a Hair-on-end appearance within the cranium, failure of sinus development, thinning of cortical bone and a reduced number of trabeculae in both the vertebrae and long bones, and infarcts (osteonecrosis) in long bones (Brickley et al. 2020b; Sullivan 2005). Bone infarcts are commonly mistaken as osteomyelitis (Brickley et al. 2020b; Sullivan 2005). Hair-on-end (Fig. 3.9) refers to appearance of the cranial vault in a cranial radiograph in which there are vertical striations that look like hairs standing at right angles to the ectocranial surface within the diploë. In cases of thalassemia, this radiographic indicator is more pronounced than in other anaemias (Lewis 2012).

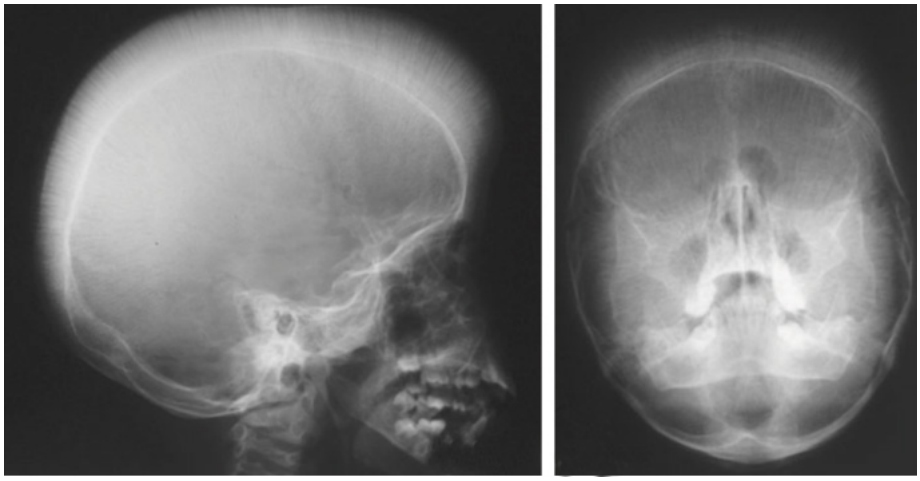

Figure 3.9. Radiograph of skull with Hair-on-end appearance associated with thalassaemia (Adapted from Basu and Kumar 2009: 807).

There can also be microscopic indicators of general anaemia on the orbital roof. On a histological section from a porous orbital roof, anaemia could present as enlarged marrow spaces, an opened orbital lamina, and lessened trabeculae (Wapler et al. 2004) (Fig. 3.10). Without histology or micro-CT, cribra orbitalia cannot be concretely designated as being an anaemic or scorbutic lesion. For it to be associated with anaemia there needs to be clear evidence of marrow expansion and intrusion into the diploë (Brickley et al. 2020b). With these skeletal signs,

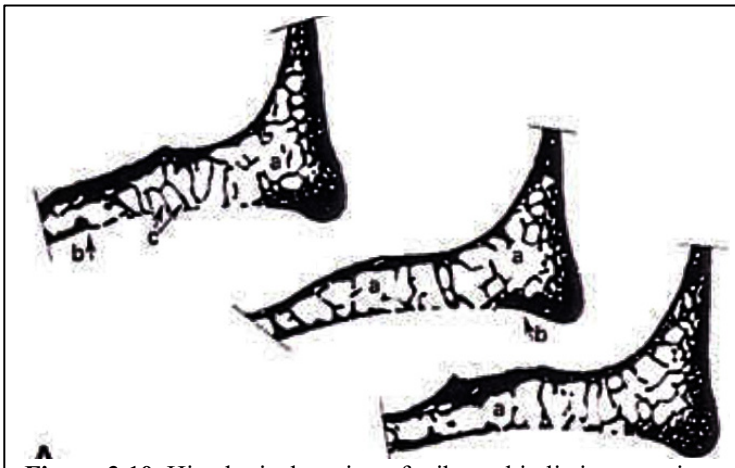

Figure 3.10. Histological section of cribra orbitalia in anaemia. "a" refers to marrow spaces, "b" to orbital lamina, and "c" to the remaining trabeculae (Adapted from Wapler et al. 2004: 335).

it is clear when providing a differential diagnosis of anaemia for human remains all possible indicators should be documented and discussed given their non-specificity.

3.3.2 Archaeological examples of anaemia

A differential diagnosis often provides only a general diagnosis of anaemia. The use of historical documents can be used to more specifically link anemia to chronic disease, dietary inadequacy, or inadequate resorption. Distinguishing between conditions based solely on skeletal evidence may not be possible.

Sullivan (2005) assessed the remains of 147 adults, each with at least one complete orbit, from the Medieval St. Andrews church cemetery in York, UK (750 to 412 cal B.P.). During its time of use, the church's congregation was generally of lower socioeconomic status. Status was determined via historical records, archaeological information regarding medieval burial practices, and the original excavation report. As status decreased, the rates of anaemia increased in this population. Across the social classes in this sample, more women exhibited cribra orbitalia than men. This may have been due to the high iron-demand of their reproductive functions, which in turn may have made iron deficiency anaemia (IDA) chronic for women. Additionally, there was a lack of economic mobility and few employment opportunities available to the lower classes likely contributed to the lower classes having higher rates of anaemia than those of upper classes (Sullivan 2005). Having less access to resources would also contribute to what foods were available to the lower classes, and result in less access to adequate vitamins and iron. During the Medieval Period, York was known to have a lack of sanitation, and had cramped, overcrowded dwellings for the poor. Analysis of phosphatic fecal concretions and other organic materials showed that GI tract parasitic infection was a major problem at this time. Sullivan (2005) posits that many residents, including those in the upper classes, would have developed anaemia of chronic disease (ACD) as a defence against parasites and infectious diseases. ACD is a form of anaemia which stems from the body's iron-withholding system, which starves host-dependent microbial invaders of the iron they need to survive. Although anaemia was present throughout all classes of people, those impacted the most belonged to low status groups (Sullivan 2005). While this case is focused on adults, it provides insight into how past dietary practices might have informed life in past lived society. Additionally, if adults were

living with anaemia, it is entirely possible that the subadults of this population were also affected.

3.4 Fluorosis

Fluorosis is not a MBD related to dietary intake of a vitamin, or lack thereof, but rather is related to the location of an individual's or group's water source. Fluorosis is a metabolic bone disease which stems from chronic exposure to high levels of fluoride (Mehta and Shah 2013; Nelson et al. 2019; Ozsvath 2009; Perumal et al. 2013). Fluoride is an essential trace element (Nelson et al. 2019) that is required for the maintenance of good bone and dental health, however, at chronically high levels it can become detrimental (Farley et al. 1983; Mehta and Shah 2013; Nelson et al. 2019; Perumal et al. 2013). Fluoride is a naturally occurring element and can enter the human body through several pathways such as water and food. Some areas in the world have naturally high levels of fluoride in the ground water including Africa, China, the Middle East, and southern Asia, such as India and Sri Lanka. Consumption of sources with a low fluoride concentration (0.8–1.2 mg/L) is necessary for the maintenance of healthy bones and teeth but chronic exposure to fluoride levels 1.5 mg/L or higher results in fluorosis (Perumal et al. 2013).

In children close to 80% of orally ingested fluoride is retained because their developing bones and teeth take up more of the fluoride (Institute of Medicine (US) Standing Committee on the Scientific Evaluation of Dietary Reference Intakes 1997). Chronic exposure to high levels of fluoride is detrimental to the skeletal system, bone being the principal site of fluoride accumulation (Perumal et al. 2013), as fluoride replaces the hydroxyl groups in hydroxyapatite (Izuora et al. 2011; Nelson et al. 2019). Fluoride stimulates rapid growth of osteoblasts (involved in both bone modelling and remodelling) which gradually builds up bones by increasing calcium uptake (Farley et al. 1983). The combination of rapid growth and stimulation of osteoblasts, with fluoride replacing hydroxyl within hydroxyapatite results in skeletal fragility (Izuora et al. 2011). Bone and tooth quality decreases and can result in brown staining and pitting on dental enamel (Gupta et al. 2016). While skeletal fluorosis can occur at any time due to bone turnover occurring continuously throughout life, dental fluorosis requires over-exposure to fluoride during childhood when tooth crowns are developing (Aoba and Fejerskov 2002). Other than teeth, the

areas of the skeleton most impacted by fluorosis are the ribs, spine, and pelvis (Gupta et al. 2016) which would be preserved in the archaeological record.

3.4.1 Skeletal indicators of fluorosis

As fluorosis directly affects bone maintenance during life and tooth formation during childhood, there are changes that can be seen post-mortem. For example, if someone had fluorosis during life then in the archaeological record their teeth may have brown discolouration and mottled enamel (Yoshimura et al. 2006) (Fig. 3.11). Hypomineralization of teeth, like that in fluorosis, can be distinguished from taphonomic change via x-ray fluorescence (Garot et al. 2017). Compared to normal enamel, such as that of teeth exposed to taphonomic processes which change colouration, hypomineralized enamel has a decreased mineral density and increased phosphate/β-carbonate ratio (Garot et al. 2017). Depending on the stage of lived fluorosis, the teeth may be a better starting indicator as dental fluorosis precedes skeletal fluorosis (Perumal et al. 2013). In terms of the skeleton itself there are a few systemic changes to look for: periosteal thickening, calcified ligaments and tendons, and bony exostoses at ligamentous and tendon bone attachment sites (Resnick and Niwayama 1983).

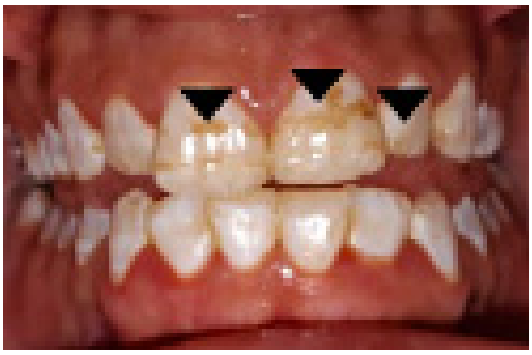

Figure 3.11. Dental fluorosis, arrowheads indicate the enamel discolouration (Adapted Sellami et al. 2020: 347).

Radiographic indicators of fluorosis include osteosclerosis (increased bone density), and osteopenia (Boillat et al. 1980; Gupta et al. 2016; Mithal et al. 1993). Osteosclerosis and osteopenia are opposite effects and do not present within the same individual at the same time. Those who demonstrate osteopenia have a lower dietary intake of calcium than patients who showcase osteosclerosis (Mithal et al. 1993). Specifically, osteosclerosis in fluorosis patients is located on the knees, wrists, pelvis, and vertebral column (Gupta et al. 2016). Osteopenia is widespread throughout the skeleton but more pronounced in the limbs (Mithal et al. 1993). Another radiological indicator is the thickening of trabecular bone, at the distal and proximal ends of long bones (Mithal et al. 1993). These radiographic indicators would be visible on skeletal remains as well.

3.4.2 Archaeological examples of fluorosis

Several archaeological studies demonstrate what this means in practice. For example, a case from the site of Herculaneum, near Mount Vesuvius, demonstrates evidence of fluorosis (Petrone et al. 2011). In the study population 73.5% exhibited diffuse osteosclerosis in both the axial and appendicular skeleton. Increased cortical and trabecular thickness, as well as bony exostoses along the periosteum were observed. Elements of dental change were also observed. Of the study population 96.1% had linear enamel hypoplasia (LEH), a non-specific indicator of stress on teeth which appears as horizontal grooves, as well as there was mottling, pitting, and staining of tooth enamel. The pathological changes were described as endemic since both adults and subadults were equally affected. It is important to note that fluorosis can be a major problem in volcanic areas, and given Herculaneum's proximity to an active volcano, the presence of fluorosis in this population is not entirely surprising. Due to both the skeletal indicators and environmental information, a high prevalence of fluorosis was suggested (Petrone et al. 2011). In this case, knowing that in volcanic areas, fluorosis can be a problem provides context for the non-specific skeletal changes observed.

A study by Nelson and colleagues (2019) examined a set of individuals from the Ray site in Illinois, dated to the Middle Woodland period (2000 to 1550 cal B.P.). The human remains were uncovered from a series of pit burials, grouped in four clusters which extended across a ridge above a flood plain (Nelson et al. 2019). Eight individuals were found to demonstrate pathological changes: osteosclerosis, high frequency of fractures, and dental abnormalities. The axial skeletons of these individuals displayed excessive abnormal bone formation more often than their appendicular skeletons. A diagnosis of fluorosis was corroborated by considering the environment in which the remains were recovered. There is a naturally high level of fluoride in both the soil and water in Illinois which put people at risk for excessive consumption and exposure to fluoride, leading to fluorosis, in both modern and past populations (Nelson et al. 2019). Having the required knowledge of environmental factors which may lead to pathology provides both a possible basis and direction for a differential diagnosis.

Seh Gabi, Iran, is located in a part of the world in which high levels of fluoride are known to occur (Perumal et al. 2013). This environmental context information is valuable for a differential diagnosis if any of these skeletal changes are noted within the population.

3.5 Hyperostosis

Although hyperostosis is unrelated to diet and environment, hyperostosis has been identified in the archaeological record. Hyperostosis refers to a variety of conditions in which there is a thickening of the endosteal surface of bones (Brickley and Ives 2008a; She and Szakacs 2004; Stiene and Frank 2002; Szeniczey et al. 2019). The main types of hyperostosis are internal frontal hyperostosis (HFI), leontiasis ossea, and infantile cortical hyperostosis (Caffey's disease) (Brickley and Ives 2008a; Stiene and Frank 2002; Szeniczey et al. 2019).

Caffey's disease and HFI have been identified in the archaeological record far more frequently than leontiasis ossea (Brickley and Ives 2008a; Stiene and Frank 2002; Szeniczey et al. 2019). As such, they will be the main focus of this discussion. Caffey's disease is characterized by acute inflammation of the surrounding soft tissues coupled with a localized thickening of the underlying bone cortex (Nistala et al. 2014). It is an inflammatory disease which begins in early infancy and characterized by cortical growth in multiple skeletal elements. Majority of the individuals associated with Seh Gabi are aged to about birth to 1 year old, thus it is possible this is a type of metabolic bone disease which could be seen. The lesions associated are often asymmetric and may occur on the cranium, mandible, tibiae, ulnae, clavicles, scapulae, ribs, humeri, femora, fibulae, ilium, and metatarsals (Kamoun-Goldrat and le Merrer 2008; Nistala et al. 2014). In HFI the frontal bones' internal tables thicken (Glab et al. 2006). Given that hyperostosis directly impacts skeletal elements, it can be visible in the archaeological record.

3.5.1 Skeletal indicators of hyperostosis

There are a few skeletal indicators of hyperostosis which can be seen in the archaeological record. A primary indicator is an increased thickness of cortical bone beyond that which is normal or expected (Kamoun-Goldrat and le Merrer 2008). Overall, there may be an increased weight to the bones as well (Allison et al. 1976). Osteal bulges may also be observed (Glab et al. 2006) which are bumps on the endocranial surface of the cranium (Antón 1997; Glab et al. 2006).

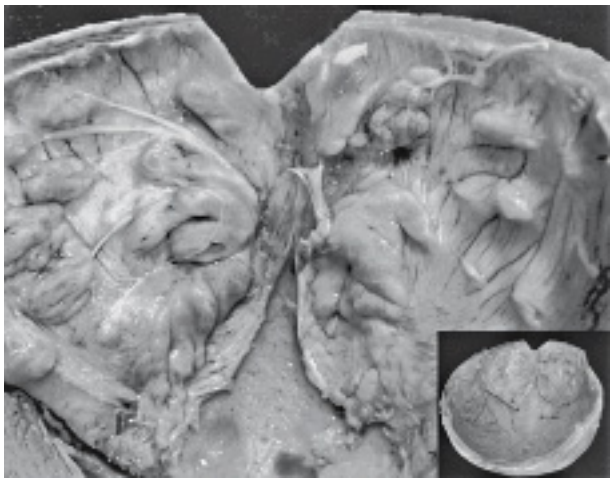

Figure 3.12. Endocranial surface of anterior frontal bone with irregular thickening associated with hyperostosis (Adapted from She and Szakacs 2004: 207).

One of the key features of HFI is the irregular thickening of the endocranial surface of the frontal bone whereas the external surface looks normal (She and Szakacs 2004). This thickening is due to an increase in trabecular bone deposition. The thickening may be bilaterally symmetrical and will be made up of multiple smooth bony ridges with nodules protruding from the inner surface (Fig. 3.12). Histological reports of this feature will show an overall thickening of the trabecular bone (She and Szakacs 2004).

In Caffey's disease, there are other indicators including irregular and excessive subperiosteal new bone formation which is most commonly found on the ribs and facial bones (Buckley 2000). These subperiosteal changes themselves are not distinguishable from other disorders which cause subperiosteal new bone formation, but in Caffey's disease, the mandible is almost always involved (Buckley 2000).

3.5.2 Archaeological examples of hyperostosis

The remains of two female skeletons from a 450 to 350 cal B.P. Dominican Church in southwest Poland were assessed (Glab et al. 2006). It was determined they had HFI due to the hypertrophic changes in the inner lamina of the frontal bone and bulges on both skulls which formed radial elevations which ran symmetrically away from the frontal crest (Glab et al. 2006).

These findings align with the archaeological indicators discussed above, and as such, the researchers determined the most appropriate diagnosis to be HFI (Glab et al. 2006).

3.6 Osteogenesis Imperfecta

Osteogenesis imperfecta (OI) is another metabolic bone disease which is unrelated to environment and diet. The term "osteogenesis imperfecta" refers to a heterogenous group of genetic disorders which are the result of type 1 collagen defects (Tournis and Dede 2018; Van Dijk and Sillence 2014; Wadanamby et al. 2022). OI encompasses a group of connective tissue disorders (Van Dijk and Sillence 2014). In most cases, 85-90%, OI is inherited through an autosomal dominant pathway and is caused by mutations in the COL1A1 and COL1A2 genes leading to defects in type 1 collagen (Tournis and Dede 2018). In general, OI increases a person's risk of fractures and bone deformities throughout their lifespan (Patel et al. 2015; Van Dijk and Sillence 2014). There are different types of OI: Type I OI is less severe, type II is lethal perinatally or shortly after birth, type III is the most severe form in which a person can survive, and type IV reflects intermediate severity (Tournis and Dede 2018). Type II may present as a stillbirth, or several fractures and deformities shortly after birth. In type III, the disease leads to extreme morbidity, disability, and mortality. In the mildest forms, fractures tend to decrease in number during adulthood but may re-emerge during a post-partum period or with menopause (Tournis and Dede 2018). Associated skeletal deformities include the bowing of long bones, kyphoscoliosis (a curved spine which can result in thoracic cage deformity), acetabular protrusion, and chest wall deformities such as a barrel chest (Forlino and Marini 2016).

3.6.1 Skeletal indicators of OI

There are some key features that palaeopathologists look for to provide a diagnosis of OI. Radiologically, a "zebra stripe" (Fig. 3.13) may be visible on the metaphyses of long bones, which refers to alternating light and dark bands (Tournis and Dede 2018). Harris lines may show up on a radiograph similarly as transverse bands (Chakraborty et al. 2017). Given this, it is difficult to distinguish between the zebra stripe sign and Harris lines, and one should not rely solely on radiographic signs.

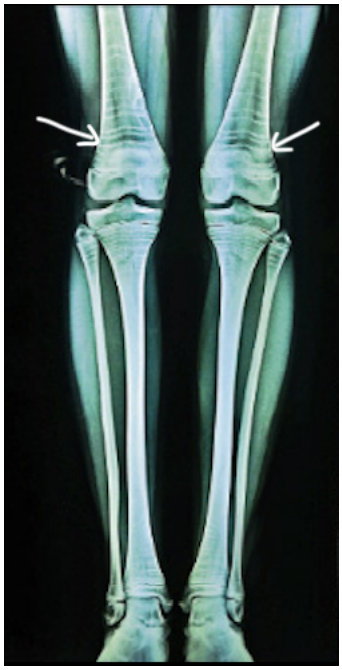

Figure 3.13. The zebra stripe sign as indicated by arrows, bilateral (Adapted from Tournis and Dede 2018: 31).

One skeletal indicator that may be present is that of osteoporosis as it develops in most OI patients (Van Dijk and Sillence 2014). The presence of only osteoporotic lesions in a skeleton would not be enough for an OI diagnosis; rather other indicators would also need to be present to support it. Additionally, it is common for the long bones to show evidence of anterior bowing (Fig. 3.14) (Gray 1970; Spranger et al. 2002) and may be accompanied by cortical thickening (Gray 1970). To distinguish from other diseases which may cause anterior bowing, like syphilis, the skeleton as a whole and radiographs must be considered (Rothschild and Rothschild 1997). Evidence of fractures could be present (Gray 1970; Lewis 2019; Spranger et al. 2002; Tournis and Dede 2018; Van Dijk and Sillence 2014). Other possible indicators would be an overall lightness and fragility to the bones, an expanded cranial vault, and elongated orbits (Gray 1970). A narrowing of long bone diaphyses, in comparison to their length, is also possible (Ortner 2003). Histologically, minimal osteon remodelling for a person with OI could be present (Ortner 2003).

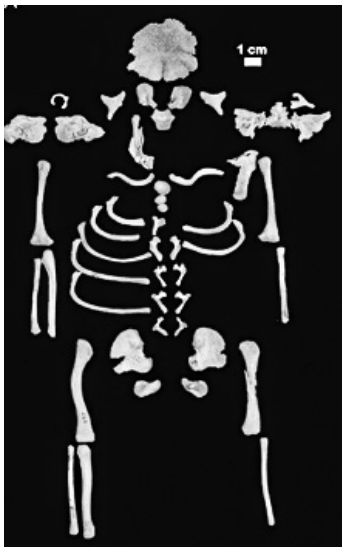

Figure 3.14. Bowing of long bones associated with OI (Adapted from Cope and Dupras 2011: 193).

3.6.2 Archaeological examples of OI

There have been several documented archaeological cases of OI. One such case is a fetal skeleton from the Dakleh Oasis, Egypt, associated with the Romano-Byzantine period and thought to date to 1900–1500 cal B.P. (Cope and Dupras 2011). The remains have been given an age estimate of 38 weeks in utero (Cope and Dupras 2011). This individual's bone was very brittle and light beige in colour which differed from the appearance for other fetal skeletons found at the site. This individual also had an exaggerated anterolateral curvature to their long bones, except for the humeri which were bent posterolaterally. Aside from bowing, this individual had a barrel-shaped rib cage which resulted from abnormally curved thin ribs. There were also fractures present in the remains, although the authors state that it is not possible to determine the timing of these due to the condition of the remains. Metaphyseal cortical development was compromised as the metaphyseal surfaces were uneven. With all these features in mind, especially the bowing and brittleness of the bone, the researchers determined OI to be the most appropriate differential diagnosis (Cope and Dupras 2011). Additionally, there are other potential cases of OI at this site (Sheldrick 1980), which may provide insight into the health of the community. While this case occurs later in the archaeological record than the occupation of Seh Gabi, it does demonstrate that OI did occur in antiquity and is a MBD that should be considered in a differential diagnosis.

3.7 Context in Differential Diagnosis

Between these different metabolic bone diseases, there is overlap of skeletal indicators which may be seen in the archaeological record. A table representing all the skeletal indicators of each metabolic bone disease is located below (Table 3.1). A second table representing all the radiographic indicators is located below (Table 3.2). With an appreciation for this overlap, there can be better possible diagnoses given. All skeletal elements present, and their associated lesions must be considered. If an individual has a lesion which is associated with multiple diseases, it is important to consider what the other lesions present on remains are associated with. As well, archaeological, historical, climatic, geographical, and cultural information must also be taken into consideration for disease applicability. This approach should then be matched with the most plausible, and most comparable disease description(s). It is not always possible to narrow it down to a singular disease as the cause but rather multiple possibilities whether that be due to

atypical presentation, non-specific lesions, or other reasons. Potential diseases are then listed in order of greatest likelihood for consideration. A thorough differential diagnosis will lead to a better overall understanding of past people's lives, estimating population health, and other archaeological parameters and questions. This could include ideas around origins of agriculture, subsistence strategies, warfare, trade, and climate change. While we will never have a complete and full picture of the past, this approach takes us one step closer. Given this, the possible cultural contexts in Iran will be discussed to provide context for the skeletal lesions which may be observed within the Seh Gabi sample.

Table 3.1. *Macroscopic Skeletal Indicators of Each Metabolic Bone Disease.*

	Scurvy	**Rickets**	**Anaemia**	**Fluorosis**	**Hyperostosis**	**OI**
General Skeleton	○ Irregular & spongy new bone formation	○ General porosity ○ Abnormal growth plates	○ Porosity ○ Osteopenia (Thal.) ○ Large bony masses (Thal.)	○ Diffuse osteosclerosis of the appendicular & axial skeleton ○ Increased cortical & trabecular thickness ○ Periosteal thickening ○ Calcified ligaments, tendons, cartilage, & inter-osseous membrane-s ○ Bony exostoses at ligament & muscle attachment zones	○ Increased weight of bones ○ Increased thickness of cortical bone ○ A lot of subperiosteal new bone formation	○ Lightness/fragility to bones ○ Fractures ○ Osteoporosis
Orbits	○ Cribra orbitalia ○ Porosity	○ Orbital roof porosity	○ Cribra orbitalia ○ Thinning of trabecular & cortical bone ○ Widening interorbital space (Thal.)			○ Elongated orbits
Cranium	Porosity on: - the greater sphenoid wing - cranial bones - facial bones - palate - basiocciput	- Frontal bone bossing - Deformed mandibular ramus	- Cranial vault porosity - Thickening of the sphenoid, maxillae, & zygomatics (Thal.) - Obliterated sutures in the cranium (Thal.)		- A lot of subperiosteal new bone formation, most commonly on facial bones (Caffey's) - Osteal bulges - Irregular thickening of internal surface of frontal bone while external surface looks normal (IFH)	- Expanded cranial vault
Dentition			- Protruding upper incisors & overbite (Thal.)	- Linear enamel hypoplasia - Brown, dis-coloured teeth, & mottled enamel		- Dentinogenesis imperfecta
Vertebral Column			- Perforations in the cortical bone of vertebrae			
Thorax		- Rib flaring	- Slight expansion of the ribs - Perforated cortical bone in ribs (Thal.) - Linear striations on the ribs (Thal.)		- A lot of subperiosteal new bone formation, most commonly on ribs	

	Scurvy	Rickets	Anaemia	Fluorosis	Hyperostosis	OI
Arms	Porosity on: - the scapulae - metaphyses of long bones	- Porosity in concave curvature of long bones - Long bone thickening & bowing - Long bone metaphyseal flaring	- Long bone porosity - Thinning of trabecular & cortical bone - Perforated cortical bone in long bones (Thal.) - Necrosis of the humeral head (SCA)			- Long bone bowing with cortical thickening - Narrowing of long bone diaphyses in comparison to their length
Hands						
Pelvis		- Ilium concavity				
Legs	Porosity on: - Metaphyses of long bones	- Porosity in concave curvature of long bones - Long bone thickening & bowing - Long bone metaphyseal flaring	- Long bone porosity - Thinning of trabecular & cortical bone - Perforated cortical bone in long bones (Thal.) - Exaggerated sulci on femora & tibiae (Thal.) - Necrosis of the femoral head (SCA)			- Long bone bowing with cortical thickening - Narrowing of long bone diaphyses in comparison to their length
Feet			- Hyper-trophic meta-carpals & phalanges (Thal.)			

Table 3.2. *Radiographic Indicators of Each Metabolic Bone Disease.*

	Scurvy	Rickets	Anaemia	Fluorosis	Hyperostosis	OI
General Skeleton	- Generalized osteopenia	- Generalized osteopenia - Thick cortex - Sharp cortical outline	- Thinning of cortical bone			
Cranium			- Hair-on-end appearance cranium - Undeveloped sinuses			
Dentition						
Vertebral Column			- Reduced number of trabeculae in vertebrae			
Thorax		- Loss of integrity in sternal rib ends				
Arms	- Long bone cortical thinning - Metaphyseal fractures - White line of Fraenkel - Wimberger's ring - Pelkan's spurs	- Long bone cortical thinning - Metaphyseal fractures - Metaphyseal trabecular coarsening - Fraying of epiphyses - Distinction at the end of the epiphysis	- Infarcts in long bones - Reduced number of trabeculae in long bones			- Zebra stripe
Hands						
Pelvis						
Legs	- Long bone cortical thinning - Metaphyseal fractures - White line of Fraenkel - Wimberger's ring - Pelkan's spurs	- Long bone cortical thinning - Metaphyseal fractures - Fraying of epiphyses - Distinction at the end of the epiphysis	- Infarcts in long bones - Reduced number of trabeculae in long bones			- Zebra stripe
Feet						

3.8 Epidemiology in Modern Iran

Epidemiology is the study of the distribution of diseases, as well as the determinants of health within a given population (Public Health Ontario 2022). When it comes to vitamin C deficiency, or scurvy, in modern Iran, there is not enough research published in European languages to have a complete picture of the epidemiology. However, using literature on scurvy in the neighbouring nations of Afghanistan and Pakistan as well as studies of nutrition and diet, an approximation can be made. Afghanistan and Pakistan are used as a proxy since these countries have mountainous regions which have the same altitude and climate as Iran, as well as encompassing the collision site of the Arabian/Indian plates with the Eurasian plate, as Iran does. The arid landscape in these countries is similar to that of Iran (Hole 2007). Eastern Turkey is also similar geographically and climatically (Hole 2007), but the published literature reflects case studies rather than population assessments (Bursalli et al. 2009; Küçükaydin et al. 2018). Scurvy outbreaks often occur in Afghanistan (Assefa et al. 2001; Bagchi 2008; Cheung et al. 2003). For example, there was an epidemic of scurvy in the mountainous regions of Afghanistan which may be related to a typical Afghan diet which is mostly bread (Cheung et al. 2003). In these mountainous regions there is little to no consumption of fruits and vegetables during the winter, which is related to reduced produce availability. Food insecurity (Cheung et al. 2003) and acute malnutrition (Assefa et al. 2001) are also factors in Afghanistan. In Pakistan people are also susceptible to malnutrition and scurvy due to seasonality, the increasing temperatures associated with climate change, and poverty (Bagchi 2008; Malik et al. 2012). These factors combined with the elevated risk of scurvy in developing countries (Cheah et al. 2020), and the high prevalence of malnutrition in Iran (Motedayen et al. 2019; Sarraf et al. 2005), suggests that modern Iranians are very likely at risk of scurvy.

However, the context of the modern Iranian diet must also be taken into consideration. A limited diet breadth contributes to the development of scurvy (Hahn et al. 2019), and Iran has a history of famine and food scarcity (Afkhami 2019; Kazemi 2016). Fresh and frugal were words that symbolized the meaning of food in traditional Iranian society (Matthee 2016). However, after 1970 in the more urban areas there was a switch in dietary practices to mirror that of the United States of America — large amounts of white rice, meats, sugar, with few vegetables and fruits being consumed (Floor 2021). But it is important to note that there are regional differences in diet (Floor 2021). Diet in more rural areas is more basic (Matthee 2016), containing sufficient

calories but lacking in protein and vitamins (Floor 2021). This suggests that if the diet is lacking in protein and vitamins scurvy could very well be present in populations within Iran, particularly in rural areas, such as the Kangavar Valley where Seh Gabi is located. Fruit and vegetable consumption appears to be more seasonal as the lowest levels of vitamin C intake occur during autumn (Toorang et al. 2013). This holds true especially in the mountainous and rural areas. Higher amounts of citrus were consumed in the winter, causing a higher level of vitamin C intake in the winter than in the fall (Toorang et al. 2013). This aligns with the Iranian citrus harvest occurring throughout the months of October to February (IFP Editorial Staff 2021). Additionally, there is a high level of consumption of vegetables during the summer while this is low during the winter (Toorang et al. 2013). Both canned fruit and vegetables are consumed throughout the year, but both at the lowest rate during the winter. Canned produce would not have been available to populations in the past (Toorang et al. 2013). For example, the diet of the Qashq'ai, a group in a rural area of the Fars province, varies substantially with seasonal availability of food (Sarraf et al. 2005). During the winter, the Qashq'ai rely on grains and beans as their dietary staples with minimal fruit, meat, and dairy supplementation (Sarraf et al. 2005).

In modern-day Iran, there is seasonality to diet which may differ to the seasonality seen in the past due to globalization and an increased likelihood of having access to fresh fruit and vegetables in the cold months. Seh Gabi is located in the Kermanshah province, which neighbours the Fars province mentioned above, which may have had similar patterns to this modern rural group due to geographical similarities of the areas. With the factors of local rural differences in diet, seasonal variability of diet, composition of modern diet, and scurvy being a problem in geographically related countries, the inference that scurvy may be a problem in modern Iran is entirely reasonable. This suggests the people of the Central Zagros could also have been at risk for development of scurvy as early as the Late Neolithic and Early Chalcolithic.

Vitamin D deficiency (VDD) is a common medical condition (Hovsepian et al. 2011) that has been estimated to afflict more than 1 billion people worldwide (Amrein et al. 2020; Hochberg and Hochberg 2019; Robinowitz 2009; World Medical Association 2017). Contrary to popular belief, rickets was widespread at least 2000 years before the Industrial Revolution (Mays et al. 2018). The highest levels of VDD are reported in some of the sunniest places, like South Asia and the Middle East (Mithal et al. 2009) and in the associated countries of Afghanistan,

Pakistan, and Turkey, VDD is a known problem (Majeed et al. 2007; Manaseki-Holland et al. 2008; Pettifor 2008; Özkan et al. 2009; Özkan 2010a, 2010b; Thacher et al. 2006). Rickets due to VDD is also a common disorder in Iran (Jokar et al. 2008; Mithal et al. 2009; Vatandost et al. 2018), even in sunny regions (Hovsepian et al. 2011). The prevalence of VDD is especially high amongst women and children (Badfar et al. 2017; Hovsepian et al. 2011; Jazayeri et al. 2018) as they tend to spend much more time indoors than men do in Middle Eastern cultural groups (Baroncelli et al. 2008; Jokar et al. 2008; Kazemi et al. 2009). Reasons for this may be directly related to cultural practices that limit exposure to UVB radiation, such as wearing concealing clothing (Hatun et al. 2005) and sun avoidance in hotter climates (Mithal et al. 2009). For example, women who wear a veil for cultural or religious reasons have lower levels of vitamin D and a higher prevalence of VDD (El-Hajj Fuleihan et al. 2006; Mithal et al. 2009). In modern-day Iran, long sleeves and a veil are required by law for women (Hovsepian et al. 2011). While there may be regional differences, the limiting of outdoor activities for women and girls no doubt contributes to this trend (Mithal et al. 2009). As we do not have information about clothing customs and cultural practices regarding time spent indoors in the Late Neolithic and Early Chalcolithic, this cannot be directly tied to the Seh Gabi population.

The practice of prolonged breast-feeding without vitamin D supplementation in the Middle East is likely another contributing factor (Baroncelli et al. 2008). These factors are echoed in Afghanistan, Pakistan, and Turkey (Dawodu et al. 2003; Majeed et al. 2007; Manaseki-Holland et al. 2008; Özkan et al. 2009; Özkan 2010a). The consumption of food sources which contain vitamin D, like egg yolks, and fatty fish in Iranian women and children is low (Delavari et al. 2009). The pooled prevalence of VDD in Iranian children is estimated to be 60.1% (Tabrizi et al. 2018), and up to 70% of adolescent girls in Iran (Moussavi et al. 2005). It was also found through a meta-analysis of published studies that 56.4% of under 20-year-olds in Iran had VDD (Vatandost et al. 2018).

Time of onset of VDD varies with the season. Spring has been found to be the most common time for onset of VDD whereas fall was the least common (Jokar et al. 2008) and in the summer, acute malnutrition or wasting in young children is the greatest (Rabiee and Geissler 1992). Most women who worked in agricultural settings ceased breast-feeding during the spring and summer because of their high workload, which along with high market prices, caused children to receive diluted milk (Rabiee and Geissler 1992). As indicated above, a child's

vitamin D status is directly related to quality of their mothers' milk and other kinds of milk they may receive. Additionally, if these children's diets were being supplemented with cereals, the phytic acid within those cereals could lessen calcium absorption (Jokar et al. 2008), thus further contributing to the possibility of VDD. It should be noted that different cereals contain different levels of phytic acid (Hídvégi and Lásztity 2002), so different cereal types could have differing impacts on calcium absorption. Rickets is also common amongst the children of families with low socioeconomic status (SES), especially in villages (Amirhakimi 1973). While related to SES and the ability to provide vitamin D rich foods, infants are traditionally kept out of the sunlight (Amirhakimi 1973). However, VDD does not just impact the children of rural settings but also those within an urban context. In cities like Tehran, rickets is a common disease amongst children (Salimpour 1975). In this study most of the children were undernourished, as well as living in homes which were high-walled and did not have a lot of sunlight (Salimpour 1975). The buildings at Seh Gabi did not have any windows (Hamlin 1973, 1974), and as such perhaps this pattern of VDD susceptibility may also be visible in the past.

Geographic and climatic factors can also influence the likelihood and occurrence of VDD. For example, the latitude of geographical location will affect the zenith angle of the sun, and as such the amount of ultraviolet B (UVB) radiation which is able to penetrate the ozone layer and reach the earth (Holick 2008; Mithal et al. 2009). Hence, people living closer to the equator will be exposed to more UVB radiation on an annual basis (Holick 2008; Mithal et al. 2009). As such, the reverse can also be inferred. The amount of cloud cover and altitude will also impact the amount of UVB radiation available (Brickley et al. 2014). Increases in altitude result in increases of UV radiation (Blumthaler et al. 1997). Seh Gabi is located at a higher altitude within the Zagros Mountains, so it is possible that at the time of occupation the amount of UVB radiation received by inhabitants was higher than those living at a lower altitude, thus possibly receiving more exposure to sunlight for vitamin D production at Seh Gabi.

Additionally, the amount of calcium and phosphorus which are bioavailable to individuals also plays a role. Adequate levels of both minerals are needed to prevent metabolic bone disease and to allow for the interactions between vitamin D, phosphorus, and calcium (Lips 2012). Diarrhea is common amongst the children of Tehran, which may impair calcium absorption, furthering the problem of vitamin D deficiency (Salimpour 1975). Vitamin D deficiency is common in modern Iran for a variety of reasons, including those of cultural basis.

It is also possible that VCD and VDD can be comorbid (Barlow 1883; Schattmann et al. 2016) but literature discussing the epidemiology of comorbidity in Iran was not found to be sufficient to make a statement. However, it has been shown in bioarchaeology studies (e.g., Schattmann et al. 2016) and clinical literature (e.g., Barlow 1883) that comorbidity is possible (Fig. 3.15). For example, in child burials (110 to 81 cal B.P.) associated with the area of Bethnal Green, London, England (Ives 2018), which was very poor and crowded at that time, 21.4% of children had rickets and 12.3% of those children with rickets also had scurvy (Ives 2018).

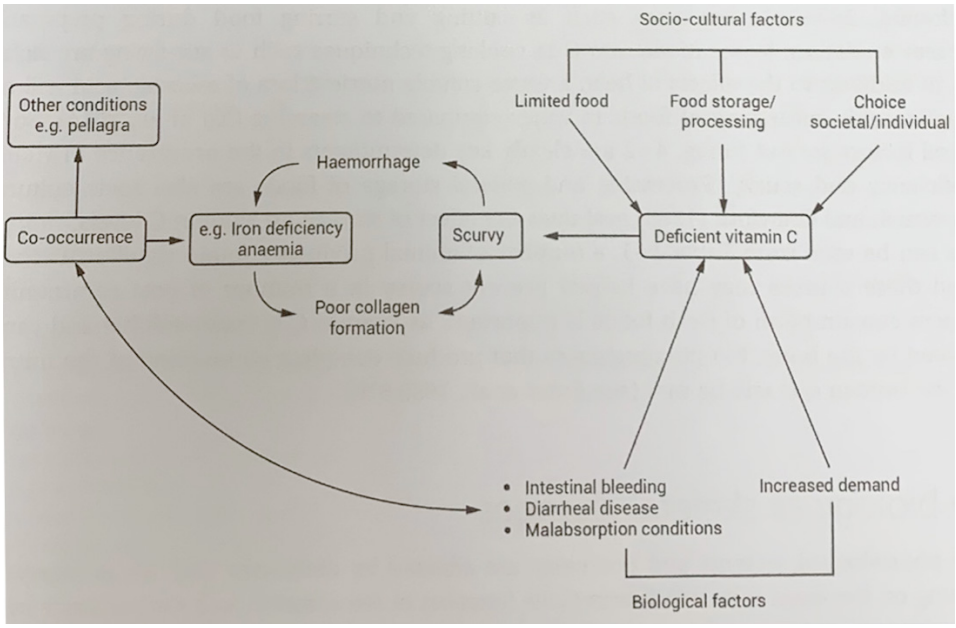

Figure 3.15. Pathway of how comorbidity may develop (Adapted from Brickley et al. 2020a: 45).

3.9 Conclusion

This detailed examination of VCD and VDD, and their influencing factors, along with anaemia, fluorosis, hyperostosis, and osteogenesis imperfecta will play a key role in the understanding of any lesions present within the Seh Gabi skeletal sample. Each of these diseases are included due to the archaeological context of Seh Gabi. Additionally, it is possible that the location of Seh Gabi and its cultural practices could have contributed to the presence of vitamin deficiencies, if any are present. The discussion of anaemia, fluorosis, hyperostosis, and osteogenesis imperfecta will also inform understanding any lesions within this skeletal sample as these diseases have been seen in juvenile populations in antiquity.

Chapter 4: Materials & Methods

4.1 Materials

Thirty-two non-adult skeletons excavated from the site of Seh Gabi and were analyzed for this thesis. Each burial had previously been assigned a number and have been assessed according to that number. Every individual has an associated burial sheet, skeletal inventory, and in most cases, radiographs.

All analyses, as indicated in this thesis, were completed at Lakehead University, Thunder Bay Campus. All photography of skeletal elements and radiographs was completed using a Canon EOS Rebel T2i camera. Radiographs were placed on a light box for photography.

4.2 Age Estimation

The age ranges for individuals in this population were primarily based on dental development and eruption. Table 4.1, below on p. 59–60, gives the age ranges for individuals included. Dental development and eruption was the preferred method of age estimation as it is less susceptible to environmental pressures on growth than other skeletal areas (Conceição and Cardoso 2011; Office of the Surgeon General 2004). The Atlas of Human Tooth Development and Eruption (AlQahtani et al. 2010) was used in conjunction with raw observational data (Merrett 2006) for dental ages, both of which are based on the Moorrees et al. (1963) criteria. Cross-striation ages (which should be considered a minimum age estimate, Merrett 2018), where available, are noted within the table.

If raw dental observational data were not available, then a skeletal age range was used, as indicated in the notes within the table. This skeletal age range was based upon cranial development first, if data were available. Where applicable, specific cranial elements used for the age range are identified within the notes column of Table 4.1. The cranial development age ranges presented within this thesis were based upon Merrett's raw observational data (2006) and the descriptions of cranial development and associated ages within Schaefer, Black and Scheuer's (2009) Field Manual. The ages identified within the Field Manual (2009) and their associated stages of cranial development are based on several primary sources (Fazekas and Kósa 1978; Madeline and Elster 1995; Molleson and Cox 1993; Redfield 1970; Tillman and Lorenz 1978).

When neither dental or cranial development data were available, an age range based on long bone length or girdle size raw observational data (Merrett 2006) was completed. The equations for long bone ages were taken from Scheuer and Black (2000 p. 288, 297, 307, 394, 415), adapted from Scheuer et al. (1980). Girdle size ages were also taken from Scheuer and Black (2000 p. 271, 373), adapted from Fazekas and Kósa (1978).

While the majority of individuals have an age estimation of under one year old, there are two children (SG29 [2.5 to 5.5 years old] and SG30 [3.5 to 7.5 years old]) and one adolescent individual (SG32 [16.5 to 18.5 years old]). Additionally, SG31 was comprised of one skeletal element (a clavicle), and no age estimate was possible.

Table 4.1. *Age Estimates for Seh Gabi Subadults.*

Individual	Age	Note
SG1	1.5 to 10.5 mo	A cross-striation age of 13.5 wks post-partum was available for this individual [a], which falls within the age range presented in this table.
SG2	3 to 6 mo	Based on long bone lengths [b, c, d] (left humerus, radius, ulna, tibia, fibula, and right femur [e]). Pectoral girdle size provides a broader age estimate of 4 to 9 mo [f, g] (left ilium width and length [e]).
SG3	1.5 to 4.5 mo	
SG4	1.5 to 3.5 yrs	A cross-striation of 71 wks post-partum was available for this individual [a], which falls within the younger end of the age range presented in this table.
SG5	32 to 36 wks in utero	Both long bone length [c, h, i] (right radius, right ulna, and left humerus were present and measured [e]) and pelvic girdle size [j] (ilium present and measured [e]) indicate this age range.
SG6	38 wks in utero to 1.5 mo	
SG7	38 wks in utero to 4.5 mo	A cross-striation age of 14.5 wks post-partum was available for this individual [a], which falls within the age range presented within this table.
SG8	1.5 to 7.5 mo	
SG9	Birth to 4.5 mo	A cross-striation age of 21 wks post-partum was available for this individual [a], which falls within the age range presented within this table.
SG10	1.5 to 7.5 mo	
SG11	1.5 to 7.5 mo	A cross-striation age of 15 wks post-partum was available for this individual [a], which falls within the age range presented within this table.
SG12	1.5 to 7.5 mo	
SG13	4.5 mo ±3 mo	
SG14	4.5 to 7.5 mo	
SG15	4.5 to 7.5 mo	A cross-striation age of 23 wks post-partum was available for this individual [a], which falls within the age range presented within this table.

Individual	Age	Note
SG16	4.5 to 10.5 mo	A cross-striation age of 25 wks post-partum was available for this individual [a], which falls within the age range presented within this table.
SG17	10 to 12 mo	Based on pelvic girdle size [f, g, j]. This individual's ilium was present and length was measured [e].
SG18	30 to 36 wks in utero	Both long bone length [b] (right humerus length and width [e]) and pectoral girdle size [k] (right scapular length and width [d]) indicate this age range.
SG19	1 to 9 mo	Based on cranial development [l] (foramen ovale, body to the lesser wings of sphenoid, greater wings to the body of the sphenoid, petromastoid to squamotympanic of the temporal, all occipital features mentioned, metopic suture, and mandibular symphysis were assessed [e]).
SG20	34 wks in utero to birth	
SG21	38 wks in utero to 1.5 mo	A cross-striation age of 12 wks post-partum was available for this individual [a], which falls outside the age range presented within this table.
SG22	38 wks in utero to 4.5 mo	
SG23	34 wks in utero to 4.5 mo	
SG24	38 to 43 wks	Based on long bone length equations [c, h] (right ulna and right radius present and measured [e]).
SG25	4.5 to 7.5 mo	
SG26	4.5 to 10.5 mo	
SG27	4.5 to 7.5 mo	
SG28	7.5 mo to 1.5 yrs	

Table 4.1 Legend
mo = months
yrs = years
[a] Merrett 2018
[b] Scheuer and Black 2000:289
[c] Scheuer and Black 2000:307
[d] Scheuer and Black 2000:298, 394, 415, 426
[e] Merrett 2006
[f] Molleson and Cox 1993
[g] Schaefer et al. 2009
[h] Scheuer and Black 2000:297
[i] Scheuer and Black 2000:288
[j] Scheuer and Black 2000:373
[k] Scheuer and Black 2000:270
[l] Schaefer et al. 2009:353.

4.3 Macroscopic Analysis

All available elements for each individual were assessed macroscopically for any possible lesions. A lesion is an area on the bone that demonstrates appearance beyond the range of normal. Potential lesions were compared to other individuals within the sample to check whether the morphology seen were normal or pathological. Comparisons were also made to published material on the normal development of subadult skeletons (e.g., Scheuer and Black 2000). For example, the presence of subperiosteal new bone formation (SPNB) and porosity that were beyond expectations for normative morphology would be considered a lesion. Possible lesions were then examined under a Wolfe 906187 dissecting microscope at a magnification of 40x. Based on the morphology of a lesion's edges and comparison with others in the population, a decision was made regarding whether the lesion was active or not. To be considered active, the lesion would need to have bony appearance which was not finished remodelling (DeWitte 2014). The lesion was recorded in an observation chart that reflected the skeletal area and individual (Appendix A, Table A.1.). If radiographs were available, they were assessed for radiological signs that could indicate possible metabolic bone disease (see Chapter 3, p. 51). From these observations, in conjunction with pertinent contextual information (e.g., geographic location and diet), possible causes of the lesions were considered.

A pathology table for each person which compared all the possible lesions associated with possible metabolic bone diseases was completed; a blank version of this pathology table is provided as Table 3.1 in Chapter 3 (p. 49–50). The completed table for each person is provided in Appendix B, along with a brief description of any lesions and the possible metabolic bone diseases that may be associated with them. The number of lesions an individual exhibited and the pattern of their distribution of the lesions were considered in the differential diagnosis (see Chapter 3, p. 21–22). The closer the fit to what is known to present in a particular disease process was taken as stronger evidence for the final diagnosis.

4.4 Statistical Analyses

Prevalence for lesions are based on the number of individuals who demonstrate a lesion divided by the number of individuals who had that skeletal element present (given in Chapter 5). The individuals were arranged in two age groups: under the age of six months, and over the age

of six months. Given that age estimates are a range, the midpoint of the range was taken for each individual for the purposes of these groupings. Under the age of six months, lesions seen in an infant are more likely to be tied to a mother's nutritional status while they were pregnant, whereas over the age of six months, lesions are more likely to have developed after birth and be tied directly to the infant's diet and health (Algahtani 2010; Brickley and Mays 2019; Brickley et al. 2014; Fain 2005; Maghbooli et al. 2007; Maiyegun et al. 2002; Mays 2008).

Individuals SG29, SG30, and SG32 were removed from the statistical tests because they were much older in age than the other individuals, and as such are considered exclusions. SG31 was also removed from statistical tests as it is represented by only one bone, and as such there was not enough skeletal remains present for assessment. An individual needed at least three separate skeletal elements present for assessment to be included for analysis. The removal of these four individuals from statistical analyses reduced the sample size to 28.

If there were lesions which were repeatedly seen among the sample, they were considered to be a common lesion. A Fisher's Exact Test (in SPSS [Version 29.0.2.0]) was then done for each common lesion to see if there was a significant difference between the two age groups. A Fisher's Exact Test is the most appropriate given that this is a small, nominal data set.

Chapter 5: Results

5.1 Assessment of Pathology

All observations of pathology for individuals in this population can be found in Table A.1. within Appendix A including the type of lesions observed (e.g., porosity and subperiosteal new bone formation), the location, and the distribution of lesions present in each individual. In this chapter, the most common lesions within the population are given, and are divided by type of appearance (i.e., subperiosteal new bone formation, porosity). Additionally, a category to represent other types of pathology is included, which includes long bone bowing, dental changes (e.g., linear enamel hypoplasia), and other cranial changes.

5.2 Common Areas of Porotic Lesions within the Seh Gabi Population

5.2.1 Porosity on the ectocranial surface of the cranial vault

In this population, 23 individuals had cranial vault remains present. Of those 23 subadults, only three demonstrated cranial vault porosity on the ectocranial surface (13%, N=3/23) (Table 5.1). In two of these three individuals this porosity occurs on the temporals while in the third individual it occurs on unidentifiable cranial vault fragments. There is no significant difference between those under the age of six months and those over the age of six months (Fisher's Exact Test, p=1.000).

Age Group	Absent	Present	Total
<6 months	12	2	14
≥6 months	8	1	9

Table 5.1. Frequency of cranial vault porosity on the ectocranial surface by age group.

5.2.2 Porosity on the endocranial surface of the cranial vault

Twenty-three individuals had cranial vault remains present for assessment. Of these, only one individual demonstrated porosity on the endocranial surface (4.3%, N=1/23) (Table 5.2). This porosity occurs on this individual's temporal, and this individual is represented within the porosity on the ectocranial surface group as well. There is no significant difference between the two age groups tested (Fisher's Exact Test, p= 1.000).

Age Group	Absent	Present	Total
<6 months	13	1	14
≥6 months	9	0	9

Table 5.2. Frequency of cranial vault porosity on the endocranial surface by age group.

5.2.3 Orbital roof porosity

Of the 28 individuals included for statistical testing, 21 had an orbital roof present for assessment. Of these 21 subadults, nine showed orbital roof porosity (42.9%, N=9/21) (Table 5.3). An example of this type of lesion can be seen in Figure 5.1. There is a significant difference between the two age groups (Fisher's Exact Test, p=0.032), with more individuals having this lesion in the over six months old age group.

Figure 5.1. Endocranial surface of the right frontal of SG12, demonstrating the right orbital porosity (arrow). 1 cm scale bar.

Age Group	Absent	Present	Total
<6 months	10	3	13
≥6 months	2	6	8

Table 5.3. Frequency of orbital roof porosity by age group.

5.2.4 Maxillary palate porosity

Fourteen individuals had at least a partial maxillary palate present for assessment. Of these 14 individuals, six individuals presented with palate porosity on the palatine process (42.6%, N=6/14) (Table 5.4). There is no significant difference in the prevalence of maxillary palate porosity in the two age groups (Fisher's Exact Test, p=1.000).

Age Group	Absent	Present	Total
<6 months	5	4	9
≥6 months	3	2	5

Table 5.4. Frequency of maxillary palate porosity by age group.

5.2.5 Scapular supraspinous fossa porosity

Twenty-three individuals had this portion of the scapula present, and of those 23, one individual had the lesion present (4.3%, N=1/23) (Table 5.5). There is no significant difference in the prevalence of this lesion between the two age groups under comparison (Fisher's Exact Test, p=1.000).

Age Group	Absent	Present	Total
<6 months	13	1	14
≥6 months	9	0	9

Table 5.5. Frequency of porosity on the scapular supraspinous fossa by age group.

5.3 Common Areas of Subperiosteal New Bone Formation (SPNB) Lesions within the Seh Gabi Population

5.3.1 SPNB on the orbital roof

Of the 28 individuals from Seh Gabi, 21 had an orbital roof present for assessment. Four of the individuals demonstrated SPNB on their orbital roof (19%, N=4/21) (Table 5.6). An example of this SPNB can be seen in Figure 5.2. There is no significant difference in the prevalence of orbital roof SPNB between the two age groups (Fisher's Exact Test, p=0.618).

Age Group	Absent	Present	Total
<6 months	11	2	13
≥6 months	6	2	8

Table 5.6. Frequency of SPNB on the orbital roof by age group.

Figure 5.2. Anterior view of SPNB (arrow) in the right orbital roof of SG9. 1 cm scale bar.

5.3.2 SPNB on the diaphyses of both upper and lower limbs

Twenty-five individuals had upper and lower limbs present for assessment. To be included in this count an individual needed to have a total count of at least three upper and lower limbs present with a diaphysis (e.g., one humerus and two femora, or two humeri and one femur, etc.). Upper and lower limbs are grouped together to

Age Group	Absent	Present	Total
<6 months	15	1	16
≥6 months	9	0	9

Table 5.7. Frequency of SPNB on the diaphyses of the upper/lower limbs by age group.

be consistent with other studies (e.g., Eggington et al. 2024). Of these 25 individuals, only one subadult showed SPNB on the diaphyses of both their upper and lower limbs (4.0%, N=1/25) (Table 5.7). There is no significant difference between the two age groups (Fisher's Exact Test, p=1.000).

5.4 Common SPNB Lesions with Porosity within the Seh Gabi Population

5.4.1 Location of porosity with SPNB observed

5.4.1.1 Ectocranial cranial vault SPNB with porosity.

Twenty-three individuals had cranial vault remains present for assessment. Seven of these 23 individuals displayed SPNB with porosity (30.4%, N=7/23) (Table 5.8). There is no significant difference in the prevalence of cranial vault SPNB and porosity (Fisher's Exact Test, p=1.000).

Age Group	Absent	Present	Total
<6 months	10	4	14
≥6 months	6	3	9

Table 5.8. Frequency of cranial vault SPNB and porosity by age group.

5.4.1.2 SPNB/porosity on the greater wing of the sphenoid.

Only 17 individuals had a greater wing of the sphenoid present for assessment. Of these 17 individuals, two had both SPNB and porosity present on the inner table (11.8%, N=2/17) (Table 5.9). There is no significant difference in the prevalence of this SPNB/porosity between the two age groups tested (Fisher's Exact Test, p=1.000).

Age Group	Absent	Present	Total
<6 months	10	2	12
≥6 months	5	0	5

Table 5.9. Frequency of SPNB and porosity on the greater wing of the sphenoid by age group.

5.4.1.3 SPNB and porosity on the orbital roof.

Of the 28 individuals in this population, 21 had an orbital roof present for assessment. Three of these 21 individuals had both SPNB and porosity present in their orbital roof (14.3%, N=3/21) (Table 5.10). These three individuals are also represented within the sections on both orbital roof porosity (5.2.3) and orbital roof SPNB (5.3.1) as individuals with those lesions. An example of SPNB and porosity together can be seen in Figure 5.3. There is no significant difference between those under six months old, and those over six months (Fisher's Exact Test, p=0.531).

Age Group	Absent	Present	Total
<6 months	12	1	13
≥6 months	6	2	8

Table 5.10. Frequency of SPNB and porosity in the orbital roof by age group.

Figure 5.3. Anterior view of the right orbit of SG25, showing orbital porosity and subperiosteal new bone formation (arrow), 1 cm scale bar.

5.4.1.4 SPNB and porosity on the posterior aspect of the maxilla (maxillary tuber).

Thirteen individuals within this population had the posterior aspect of the maxilla present for assessment, and of these 13, two had evidence of SPNB and porosity on this element (15.4%, N=2/13) (Table 5.11). There is no

Age Group	Absent	Present	Total
<6 months	7	2	9
≥6 months	4	0	4

Table 5.11. Frequency of SPNB and porosity on the posterior aspect of the maxilla by age group.

significant difference in the prevalence of this lesion amongst the two age groups compared (Fisher's Exact Test, p=1.000).

5.4.1.5 SPNB and porosity around the infraorbital foramen of the maxilla.

Fifteen of the individuals had the portion of their maxilla with the infraorbital foramen intact for assessment. Of these 15 subadults, one had SPNB and porosity on that area (6.7%, N=1/15) (Table 5.12). There is no significant difference between the two age groups which were assessed (Fisher's Exact Test, p=1.000).

Age Group	Absent	Present	Total
<6 months	8	1	9
≥6 months	6	0	6

Table 5.12. Frequency of SPNB/porosity on the infraorbital foramen of the maxilla by age group.

5.4.1.6 SPNB and porosity on the infraspinous fossa of the scapula.

Twenty-three individuals had this portion of the scapula present for assessment. Of these 23, two individuals had the lesions present (8.7%, N=2/23) (Table 5.13). There is no significant difference between the two age groups (Fisher's Exact Test, p=1.000).

Age Group	Absent	Present	Total
<6 months	13	1	14
≥6 months	8	1	9

Table 5.13. Frequency of SPNB/porosity on the scapular infraspinous fossa by age group.

5.5 Other Pathologies Noted

5.5.1 Long bone metaphyseal flaring of the upper and lower limbs

Twenty-five individuals had upper and lower limbs present for assessment. As mentioned in section 5.3.2, a combination of at least three upper and lower limb long bones with a metaphysis present were required (e.g., one humerus and two femora) for assessment. Only one individual showed metaphyseal flaring in their upper and lower limbs (4.0%, N=1/25) (Table 5.14). There is no significant difference between the two age groups assessed (Fisher's Exact Test, p=0.360). There were no individuals who had metaphyseal flaring in only their upper or lower limbs, when multiple upper or lower limb bones were present for assessment.

Age Group	Absent	Present	Total
<6 months	16	0	16
≥6 months	8	1	9

Table 5.14. Frequency of metaphyseal flaring of the upper/lower limbs by age group.

5.5.2 Dental pathology

Localized hypoplasia of the primary canine (LHPC), a non-specific indicator of stress, and enamel defects (missing spots of enamel) were common among the subadults of Seh Gabi. Two of the 28 individuals included for statistical analyses (SG7 and SG15) had LHPC present (7.1%, N=2/28). Six individuals had enamel defects present (SG3, SG7, SG14, SG22, SG23, SG27) which results in a prevalence of 21.4% (N=6/28). Linear enamel hypoplasia (LEH), another non-specific indicator of stress, was present in two of the older individuals who are not included in statistical analyses (SG29 and SG30). An example of Linear Enamel Hypoplasia (LEH) is shown in Figure 5.4.

Figure 5.4. Dentition of SG29, demonstrating multiple teeth affected by LEH (arrow), 1 cm scale bar.

5.5.3 Other pathologies

Additionally, three individuals showed evidence of a healed or healing clavicular fracture (SG12, SG16, SG23). Finally, one individual showed evidence of hydrocephalus (D.C. Merrett, pers. comm., 2022) due to the shape of their cranial bones and the associated cranial vault expansion (SG16).

5.6 Lesions Associated With MBD Which Are Not Visible On The Seh Gabi Subadults

5.6.1 Frontal bone bossing

In this population, 18 individuals had a large enough portion of their frontal bone present for the assessment of the presence of bossing. None demonstrated frontal bone bossing (0%).

5.6.2 SPNB on the lesser wings of the sphenoid

Fourteen individuals had the lesser wings of the sphenoid present for assessment. None of these individuals presented with this lesion (0%).

5.6.3 Maxillary/mandibular alveolar process SPNB/porosity

In this population sample, 22 individuals had a maxilla, mandible, or both present for assessment of this lesion. None of these individuals presented with this lesion (0%)

5.6.4 SPNB/porosity on the mental coronoid process of the mandible

Seventeen individuals in this population had this portion of their mandible present for assessment. In this group of 17, none presented with this lesion (0%).

5.6.5 Deformed mandibular ramus

Nineteen of the Seh Gabi subadults had a mandibular ramus present for assessment; none had evidence of a deformity (0%).

5.6.6 Porosity of the orbital surface of the zygomatic

Of the 28 individuals who make up this population sample, 20 had the orbital surface of the zygomatic present. None of these 20 individuals had this lesion (0%).

5.6.7 Rib changes

Twenty-six individuals had ribs present with their remains for assessment. None of these individuals demonstrated rib cupping or flaring (0%). There are two types of lesions that focus on the sternal ends of ribs which could be related to MBD. One of these is sternal rib end flaring, if cupped. Of the 26 individuals who had their sternal rib ends present, none showed evidence of this lesion (0%). Porosity on the sternal rib ends can also be associated with MBD. Again, of the 26 subadults who had sternal rib ends, none had porosity on that area (0%).

5.6.9 Rib deformity with a sharp angle

Twenty-six individuals in the Seh Gabi population had multiple ribs present for assessment. Of these 26 subadults, none displayed this type of lesion (0%).

5.6.10 Ilium porosity

Twenty-two individuals had an ilium present for assessment, and none had porosity present (0%).

5.6.11 Ilium concavity

In the Seh Gabi population, 22 individuals had an ilium present for assessment. Of these 22 individuals, none displayed this lesion (0%).

5.6.12 Deformed arm & leg bones with a clear bend

In the Seh Gabi population, 25 individuals had multiple arm and leg bones present for assessment. None of these 25 individuals had this lesion present (0%).

5.6.13 Abnormal distal growth plates

Twenty-six of the subadults from Seh Gabi had distal ends of long bones present for assessment, and of these 26 individuals, none demonstrated this lesion (0%).

5.6.14 Flattening of femoral metaphysis and coxa vara

Of the Seh Gabi individuals, only 24 had these femoral areas present for assessment. None of these 24 individuals showed evidence of this type of pathological lesion (0%).

5.6.15 Bilateral thickening of long bones

Of the 28 individuals associated with Seh Gabi, 24 had both right and left long bones. In this group of 24, none demonstrated this lesion (0%).

5.6.16 Long bone concave curvature porosity

Twenty-seven Seh Gabi subadults had a long bone present for the assessment of this lesion. None showed the lesion (0%).

5.6.17 Irregular & porous metaphyseal cortex of long bones

Twenty-five of the Seh Gabi subadult population had multiple long bones present with enough metaphyseal cortex for the assessment of lesion presence. None showed this lesion (0%).

5.8 Summary

A variety of lesions can be seen in the Seh Gabi population, the majority of which are changes represented by porosity and subperiosteal new bone formation (SPNB) on the cranial bones. There are also other signs of non-specific stress (LEH) in this population, including on individuals who were excluded from statistical testing. SG16 is a pathological outlier as they present with changes associated with hydrocephalus. To the data above a differential diagnosis (Chapter 6) was applied to assess what these lesions might mean and to better understand life at Seh Gabi.

Chapter 6: Discussion & Interpretations

6.1 Introduction

The cultural materials associated with Seh Gabi indicate a date range of about 7450 to 5450 cal B.P. (Hamlin 1973, 1974) while the radiocarbon dating of human skeletal remains are specifically tied to the period from 6850±50 cal B.P. to 5070±30 cal B.P. (Lazaridis et al. 2016; Narasimhan et al. 2019). The dates which are associated with the human skeletal remains themselves overlap with the Chalcolithic period in the Zagros; 7450 to 5150 cal B.P. (Matthews and Fazeli Nashli 2022). While the sample size for this population is small, especially when divided between mounds, the number of subadult individuals recovered from Seh Gabi is unique for this time period and region. This illustrates the importance of the assessment and resulting interpretations about the population. The focus of this study is on the presence or absence for skeletal evidence of vitamin deficiencies, using differential diagnosis, informing our understanding of diet and population health.

6.2 Differential Diagnosis

6.2.1 Lesions within the Seh Gabi skeletal population

Multiple areas of the skeleton had visible lesions on multiple individuals within the Seh Gabi sample. A summary of these lesions is provided in section 6.2.1.1 and 6.2.1.2 beginning with the cranium and then the infracranial skeleton. This is followed by a consideration of the possible causes.

6.2.1.1 Cranial lesions.

There were several types of cranial lesions seen in the Seh Gabi subadults. On the cranial vault, porosity could be seen on the ectocranial surface (13%; N=3/23) and the endocranial surface (4.3%; N=1/23) (see Appendix C, Tables C.1. and C.2. for complete list of individuals with this lesion, and others mentioned). This porosity can be associated with anaemia (Brickley et al. 2020b; Lewis 2012; Rinaldo et al. 2019; Sullivan 2005) and rickets (Mays et al. 2006; Ortner and Mays 1998). However, if the porosity on the ectocranial surface presents with subperiosteal new bone formation (SPNB with porosity: 30.4%; N=7/23) as well, then scurvy could have been present (Eggington et al. 2024; Geber and Murphy 2012).

If both SPNB and porosity are present on the greater wing of the sphenoid, this is considered to be a clear indicator of scurvy (Brown and Ortner 2011; Eggington et al. 2024; Geber and Murphy 2012; Klaus 2017; Ortner and Ericksen 1997; Schattmann et al. 2016; Snoddy et al. 2018) and has not been found in association with other metabolic bone diseases. The combination of SPNB and porosity on the greater wing of the sphenoid was visible in 11.8% (N=2/17) of the population sample for Seh Gabi.

On the orbital roofs, the presence of porosity was seen in 42.9% (N=9/21) of individuals. This type of lesion can be associated with scurvy (Brickley and Ives 2006; Mays 2008; Moore and Koon 2017; Ortner et al. 2001; Ortner and Ericksen 1997), rickets (Mays et al. 2006; Ortner and Mays 1998; Schattmann 2014), anaemia (Rinaldo et al. 2019), and pellagra (Brenton and Paine 2007). For this lesion to be tied to anaemia specifically, there must be evidence of thickened diploë representing marrow expansion (Brickley et al. 2020b), which was not observed in this population. Also seen in the orbital roof was the occurrence of SPNB (19%; N=4/21), which is typically associated with scurvy (Brown and Ortner 2011; Eggington et al. 2024; Klaus 2017; Snoddy et al. 2018). Three individuals (SG9, SG25, SG27) had both porosity and SPNB present in their orbital roof, 14.3% (N=3/21). These three individuals are represented within the separate groups of porosity in the orbital roof and SPNB in the orbital roof groups mentioned above.

Porosity was seen in 42.6% (N=6/14) of the individuals with the maxillary palate present for assessment, which is often associated with scurvy (Brown and Ortner 2011; Eggington et al. 2024; Ortner and Ericksen 1997). Also seen in the maxilla was subperiosteal new bone formation and porosity on the posterior aspect (15.4%; N=2/13), also typically linked to scurvy (Eggington et al. 2024; Geber and Murphy 2012; Klaus 2017; Ortner and Ericksen 1997; Schattmann et al. 2016; Snoddy et al. 2018). SPNB and porosity were present around the infraorbital foramen of the maxilla for 6.7% (N=1/15) of the sample. Again, this lesion combination is associated with scurvy and no other metabolic bone diseases (Brown and Ortner 2011; Eggington et al. 2024; Geber and Murphy 2012; Schattmann et al. 2016).

6.2.1.2 Infracranial lesions.

Porosity on the scapulae seen in the supraspinous fossa (4.3%; N=1/23) has been generally associated with scurvy (Brown and Ortner 2011; Eggington et al. 2024; Klaus 2017;

Schattmann et al. 2016; Snoddy et al. 2018). Porosity and SPNB of the scapular infraspinous fossa were seen in 8.7% (N=2/23) of the sample; this type of lesion is, again, typically related to scurvy (Brown and Ortner 2011; Eggington et al. 2024; Klaus 2017; Schattmann et al. 2016; Snoddy et al. 2018).

Subperiosteal new bone formation of the upper and lower limb diaphyses was seen on 4.0% (N=1/25) of the population sample. This lesion is often seen in scurvy cases (Eggington et al. 2024; Geber and Murphy 2012) and is not associated with other metabolic bone diseases.

Metaphyseal flaring of the upper and lower limbs was present in 4.0% (N=1/25) of the individuals. Typically, this lesion type is related to both scurvy (Eggington et al. 2024; Snoddy et al. 2018) and rickets (Mays et al. 2006; Schattmann 2014; Ortner and Mays 1998). However, it can also be linked to osteopetrosis when it is located at the proximal humerus, and distal femur and tibia (Beighton et al. 1977), which was not seen in the Seh Gabi individuals in association with metaphyseal flaring.

6.2.1.3 Patterning.

There are some areas of patterning within the lesions that were seen among the subadults of this population. Much of the patterning that can be seen has to do with porotic lesions. Of the individuals who had ectocranial vault porosity, one individual also had orbital roof porosity. Thus, 33% of the individuals with ectocranial vault porosity had orbital roof porosity (N=1/3) or 11% of individuals with orbital roof porosity had ectocranial vault porosity (N=1/9). Also, of the those with ectocranial vault porosity, two individuals also had maxillary palate porosity (66%; N=2/3), or, 33% of individuals with maxillary palate porosity also had ectocranial vault porosity (N=2/6). Of those six individuals with maxillary palate porosity, three individuals also had porosity present on an orbital roof (50%, N=3/6) or 33% of the individuals with orbital roof porosity also had maxillary palate porosity (N=3/9). Nine individuals had orbital roof porosity, one of whom also had porosity on their scapular supraspinous fossa (11%, N=1/9). This same individual also had maxillary palate porosity, meaning that of the six individuals with maxillary palate porosity one had scapular supraspinous fossa porosity (16.6%, N=1/6).

Some patterning can be seen in the lesions that focus on SPNB changes. There is overlap between the groups of SPNB in the orbital roof, and SPNB with porosity of the greater wing of the sphenoid. Of the four individuals who have SPNB in their orbital roof, one individual also

has SPNB and porosity on the greater wing of their sphenoid (25%, N=1/4). Only two individuals have SPNB and porosity on the greater wing of the sphenoid, meaning that 50% of this group present with SPNB in their orbital roof (N=1/2). Also, there is one individual who has SPNB on their long bones, also has SPNB on their ectocranial vault. This means that of the seven individuals with SPNB on their ectocranial vault 14.3% have SPNB on the long bone diaphyses (N=1/7).

There is also overlap between different SPNB associated with porosity lesions. Of the three individuals who have SPNB and porosity in their orbital roof, one also has SPNB and porosity on the posterior aspect of the maxilla (33%, N=1/3). This means that of the two individuals who have these changes on the posterior aspect of the maxilla (maxillary tuber), 50% also have orbital roof SPNB and porosity (N=1/2). Two individuals have SPNB and porosity on the greater wing of the sphenoid, and one of these individuals also has SPNB and porosity around the infraorbital foramen of their maxilla (50%, N=1/2). This individual (SG21) is the only one in the sample to have this lesion combination (SPNB and porosity around the infraorbital foramen of the maxilla). SG21 also has SPNB and porosity on the infraspinous fossa of their scapula, meaning that of the group with greater wing of the sphenoid changes, 50% have SPNB and porosity on this area of the scapula (N=1/2). Additionally, this means that 100% of the individuals with SPNB and porosity around the infraorbital foramen of the maxilla also have SPNB and porosity on the infraspinous fossa of the scapula. Thus, the most common lesion combinations are: ectocranial vault porosity with maxillary palate porosity, maxillary palate porosity and orbital roof porosity, SPNB and porosity on the greater wing of the sphenoid with SPNB in the orbital roof, posterior aspect of the maxilla changes with orbital roof SPNB and porosity, and SPNB and porosity on the greater wing of the sphenoid with SPNB and porosity around the infraorbital foramen of the maxilla.

6.2.1.4 What cause(s) should be considered most likely for the subadults of Seh Gabi?

Most lesions seen in this population occurred in the cranium. The most commonly noted lesions had possible links to anaemia, pellagra, and osteopetrosis however, the majority of those lesions are typically associated with scurvy and rickets. Anaemia is a factor that needs to be considered, especially when the probability of dietary stressors is high. But only two of the common lesions in this sample are associated with anaemia (orbital roof porosity and porosity on

the ectocranial surface of the cranial vault). Also, the orbital roof porosity did not show evidence of connection with the diploë or marrow expansion, which is required for an anaemia diagnosis (Brickley et al. 2020b). Pellagra is also considered to be unlikely as it is tied to only one of the most common lesions (orbital roof porosity) noted. Osteopetrosis is not considered, as the lesion location criteria (at the distal femur and tibia, the proximal humerus) needed to be associated with metaphyseal flaring, which was not evident in the individual with metaphyseal flaring.

It will also be noted that the skeletal changes associated with rickets can also be caused by celiac disease, chronic biliary status, and biliary fistula as these conditions impede vitamin D absorption (Ortner and Putschar 1985). In scurvy, as noted above, some of the changes observed can be associated with other metabolic bone diseases such as rickets and anaemia.

Multiple lesions discussed above are linked only to scurvy. One such indicator seen in the Seh Gabi sample is SPNB and porosity on the greater wing of the sphenoid (Brown and Ortner 2011; Eggington et al. 2024; Geber and Murphy 2012; Klaus 2017; Ortner and Ericksen 1997; Schattmann et al. 2016; Snoddy et al. 2018). Another lesion typically only linked to scurvy which is seen within this sample is that of SPNB in the orbital roof (Brown and Ortner 2011; Eggington et al. 2024; Klaus 2017; Snoddy et al. 2018). The lesions seen in the maxilla discussed above are also associated only with scurvy: maxillary palate porosity (Brown and Ortner 2011; Eggington et al. 2024; Ortner and Ericksen 1997); SPNB and porosity on the posterior aspect (Eggington et al. 2024; Geber and Murphy 2012; Klaus 2017; Ortner and Ericksen 1997; Schattmann et al. 2016; Snoddy et al. 2018), and SPNB and porosity around the infraorbital foramen (Brown and Ortner 2011; Eggington et al. 2024; Geber and Murphy 2012; Schattmann et al. 2016). Additionally, both porosity on the scapular supraspinous fossa and SPNB and porosity on the scapular infraspinous fossa are typically tied to scurvy (Brown and Ortner 2011; Eggington et al. 2024; Klaus 2017; Schattmann et al. 2016; Snoddy et al. 2018).

Given that many of the lesions seen in the Seh Gabi sample are typically associated with scurvy, and that the other possible MBD (anaemia, pellagra, and osteopetrosis) are thought to be unlikely due to the possible associated lesions not fully aligning with those diseases (e.g., no sign of marrow expansion associated with orbital roof porosity), it is concluded that scurvy is a possible lived experience for the population of Seh Gabi. It should also be noted that in cases of non-adult scurvy the long bones are less affected (Brown and Ortner 2011; Ortner 2003), and osseus evidence can be restricted to the cranium, especially in cases of infantile scurvy (e.g.,

Geber and Murphy 2012). It is thus, not surprising that many of the more common lesions among the Seh Gabi sample are restricted to the cranium.

6.2.2 Individual diagnoses

6.2.2.1 Framework for diagnosis.

An operational definition requires a certain set of criteria to be fulfilled for a disease to be identified (Waldron 2009). In this study, a probable diagnosis of scurvy or rickets requires an individual to have at least two diagnostic lesions, or a combination of three suggestive or non-diagnostic lesions associated with scurvy or rickets (e.g., Eggington et al. 2024; Schattmann 2014; Snoddy et al. 2018). These criteria are considered to be the operational definitions for either scurvy or rickets within this study. Individuals with one diagnostic lesion, one suggestive lesion, or at least two suggestive and non-diagnostic lesions were categorized as possible cases with insufficient skeletal evidence for both rickets and scurvy. This framework is consistent with other studies of scurvy and rickets in skeletal populations (e.g., Eggington et al. 2024; Schattmann 2014; Srienc-Ścies iek et al. 2024). The diagnostic, suggestive, and non-diagnostic lesions for scurvy are presented in Table 6.1 (p. 80) while the diagnostic, suggestive, and non-diagnostic lesions for rickets are shown in Table 6.2 (p. 81). Comorbidity was identified as a possibility if multiple features of both scurvy and rickets were present in individuals. A complete summary of all these diagnostic, suggestive, and non-diagnostic scorbutic and rachitic lesions for each individual is provided in Appendix C. It will be noted that there are other slightly different frameworks that could be used (i.e., Brickley and Morgan 2023) which offer alternatives to the labels of probable and possible cases. But, given the age of these individuals and the amount of growth and development that is occurring at that time of life, lesions are sometimes difficult to distinguish on subadult skeletal remains. Given this, the decision was made to use probable and possible diagnoses, as to not underrepresent those cases.

Table 6.1. *Types of Scorbutic Lesions for Diagnosis.*

Diagnostic	Suggestive	Non-Diagnostic
Sphenoid: greater wing SPNB/porosity [a, b, c, d, e, f, g]	Sphenoid: lesser wings SPNB [b, c, f]	Cranial Vault: SPNB/porosity [a, b]
Maxilla: posterior aspect SPNB/porosity [b, c, d, e, f, g]	Mandible: mental coronoid process SPNB/porosity [b, f]	Ilium: porosity [b, f]
Scapula: Supraspinous fossa porosity [a, b, d, f, g]	Zygomatic: orbital surface porosity [a, b, c, f, g]	
Scapula: Infraspinous fossa SPNB/porosity [a, b, d, f, g]	Maxilla: infraorbital foramen SPNB/porosity [a, b, c, f]	
Frontal: orbital roof SPNB [a, b, d, g]	Upper/Lower limbs: diaphysis SPNB [b, c]	
	Upper/Lower limbs: metaphyseal flaring [b, g]	
	Maxilla: palate porosity [a, b, e]	
	Maxilla/Mandible: alveolar process SPNB/porosity [a, b, c, e]	
	Rib flaring/cupping [b, g]	

[a] Brown and Ortner 2011
[b] Eggington et al. 2024
[c] Geber and Murphy 2012
[d] Klaus 2017
[e] Ortner and Ericksen 1997
[f] Schattmann et al. 2016
[g] Snoddy et al. 2018.

Table 6.2. *Types of Rachitic Lesions for Diagnosis.*

Diagnostic	Suggestive	Non-Diagnostic
Deformed arm & leg long bones when multiple bones affected & clear bend, radiography rules out trauma [a, b, c, d]	Sternal rib end porosity [b, c, d]	Cranial vault porosity ecto & endocranial [b, c, d]
Abnormal growth plate distally [b, c, d]	Rib deformity with a sharp angle if multiple bones affected [b, c, d]	Frontal bone bossing [a, c]
Flattening of femoral metaphysis & coxa vara [b, c]	Deformed mandibular ramus [b, c, d]	Orbital roof porosity [b, c, d]
Thickened long bones bilaterally & confirmed radiographically [b, c, d]	Ilium concavity [b, c, d]	Irregular & porous metaphyseal cortex of long bones [b, c, d]
Sternal rib end flaring if cupped [b, c, d]	Long bone metaphyseal flaring; arms & legs [b, c]	
	Long bone concave curvature porosity [b, c]	

[a] Brickley and Ives 2008b
[b] Mays et al. 2006
[c] Schattmann 2014
[d] Ortner and Mays 1998.

6.2.3 Presence of possible scorbutic vs rachitic lesions

Based on prevalence alone (see Table 6.3), the possible scorbutic lesions (see Table 6.1, p. 80) appear to be more common than possible rachitic lesions (see Table 6.2, above); possible in this case referring to lesions which could be possibly associated with each disease. However, the most common rachitic lesion of orbital roof porosity has a higher prevalence rate than any of the common scorbutic lesions. It is entirely possible that other individuals may have also displayed the rachitic and scorbutic lesions, but do not have the relevant skeletal elements available to assess. Nineteen individuals presented with lesions that have been identified as diagnostic, suggestive, and non-diagnostic for rickets and scurvy. The frequencies by age group can be seen in Table 6.3. A Fisher's exact test was done to test whether there is a significant

	Possible Scorbutic Lesions	Possible Rachitic Lesions	Both	Total
<6 months	6	2	3	11
≥6 months	1	1	6	8
Total	7	3	9	19

Table 6.3. Frequency of individuals with scorbutic and/or rachitic lesions by age group.

relationship between the possible scorbutic and rachitic lesions within this population and/or by age group which resulted in a p-value of 0.150, meaning that there was no significant difference between lesions and age in this sample.

6.3 Analysis Method of Disease Prevalences

Prevalences were calculated for scurvy, rickets, and comorbidity in this population. In living populations, prevalences are calculated as the number of cases/total population. As the total population of this site cannot be known, total sample size is used instead of total population.

Different mounds have been dated to different time periods. Comparisons were made between mound groupings to determine if there was a change in the prevalence of scurvy and rickets through time. As such, mounds will be separated into three groups for analysis: oldest (Mound C), intermediate (Mound E and B), and most recent (Mound F and A). The location of the mounds can be seen in Figure 2.1 (p. 6).

6.4 Location of Burials and Diagnoses

Table 6.4 outlines where individuals were buried, and the metabolic bone disease condition, if any, they may have experienced. The calibrated radiocarbon dates come from aDNA studies of human bone (Lazaridis et al. 2016; Narasimhan et al. 2019). The dates associated with skeletal material have been preferentially used, when available, for the purposes of analysis here as they are more concrete and not estimates. Other dates are uncalibrated and come from Hamlin's excavation report (1974), which have been converted to cal B.P.

Table 6.4. *Burial Location & Diagnoses of the Seh Gabi Population.*

Burial	Mound C 6850±50 cal B.P.[a] (7450 cal B.P.[b])	Mound E 5950 to 5450 cal B.P.[b]	Mound B 5870±40 to 5740±40 cal B.P.[a] (6950–6450 cal B.P.[b])	Mound F 5450 cal B.P.[b]	Mound A 5105±35 to 5070±30 cal B.P.[a]
1	SG 1	SG 22: possible scurvy	SG 5	SG 24	SG 18
2	SG 2	SG 23: possible scurvy	SG 6	*SG 29	SG 19
3	SG 3: possible scurvy	SG 25: possible scurvy	SG 7: probable scurvy		SG 20
4	SG 4: possible scurvy & rickets	SG 26: possible scurvy	SG 8: possible scurvy		SG 21: probable scurvy
5		SG 27: possible scurvy	SG 9: probable scurvy		*SG 30
6		SG 28	SG 10		*SG 31
7		*SG 32: possible scurvy	SG 11: possible scurvy		
8			SG 12		
9			SG 13		
10			SG 14: possible scurvy& rickets		
11			SG 15		
12			SG 16: possible scurvy		
13			SG 17		
Prevalence probable scurvy	0%	0%	15.4% (N=2/13)	0%	25% (N=1/4)
Prevalence possible scurvy	50% (N=2/4)	83.3% (N=5/6)	30.8% (N=4/13)	0%	0%
Prevalence possible rickets	25% (N=1/4)	0%	7.7% (N=1/13)	0%	0%
Prevalence possible scurvy and rickets	25% (N=1/4)	0%	7.7% (N=1/13)	0%	0%

[a] Lazaridis et al. 2016; Narasimhan et al. 2019
[b] Hamlin 1974
*= not included for analysis due to age estimations.

6.5 Scurvy

Within the framework of diagnostic, suggestive, and non-diagnostic scorbutic lesions outlined in Table 6.1, the identification of scurvy in these subadults was possible. With these requirements in mind, three of these subadults (SG7, SG9, and SG21) exhibited two diagnostic or three suggestive and non-diagnostic lesions which is indicative of probable scurvy at a prevalence of 10.7% (N=3/28) in this population. There are an additional eleven cases (SG3, SG4, SG8, SG11, SG14, SG16, SG22, SG23, SG25, SG26, SG27) of possible scurvy with insufficient skeletal evidence (39.3%, N=11/28) that consisted of one diagnostic or suggestive lesion, or two non-diagnostic lesions.

6.5.1 Within and Between Mounds

The occurrence of scurvy diagnosis by mound grouping is summarized in Table 6.5, below. The oldest mound, Mound C (6850±50 cal B.P., Lazaridis et al. 2016), had no probable scorbutic individuals, or a prevalence of 0% (0/4). Mounds B and E are part of the intermediate dated group of mounds. Mound B (5870±40 to 5740±40 cal B.P., Lazaridis et al. 2016) contained two probable scorbutic individuals resulting in a prevalence of 15.4% (N=2/13). Mound E (5950 to 5450 cal B.P., Hamlin 1974) had no probable scorbutic individuals or a prevalence of 0%. Mound F and Mound A are the most recent mounds. Mound F (5450 cal B.P., Hamlin 1974) had no probable scorbutic individuals, or a prevalence of 0%. Mound A (5105±35 to 5070±30 cal B.P., Lazaridis et al. 2016) contained one individual with probable scurvy, resulting in a scurvy prevalence of 25% (N=1/4), making it slightly more common in this more recent mound. The results indicate that the earliest mound (Mound C) had a prevalence of 0%; the intermediate group of mounds (Mounds B and E) had a probable scurvy prevalence of 10.5% (N=2/19); while the most recent mound group (Mounds F and A) has a probable scurvy prevalence of 20% (N=1/5). This indicates that the prevalence of probable scurvy increases with time.

There are nine individuals who have lesions possibly associated with scurvy, but with insufficient indicators for a probable diagnosis. Mound C contained four individuals, two of which are possible scurvy cases for a prevalence of 50% (N=2/4). Of the intermediate mounds, Mound E has 6 individuals for analysis, five of whom are possible scurvy cases (83.3%, N=5/6) and Mound B, four individuals are possible scurvy cases indicating a prevalence of 30.1% (N=4/13). In the most recent mounds, both Mound F and Mound A have no possible cases, with a prevalence of 0% for both. Combined, the oldest mound group (Mound C) has a possible scurvy prevalence of 50%, the intermediate grouping of mounds (Mound E and B) 47.4% (N=9/19), and the most recent group (mound F and A) has a prevalence of 0%. Contrary to that for probable scurvy, the prevalence of possible scurvy decreases through time.

Mound Grouping	Probable Scurvy	Possible Scurvy	Absent	Total
Oldest (Mound C)	0	2	2	4
Intermediate (Mound E & B)	2	7	10	19
Most Recent (Mounds A &F)	1	0	4	5
Totals	3	9	16	28

Table 6.5. Frequency of individuals with probable scurvy, possible scurvy, and absent scorbutic lesions by mound grouping.

The frequencies of scurvy diagnosis by mound grouping can be seen in Table 6.5. There is no significant difference between the mound groupings and the number of cases of probable scurvy, possible scurvy, and the absence of scorbutic lesions (Fisher-Freeman-Halton Exact Test, p=0.461).

6.6 Rickets

The identification of rachitic lesions was possible using the previously established framework (p. 79). None of the individuals in this study met the requirements for probable diagnosis (two diagnostic or three suggestive and non-diagnostic lesions, see Table 6.2 p. 81), thus there is a prevalence of 0% for probable rickets. However, two individuals presented as possible rickets cases (SG4, SG14) with a prevalence of 7.1% (N=2/28). To qualify for possible rickets with insufficient skeletal evidence, these individuals needed to have one diagnostic or

suggestive lesion, or two non-diagnostic lesions (Table 6.2, p. 81). It is important to note that more individuals may have experienced rickets than is visible macroscopically on their remains. It is also possible that they did not have rickets long enough to leave skeletal evidence or, as discussed in Chapter 3 (p. 35), that they also had scurvy which can mask the rachitic lesions on skeletal remains (Follis et al. 1940; Fouron and Chicoine 1962; Schattmann et al. 2016).

The presence of interglobular dentin has been linked to the onset of vitamin D deficiency (D'Ortenzio et al. 2018) and can only be seen in cross-sections of the teeth. In cross-sections of teeth from eight Seh Gabi infants, evidence of interglobular dentin was observed in two individuals (Merrett 2019). This study is used as a point of comparison, since the methodology and the criteria required for diagnosis differs from this thesis. The two individuals (SG15 and SG26) identified had interglobular dentin present within their teeth at different ages of onset. Neither of these individuals had macroscopic lesions which are consistent with the possible rachitic lesions outlined in Table 6.2 (p. 81). SG15 experienced this within a week of birth whereas SG26 had interglobular dentin appear 24 weeks after birth. The timing of this interglobular dentin would then suggest it was the mothers of SG15 and SG26 that were deficient in vitamin D (Merrett 2019). Thus, it is possible that both infants experienced vitamin D deficiency without leaving any macroscopic skeletal evidence and corroborates the presence of vitamin D deficiency in the Seh Gabi population. Additionally, this would indicate that it is possible that other individuals within the population could have experienced metabolic bone diseases such as rickets, without having any macroscopic evidence of it on their skeletal remains.

6.6.1 Within and Between Mounds

Two possible cases of rickets were identified among the subadults from Seh Gabi; the frequencies of possible rickets within mound groupings can be seen in Table 6.6. One individual with possible rickets was identified within Mound C (25%, N=1/4), and one individual from Mound B (7.7%, N=1/13). Comparing mound groupings, the earliest grouping (Mound C) has a prevalence of 25% (N=1/4) while the intermediate grouping (Mounds B and E) has a possible rickets prevalence of 5.3% (N=1/19). No cases of possible rickets were identified from the most recent mounds (Mounds F and A) for a prevalence of 0%. Together, this indicates that prevalence of possible rickets decreases over time. However, there is no significant difference between the mounds and cases of probable rickets, possible rickets, or absence of rachitic lesions (Fisher-Freeman-Halton Exact Test, p=0.296).

Mound Grouping	Probable Rickets	Possible Rickets	Absent	Total
Oldest (Mound C)	0	1	3	4
Intermediate (Mound E & B)	0	1	18	19
Most Recent (Mounds A &F)	0	0	5	5
Totals	0	2	26	28

Table 6.6. Frequency of individuals with probable rickets, possible rickets, and absent rachitic lesions by mound.

6.7 Comorbidity

As discussed in Chapter 3 (p. 35), scurvy and rickets can occur as co-morbid conditions within an individual and, depending on the timing of the onset of skeletal symptoms, scurvy can mask rickets and vice versa (Brickley and Morgan 2023; Follis et al. 1940; Fouron and Chicoine 1962; Schattmann et al. 2016). The two individuals identified as possible rickets cases (SG4 and SG14) were also identified as possible scurvy cases. This would give the Seh Gabi population a prevalence of 7.1% (N=2/28) for possible comorbid cases of scurvy and rickets.

An infant, under the age of six months, presenting with both scurvy and rickets suggests that their mother may have had scurvy and osteomalacia, or alternatively, not enough vitamin

stores to provide their child with sufficient vitamins either *in utero* or during breastfeeding (Brickley and Mays 2019; Maghbooli et al. 2007; Roberts and Manchester 2007). Both SG4 and SG14 were over the age of six months at the time of death, indicating that their lesions were more likely to be directly tied to diet and their own health rather than solely that of their mother. When over the age of six months, it is thought that dietary deficiencies reflect more of the diet of the individual due to lessened impacts related to maternal nutritional status during pregnancy (Algahtani 2010; Brickley and Mays 2019; Brickley et al. 2014; Fain 2005; Maghbooli et al. 2007; Maiyegun et al. 2002; Mays 2008). These two individuals appear to have been lacking in vitamin C and may not have received enough vitamin D either through sun exposure and/or breastfeeding.

Seh Gabi's location in a rain shadow is indicative of a marginal location (Zohary 1973) which would have influenced farming and pastoralism (Hamlin 1973, 1974). Farming in a marginal location involved planting in soils which have fewer micronutrients in the soils and decreasing organic matter (Moreno-Jiménez et al. 2019) which could have led to lower crop yield overall at Seh Gabi. Thus, this marginal location could have reduced the amount of vitamin C available to the adult population, therefore reducing the amount available to infants.

6.8 The Population of Seh Gabi

From this point forward, only probable cases will be discussed since there is insufficient evidence for diagnosis in the possible cases.

It was determined that three of the individuals of the Seh Gabi population had probable cases of scurvy. The oldest mound group (Mound C) had no probable scurvy (0%) while the intermediate group of mounds (Mound E and B) have had a probable scurvy prevalence of 10.5% (N=2/19) The most recent mound group (Mound F and A) has a probable scurvy prevalence of 20% (N=1/5). Given that there are probable cases of scurvy within this population, presumably both adults and children encountered nutritional deficiencies and possible metabolic bone disease. It should be noted however that there is a mortality bias as this study is based on the children who died. Presumably there would have been other children who could have experienced the same health issues to varying degrees but survived into older age categories.

6.9 Maternal Health

Maternal health and diet are known to impact the health of children. It has been found that understanding nutritional stress and disease in children under three years of age provides context for both adult and maternal health (Barker 2012; Gowland 2015; Waterland and Michaels 2007). For example, maternal vitamin D status can influence the amount of *in utero* fetal bone mineralization (Williams et al. 2009). Scorbutic neonate, individuals up to 28 days old (World Health Organization n.d.), and post neonate (infant) remains, aged 1 month to 1 year, (28% and 32% respectively) from a mass burial in Ireland reflected scurvy in their mothers (Geber and Murphy 2012). For individuals under the age of six months, lesions are likely to be tied to a mother's nutritional status while they were pregnant (Algahtani 2010; Brickley and Mays 2019; Brickley et al. 2014; Fain 2005; Maghbooli et al. 2007; Maiyegun et al. 2002; Mays 2008). All the probable scurvy cases in the Seh Gabi subadults occur in the under six months old age group (Table 6.7). Thus, it is reasonable to conclude that the probable scorbutic Seh Gabi individuals also had scorbutic mothers. Although, there is no significant difference between age group and/or cases of probable, possible, and absent scurvy (Fisher-Freeman-Halton Exact Test, p=0.542), the small sample size may be influencing that result.

Age	Probable Scurvy	Possible Scurvy	Absent	Total
<6 months	3	5	10	18
≥6 months	0	4	6	10
Totals	3	9	16	28

Table 6.7. Frequency of individuals with probable scurvy, possible scurvy, and absent scorbutic lesions by age group.

6.10 Cultural Practices

6.10.1 Diet

The occurrence of scurvy is directly tied to the diet of an individual or a population (Fain 2005). The question remains whether possible food sources would be enough to provide the inhabitants of Seh Gabi with enough daily vitamin C. There is archaeological evidence, either from the site itself or similar sites in the same region, to at least partially reconstruct dietary sources of nutrients.

At Seh Gabi, there is evidence for cultivated grains in their diet with storage rooms built into structures (Hamlin 1973, 1974). A stable isotopic analysis of human bone found their diet was largely based on a C3 terrestrial diet throughout the occupation (Scott 2018). This is consistent with findings at Godin Tepe (nearby Chalcolithic site) which indicated utilization of wheat, barley, lentils, chickpeas, and coriander (Miller 1990), (Chapter 2, p. 18). Thus, it is possible that these resources were being used Seh Gabi as well although it is not possible to know the volume of what was being eaten.

The grains and legumes mentioned would not have provided much vitamin C in the diet. Wheat and barley do not contain any vitamin C per cup at all (University of Rochester 2026a, b) while chickpeas have about nine milligrams (University of Rochester 2026c) and lentils have about three milligrams per cup (University of Rochester 2026d). However, if raw coriander leaves were being utilized in diet, then this would increase levels of vitamin C as it contains thirty milligrams of ascorbic acid per 100 grams of leaves (Australian Food Composition Database n.d.). Another possible food source to consider are pistachios and almonds as those were the dominant forests in the region (Rothman 2011; van Zeist and Wright 1963; van Zeist 1967). Almonds have no vitamin C content (University of Rochester 2026e) while pistachios contain very little, about six milligrams per cup (University of Rochester 2026f). It will be noted that the serving sizes outlined here may not correspond to what a serving size was at the time of Seh Gabi's occupation.

Although there are many faunal remains present at Seh Gabi (Hamlin 1973, 1974) it is unclear which animals and parts of animals were primarily eaten, or how much animal products were being consumed. Organ meats are a good source of vitamin C, but muscle meats are not as animals do not store much vitamin C in their tissues (World Health Organization 1999). It was also discussed in Chapter 2, p. 18, that dairying was possible at Seh Gabi given the faunal assemblage present, and the evidence at nearby sites, however it is again impossible to know to what extent this was being utilized and how much was being consumed. Caprine dairy does contain vitamin C, around 5.5 milligrams per 100 millilitres (Kondyli et al. 2007). Thus, some of these potential food sources, both plant and animal, would have contained some ascorbic acid.

However, it seems that these potential sources of dietary vitamin C would not have been sufficient to avoid symptoms of scurvy or scurvy itself at Seh Gabi for most people. The daily recommended amount of vitamin C intake for adults is 75–90 mg, 40–50 mg for infants, and 15–

65 mg per day for children (Monsen 2000). This would depend on the volume consumed of course and what meats were consumed, but based on a serving size of each source, as outlined above and adding the amount of ascorbic acid from a serving size of each source together, individuals could receive 0–107 mg per day of vitamin C. This range is reflective of zero to two servings of the dietary sources described. The middle point of the range, (1 serving of each), 53.5 mg per day is within range for infants. Infants rely on maternal dietary habits for their vitamin C intake via breastfeeding, and if the mother is lacking in vitamin C, then this translates to the infants as well (Brickley and Mays 2019). This amount of 53.5 mg per day would be in range for children as they can survive with less vitamin C than adults and infants (Monsen 2000). The ascorbic acid associated with two servings would also be in range for children. There are only possible cases of scurvy in individuals over the age of six months and thus thought to be attributed more to the individual's diet rather than the maternal diet (Algahtani 2010; Brickley and Mays 2019; Brickley et al. 2014; Fain 2005; Maghbooli et al. 2007; Maiyegun et al. 2002; Mays 2008). With these possible cases it may be more of an individualized reason for the lesions rather than a societal level dietary issue, given the amount of vitamin C a child needs. However, this would change with adults for which 53.5 mg would be insufficient and could lead to either deficiency or some symptoms within a few months of sustained low levels of vitamin C intake (Brickley and Ives 2006; Léger 2008). If adults were consuming two servings of each dietary source outlined (107 mg), then this would be in range of required daily ascorbic acid (Monsen 2000). It should be noted that there may have been other food sources which could have influenced the amount of vitamin C in the diet which have not yet been recorded, reported or preserved in the archaeological record. Alternatively, it is possible that these plant sources were not used, and the inhabitants of Seh Gabi were cultivating different crops.

Additionally, there are no probable cases of scurvy in Mound C, the oldest mound. Mound C had a subsistence strategy which did not utilize animal husbandry (McDonald 1979) which is different than the temporally later mounds. In Mound C, they could have been incorporating more hunting and foraging to supplement. This could be reflective a greater reliance on agriculture and domesticated caprines influencing the amount of probable scurvy in the later mounds of occupation.

6.10.2 Weaning

Although the number of individuals over the age of one year at Seh Gabi is limited, Scott (2018) found that weaning had ceased by 3.3 years, with evidence that several of the individuals were enriched in ^{15}N because of breastfeeding. There was also evidence of breast milk still being incorporated in diet at 1.6 years of age. It is recommended that dietary supplementation to breastfeeding begin around the age of six months old (World Health Organization 2023) and supplementation has been noted as a possibility in the archaeological sample from Ganj Dareh (Merrett et al. 2021) As most of the Seh Gabi subadults are under the age of one year, it is plausible that most were not yet completely weaned, and their diet still contained breast milk (Scott 2018). Additionally, this could mean that if their mother's diet did not contain sufficient levels of vitamin C, then the child would also have insufficient vitamin C (Brickley and Mays 2019). Since maternal health and breastfeeding impact an infant, it is also plausible that the under six-month-old individuals at Seh Gabi were impacted by their mother's vitamin deficiency. All the probable scurvy cases occurred in individuals under six months old, therefore, it can again be postulated that their mothers had scurvy as well (see Table 6.7, p. 89).

However, there is also a possible case of scurvy in an individual (SG4) over the age of six months who could have been over the age of 1.6 years old, when weaning could have been in progress (Scott 2018), when they died. In this case, if they did in fact have scurvy, it could be attributed more to the individual's diet (Algahtani 2010; Brickley and Mays 2019; Brickley et al. 2014; Fain 2005; Maghbooli et al. 2007; Maiyegun et al. 2002; Mays 2008), rather than strictly their mothers' or a combination of the two.

6.10.3 Other cultural practices

Other cultural practices could have impacted infant health. The windowless buildings found at Seh Gabi (Hamlin 1973, 1974) could potentially lead to vitamin D deficiency through inadequate sun exposure if children were frequently kept indoors. Additionally, clothing choices could reduce the amount of skin that sunlight is able to come into contact with, resulting in less vitamin D synthesis being activated (Hatun et al. 2005). However, since there are no probable cases of rickets by skeletal lesions represented within the population there is no concrete evidence of inadequate sun exposure at least through macroscopic and radiographic analyses. That being said, there are the two cases of interglobular dentin (SG15, SG26) which indicate

vitamin D deficiency (Merrett 2019) which could be indicative of inadequate sun exposure, possibly due to the windowless buildings present at Seh Gabi (Hamlin 1973, 1974).

6.11 Comparisons to other Chalcolithic Populations

While Seh Gabi is a relatively unique site given the number of subadults present, there are few other Chalcolithic sites in the same region for comparison. At Tepe Hissar in Iran, the remains of 313 adults from different Chalcolithic time periods were assessed and found to have a prevalence of 0-1 % for scurvy and 47-68% for osteomalacia respectively (Afshar 2016). This varies greatly from what was seen in the Seh Gabi population. However, this could suggest that the prevalence of rickets may have been higher than what was visible macroscopically among the Seh Gabi subadults. A subadult aged to be around one year old from the Chalcolithic occupation at Aswan, Egypt was found to have scurvy which was thought to be related to maternal health status and breastfeeding (Pitre et al. 2016). While this study does not give us a population level assessment, it confirms that scurvy was present in subadults during the Chalcolithic, indicating that the probable scurvy at Seh Gabi could be related to maternal health. Further afield, in Europe a case of comorbid rickets and scurvy was identified in one complete subadult skeleton (about six years old) at the El Portalón site in Spain (Castilla et al. 2014). While there are no population level prevalences with which to compare Seh Gabi, this study does show that comorbidity of the two vitamin deficiencies during the Chalcolithic was present.

A Neolithic site which can be compared is Ganj Dareh, Iran. Ganj Dareh is also located in the Central Zagros Mountains but unlike Seh Gabi, it is not located in a rain shadow and no individuals had visible osseous evidence of cribra orbitalia or scurvy (Merrett 2004, 2006) unlike what was seen in the subadults from Seh Gabi.

These sites illustrate that metabolic bone disease prevalence varied between different sites during the Chalcolithic and earlier Neolithic periods. However, the prevalence at which probable scurvy was experienced at Seh Gabi is much higher than these other sites and is unique which could be due to a variety of factors like diet and location.

6.12 Implications for Modern Iranian Groups

Vitamin deficiencies are commonly experienced within the modern Iranian population due to both diet and cultural practices. In modern groups, diet varies seasonally, especially in

rural areas (e.g., Toorang et al. 2013). These rural and remote communities in Iran, in locations like Seh Gabi, may not have the same access to fresh produce as those in major cities (Sarraf et al. 2005). Additionally, this can be exacerbated by the high cost associated with imported fresh produce which not everyone may be able to afford. Other options such as vitamin C supplements may be more accessible depending on factors like socioeconomic status (Ghodsi et al. 2023). As seen with Seh Gabi, diet and nutritional deficiencies impacted the health of past populations; this patterning could also be applied to understanding the impact of diet in a modern context. With intensive agriculture, like that seen at Seh Gabi, there is an increased reliance on cultivated products and a more sedentary lifestyle (Flannery 1971; Larsen 1995; McDonald 1979; Melville 1984) which could lead to an increased susceptibility to disease (Larsen 1995; Rowan and Golden 2009; Şener et al. 2026). Many of the same factors that affected past populations continue to be an influence on modern populations health. However, measures like vitamin C supplementation can ameliorate deficiency.

6.13 Limitations of the Study

There are numerous limitations which impacted the accuracy of identifying features of scurvy and rickets and then making interpretations from them. Firstly, the sample population is comprised of very young individuals. Differentiating between normative new bone formation and pathological change presents its own challenge as this is a time when the skeleton is undergoing massive amounts of growth and development. Given this, lesions were only identified as such when they were obvious. Additionally, there may be cases of comorbidity of diseases in this population which were not identifiable macroscopically given that both scurvy and rickets inhibit the other's expression (Brickley et al. 2020a; Brickley and Morgan 2023; Follis et al. 1940; Fouron and Chicoine 1962; Schattmann et al. 2016). Post-mortem damage was an issue encountered, with some individuals having widespread post-mortem damage across their remains which could have obscured the presence of lesions. Thus, there is a possibility that there are lesions present in this population which were not visible macroscopically either due to cooccurrence or post-mortem damage. Additionally, it is possible that some individuals had scurvy or rickets during life, but the skeletal elements impacted were not present in the archaeological record, or that the disease had not progressed to their skeleton at the time of their death. As such, the prevalences noted within this thesis are minimal estimates of prevalence.

There are also limitations in terms of interpretations for this study. For one, there is limited information available about diet at Seh Gabi, which impacts interpretations as to why lesions are present and what those lesions meant for the population. Different food sources have different implications for vitamin C consumed, and thus the likelihood of deficiency or symptoms experienced. Also, there are no adult remains present for assessment, so assumptions are made when it comes to what these lesions in subadults mean for the adult population.

6.14 Summary

Among the subadults of Seh Gabi, lesions were visible on their skeletal remains. Most of these lesions occurred on the crania and were most associated with scurvy. The framework of probable and possible diagnoses led to the identification of three probable scurvy cases, or 10.7% of the sample. Another 39.3% of the population were identified as possible scurvy cases. Based on the prevalence of probable scurvy within and between mounds, it appears that the prevalence of probable scurvy increased through time. While no probable cases of rickets were identified within this diagnosis framework, there were two possible cases, or 7.1% of the sample. Both possible rickets cases were also possible cases of comorbid rickets and scurvy. The prevalence of possible rickets cases decreases through time, based on the mounds of occupation. It was noted, however, that in a microscopic analysis two individuals were identified as having experienced interglobular dentin, indicating vitamin D deficiency (Merrett 2019), although this was not visible macroscopically.

The influencing factors of location, maternal health, and diet were discussed. The site's location in a rain shadow (a marginal zone) could have influenced nutrition as it would have impacted farming practices. A rain shadow is an arid area, meaning there is less moisture available for crops, and thus a reduced level of micronutrients in soils. Given the relatively lower number of micronutrients and organic matter in the soils associated with this type of environment (Moreno-Jiménez et al. 2019) this could have led to lower crop yields overall at Seh Gabi. Thus, potentially resulting in dietary deficiencies, if there are not resources to provide adequate nutrition for the entire population.

Maternal health could have also contributed to dietary deficiencies. If a mother was vitamin deficient during pregnancy or during breastfeeding, this could impact the infant's health as well (Algahtani 2010; Brickley and Mays 2019; Brickley et al. 2014; Fain 2005; Maghbooli et

al. 2007; Maiyegun et al. 2002; Mays 2008). Thus, it is likely that the mothers of the infants who had probable scurvy, were likely to have experienced scurvy themselves. The possible diet sources at Seh Gabi were discussed and shown to have probably reflected insufficient vitamin C intake. However, the volume of food being consumed is unknowable, and there is the possibility that other food sources were being utilized which are not recorded, reported, or present in the archaeological record. The prevalence of probable scurvy for this population (10.7%) appears to be higher when compared to other Chalcolithic sites in the region (0-1%) (Afshar 2016). Investigating vitamin deficiencies in the past could provide a way to understand disease patterning in the present and inform ways to counteract scurvy and rickets.

Chapter 7: Conclusion

Seh Gabi, Iran is an Early to mid-Chalcolithic site located in a rain shadow and thus a marginal zone (Henrickson 1983; Kramer 1982; McDonald 1979; Moreno-Jiménez et al. 2019; Zohary 1973). A rain shadow is an arid area with the environment affected by the location of mountains, with less moisture and a reduced level of micronutrients available for crops (Moreno-Jiménez et al. 2019). This site is comprised of seven mounds of occupation, which were mainly occupied during the Chalcolithic. Recent estimates place the Chalcolithic as having occurred through 7450 to 5150 cal B.P. in Iran (Matthews and Fazeli Nashli 2022).

Thirty-two subadult skeletons were excavated from Seh Gabi (Hamlin 1973, 1974). Radiocarbon dating of skeletal material directly ties the period of occupation from 6850±50 cal B.P. to 5070±30 cal B.P. (Lazaridis et al. 2016; Narasimhan et al. 2019). The inhabitants of Seh Gabi used intensive cultivation coupled with limited pastoralism, and foraging to supplement their diet as their means of subsistence (Henrickson 1985b; Kramer 1982; McDonald 1979). The location of Seh Gabi in a marginal zone, coupled with their subsistence method and increased population density during this period in the region would have led to an increased reliance on cultivated products (Flannery 1971; Larsen 1995; McDonald 1979; Melville 1984). This reliance could have had a direct impact on the population of Seh Gabi's susceptibility to dietary stressors including nutritional deficiencies.

Due to these factors, an overview of metabolic bone diseases which are known to exist in antiquity and to affect subadults was provided. There are, of course, other metabolic bone diseases (i.e., pellagra, osteoporosis and osteopenia, Paget's Disease, hyperparathyroidism, hypophosphatasia, osteopetrosis) which were not discussed due to being rarer in children (Arumugam et al. 2015; Cleveland Clinic 2024; Genetic and Rare Diseases Information Center; Naveen et al. 2013; National Institute of Arthritis and Musculoskeletal and Skin Diseases; Walczyk et al. 2011). It was noted that in a differential diagnosis these diseases should still be considered, where applicable (see Chapter 6). This overview included tables identifying which lesions could be associated with each disease (see Tables 3.1 and 3.2, p. 49–51). In modern Iran, scurvy could be common due to limited diet breadth (Hahn et al. 2019), and Iran has a history of food scarcity and famine (Afkhami 2019; Kazemi 2016). Additionally, rickets is known to be widespread in Iran (Jokar et al. 2008; Mithal et al. 2009; Vatandost et al. 2018).

To determine if any lesions were present on the skeletal remains of the subadults, a macroscopic visual analysis was undertaken. Three individuals were removed from statistical tests of these common lesions as their age estimates placed them as much older than the majority of the population (SG29, SG30, and SG32). One other individual (SG31) was removed from statistical tests as an age estimate was not possible. Based on this macroscopic visual analysis, common areas where lesions were present were identified within the population which consisted of either porotic changes, subperiosteal new bone formation changes, or a combination of both. Only one of these common areas (orbital roof porosity) had a statistically significant difference between the over and under six months old age groups, with more individuals in the over six months category having the lesion present. There were also signs of non-specific stress on some of the individuals in the form of linear enamel hypoplasia.

The sample of 28 subadults were macroscopically assessed for any lesions, and then a differential diagnosis was completed. The majority of lesions seen were present on cranial bones. Of the most commonly occurring lesions, there were links to scurvy, rickets, anaemia, pellagra, and osteopetrosis. However, the lesions seen are most typically linked to scurvy. From these subadult human remains it has been shown that 10.7% of the population sample experienced a probable metabolic bone disease due to vitamin C deficiency within their lifetime. The most recent mounds (Mounds F and A) had the highest prevalence of probable scurvy, while the oldest mound (Mound C) had the lowest prevalence of probable scurvy. Thus, it appears that cases of probable scurvy are increasing through time. These cases of probable scurvy could be a result of diet, the vitamin C status of mothers, or cultural practices. Given that all the probable cases of scurvy are in individuals who are under the age of six months, their lesions are likely linked to their mother's nutritional status while they were pregnant (Algahtani 2010; Brickley and Mays 2019; Brickley et al. 2014; Fain 2005; Maghbooli et al. 2007; Maiyegun et al. 2002; Mays 2008), which could have been impacted by insufficient intake of ascorbic acid. Additionally, at Seh Gabi, weaning has been shown to not be complete until 3.3 years of age (Scott 2018). If a mother continued to have scurvy while breastfeeding this would impact the infant (Brickley and Mays 2019). Although there were no macroscopically identified cases of probable rickets, two individuals (SG15 and SG26) have been identified as having interglobular dentin present in a previous microscopic study (Merrett 2019), which is linked to the onset of vitamin D deficiency (D'Ortenzio et al. 2018). It is possible that more of the sample experienced vitamin C or D

deficiency than what was visible macroscopically, as both metabolic bone diseases can mask the other's presentation. The results of this study suggest that Seh Gabi was unique in its experience of a high level of probable scurvy when compared to other contemporaneous sites. This was then explored in terms of population health, and in turn how this could inform understandings of metabolic bone disease and nutritional deficiencies in modern Iranian populations, especially those who live in rural areas that could be compared to the location of Seh Gabi. However, I believe that through further research there is still more to learn from Seh Gabi.

In terms of future research on metabolic bone disease in this population, ancient DNA analysis (aDNA) could provide further understanding of the represented population demographics by providing sex estimations. These sex estimations could give insight into any correlations between sex and both probable scorbutic individuals and possible comorbid (scurvy and rickets) individuals. However, it will be noted that aDNA is not always successful and can be quite destructive.

There is still more to learn from the skeletal remains themselves as well. It seems that several individuals have a healed or healing clavicular fracture, and research into why this is the case, could be useful. While Seh Gabi is unique in its prevalence of scurvy, it would be helpful to see if this extends to other conditions, like interglobular dentin. Further studies could be done to see if interglobular dentin is present in more individuals to refine the prevalence of vitamin D deficiency, as individuals may not have lived with rickets long enough to see it on their skeletal remains. If there are more individuals that are identified as having interglobular dentin, it would be interesting to see if there is overlap with genetic predispositions. Additionally, comparison studies between disease patterning between Seh Gabi to other temporally and geographically related sites could provide further insight. Perhaps Seh Gabi was unique in that the population had higher levels of genetic predisposition to scurvy whereas at another site with a lower genetic predisposition but similar diet and location there could be a lower prevalence of scurvy.

While there is not much erupted permanent dentition present in the skeletal remains associated with Seh Gabi due to the age of most of the individuals, the adolescent (SG32) has permanent dentition which showed signs of wear and potential caries. A specific study on SG32's dentition and how that could relate to diet (i.e., grains and dairy) would also provide more insight into the practices of the population. Caries and dental calculus can stem from carbohydrate-rich foods, like cereals (Santiago-Marrero et al. 2025). Additionally, sometimes

micro botanicals like phytoliths and starch grains can be recovered from dental calculus (Santiago-Marrero et al. 2025). If micro botanicals are present in any dental calculus that SG32 might have and can be identified, these micro botanicals could provide further insight into the plants consumed at Seh Gabi.

Studies into the cultural materials would be beneficial as well. Research into the associated funerary objects, burial type, and burial positioning could provide more insight into the cultural practices associated with the different mounds, and thus time periods of site occupation. Perhaps this could also inform understanding into information and material culture dissemination across the broader area of the Eastern Fertile Crescent. As well, further faunal assessment could provide more information about diet and subsistence at this site. For example, if there are certain patterns of butchery and burning present among the faunal assemblage this could provide insight into which animals were being preferentially consumed at Seh Gabi. Finally, residue analysis on the ceramic wares from Seh Gabi could indicate what was stored in the vessels, and inform our understanding of diet, including dairy (e.g., Casanova et al. 2026), plant, and animal consumption (e.g., Morton and Schwarcz 2004; Taché and Craig 2015; Taché et al. 2019). Improved understanding of diet could help inform interpretations as to why vitamin deficiency was experienced at Seh Gabi.

In summary, it is likely that vitamin C deficiency was experienced by the inhabitants of Seh Gabi. This study identified three cases of probable scurvy, along with nine additional cases of possible scurvy and two cases of possible comorbid scurvy and rickets in the subadults from Seh Gabi. Further research into aDNA, diet, and indicators of rickets are highly encouraged as these could further our understanding of disease at Seh Gabi, and interpretations as to why the prevalence of vitamin C deficiency was so high at this Chalcolithic site.

References

Abdi, Kamyar.
2003. The Early Development of Pastoralism in the Central Zagros Mountains. *Journal of World Prehistory* 17(4): 395–448.

Abdi, Kamyar, Gabriel Nokandeh, Ali Azadi, Fereydoun Biglari, Saman Heydari, Dariush Farmani, Akbar Rezaii, and Marjan Mashkour.
2002. Tuwah Khoshkeh: A middle Chalcolithic mobile pastoralist camp-site in the Islamabad Plain. *Iran Journal of the British Institute of Persian Studies* 40(1): 43–74. DOI: 10.1080/05786967.2002.11834411.

Afkhami, Amir A.
2019. *A Modern Contagion: Imperialism and Public Health in Iran's Age of Cholera*. John Hopkins University Press, Baltimore.

Afshar, Zahra.
2017. Palaeopathological analyses of human skeletons: Statistical analysis of health and disease among the Chalcolithic and Bronze Age populations at Tepe Hissar. *International Journal of the Society of Iranian Archaeologists* 3(5): 31–44.

Aghajanian, Patrick, Susan Hall, Montri D. Wongworawat, and Subburaman Mohan.
2015. The roles and mechanisms of actions of vitamin C in bone: New developments. *Journal of Bone and Mineral Research* 30(11): 1945–1955. DOI: 10.1002/jbmr.2709.

Albahri, A. S., Jwan K. Alwan, Zahraa K. Taha, Sura F. Ismail, Rula A. Hamid, A. A. Zaidan, O. S. Albahri, B. B. Zaidan, A. H. Alamoodi, and M. A. Alsalem.
2021. IoT-based telemedicine for disease prevention and health promotion: State-of-the-Art. *Journal of Network and Computer Applications* 173. DOI: 10.1016/j.jnca.2020.102873.

Algahtani, Hussein A., Abduljaleel P. Abdu, Imad M. Khojah, and Ali M. Al-Khathaami.
2010. Inability to walk due to scurvy: A forgotten disease. *Annals of Saudi Medicine* 30(4): 325–328. DOI: 10.4103/0256-4947.65266.

Alijani, Bohloul.
2008. Effect of the Zagros Mountains on the spatial distribution of precipitation. *Journal of Mountain Science* 5: 218–231. DOI: 10.1007/s11629-008-0126-8.

Allison, Marvin J., Enrique Gerszten, and Raul Sotil.
1976. Primary generalized hyperostosis in ancient Peru. *MCV Quarterly* 12(2): 49–51.

AlQahtani, Sakher J., Mark Hector, and Helen M. Liversidge.
2010. Brief communication: The London atlas of human tooth development and eruption. *American Journal of Physical Anthropology* 142(3): 481–490.

Amirhakimi, G. H.
1973. Rickets in a developing country: Observations of general interest from Southern Iran. *Clinical Pediatrics* 12(2): 88–92.

Amrein, Karin, Mario Scherkl, Magdalena Hoffmann, Stefan Neuwersch-Sommeregger, Markus Köstenberger, Adelina Tmava Berisha, Gennaro Martucci, Stefan Pilz, and Oliver Malle.
2020. Vitamin D deficiency 2.0: An update on the current status worldwide. *European Journal of Clinical Nutrition* 74: 1498–1513. DOI: 10.1038/s41430-020-0558-y.

Anderson, Emma, Matthew J. Almond, Wendy Matthews, Gianfelice Cinque, and Mark D. Frogley.
2014. Analysis of red pigments from the Neolithic sites of Çatalhöyük in Turkey and Sheikh-e Abad in Iran. *Spectrochimica Acta Part A: Molecular and Biomolecular Spectroscopy* 131: 373–383. DOI: 10.1016/j.saa.2014.03.126.

Antón, Susan C.
1997. Endocranial hyperostosis in Sangiran 2, Gibraltar 1, and Shanidar 5. *American Journal of Physical Anthropology* 102: 111–122. DOI: 10.1002/(SICI)1096-8644(199701)102:1<111::AID-AJPA9>3.0.CO;2-3.

Aoba, T., and O. Fejerskov.
2002. Dental fluorosis: Chemistry and biology. *Critical Reviews in Oral Biology & Medicine* 13(2): 155–170.

Armelagos, George J., Kendra Sirak, Taylor Werkema, and Bethany L. Turner.
2014. Analysis of nutritional disease in prehistory: The search for scurvy in antiquity and today. *International Journal of Paleopathology* 5: 9–17. DOI: 10.1016/j.ijpp.2013.09.007.

Arsalani, Mohsen, Ghasem Azizi, and Achim Bräuning.
2015. Dendroclimatic reconstruction of May-June maximum temperatures in the central Zagros Mountains, western Iran. *International Journal of Climatology* 35: 408–416. DOI: 10.1002/joc.3988.

Arumugam, Eswaran, Maheswari Harinathbabu, Ranjani Thillaigovindan, and Geetha Prabhu.
2015. Marble bone disease: A rare bone disorder. *Cureus* 7(10): e339.

Assefa, Fitsum, Mohammed Zahir Jabarkhil, Peter Salama, and Paul Spiegel.
2001. Malnutrition and mortality in Kohistan District, Afghanistan, April 2001. *Journal of the American Medical Association* 286(21): 2723–2728.

Australian Food Composition Database.
2026. FOO3192: Coriander, fresh, raw. https://afcd.foodstandards.gov.au/fooddetails.aspx?PFKID=F003192. Accessed March 8, 2026.

Badfar, Gholamreza, Masoumeh Shohani, Akram Mansouri, Ali Soleymani, and Milad Azami.
2017. Vitamin D status in Iranian pregnant women and newborns: A systematic review and meta-analysis study. *Expert Review of Endocrinology and Metabolism* 12(5): 379–389. DOI: 10.1080/17446651.2017.1365596.

Bagchi, Kunal.
2008. Nutrition in the Eastern Mediterranean Region of the World Health Organization. *Eastern Mediterranean Health Journal* 14(Special Issue): S107–S113.

Barker, D. J.P.
2012. Developmental origins of chronic disease. *Public Health* 126: 185–189. DOI: 10.1016/j.puhe.2011.11.014.

Barlow, Thomas.
1883. *Cases described as "acute rickets" which are probably a combination of scurvy and rickets, the scurvy being an essential, and the rickets a variable element.*

Baroncelli, G., A. Bereket, M. El Kholy, L. Audì, Y. Cesur, B. Ozkan, M. Rashad, M. Fernández-Cancio, Y. Weisman, G. Saggese, and Z. Hochberg.
2008. Rickets in the Middle East: Role of the environment and genetic predisposition. *The Journal of Clinical Endocrinology and Metabolism* 93(5): 1743–1750.

Basu, Sriparna, and Ashok Kumar.
2009. Hair-on-end appearance in radiograph of skull and facial bones in a case of beta thalassaemia. *British Journal of Haematology* 144: 807. DOI: 10.1111/j.1365-2141.2008.07404.x.

Beighton, P., F. Horan, and H. Hamersma.
1977. A review of the osteopetroses. *Postgraduate Medical Journal* 53(622): 507–516.

Biale, Y., S. Shany, M. Levi, R. Shainkin-Kestenbaum, and G.M. Berlyne.
1979. Hydroxycholecalciferol levels in Beduin women in labor and cord blood of their infants. *The American Journal of Clinical Nutrition* 32: 2380–2382.

Binford, L.R.
1968. Post-Pleistocene adaptations. In *New Perspectives in Archeology*, edited by S.R. Binford and L.R. Binford. Aldine, Chicago, pp. 313–341.

Blumthaler, M., W. Ambach, and R. Ellinger.
1997. Increase in solar UV radiation with altitude. *Journal of Photochemistry and Photobiology B: Biology* 39: 130–134.

Boillat, M.A., J. Garcia, and L. Velebit.
1980. Radiological criteria of industrial fluorosis. *Skeletal Radiology* 5(3): 161–165.

Bordelon, Paula, Maria V. Ghetu, and Robert Langan.
2009. Recognition and management of Vitamin D deficiency. *American Family Physician* 80(8): 841–846.

Brenton, Barrett P., and Robert R. Paine.
2007. Reevaluating the health and nutritional status of maize-dependent populations: Evidence for the impact of pellagra on human skeletons from South Africa. *Ecology of Food and Nutrition* 46: 345–360. DOI: 10.1080/03670240701486545.

Brickley, Megan B., Lori D'Ortenzio, Bonnie Kahlon, Annabelle Schattmann, Isabelle Ribot, Emeline Raguin, and Benoit Bertrand.
2017. Ancient vitamin D deficiency: Long-term trends. *Current Anthropology* 58(3): 420–427. DOI: 10.1086/691683.

Brickley, Megan, and Rachel Ives.
2006. Skeletal manifestations of infantile scurvy. *American Journal of Physical Anthropology* 129(2): 163–172. DOI: 10.1002/ajpa.20265.

2008a. Hyperostosis. In *The Bioarchaeology of Metabolic Bone Disease*. 1st ed. Academic Press, Elsevier, Oxford, pp. 258–259.

2008b. *The Bioarchaeology of Metabolic Bone Disease*. 1st ed. Academic Press, Elsevier, Oxford.

Brickley, Megan B., Rachel Ives, and Simon Mays.
2020a. *The Bioarchaeology of Metabolic Bone Disease*. 2nd ed. Academic Press: Elsevier, Oxford.

2020b. Anaemia. In *The Bioarchaeology of Metabolic Disease*. 2nd ed. Academic Press, Elsevier, Oxford, pp. 201–225.

Brickley, Megan B., and Simon Mays.
2019. Metabolic disease. In *Ortner's Identification of Pathological Conditions in Human Skeletal Remains*. Elsevier, January 1, pp. 531–566.

Brickley, Megan B., Tina Moffat, and Lelia Watamaniuk.
2014. Biocultural perspectives of vitamin D deficiency in the past. *Journal of Anthropological Archaeology* 36(1): 48–59. DOI: 10.1016/j.jaa.2014.08.002.

Brickley, Megan, and Brianne Morgan.
2023. Assessing diagnostic certainty for scurvy and rickets in human skeletal remains. *American Journal of Biological Anthropology* 181: 637–645.

Brown, Matthew, and Donald J. Ortner.
2011. Childhood scurvy in a medieval burial from Mačvanska Mitrovica, Serbia. *International Journal of Osteoarchaeology* 21(2): 197–207. DOI: 10.1002/oa.1124.

Buckley, Hallie R.
2000. Subadult health and disease in prehistoric Tonga, Polynesia. *American Journal of Physical Anthropology* 113: 481–505.

Buikstra, Jane E., Della C. Cook, and Katelyn L. Bolhofner.
2017. Introduction: Scientific rigor in paleopathology. *International Journal of Paleopathology* 19: 80–87. DOI: 10.1016/j.ijpp.2017.08.005.

Bursalli, Aysegul, Sarper Gursu, Alper Gursu, and Timur Yildirim.
2009. A case of infantile scurvy treated only with vitamin C: A forgotten disease. *Acta Orthopaedica Belgica* 75(3): 428–430.

Carter, D.R., M.C.H. Van Der Meulen, and G.S. Beaupré.
1996. Mechanical Factors in Bone Growth and Development. *Bone* 18(1, Supplement): 5S-10S.

Casanova, Emmanuelle, Hossein Davoudi, Antonie Zazzo, Séverine Zirah, Jérémy Jacob, Christine Hatté, Audrey Boco-Simon, François Thil, Caroline Gauthier, Jebrael Nokandeh, Abbas Alizadeh, Fereidoun Biglari, Reinhard Bernbeck, Susan Pollock, Akira Tsuneki, Omolbanin Ghafoori, Homa Fathi, Frank Hole, Emmanuelle Demey-Thomas, Joëlle Vinh, and Marjan Mashkour.
2026. Caprine dairy exploitation on the Iranian Plateau from the seventh millennium BC. *Nature Human Behaviour*: 1–11.

Castilla, Maria, José-Miguel Carretero, Ana Gracia, and Juan-Luis Arsuaga.
2014. Evidence of rickets and/or scurvy in a complete Chalcolithic child skeleton from the El Portalón site (Sierra de Atapuerca, Spain). *Journal of Anthropological Sciences* 92: 257–271. DOI: 10.4436/jass.89003.

Chakraborty, Partha Pratim, Sugata Narayan Biswas, Shinjan Patra, and Gouranga Santra.
2017. “Zebra stripe” sign and “bone in bone” sign in cyclical bisphosphonate therapy. *Journal of Clinical and Diagnostic Research* 11(2): RJ01–RJ02. DOI: 10.7860/JCDR/2017/24349.9177.

Cheah, Siew Chung, Ing Ping Tang, Tong Jong Haw Matthew, Mong How Ooi, and Salina Husain.
2020. Spontaneous orbital haematoma in a scurvy child: A forgotten diagnosis. *International Journal of Pediatric Otorhinolaryngology* 137: 110224.

Cheung, Edith, Roya Mutahar, Fitsum Assefa, Mija-Tesse Ververs, Shah Mahmood Nasiri, Annalies Borrel, and Peter Salama.
2003. An epidemic of scurvy in Afghanistan: Assessment and response. *Food and Nutrition Bulletin* 24(3): 247–255.

Cleveland Clinic.
2024. Hypophosphatasia. https://my.clevelandclinic.org/health/diseases/hypophosphatasia. Accessed March, 2026.

Conceição, E. L.N., and H. F.V. Cardoso.
2011. Environmental effects on skeletal versus dental development II: Further testing of a basic assumption in human osteological research. *American Journal of Physical Anthropology* 144: 463–470. DOI: 10.1002/ajpa.21433.

Cope, Darcy J., and Tosha L. Dupras.
2011. Osteogenesis imperfecta in the archeological record: An example from the Dakhleh Oasis, Egypt. *International Journal of Paleopathology* 1(3–4): 188–199. DOI: 10.1016/j.ijpp.2012.02.001.

Cotran, R.S., V. Kumar, and T. Collins.
1999. *Robbins Pathologic Basis of Disease*. 6th ed. W.B. Saunders Company, Philadelphia, P.A.

Dadaneh, M.Z., S. Renette, and A.S. Mucheshi.
2021. Connections between the northern Zagros and Mesopotamia during the fifth millennium BCE: New insights from Tepe Namashir in western Iran. *Review of Prehistory and Protohistory of Ancient Civilizations* 45: 7–34.

Darabi, Hojjat, Tobias Richter, and Peder Mortensen.
2019. Neolithisation process in the central Zagros: Asiab and Ganj Dareh revisited. *Documenta Praehistorica XLVI*: 44–56.

Dawodu, Adekunle, Mukesh Agarwal, Moshaddeque Hossain, Jose Kochiyil, and Reem Zayed.
2003. Hypovitaminosis D and vitamin D deficiency in exclusively breast-feeding infants and their mothers in summer: A justification for vitamin D supplementation of breast-feeding infants. *Journal of Pediatrics* 142(2): 169–173. DOI: 10.1067/mpd.2003.63.

Dawodu, Adekunle, and Reginald C. Tsang.
2012. Maternal vitamin D status: Effect on milk vitamin D content and vitamin D status of breastfeeding infants. *Advances in Nutrition* 3: 353–361. DOI: 10.3945/an.111.000950.

Delavari, A., S. Alikhani, and F. Aladini.
2009. *Report on the status of risk factors for the non-transmissible diseases in the Islamic Republic of Iran*. Tehran.

Dent, C.E., and R Smith.
1969. Nutritional osteomalacia. *Quarterly Journal of Medicine* 38(2): 195–209.

DeWitte, Sharon N., and Christopher M. Stojanowski.
2015. The osteological paradox 20 years later: Past perspectives, future directions. *Journal of Archaeological Research* 23(4): 397–450. DOI: 10.1007/s10814-015-9084-1.

DeWitte, Sharon N.
2014. Differential survival among individuals with active and healed periosteal new bone formation. *International Journal of Paleopathology* 7: 38–44.

Van Dijk, F.S., and D.O. Sillence.
2014. Osteogenesis imperfecta: Clinical diagnosis, nomenclature and severity assessment. *American Journal of Medical Genetics, Part A* 164(6): 1470–1481. DOI: 10.1002/ajmg.a.36545.

D'Ortenzio, Lori, Isabelle Ribot, Emeline Raguin, Annabelle Schattmann, Benoit Bertrand, Bonnie Kahlon, and Megan Brickley.
2016. The rachitic tooth: A histological examination. *Journal of Archaeological Science* 74: 152–163. DOI: 10.1016/j.jas.2016.06.006.

D'Ortenzio, Lori, Bonnie Kahlon, Taylor Peacock, Hana Salahuddin, and Megan Brickley.
2018. The rachitic tooth: Refining the use of interglobular dentine in diagnosing vitamin D deficiency. *International Journal of Paleopathology* 22: 101–108.

Dusso, A.S., A.J. Brow, and E.A. Slatopolsky.
2005. Vitamin D and renal failure. In *Vitamin D*, edited by D. Feldman, J.W. Pike, and F.H. Glorieux. 2nd ed. Elsevier Academic Press, London, pp. 1313–1338.

Econs, M.J., and P.T. McEnery.
1997. Autosomal dominant hypophasphatemic rickets/osteomalacia: A clinical characterization of a novel renal phosphate-wasting disorder. *The Journal of Clinical Endocrinology and Metabolism* 82(2): 674–681.

Eggington, Jack, Rebecca Pitt, and Claire Hodson.
2024. A macroscopic assessment of porosity and new bone formation on the inferior pars basilaris: Normal growth or an indicator of scurvy? *International Journal of Paleopathology* 45: 62–72. DOI: 10.1016/j.ijpp.2024.05.001.

El-Hajj Fuleihan, G., M. Nabulsi, H. Tamim, J. Maalouf, M. Salamoun, H. Khalife, M. Choucair, A. Arabi, and R. Vieth.
2006. Effect of vitamin D replacement on musculoskeletal parameters in school children: A randomized control trial. *The Journal of Endocrinology and Metabolism* 91(1): 405–412.

El-Moslimany, Ann P.
1987. The late Pleistocene climates of the Lake Zeribar region (Kurdistan, western Iran) deduced from the ecology and pollen production of non-arboreal vegetation. *Vegetation* 72: 131–139.

Fain, Olivier.
2005. Musculoskeletal manifestations of scurvy. *Joint Bone Spine* 72: 124–128. DOI: 10.1016/j.jbspin.2004.01.007.

Farley, J.R., J.E. Wergedal, and D.J. Baylink.
1983. Fluoride directly stimulates proliferation and alkaline phosphatase activity on bone forming cells. *Science* 222: 330–332.

Fazekas, István Gyula, and Ferenc Kòsa.
1978. *Forensic fetal osteology.* Akadémiai Kiadó, Budapest.

Flannery, K.V.
1971. The origins and ecological effects of early Near Eastern domestication (reprint). In *Prehistoric Agriculture*, edited by S. Struever. American Museum of Natural History, Garden City, New York, pp. 50–79.

1983. Early pig domestication in the fertile crescent: a retrospective look. In *The Hilly Flanks and Beyond: Essays on the Prehistory of Southwestern Asia*, edited by T.C. Jr Young, P.E.L Smith, and P. Mortensen, 36: pp. 163–188.

Floor, Willem.
2021. From quasi-vegetarians to quasi-carnivores: The changing diet of Iranians. *Iranian Studies* 54(5–6): 931–946. DOI: 10.1080/00210862.2020.1810603.

Follis, R.H., D.A. Jackson, and E Park.
1940. The problem of the association of rickets and scurvy. *The American Journal of Disease of Children* 60: 745–747.

Forlino, A., and J.C. Marini.
2016. Osteogenesis imperfecta. *Lancet* 387: 1657–1671.

Fouron, J., and L. Chicoine.
1962. Le scorbut: aspects particuliers del'association rachitisme-scorbut. *Canadian Medical Association Journal* 86: 1191.

Freitag, H.
1977. The pleniglacial, late-glacial, and early postglacial vegetations of Zeribar and their present day counterparts. *Palaeohistoria* 19: 87–95.

Gallego-Llorente, M., S. Connell, E. R. Jones, D.C. Merrett, Y. Jeon, A. Eriksson, V. Siska, C. Gamba, C. Meiklejohn, R. Beyer, S. Jeon, Y. S. Cho, M. Hofreiter, J. Bhak, A. Manica, and R. Pinhasi.
2016. The genetics of an early Neolithic pastoralist from the Zagros, Iran. *Scientific Reports* 6: 1–7. DOI: 10.1038/srep31326.

Garot, Elsa, Christine Couture-Veschambre, David Manton, Vincent Rodriguez, Yannick Lefrais, and Patrick Rouas.
2017. Diagnostic guide enabling distinction between taphonomic stains and enamel hypomineralisation in an archaeological context. *Archives of Oral Biology* 74: 28–36. DOI: 10.1016/j.archoralbio.2016.11.008.

Geber, Jonny, and Eileen Murphy.
2012. Scurvy in the great Irish famine: Evidence of vitamin C deficiency from a mid-19th century skeletal population. *American Journal of Physical Anthropology* 148: 512–524. DOI: 10.1002/ajpa.22066.

Genetic and Rare Diseases Information Center.
Juvenile Paget disease. *National Center for Advancing Translational Sciences.* https://rarediseases.info.nih.gov/diseases/2831/juvenile-paget-disease. Accessed March, 2026.

Ghazala, Nasim.
2022. Rain Shadow deserts. *EBSCO*. ebsco.com/research-starters/earth-and-atmospheric-sciences/rain-shadow-deserts. Accessed October 28, 2025.

Ghodsi, Delaram, Bahareh Nikooyeh, Maryam Amini, Samira Rabiei, Azam Doustmohammadian, Zahra Abdollahi, Mina Minaie, Farzaneh Sadeghi, Cain C.T. Clark, Tirang R. Neyestani, and Hamid Rasekhi.
2023. Dietary supplement use among Iranian households during COVID-19 epidemic lockdown: Less access in those who may need more national food and nutrition surveillance. *International Journal of Preventative Medicine* 14(99): 1–7.

Glab, H., K. Szostek, and K. Kaczanowski.
2006. Hyperostosis frontalis interna, a genetic disease?: Two medieval cases from Southern Poland. *Journal of Comparative Human Biology* 57: 19–27. DOI: 10.1016/j.jchb.2005.08.001.

Glorieux, F.H., and R. St-Arnaud.
2005. Vitamin D pseudoinsufficiency. In *Vitamin D,* edited by D. Feldman, J.W. Pike, and F.H. Glorieux. 2nd ed. Elsevier Academic Press, London, pp. 1197–1206.

González Martín, A., F.J. Robles Rodríguez, O. Cambra-Moo, J. Rascón Pérez, and M. Campo Martín.
2018. Comment upon "Basilar portion porosity: A pathological lesion possibly associated with infantile scurvy." *International Journal of Paleopathology* 20: 114–115. DOI: 10.1016/j.ijpp.2017.09.003.

Gowland, Rebecca L.
2015. Entangled lives: Implications of the developmental origins of health and disease hypothesis for bioarchaeology and the life course. *American Journal of Physical Anthropology* 158: 530–540. DOI: 10.1002/ajpa.22820.

Gray, P.H.K.
1970. A case of osteogenesis imperfecta, associated with dentinogenesis imperfecta, dating from antiquity. *Clinical Radiology* 20: 106–108.

Gresky, Julia, Roman Sokiranski, Florian Witzmann, and Emmanuele Petiti.
2020. The oldest case of osteopetrosis in a human skeleton: exploring the history of rare diseases. *The Lancet Diabetes and Endocrinology* 8: 806–808. DOI: 10.1016/S2213-8587(20)30307-7.

Gulko, Edwin, Lee K. Collins, Robyn C. Murphy, Beverly A. Thornhill, and Benjamin H. Taragin.
2015. MRI findings in pediatric patients with scurvy. *Skeletal Radiology* 44: 291–297. DOI: 10.1007/s00256-014-1962-y.

Gupta, Nishtha, Nikhil Gupta, and Puneet Chhabra.
2016. Image diagnosis: Dental and skeletal fluorosis. *The Permanente journal* 20(1): e105–e106. DOI: 10.7812/TPP/15-048.

Hahn, Timothy, Whitney Adams, and Keith Williams.
2019. Is vitamin C enough? A case report of scurvy in a five-year-old girl and review of the literature. *BMC Pediatrics* 19(74): 1–6. DOI: 10.1186/s12887-019-1437-3.

Hamlin, Carol.
1973. The 1971 Excavations at Seh Gabi, Iran. *Archaeology* 26(3): 224–227.

1974. Seh Gabi, 1973. *Archaeology* 27(4): 274–277.

Hanly, J.G., M.J. McKenna, C. Quigley, R. Freaney, F.P. Muldowney, and M.X. Fitzgerald.
1985. Hypovitaminosis D and response to supplementation in older patients with cystic fibrosis. *Quarterly Journal of Medicine* 56(1): 377–385.

Hatun, S., O. Islam, F. Cizmecioglu, B. Kara, K. Babaoglu, F. Berk, and A.S. Gokalp.
2005. Subclinical vitamin D deficiency is increased in adolescent girls who wear concealing clothing. *Journal of Nutrition* 135(2): 218–222.

Heathcote, Isobel.
1974. The Seh Gabi osteological material. In *Excavations of the Godin project: Second progress report. Archive of Mesopotamian Archaeological Reports (AMAR)*, T. Cuyler Young and Louis D. Levine, 132: pp. 40–41.

Henrickson, Elizabeth F.
1983. *Ceramic Styles and Cultural Interaction in the Early and Middle Chalcolithic of the Central Zagros, Iran*. University of Toronto, Toronto.

1985a. An Updated Chronology of the Early and Middle Chalcolithic of the Central Zagros Highlands, Western Iran. *Iran* 23: 63–108.

1985b. The Early Development of Pastoralism in the Central Zagros Highlands (Luristan). *Iranica Antiqua* 20: 1–42.

1988. Chalcolithic seals and sealing from Seh Gabi, central western Iran. *Iranica Antiqua* 23: 1–22.

1991a. CERAMICS iv: The Chalcolithic period in the Zagros Highlands. *Encyclopaedia Iranica*. https://www.iranicaonline.org/articles/ceramics-iv/.

1991b. CHALCOLITHIC ERA. *Encyclopaedia Iranica.* https://www.iranicaonline.org/articles/chalcolithic-era-in-persia/.

Henrickson, Elizabeth F, and Vanda Vitali.
1987. The Dalma Tradition: Prehistoric inter-regional cultural integration in highland western Iran. *Paléorient* 13(2): 37–45.

Hesse, Brian C.
1978. *Evidence for husbandry from the early Neolithic site of Ganj Dareh in western Iran*. Columbia University.

1982. Slaughter patterns and domestication: The beginnings of pastoralism in western Iran. *Man, New Series* 17(3): 403–417.

1984. These are our goats: The origins of herding in west central Iran. In *Animals and Archaeology: 3: Early Herders and Their Flocks*, edited by J. Clutton and C. Grigon. Oxford: British Archaeological Reports International Series, pp. 243–264.

Hídvégi, Máté, and Radomir Lásztity.
2002. Phytic acid content of cereals and legumes and interactions with proteins. *Periodica Polytechnica Ser. Chem. Eng.* 46(1–2): 59–64.

Hochberg, Ze'ev, and Irit Hochberg.
2019. Evolutionary perspective in rickets and vitamin D. *Frontiers in Endocrinology* 10: 1–10. DOI: 10.3389/fendo.2019.00306.

Hodges, R.E., J. Hood, J.E. Canham, H.E. Sauberlich, and E.M. Baker.
1971. Clinical manifestations of ascorbic acid deficiency in man. *American Journal of Clinical Nutrition* 24(4): 432–443.

Hole, Frank.
1984. A Reassessment of the Neolithic Revolution. *Paléorient* 10(2): 49–60.

1987. *The Archaeology of Western Iran: Settlement and Society from Prehistory to Islamic Conquest*. Ed. Frank Hole.

2007. Agricultural sustainability in the semi-arid Near East. *Climate of the Past* 3: 193–203.

Holick, M.F.
1996. Vitamin D and bone health. *Journal of Nutrition* 126(4 Suppl): 1159S.

1999. Evolution, biologic functions, and recommended dietary allowance for vitamin D. In *Vitamin D: Physiology, molecular biology and clinical applications*, edited by M.F. Holick. Humana Press, Totowa, New Jersey, pp. 1–16.

2002. Vitamin D: The under appreciated D-lightful hormone that is important for skeletal and cellular health. *Current Opinion in Endocrinology, Diabetes and Obesity* 9: 87–98.

2004. Sunlight and vitamin D for bone health and prevention of autoimmune diseases, cancers, and cardiovascular disease. *The American Journal of Clinical Nutrition* 80(6): 1678S-1688S.

2006. Resurrection of vitamin D deficiency and rickets. *Journal of Clinical Investigation* 116(8): 2062–2072.

2007. Vitamin D deficiency. *The New England Journal of Medicine* 357: 266–281.

2008. Vitamin D: A D-Lightful health perspective. *Nutrition Reviews* 66(2): S182–S194.

Holmes, Arthur D., Carleton P. Jones, Anne W. Wertz, John W. Kuzmeski.
1943. The ratio of ascorbic acid, riboflavin and thiamine in raw and pasteurized milk. *The Journal of Nutrition* 26(4): 337–345.

Hovsepian, Silva, Massoud Amini, Ashraf Aminorroaya, Peyvand Amini, and Bijan Iraj.
2011. Prevalence of vitamin D deficiency among adult population of Isfahan City, Iran. *Journal of Health, Population, and Nutrition* 2: 149–155.

HYP Consortium.
1995. A gene (PEX) with homologies to endopeptidases is mutated in patients with X-linked hypophosphatemic rickets. *Natural Genetics* 11: 130–136.

IFP Editorial Staff.
2021. Citrus fruits harvest season begins in North Iran. *Iran Front Page*. November 7. ifpnews.com/citrus-fruits-harvest-season-begins-in-north-iran/. Accessed.

Institute of Medicine (US) Standing Committee on the Scientific Evaluation of Dietary Reference Intakes.
1997. *Dietary reference intakes for calcium, phosphorus, magnesium, vitamin D, and fluoride*. National Academies Press (US), Washington, DC.

Ives, Rachel.
2018. Rare paleopathological insights into vitamin D deficiency rickets, co-occurring illnesses, and documented cause of death in mid-19th century London, UK. *International Journal of Paleopathology* 23: 76–87. DOI: 10.1016/j.ijpp.2017.11.004.

Izuora, Kenneth, Jennifer G. Twombly, Gary M. Whitford, Jennifer Demertzis, Roberto Pacifici, and Michael P. Whyte.
2011. Skeletal fluorosis from brewed tea. *Journal of Clinical Endocrinology and Metabolism* 96(8): 2318–2324. DOI: 10.1210/jc.2010-2891.

Jacob, Robert A.
1990. Assessment of Human Vitamin C Status. *The Journal of Nutrition* 120(suppl_11): 1480–1485.

Jaffe, H.L.
1972. *Metabolic, Degenerative, and Inflammatory Diseases of Bones and Joints*. Lea & Febiger, Philadelphia.

Jazayeri, Maryam, Yousef Moradi, Arezoo Rasti, Manouchehr Nakhjavani, Mahboobeh Kamali, and Hamid Reza Baradaran.
2018. Prevalence of vitamin D deficiency in healthy Iranian children: A systematic review and meta-analysis. *Medical Journal of the Islamic Republic of Iran* 32(83): 1–6. DOI: 10.14196/mjiri.32.83.

Jokar, Mohammadhassan, Mohammadreza Hatef Fard, and Zahra Mirfeizi.
2008. Rickets and osteomalacia in northeast Iran: report of 797 cases. *International Journal of Rheumatic Diseases* 11: 170–174.

Kamoun-Goldrat, Agnès, and Martine le Merrer.
2008. Infantile Cortical Hyperostosis (Caffey Disease): A review. *Journal of Oral and Maxillofacial Surgery* 66: 2145–2150. DOI: 10.1016/j.joms.2007.09.007.

Kazemi, Alinaghi, Faranak Sharifi, Nahid Jafari, and Nouraddin Mousavinasab.
2009. High prevalence of Vitamin D Deficiency among pregnant women and their newborns in an Iranian population. *Journal of Women's Health* 18(6): 835–839.

Kazemi, Ranin.
2016. Of diet and profit: on the question of subsistence crises in nineteenth-century Iran. *Middle Eastern Studies* 52(2): 335–358. DOI: 10.1080/00263206.2015.1119123.

Kimball, S., G.E.H. Fuleihan, and R. Vieth.
2008. Vitamin D: A growing perspective. *Critical Reviews in Laboratory Sciences* 45: 339–414.

Klaus, H.D.
2017. Paleopathological rigor and differential diagnosis: Case studies involving terminology, description, and diagnostic frameworks for scurvy in skeletal remains. *International Journal of Paleopathology* 19: 96–110.

Kondyli, Efthymia, Maria C. Katsiari, Leandros P. Voutsinas.
2007. Variations of vitamin and mineral contents in raw milk of the indigenous Greek breed during lactation. *Food Chemistry* 100(1): 226–230.

Koon, Hannah.
2010. Scurvy bones: A collagen biomarker to detect vitamin C deficiency in archaeological bone. In *Fourth International Symposium on Biomolecular Archaeology Conference Programme and Abstracts*, pp. 79.

Kramer, Carol.
1982. *Village Ethnoarchaeology: Rural Iran in Archaeological Perspective*. Academic Press, New York.

Küçükaydin, Zeynep, Ismail Dursun, Burcu Daldaban, Alper Özcan, and Ekrem Ünal.
2018. Scurvy: A rare cause of arthritis in a child with neurologic disorder. *European Journal of Rheumatology* 5(4): 283–284. DOI: 10.5152/eurjrheum.2018.17165.

Larsen, Clark S.
1995. Biological changes in human populations with agriculture. *Annual Review of Anthropology* 24: 185–213.

Lazaridis, Iosif, Dani Nadel, Gary Rollefson, Deborah C. Merrett, Nadin Rohland, Swapan Mallick, Daniel Fernandes, Mario Novak, Beatriz Gamarra, Kendra Sirak, Sarah Connell, Kristin Stewardson, Eadaoin Harney, Qiaomei Fu, Gloria Gonzalez-Fortes, Eppie R. Jones, Songül Alpaslan Roodenberg, György Lengyel, Fanny Bocquentin, Boris Gasparian, Janet M. Monge, Michael Gregg, Vered Eshed, Ahuva Sivan Mizrahi, Christopher Meiklejohn, Fokke Gerritsen, Luminita Bejenaru, Matthias Blüher, Archie Campbell, Gianpiero Cavalleri, David Comas, Philippe Froguel, Edmund Gilbert, Shona M. Kerr, Peter Kovacs, Johannes Krause, Darren McGettigan, Michael Merrigan, D. Andrew Merriwether, Seamus O'Reilly, Martin B. Richards, Ornella Semino, Michel Shamoon-Pour, Gheorghe Stefanescu, Michael Stumvoll, Anke Tönjes, Antonio Torroni, James F. Wilson, Loic Yengo, Nelli A. Hovhannisyan, Nick Patterson, Ron Pinhasi, and David Reich.
2016. Genomic insights into the origin of farming in the ancient Near East. *Nature* 536(7617): 419–424. DOI: 10.1038/nature19310.

Léger, Daniel.
2008. Scurvy: Reemergence of nutritional deficiencies case description. *Canadian Family Physician* 54: 1403–1406.

Levine, Louis D.
1974. Survey of excavations in Iran during 1972-73. The Godin Project: Seh Gabi. *Iran* 12: 211–213.

1990. *Microprovenance Studies of Archaeological Ceramics: A Case Study from the Kangavar and Mahidasht Valleys, Central Western Iran*.

Lewis, Mary E.
2012. Thalassaemia: Its diagnosis and interpretation in past skeletal populations. *International Journal of Osteoarchaeology* 22(6): 685–693. DOI: 10.1002/oa.1229.

2019. Skeletal dysplasias and related conditions. In *Ortner's Identification of Pathological Conditions in Human Skeletal Remains*, edited by Jane E. Buikstra. Academic Press, pp. 615–637.

Libby, Peter, and Masanori Aikawa.
2002. Vitamin C, collagen, and cracks in the plaque. *Circulation* 105(12): 1396–1398. DOI: 10.1161/01.CIR.0000012513.58079.EA.

Lips, P.
2012. Interaction between vitamin D and calcium. *Scandinavian Journal of Clinical and Laboratory Investigation* Suppl. 72(Suppl. 243): 60–64.

Loria, Catherine M., Paul K. Whetton, Laura E. Caulfield, Moyses Szklo, Michael J. Klag, and Catherine Loria.
1998. Agreement among Indicators of Vitamin C Status. *American Journal of Epidemiology* 147(6): 587–596.

Maakaron, J.E., A.T. Taher, and M.E. Conrad.
2016. Anemia practice essentials, pathophysiology, etiology. *MedScape*.

Madeline, Lee A., and Allen D. Elster.
1995. Suture closure in the human chondrocranium: CT assessment. *Radiology* 196(3): 747–756.

Maghbooli, Zhila, Arash Hossein-Nezhad, Ali Reza Shafaei, Farzaneh Karimi, Farzaneh Sadat Madani, and Bagher Larijani.
2007. Vitamin D status in mothers and their newborns in Iran. *BMC Pregnancy and Childbirth* 7. DOI: 10.1186/1471-2393-7-1.

Maiyegun, S.O., A.H. Malek, L.V. Devarajan, and M.H. Dahniya.
2002. Severe congenital rickets secondary to maternal hypovitaminosis D: A case report. *Annals of Tropical Paediatrics* 22: 191–195.

Majeed, Rehana, Yasmeen Memon, Mansoor Khowaja, Farrukh Majeed, Mohammad Usman Ali, and Uzma Rajar.
2007. Contributing factors of rickets among children at Hyderabad. *Journal of Liaquat University of Medical and Health Sciences* 6(2): 60–65.

Malik, Sadia M., Haroon Awan, and Niazullah Khan.
2012. Mapping vulnerability to climate change and its repercussions on human health in Pakistan. *Globalization and Health* 8(31): 1–10. DOI: 10.1186/1744-8603-8-31.

Malloy, P.J., and D. Feldman.
2003. Hereditary 1,25-dihydroxyvitamin-D resistant rickets. In *Vitamin D and Rickets*, edited by Z. Hochberg. Karger AG, Basel, pp. 1–13.

Ma'luf, R., W. Zein, M. El Deiri, and Z. Bashshur.
2002. Bilateral subperiosteal hematomas and Henoch-Schonlein purpura. *Archives of Ophthalmology* 120: 1398–1399.

Manaseki-Holland, Semira, M. Zulf Mughal, Zulfiqar Bhutta, and M. Qasem Shams.
2008. Vitamin D status of socioeconomically deprived children in Kabul, Afghanistan. *International Journal for Vitamin and Nutrition Research* 78(1): 16–20. DOI: 10.1024/0300-9831.78.1.16.

Mardi, Golnaz Hossein.
2025. A petrographic approach to study Dalma pottery at the sites of Seh Gabi, Godin Tepe, and Tepe Siahbid in the Central Zagros of Iran. *Journal of Archaeological Science: Reports* 63, pp. 1–17.

Marini, J.C., W.A. Cabral, A.M. Barnes, and W. Chang.
2007. Components of the collagen prolyl 3-hydroxylation complex are crucial for normal bone development. *Cell Cycle* 6(14): 1675–1681.

Matthee, Rudolph.
2016. Patterns of Food Consumption in Early Modern Iran. In *Oxford Handbooks Online.* Oxford University Press, February 11, pp. 1–28.

Matthews, Roger, Wendy Matthews, and Amy Richardson.
2013. Radiocarbon dating of Sheikh-e Abad and Jani. In *The earliest Neolithic of Iran: 2008 excavations at Sheik-e Abad and Jani*, edited by R. Matthews, W. Matthews, and Y. Mohammadifar. Oxbow Books, pp. 61–66.

Matthews, Rogers, and Hassan Fazeli Nashli.
2022. *The archaeology of Iran from the Palaeolithic to the Achaemenid Empire.* Routledge.

Mays, Simon A.
2008. A likely case of scurvy from early bronze age Britain. *International Journal of Osteoarchaeology* 18: 178–187. DOI: 10.1002/oa.930.

2020. A dual process model for paleopathological diagnosis. *International Journal of Paleopathology* 31: 89–96. DOI: 10.1016/j.ijpp.2020.10.001.

Mays, Simon, Tracy Prowse, Michele George, and Megan Brickley.
2018. Latitude, urbanisation, age and sex as risk factors for vitamin D deficiency disease in the Roman Empire. *American Journal of Physical Anthropology* 167(3): 484–496.

Mays, Simon, Megan Brickley, and Rachel Ives.
2006. Skeletal manifestation of rickets in infants and young children in a historic population from England. *American Journal of Physical Anthropology* 129: 362–374. DOI: 10.1002/ajpa.20292.

McDonald, M.M.A.
1979. *An Examination of Mid-Holocene Settlement Patterns in the Central Zagros Region of western Iran*. PhD Dissertation, University of Toronto.

Mehta, Dhaval, and Jigna Shah.
2013. Reversal of dental fluorosis: A clinical study. *From: Journal of Natural Science* 4(1).

Meiklejohn, Christopher, Deborah C. Merrett, David Reich, and Ron Pinhasi.
2017. Direct dating of human skeletal material from Ganj Dareh, early Neolithic of the Iranian Zagros. *Journal of Archaeological Science: Reports* 12: 165–172.

Melville, Charles.
1984. Meteorological hazards and disasters in Iran: A preliminary survey to 1950. *Iran* 22: 113–150.

Melvin, K.E.W., G.W. Hepner, P. Bordier, G. Neale, and G.F. Joplin.
1970. Calcium metabolism and bone pathology in adult coeliac disease. *Quarterly Journal of Medicine* 39(153): 83–113.

Merrett, Deborah C.
2004. *Bioarchaeology in Early Neolithic Iran: Assessment of Health Status and Subsistence Strategy*. University of Manitoba, Winnipeg.

2006. Infant health: Assessing adaptation and stability of transitional early neolithic subsistence economies in the Zagros Mountains. In *American Association of Physical Anthropology.* Anchorage, Alaska.

2018. Infant age estimation. In *Frontiers in Archaeological Science 2.* Burnaby, British Columbia.

2019. Vitamin D Deficiency in Chalcolithic Iran: Links between maternal and childhood health. In *American Anthropological Association*. Vancouver.

Merrett, Deborah C., Christina Cheung, Christopher Meiklejohn, and Michael P. Richards.
2021. Stable isotope analysis of human bone from Ganj Dareh, Iran, ca. 10,100 calBP. *PLoS ONE* 16(3): 1–15. DOI: 10.1371/journal.pone.0247569.

Miller, Naomi F.
1990. Godin Tepe, Iran: Plant remains from Period V, the late fourth millennium B.C. *MASCA Ethnobotanical Report* 6: 1–12.

Mimasaka, S., M. Funayama, N. Adachi, M. Nata, and M. Morita.
2000. A fatal case of infantile scurvy. *International Journal of Legal Medicine* 114: 122–124.

Mithal, A., N Trivedi, S.K. Gupta, S Kumar, and R.K. Gupta.
1993. Radiological spectrum of endemic fluorosis: Relationship with calcium intake. *Skeletal Radiology* 22(4): 257–261.

Mithal, A., D. A. Wahl, J. P. Bonjour, P. Burckhardt, B. Dawson-Hughes, J. A. Eisman, G. El-Hajj Fuleihan, R. G. Josse, P. Lips, and J. Morales-Torres.
2009. Global vitamin D status and determinants of hypovitaminosis D. *Osteoporosis International* 20: 1807–1820. DOI: 10.1007/s00198-009-0954-6.

Molleson, T., and M. Cox.
1993. *The Spitalfields Project, Volume 2: The Anthropology*. Council for British Archaeology, York, UK.

Monsen, E.R.
2000. Dietary reference intakes for the antioxidant nutrients: vitamin C, vitamin E, selenium, and carotenoids. *Journal of the American Dietetic Association* 100(6): 637–640.

Moore, Joanna, and Hannah E.C. Koon.
2017. Basilar portion porosity: A pathological lesion possibly associated with infantile scurvy. *International Journal of Paleopathology* 18: 92–97. DOI: 10.1016/j.ijpp.2017.05.010.

Moorrees, Coenraad FA., Elizabeth A. Fanning, and Edward E. Hunt Jr.
1963. Age variation of formation stages for ten permanent teeth. *Journal of Dental Research* 42(6): 1490–1502.

Moreno-Jiménez, Eduardo, César Plaza, Hugo Saiz, Rebeca Manzano, Maren Flagmeier, and Fernando T. Maestre.
2019. Aridity and reduced soil micronutrient availability in global drylands. *Nature Sustainability* 2(5): 371–377.

Morley, R., J. Carlin, J. Pasco, and J. Wark.
2006. Maternal 25-hydroxyvitamin D and parathyroid hormone concentrations and offspring birth size. *The Journal of Clinical Endocrinology and Metabolism* 91(3): 906–912.

Morton, June D., and Henry P. Schwarcz.
2004. Paleodietary implication from stable isotopic analysis of residues on prehistoric Ontario ceramics. *Journal of Archaeological Science* 31: 503–517.

Motarjem, Abbas, and Mahnaz Sharifi.
2014. Cultural development of Chalcolithic era in the east of Central Zagros based on archaeological excavations at Tepe Gheshlagh. *IRANIAN JOURNAL OF ARCHAEOLOGICAL STUDIES* 4: 49–65.

Motedayen, Morteza, Majid Dousti, Fatemeh Sayehmiri, and Aziz A. Pourmahmoudi.
2019. An Investigation of the Prevalence and Causes of Malnutrition in Iran: A Review Article and Meta-analysis. *Clinical Nutrition Research* 8(2): 101. DOI: 10.7762/cnr.2019.8.2.101.

Moussavi, Mohammad, Reza Heidarpour, Ashraf Aminorroaya, Zahra Pournaghshband, and Massoud Amini.
2005. Prevalence of vitamin D deficiency in Isfahani high school students in 2004. *Hormone Research* 64: 144–148. DOI: 10.1159/000088588.

Narasimhan, Vagheesh M., Nick Patterson, Priya Moorjani, Nadin Rohland, Rebecca Bernardos, Swapan Mallick, Iosif Lazaridis, Nathan Nakatsuka, Iñigo Olalde, Mark Lipson, Alexander M. Kim, Luca M. Olivieri, Alfredo Coppa, Massimo Vidale, James Mallory, Vyacheslav Moiseyev, Egor Kitov, Janet Monge, Nicole Adamski, Neel Alex, Nasreen Broomandkhoshbacht, Francesca Candilio, Kimberly Callan, Olivia Cheronet, Brendan J. Culleton, Matthew Ferry, Daniel Fernandes, Suzanne Freilich, Beatriz Gamarra, Daniel Gaudio, Mateja Hajdinjak, Éadaoin Harney, Thomas K. Harper, Denise Keating, Ann Marie Lawson, Matthew Mah, Kirsten Mandl, Megan Michel, Mario Novak, Jonas Oppenheimer, Niraj Rai, Kendra Sirak, Viviane Slon, Kristin Stewardson, Fatma Zalzala, Zhao Zhang, Gaziz Akhatov, Anatoly N. Bagashev, Alessandra Bagnera, Bauryzhan Baitanayev, Julio Bendezu-Sarmiento, Arman A. Bissembaev, Gian Luca Bonora, Temirlan T. Chargynov, Tatiana Chikisheva, Petr K. Dashkovskiy, Anatoly Derevianko, Miroslav Dobeš, Katerina Douka, Nadezhda Dubova, Meiram N. Duisengali, Dmitry Enshin, Andrey Epimakhov, Alexey V. Fribus, Dorian Fuller, Alexander Goryachev, Andrey Gromov, Sergey P. Grushin, Bryan Hanks, Margaret Judd, Erlan Kazizov, Aleksander Khokhlov, Aleksander P. Krygin, Elena Kupriyanova, Pavel Kuznetsov, Donata Luiselli, Farhod Maksudov, Aslan M. Mamedov, Talgat B. Mamirov, Christopher Meiklejohn, Deborah C. Merrett, Roberto Micheli, Oleg Mochalov, Samariddin Mustafokulov, Ayushi Nayak, Davide Pettener, Richard Potts, Dmitry Razhev, Marina Rykun, Stefania Sarno, Tatyana M. Savenkova, Kulyan Sikhymbaeva, Sergey M. Slepchenko, Oroz A. Soltobaev, Nadezhda Stepanova, Svetlana Svyatko, Kubatbek Tabaldiev, Maria Teschler-Nicola, Alexey A. Tishkin, Vitaly V. Tkachev, Sergey Vasilyev, Petr Velemínský, Dmitriy Voyakin, Antonina Yermolayeva, Muhammad Zahir, Valery S. Zubkov, Alisa Zubova, Vasant S. Shinde, Carles Lalueza-Fox, Matthias Meyer, David Anthony, Nicole Boivin, Kumarasamy Thangaraj, Douglas J. Kennett, Michael Frachetti, Ron Pinhasi, and David Reich.

2019. The formation of human populations in South and Central Asia. *Science* 365(6457). DOI: 10.1126/science.aat7487.

National Institute of Arthritis and Musculoskeletal and Skin Diseases.

Juvenile Osteoporosis. https://www.niams.nih.gov/health-topics/juvenile-osteoporosis#:~:text=What%20is%20juvenile%20osteoporosis?,on%20how%20osteoporosis%20is%20diagnosed.

Naveen, Kikkeri Narayanashetty, Varadraj V. Pai, Praveen Bagalkot, Vijay Kulkarni, Priyanka Rashme, and Sharatchandra Athanikar.

2013. Pellagra in a child – A rare entity. *Nutrition* 29: 1426–1428.

Nekouei, Parisa, and R. Yousefi Zoshk.

2021. Cultural interactions of prehistoric societies of central Iranian plateau with residents of Central Zagros, Fars and southwestern of Iran during the fifth millennium BC. *Journal of Archaeological Studies* 13(1): 223–258. DOI: 10.22059/jarcs.2020.

Nelson, Elizabeth A., Christine L. Halling, and Jane E. Buikstra.

2019. Evidence of skeletal fluorosis at the Ray Site, Illinois, USA: A pathological assessment and discussion of environmental factors. *International Journal of Paleopathology* 26: 48–60. DOI: 10.1016/j.ijpp.2019.05.003.

Nistala, Harikiran, Outi Mäkitie, and Harald Jüppner.
2014. Caffey disease: New perspectives on old questions. *Bone* 60: 246–251. DOI: 10.1016/j.bone.2013.12.030.

Nord, Anders G., Henk Kars, Inga Ullén, Kate Tronner, and Eva Kars.
2005. Deterioration of archaeological bone — a statistical approach. *Journal of Nordic Archaeological Science* 15: 77–86.

Oberhelman, S., and T. Thacher.
2013. Vitamin D in the 21st Century: An overview. In *Handbook of Vitamin D in Human Health. Prevention, Treatment and Toxicity*, edited by R.R. Watson. Wageringen Academic Publishers, Wageringen, pp. 13–38.

Office of the Surgeon General (US).
2004. *Bone Health and Osteoporosis: A Report of the Surgeon General*.

Ortner, Donald J.
2003. *Identification of Pathological Conditions in Human Skeletal Remains.* Academic Press, San Diego.

Ortner, Donald J., Whitney Butler, Jessica Cafarella, and Lauren Milligan.
2001. Evidence of probable scurvy in subadults from archeological sites in North America. *American Journal of Physical Anthropology* 114: 343–351.

Ortner, Donald J., and Mary Frances Ericksen.
1997. Bone changes in the human skull probably resulting from scurvy in infancy and childhood. *International Journal of Osteoarchaeology* 7: 212–220.

Ortner, Donald J., Erin H. Kimmerle, and Melanie Diez.
1999. Probable evidence of scurvy in subadults from archeological sites in Peru. *American Journal of Physical Anthropology* 108: 321–331.

Ortner, Donald J., and Simon Mays.
1998. Dry-bone manifestations of rickets in infancy and early childhood. *International Journal of Osteoarchaeology* 8(1): 45–55.

Ortner, Donald J., and Walter G.J. Putschar.
1985. *Identification of Pathological Conditions in Human Skeletal Remains.* Smithsonian Institution Press, Washington.

Özkan, Behzat.
2010a. Nutritional Rickets in Turkey. *The Eurasian Journal of Medicine* 42: 86–91. DOI: 10.5152/eajm.2010.24.

2010b. Nutritional rickets. *Journal of Clinical Research in Pediatric Endocrinology* 2(4): 137–143. DOI: 10.4274/jcrpe.v2i4.137.

Özkan, Behzat, Hakan Doneray, Mehmet Karacan, Serhat Vançelik, Zuhal Keskin Yıldırım, Asuman Ozkan, Celalettin Kosan, and Kamil Aydın.
2009. Prevalence of vitamin D deficiency rickets in the eastern part of Turkey. *European Journal of Pediatrics* 168: 95–100. DOI: 10.1007/s00431-008-0821-z.

Ozsvath, D.L.
2009. Fluoride and environmental health, a review. *Review of Environmental Science and Bio/technology* 8: 59–79.

Parfitt, A.M., J.C. Gallagher, R.P. Heaney, C.C. Johnston, R. Neer, and G.D. Whedon.
1982. Vitamin D and bone health in the elderly. *The American Journal of Clinical Nutrition* 36(5): 1014–1031.

Patel, R.M., S.C.S. Nagamani, D. Cuthbertson, P. M. Campeau, J.P. Krischer, J.R. Shapiro, R.D. Steiner, P.A. Smith, M.B. Bober, P.H. Byers, M. Pepin, M. Durigova, F.H. Glorieux, F. Rauch, B.H. Lee, T. Hart, and V.R. Sutton.
2015. A cross-sectional multicenter study of osteogenesis imperfecta in North America - results from the linked clinical research centers. *Clinical Genetics* 87(2): 133–140. DOI: 10.1111/cge.12409.

Peasnall, B.L.
2002. Iranian Chalcolithic. In *Encyclopedia of Prehistory*, edited by P.N. Peregrine and M. Ember. Pp. 160–165. Springer US.

Perumal, Ekambaram, Vanaja Paul, Vimal Govindarajan, and Lakshmikanthan Panneerselvam.
2013. A brief review on experimental fluorosis. *Toxicology Letters* 223: 236–251. DOI: 10.1016/j.toxlet.2013.09.005.

Petrone, Pierpaolo, Michele Giordano, Stefano Giustino, and Fabio M. Guarino.
2011. Enduring fluoride health hazard for the Vesuvius area population: The case of AD 79 Herculaneum. *PLoS ONE* 6(6). DOI: 10.1371/journal.pone.0021085.

Pettifor, John M.
2008. Vitamin D &/or calcium deficiency rickets in infants & children: a global perspective. *Indian J Med Res* 127: 245–249.

Pitre, Mindy C., Robert J. Stark, and Maria Carmela Gatto.
2016. First probable case of scurvy in ancient Egypt at Nag el-Qarmila, Aswan. *International Journal of Paleopathology* 13: 11–19. DOI: 10.1016/j.ijpp.2015.12.003.

Pitt, M.
1988. Rickets and osteomalacia. In *Diagnosis of Bone and Joint Disorders,* edited by D. Resnick and G. Niwayama. second. W.B. Saunders, Philadelphia, 8: pp. 2086–2119.

1995. Rickets and Osteomalacia. In *Diagnosis of Bone and Joint Disorders*, edited by D. Resnick. 3rd ed. W.B. Saunders, London, pp. 1885–1892.

Popovich, Debbie, Allison McAlhany, Abimbola O. Adewumi, and Marilyn McKim Barnes.
2009. Scurvy: Forgotten but definitely not gone. *Journal of Pediatric Health Care* 23(6): 405–415. DOI: 10.1016/j.pedhc.2008.10.008.

Priemel, M., C. von Domarus, T.O. Klatte, S. Kessler, J. Schlie, S. Meier, N. Proksch, F. Pastor, C. Netter, T. Streichert, K. Püschel, and M. Amling.
2010. Bone mineralization defects and vitamin D deficiency: histomorphometric analysis of iliac crest bone biopsies and circulating 25-hydroxyvitamin D in 675 patients. *Journal of Bone and Mineral Research* 25(2): 305–312.

Public Health Ontario.
2022. Tell me more: Epidemiology. https://www.publichealthontario.ca/en/About/News/2022/Epidemiology-Tell-Me-More. Accessed March, 2026.

Rabiee, Fatimeh, and Catherine Geissler.
1992. The impact of maternal workload on child nutrition in rural Iran. *Food and Nutrition Bulletin* 14(1): 1–6.

Rajakumar, Kumaravel, and Stephen B. Thomas.
2005. Reemerging nutritional rickets: A historical perspective. *Archives of Pediatrics and Adolescent Medicine* 159: 335–341.

Redding, Richard W.
1988. A general explanation of subsistence change: From hunting and gathering to food production. *Journal of Anthropological Archaeology* 7: 56–97.

Redfield, Alden.
1970. A new aid to aging immature skeleton: Development of the occipital bone. *American Journal of Physical Anthropology* 33(2): 207–220.

Reid, Claudia, and Rhonda Graham.
2024. A case of rickets and pediatric iron deficiency anemia in Alabama. *Cureus* 16(5): e60140.

Renette, Steve, and Sirvan Mohammadi Ghasrian.
2020. The central and northern Zagros during the Late Chalcolithic: An updated ceramic chronology based on recent fieldwork results in western Iran. *Paléorient* 46(1–2): 109–132. DOI: 10.4000/paleorient.366.

Resnick, D., and G. Niwayama.
1983. Entheses and enthesopathy. Anatomical, pathological, and radiological correlation. *Radiology* 146(1): 1–9.

Richter, Tobias, Hojjat Darabi, Sajjad Alibaigi, Amaia Arranz-Otaegui, Pernille Bangsgaard, Shokouh Khosravi, Lisa Maher, Peder Mortensen, Patrick Pedersen, Joe Roe, and Lisa Yeomans.
2021. The formation of early Neolithic communities in the Central Zagros: An 11,500 year-old communal structure at Asiab. *Oxford Journal of Archaeology* 40(1): 2–22.

Rinaldo, Natascia, Nicoletta Zedda, Barbara Bramanti, Irene Rosa, and Emanuela Gualdi-Russo.
2019. How reliable is the assessment of Porotic Hyperostosis and Cribra Orbitalia in skeletal human remains? A methodological approach for quantitative verification by means of a new evaluation form. *Archaeological and Anthropological Sciences* 11(7): 3549–3559. DOI: 10.1007/s12520-019-00780-0.

Roberts, Charlotte, and Keith Manchester.
2007. *The Archaeology of Disease*. 3rd ed. Cornell University Press, Ithaca, New York.

Robinowitz, C.
2009. Appropriate supplementation of vitamin D: Report of the Council on Science and Public Health. CSAPH Report 4-A-09. https://www.ama-assn.org/sites/ama-assn.org/files/corp/media-browser/public/about-ama/councils/Council%20Reports/council-on-science-public-health/a09-csaph-vitamin-d-supplementation.pdf. Accessed.

Rothman, M.S.
2011. The Environment of Godin Tepe. In *On the High Road: The History of Godin Tepe, Iran,* edited by H Gopnik and M.S. Rothman. Royal Ontario Museum Press, Toronto, pp. 49–66.

Rothman, M.S., and V.S. Badler.
2011. Contact and development in Godin Period VI. In *On the High Road: The History of Godin Tepe, Iran,* edited by H Gopnik and M.S. Rothman. Royal Ontario Museum Press, Toronto, pp. 67–138.

Rothschild, Bruce M., and Christine Rothschild.
1997. Congenital syphilis in the archaeological record: Diagnostic insensitivity of osseous lesions. *International Journal of Osteoarchaeology* 7: 39–42.

Rowan, Yorke.
2014. The mortuary process in the Chalcolithic period. *Masters of Fire: Copper Age Art from Israel:* 101–112.

Rowan, Yorke M., and Jonathan Golden.
2009. The Chalcolithic period of the Southern Levant: A synthetic review. *Journal of World Prehistory* 22: 1–92. DOI: 10.1007/s10963-009-9016-4.

Rowan, Yorke M., and Jaimie L. Lovell.
2011. Introduction: Culture, chronology and the Chalcolithic. In *Culture, Chronology, and the Chalcolithic: Theory and Transition*. Oxbow Books, pp. 1–11.

Roy, Sudipta, A.R.M. Luthful Kabir, Rahat Bin Habib, Masuma Khan, Armin Sultana, and Ashraf Uddin Ahmed.
2020. Co-occurrence of rickets and scurvy – A case report. *The Journal of Ad-din Women's Medical College* 8(2): 35–39.

Salimpour, R.
1975. Rickets in Tehran: Study of 200 cases. *Archives of Disease in Childhood* 50: 63–66. DOI: 10.1136/adc.50.1.63.

Santiago-Marrero, Carlos G., Ali Metin Büyükkarakaya, Ezgi Küçükel, and Jaroslav Řídký.
2025. Microbotanical analyses of dental calculus and caries occurrence at Neolithic Tepecik-Çiftlik, Türkiye: Insights into diet and oral health. *Archaeological and Anthropological Sciences* 17: 15.

Sarraf, Zahra, Dena Goldberg, Mohammad Shahbazi, Kristen Arbuckle, and Moosa Salehi.
2005. Nutritional status of schoolchildren in rural Iran. *British Journal of Nutrition* 94: 390–396. DOI: 10.1079/bjn20051487.

Schaefer, Maureen, Sue Black, and Louise Scheuer.
2009. *Juvenile osteology: A laboratory and field manual.* Academic Press.

Schats, Rachel.
2021. Cribriotic lesions in archaeological human skeletal remains. Prevalence, co-occurrence, and association in medieval and early modern Netherlands. *International Journal of Paleopathology* 35: 81–89. DOI: 10.1016/j.ijpp.2021.10.003.

Schattmann, Annabelle, Benoît Bertrand, Sophie Vatteoni, and Megan Brickley.
2016. Approaches to co-occurrence: Scurvy and rickets in infants and young children of 16-18th century Douai, France. *International Journal of Paleopathology* 12: 63–75. DOI: 10.1016/j.ijpp.2015.12.002.

Schattmann, Annabelle F.
2014. *The Co-occurrence of Scurvy and Rickets in 16th to 18th Century Skeletal Material from Douai, France*. McMaster University, Hamilton, November.

Schmandt-Besserat, Denise, and Niloufar Moghimi.
2017. Making tokens talk. In, *Non-scribal Communication Media in the Bronze Age Aegean and Surrounding Areas.* Firenze University Press, pp. 175–185.

Scheuer, Louise, and Sue Black.
2000. *Developmental Juvenile Osteology.* Academic Press.

Scheuer, Louise, Johnathan H. Musgrave, and Suzanne P. Evans.
1980. The estimation of late fetal and perinatal age from limb long bone length by linear and logarithmic regression. *Annals of Human Biology* 7(3): 257–265.

Scott, Michael.
2018. *Stable Isotope Analysis of Human Remains from Seh Gabi, Iran*.

Sellami, Meriem, Hend Riahi, Kaouther Maatallah, Hanen Ferjani, Mouna Chelli Bouaziz, and Mohamed Fethi Ladeb.
2020. Skeletal fluorosis: don't miss the diagnosis! *Skeletal Radiology* 49: 345–357. DOI: 10.1007/s00256-019-03302-0.

Şener, Elçin, Ali Taş, and Ahmet Cem Erkman.
2026. A new society emerges in Anatolia: Bioarchaeological perspectives on the Late Neolithic and Early Chalcolithic population of Gökhöyük (GH). *International Journal of Osteoarchaeology* 36: 297–309.

Senoir, N.
1983. Aspects of infant feeding in eighteenth-century France. *Eighteenth-Century Studies* 16: 376–388.

She, Rosemary, and Juliana Szakacs.
2004. Hyperostosis Frontalis Interna: Case report and review of literature. *Annals of Clinical & Laboratory Science* 34(2): 206–208.

Sheldrick, P.G.
1980. Skinny bones from Dakhleh Oasis. *Paleopathology Newsletter* 30: 7–10.

Shin, Natalya, Nader Ghotbi, and William B. Claster
2008. Increased risk of rickets among infants raised in the Uzbek Cradle, Beshik. *Acta Med. Nagasaki* 53: 55–58.

Smith, P.E.L., and T.C. Young.
1972. The evolution of early agriculture and culture in greater Mesopotamia: A trial model. In *Population Growth: Anthropological Implications*. MIT Press, Cambridge, MA, pp. 1–59.

1983. The force of numbers: Population pressure in the western Zagros 12,000-4,500 B.C. In *The Hilly Flanks and Beyond: Essays on the Prehistory of Southwestern Asia*, edited by T.C. Young, P.E.L. Smith, and P Mortensen. Oriental Institute, Chicago, pp. 141–159.

Snoddy, Anne Marie E., Hallie R. Buckley, Gail E. Elliott, Vivien G. Standen, Bernardo T. Arriaza, and Siân E. Halcrow.
2018. Macroscopic features of scurvy in human skeletal remains: A literature synthesis and diagnostic guide. *American Journal of Physical Anthropology* 167: 876–895. DOI: 10.1002/ajpa.23699.

Spranger, J.W., P.W. Brill, and A. Poznanski.
2002. *Bone Dysplasias: An Atlas of Genetic Disorders of Skeletal Development*. Oxford University Press, Oxford.

Srienc-Ściesiek, Magdalena T., Nina Richards, Sabine Ladstätter, and Sylvia Kirchengast.
2024. Evidence of non-adult vitamin C deficiency in three early medieval sites in the Jaun/Podjuna Valley, Carinthia, Austria. *International Journal of Paleopathology* 45: 18–29. DOI: 10.1016/j.ijpp.2024.02.002.

Stiene, Jennifer Michelle, and Patrick William Frank.
2022. Hyperostosis Frontalis Interna and a question on its pathology: A case report. *American Journal of Case Reports* 23: e937450-. DOI: 10.12659/AJCR.937450.

Streym, Susanna Vio, Carsten S. Højskov, Ulla Kristine Møller, Lene Heickendorff, Peter Vestergaard, Leif Mosekilde, and Lars Rejnmark.
2016. Vitamin D content in human breast milk: A 9-mo follow-up study. *American Journal of Clinical Nutrition* 103: 107–114. DOI: 10.3945/ajcn.115.115105.

Sullivan, Amy.
2005. Prevalence and etiology of acquired anemia in Medieval York, England. *American Journal of Physical Anthropology* 128: 252–272. DOI: 10.1002/ajpa.20026.

Szeniczey, Tamás, Antónia Marcsik, Zsófia Ács, Tímea Balassa, Zsolt Bernert, Katalin Bakó, Tamás Czuppon, Anna Endrődi, Sándor Évinger, Zoltán Farkas, Lucia Hlavenková, Krisztina Hoppál, Csaba Kálmán Kiss, Krisztián Kiss, Kinga Kocsis, Loránd Olivér Kovács, Péter F. Kovács, Kitti Köhler, László Költő, Ivett Kővári, Orsolya László, Gabriella Lovász, Júlia Lovranits, József Lukács, Zsófia Masek, Mónika Merczi, Erika Molnár, Csilla Emese Németh, János Gábor Ódor, László Paja, Ildikó Pap, Róbert Patay, István Rácz, Zsófia Rácz, Ágnes Ritoók, Gergely Szenthe, Gábor Szilas, Béla Miklós Szőke, Zoltán Tóth, Tivadar Vida, Katalin Wolff, Michael Finnegan, and Tamás Hajdu.
2019. Hyperostosis frontalis interna in ancient populations from the Carpathian Basin – A possible relationship between lifestyle and risk of development. *International Journal of Paleopathology* 24: 108–118. DOI: 10.1016/j.ijpp.2018.10.003.

Tabrizi, Reza, M. Moosazadeh, M. Akbari, Mohammed Hossein Dabbaghmanesh, Minoo Mohamadkhani, Zatollah Asemi, Seyed Taghi Heydari, Mojtaba Akbari, and Kamran B Lankarani.
2018. High prevalence of Vitamin D Deficiency among Iranian population: A Systematic Review and Meta-Analysis. *Iran J Med Sci* 43(2): 125–139.

Taché, Karine, and Oliver E. Craig.
2015. Cooperative harvesting of aquatic resources and the beginning of pottery production in north-eastern North America. *Antiquity* 89(343): 177–190.

Taché, Karine, Manon Bondetti, Alexandre Lucquin, Marjolein Admiraal, and Oliver E. Craig.
2019. Something fishy in the Great Lakes? A reappraisal of early pottery use in north-eastern North America. *Antiquity* 93(371): 1339–1349.

Tamura, Yoshiko, Derek C. Welch, John A. Zic, William O. Cooper, Sharon M. Stein, and Donna S. Hummell.
2000. Scurvy presenting as painful gait with bruising in a young boy. *Archives of Pediatrics and Adolescent Medicine* 154: 732–735.

Tembunde, Yazmeen, Shealinna Ge, Kathryn Turney, and Marcia Driscoll.
2022. Scurvy: A diagnosis not to be missed. *Cureus* 14(12): e33050.

Thacher, Tom D., Philip R. Fischer, Mark A. Strand, and John M. Pettifor.
2006. Nutritional rickets around the world: Causes and future directions. *Annals of Tropical Paediatrics* 26: 1–16. DOI: 10.1179/146532806X90556.

Tiesler, V., A. Coppa, P. Zabala, and A. Cucina.
2016. Scurvy-related morbidity and death among Christopher Columbus' crew at La Isabela, the first European town in the New World (1494-1498): An assessment of the skeletal and historical information. *International Journal of Osteoarchaeology* 26: 191–202. DOI: 10.1002/oa.2406.

Tillman, B., and R. Lorenz.
1978. The stress at the human atlanto-occipital joint. *Anatomy and Embryology* 153: 269–277.

Toorang, Fatemeh, Anahita HoushiarRad, Morteza Abdollahi, Mina Esmaili, and Soraya Ebrahimpour Koujan.
2013. Seasonality in Iranian fruit and vegetable dietary intake. *Thrita Journal of Medical Sciences* 2(4): 58–63. DOI: 10.5812/thrita.11634.

Tournis, Symeon, and Anastasia D. Dede.
2018. Osteogenesis imperfecta – A clinical update. *Metabolism: Clinical and Experimental* 80: 27–37. DOI: 10.1016/j.metabol.2017.06.001.

Travis, John.
2008. Old bones reveal new signs of scurvy. *Science* 322(5900): 368–369. DOI: 10.1126/science.322.5900.368b.

University of Rochester.
2026a. Nutrition facts: Barley. https://www.urmc.rochester.edu/encyclopedia/content?contenttypeid=76&contentid=20004-1. Accessed March 8, 2026.

2026b. Nutrition facts: Wheat. https://www.urmc.rochester.edu/encyclopedia/content?contenttypeid=76&contentid=20074-1. Accessed March 8, 2026.

2026c. Nutrition facts: Chickpeas (garbanzo beans, Bengal gram), mature seeds, canned. https://www.urmc.rochester.edu/encyclopedia/content?contenttypeid=76&contentid=16058-1. Accessed March 8, 2026.

2026d. Nutrition facts: Lentils, mature seeds, cooked, boiled, with salt. https://www.urmc.rochester.edu/encyclopedia/content?contenttypeid=76&contentid=16370-1. Accessed March 8, 2026.

2026e. Nutrition facts: Nuts, almonds, 1 cup, whole. https://www.urmc.rochester.edu/encyclopedia/content?contenttypeid=76&contentid=12061-4. Accessed March 8, 2026.

2026f. Nutrition facts: Nuts, pistachio nuts, raw, 1 cup. https://www.urmc.rochester.edu/encyclopedia/content?contenttypeid=76&contentid=12151-1. Accessed March 8, 2026.

University of Oxford.
Calculations. https://c14.arch.ox.ac.uk/oxcal3/math_ca.htm. Accessed March 3, 2026.

Vatandost, Salam, Marzieh Jahani, Ali Afshari, Mohammad Reza Amiri, Rashid Heidarimoghadam, and Younes Mohammadi.
2018. Prevalence of vitamin D deficiency in Iran: A systematic review and meta-analysis. *Nutrition and Health* 24(4): 269–278. DOI: 10.1177/0260106018802968.

Vitoria, Isidro, Berta López, Jacinto Gómez, Carolina Torres, María Guasp, Inmaculada Calvo, and Jaime Dalmau.
2016. Improper use of a plant-based Vitamin C-deficient beverage causes scurvy in an infant. *Pediatrics* 137(2): e1–e5. DOI: 10.1542/peds.2015-2781.

Wadanamby, S., S. El Garwany, D. J.A. Connolly, P. Arundel, N. J. Bishop, C. J. DeVile, A. D. Calder, B. Crowe, C. P. Burren, V. Saraff, and A. C. Offiah.
2022. Monitoring skull base abnormalities in children with Osteogenesis Imperfecta – Review of current practice and a suggested clinical pathway. *Bone* 154: 1–8. DOI: 10.1016/j.bone.2021.116235.

Walczyk, Agnieszka, Mieczyslaw Szalecki, and Aldona Kowalska.
2011. Primary hyperparathyroidism: A rare endocrinopathy in children. Two cases reports. *Polish Journal of Endocrinology* 62(4): 346–350.

Waldron, Tony
2009. *Palaeopathology*. Cambridge University Press, Cambridge.

Walmsley, A.R., M.R. Batten, U. Lad, and N.J. Bulleid.
1999. Intracellular retention of procollagen within the endoplasmic reticulum is mediated by prolyl 4-hydroxylase. *Journal of Biological Chemistry* 274(21): 14884–14892.

Walsh, S., and R. Matthews.
2018. Articulating the disarticulated: Human remains from the Early Neolithic of the eastern Fertile Crescent (eastern Iraq and western Iran). In *Neolithic Studies Group Seminar Papers (15): Neolithic Bodies.*, edited by P. Bickle, and E. Sibbeson. Oxbow Books, Oxford.

Wapler, Ulrike, Eric Crubézy, and Michael Schultz.
2004. Is cribra orbitalia synonymous with anemia? Analysis and interpretation of cranial pathology in Sudan. *American Journal of Physical Anthropology* 123: 333–339. DOI: 10.1002/ajpa.10321.

Waterland, Robert A, and Karin B. Michels.
2007. Epigenetic epidemiology of the developmental origins hypothesis. *Annu. Rev. Nutr.* 27(1): 363–388.

Weston, D.A.
2012. Nonspecific infection in paleopathology: interpreting periosteal reactions. In *A Companion to Palaeopathology,* edited by A.L. Grauer. Wiley-Blackwell, Chichester, pp. 492–512.

Williams, Emma L., Nicholas C. Harvey, Elaine M. Dennison, Christopher C. Edwards, and Cyrus Cooper.
2009. Maternal nutrition and bone health in the offspring. *International Journal of Clinical Rheumatology* 4(2): 133–145.

Wood, James W., George R. Milner, Henry C. Harpending, Kenneth M. Weiss, Mark N. Cohen, Leslie E. Eisenberg, Dale L. Hutchinson, Rimantas Jankauskas, Gintautas Cesnys, Gintautas Česnys, Anne M. Katzenberg, John R. Lukacs, Janet W. McGrath, Eric Abella Roth, Douglas H. Ubelaker, and Richard G. Wilkinson.
1992. The Osteological Paradox: Problems of Inferring Prehistoric Health from Skeletal Samples [and Comments and Reply]. *Current Anthropology* 33(4): 343–370.

World Health Organization.
Newborn Health. https://www.who.int/westernpacific/health-topics/newborn-health#tab=tab_1. Accessed November, 2025.

1999. *Scurvy and its prevention and control in major emergencies*. Geneva.
Newborn Health. who.int/westernpacific/health-topics/newborn-health#tab=tab_1. Accessed October 27, 2025.

2023. *WHO Guideline for complementary feeding of infants and young children 6-23 months of age*. Geneva.

World Medical Association.
2017. WMA Statement on Vitamin D Insufficiency. *World Medical Association*.

Wright, H.E., J.H. McAndrews, and Willem Van Zeist.
1967. Modern Pollen Rain in Western Iran, and Its Relation to Plant Geography and Quaternary Vegetational History. *Source: Journal of Ecology* 55(2): 415–443.

Yoshimura, K., T. Nakahashi, and K. Saito.
2006. Why did the ancient inhabitants of Palmyra suffer fluorosis? *Journal of Archaeological Science* 33(10): 1411–1418. DOI: 10.1016/j.jas.2006.01.016.

Zeder, Melinda A.
2001. A metrical analysis of a collection of modern goats (Capra hircus aegargus and C. h. hircus) from Iran and Iraq: Implications for the study of caprine domestication. *Journal of Archaeological Science* 28: 61–79. DOI: 10.1006/jasc.1999.0555.

Zeder, Melinda A., and Brian Hesse.
2000. The initial domestication of goats (Capra hircus) in the Zagros Mountains 10,000 years ago. *Science* 287(5461): 2254–2257.

van Zeist, W.
1967. Late quaternary vegetation history of western Iran. *Review of Paleobotany and Palynology* 2(1–4): 301–311.

van Zeist, W., and S. Bottema.
1977. Palynological Investigations in Western Iran. *Palaeohistoria* 19: 19–85.

van Zeist, W., P.E. Smith, R.M. Palfenier-Vegter, M. Suwijn, and W.A. Casparie.
1984. An archaeobotanical study of Ganj Dareh Tepe, Iran. *Palaeohistoria*: 201–224.

van Zeist, W., and H. E. Wright.
1963. Preliminary Pollen Studies at Lake Zeribar, Zagros Mountains, Southwestern Iran. *Science* 140(3562): 65–67.

Zeynivand, Mohsen, Hamid Hariryan, and Mahmoud Heydarian.
2013. The Dalma Settlements of Songhor and Koliyaei Plains, Central Zagros. *IRANIAN JOURNAL OF ARCHAEOLOGICAL STUDIES* 3: 39–47.

Zohary, M.
1973. *Geobotanical Foundations of the Middle East*. Fischer.

Zuckerman, Molly K., Evan M. Garofalo, Bruno Frohlich, and Donald J. Ortner.
2014. Anemia or scurvy: A pilot study on differential diagnosis of porous and hyperostotic lesions using differential cranial vault thickness in subadult humans. *International Journal of Paleopathology* 5: 27–33. DOI: 10.1016/j.ijpp.2014.02.001.

Appendix A

Table A.1. *General Observation Chart.*

Individual #	*Cranium*	*Teeth*	*Vertebral Column*	*Rib Cage*	*Shoulder Girdle*	*Arms*	*Legs*	*Pelvic Girdle*	*Hands*	*Feet*	*Notes*
1	P. NBF on right & left malar ectocranial surface. NBF on right temporal, squamous portion. Clumped porosity on basiocciput. New growth on right alisphenoid. NBF on right maxillary pieces & left maxilla (ectocranial). Slight porosity right orbit. Reconstructed vault frags have porosity on the endocranial surface.	N/A	N/A	N/A	N/A	N/A	N/A	N/A	N/A	N/A	Spongey NBF
2	N/A	N/A	N/A	N/A	N/A	P. Possible odd flaring at distal end. Post-mortem damage on left radius cortical bone.	P. fracture lines or post-mortem damage on x-ray of femur?	N/A	N/A	N/A	

Individual #	*Cranium*	*Teeth*	*Vertebral Column*	*Rib Cage*	*Shoulder Girdle*	*Arms*	*Legs*	*Pelvic Girdle*	*Hands*	*Feet*	*Notes*
3	P. Porosity & NBF basiocciput (Clumped). Porosity on the palatine process of the left maxilla. SPNB across the ectocranial surface of the right & left temporal. NBF on the ectocranial surface of the left parietal, shelf-like.	P. 3-27 (lower right deciduous canine w/ enamel defect buccal surface).	N/A	N/A	N/A	N/A	N/A	N/A	N/A	N/A	
4	N/A	4-17 fairly worn down. Upper left incisor 1 has a line across it, not LEH. Lower right DI4 has a lot of wear.	PMD & missing cortical bone on cervical arches.	N/A	Left clavicle with pronounced curvature.	P. Left humeral bowing, no right present for comparison. Left radius has white line of Fraenkel on the distal end.	P. Left femoral metaphyseal distal flaring and a White line of Fraenkel.	N/A	N/A	N/A	Box 36 (long bone frag.s) has missing cortical bone & P-M damage. General porosity throughout. Has a Wormian bone.
5	P. Porosity & NBF on endo & ectocranial surface right temporal. NBF on left exoccipital.	N/A	N/A	N/A	N/A	N/A	N/A	N/A	N/A	N/A	
6	NBF on frontal & facial bones but not necessarily pathological. Right palate process maxilla (2) w/ NBF. NBF on lesser wings of sphenoid but not necessarily abnormal given age.	N/A	Porosity on lumbar neural arches, normative.	Striations on ribs indicators of normal growth.	N/A	NBF on right ulna. NBF on left radius but not pathology. NBF left ulna non-path.	N/A	New growth on left ischium.	N/A	N/A	

Individual #	*Cranium*	*Teeth*	*Vertebral Column*	*Rib Cage*	*Shoulder Girdle*	*Arms*	*Legs*	*Pelvic Girdle*	*Hands*	*Feet*	*Notes*
7	P. Clumped porosity on basiocciput. Some porosity and new growth on left & right alisphenoid. Porosity & new growth right exoccipital. New growth on orbital roofs, shelf-like (SPNB).	P. Enamel defect UPDI1, lingual surface. Upper right DC has hypoplastic defect at the crown tip & a line across the centre of the tooth. Poor enamel formation tip hypoconid, lower right DP3.	N/A	N/A	P. Right clavicle has a bump in middle of diaphysis.	N/A	N/A	Right ilium missing cortical bone. Taphonomy right ischium. P. New growth on right ilium.	N/A	Mid phalanges missing cortical bone. 1st left metatarsal appears hollowed out.	32-86 (long bone frag.s) missing cortical bone.
8	P. Widespread porosity basiocciput. Porosity & NBF left maxilla, superior surface. Some new growth on inferior left maxilla. Porosity/NBF on cranial frag.s (most in range of normal though).	N/A	N/A	N/A	Left scapular NBF. NBF leaning towards shelf-like appearance but not completely there.	New bone growth left humerus on the anterior surface of diaphysis within normal range though.	N/A	N/A	N/A	N/A	
9	P. SPNB right orbit, porosity. Some porosity on left orbit but not to extent of right. NBF/porosity maxillae (superior & inferior views).	N/A	N/A	N/A	P. Left scapula has porosity on the ridge.	New bone growth left radius but not necessarily atypical.	New growth at distal end of right femur but normal.	N/A	N/A	N/A	
10	P. NBF & porosity left orbit. Changes in right orbit but not as much as left. Possible infection in pituitary fossa of basisphenoid.	N/A	N/A	N/A	N/A	N/A	N/A	N/A	N/A	N/A	Possible cranial deformation.

Individual #	*Cranium*	*Teeth*	*Vertebral Column*	*Rib Cage*	*Shoulder Girdle*	*Arms*	*Legs*	*Pelvic Girdle*	*Hands*	*Feet*	*Notes*
11	Post-mortem damage has removed cortical bone on cranium. P. SPNB Left petrous & partial squamous of temporal has a sheet of new growth like a layer, post-mortem damage. SPNB Right petrous & partial squamous of temporal. NBF around perimeter of orbits.	N/A	N/A	N/A	P. Left clavicle has NBF & perhaps odd curvature. Right clavicle has NBF & swollen shaft.	P. Note about subperiosteal haemorrhage on all long bones. Right ulna has evidence of NBF along diaphysis & post-mortem damage. NBF right humerus & post-mortem damage. NBF & post-mortem damage on left humerus; potential slight curvature outwards. Left radius has post-mortem damage & NBF/growth, possible curvature to diaphysis. Right radius has NBF on diaphysis.	P. Note about subperiosteal haemorrhage on all long bones. Left tibia has NBF & post-mortem damage (posterior & anterior) along diaphysis. Left femur has NBF. Right femur has NBF & post-mortem damage.	N/A	P. Metacarpals or metatarsals have NBF across diaphyses.	P. Metacarpals or metatarsals have NBF across diaphyses.	Noted clavicle x-rays appear to have odd bend to them.
12	PMD to cranium. P. Porosity in orbits; more in right than in left.	N/A	N/A	N/A	P. Weird bend to clavicular x-ray. Right clavicle has an odd bend; notes indicate healing fracture (bowed dorsally sternal end).	PMD right radius.	N/A	P. Porosity & NBF left ischium.	N/A	N/A	Widespread PMD.
13	N/A	N/A	N/A	N/A	N/A	N/A	P. New growth on left tibia.	N/A	N/A	N/A	PMD - scratches on cortical surfaces
14	P. Left orbit inner surface has NBF & porosity. Cranial frag.s have porosity & NBF. Porosity maxillae.	Crazing upper left DP3, lower left DP4, upper left DP4. P. Upper right DI1 with slight shovelling. Upper right DP4 with enamel defect & crazing.	N/A	N/A	P. Odd curvature to left clavicle.	N/A	Normal new growth on tibiae.	N/A	N/A	N/A	Widespread PMD, trowel marks.

Individual #	*Cranium*	*Teeth*	*Vertebral Column*	*Rib Cage*	*Shoulder Girdle*	*Arms*	*Legs*	*Pelvic Girdle*	*Hands*	*Feet*	*Notes*
15	N/A	P. Shovelling on upper left DI1, DI2; upper right DI1, DI2. Lower left DC pit on buccal surface. Upper left DC hypoplastic defect on crown.	N/A	N/A	P. Clavicles look odd in x-rays. Left clavicle is larger than the right & has weird shape.	N/A	PMD left femur, possible Harris lines visible via this PMD.	N/A	N/A	N/A	Possible cranial deformation/modification.
16	P. Porosity inferior right malar. Slight porosity right orbit. Cranium is oddly elongated/bulbous - at least 2 Wormian bones (from lab notes). Porosity cranial frag.s.. New growth/porosity on left maxillary frag (near palatine). Porosity/new growth left exoccipital. Porosity on right parietal frag.s; parietals in general. Porosity on frontals, endocranial surface lumpy. Porosity on the ectocranial & endocranial surface of occipital. Slight porosity consistent across the cranium.	N/A	N/A	N/A	P. Both clavicles robust for this age. May be well healed fracture, strange dent 1/3 acromially on left clavicle.	N/A	N/A	N/A	N/A	N/A	PMD on x-rays. Wormian bone. Hydrocephalus.

Individual #	*Cranium*	*Teeth*	*Vertebral Column*	*Rib Cage*	*Shoulder Girdle*	*Arms*	*Legs*	*Pelvic Girdle*	*Hands*	*Feet*	*Notes*
17	N/A	N/A	N/A	N/A	N/A	N/A	N/A	N/A	N/A	N/A	Widespread PMD. Normal - no pathological lesions; not many remains.
18	N/A	N/A	N/A	A lot of striations on ribs which may be normal - nothing else to compare to for this individual.	P. Right scapula very thin w/ NBF on the ridge & anterior surface. New growth on posterior (internal facing) surface as well.	N/A	Left & right femur have almost no medullary cavity in x-ray.	N/A	N/A	N/A	
19	N/A	N/A	N/A	Ribs thin w/ striations (growing).	PMD left clavicle. Outward growth visible on left scapula.	Odd bend to radii w/ lack of medullary cavity in x-rays. Humeri very thick at epiphyseal ends.	Odd bend to femora along w/ lack of medullary cavity in x-rays. Thickness of one of the femora.	N/A	N/A	N/A	X-rays show very small medullary cavities.
20	P. New bone growth/porosity basiocciput posteriorly. New growth/porosity basisphenoid, SPNB. Outward growth on unidentified cranial frag.s.	N/A	N/A	N/A	N/A	N/A	New growth on diaphysis of tibia (2).	N/A	N/A	N/A	Very narrow medullary cavities in x-rays. New growth on the unidentified frag.s.
21	P. Porosity on right alisphenoid on the ectocranial surface. New growth and porosity on left partial maxilla.	Teeth normal; some crazing visible on upper right DI2, upper left DI1, and lower right DI2.	N/A	N/A	P. New growth left scapula, SPNB. Also, growth on the right but not as much it appears but also PMD which makes it hard to judge.	N/A	N/A	N/A	N/A	N/A	PMD on some elements.

Individual #	*Cranium*	*Teeth*	*Vertebral Column*	*Rib Cage*	*Shoulder Girdle*	*Arms*	*Legs*	*Pelvic Girdle*	*Hands*	*Feet*	*Notes*
22	P. Inferior surface of the left maxilla has shelf-like new growth (SPNB) and porosity. Shelf-like new growth (SPNB) ectocranial surface both temporals.	Enamel defect on distal surface of lower right DI1. Enamel defects on upper left DI1, upper right DI1, and upper left DI2 (labial surface).	New growth sacral neural arches but believed to be in range of normal.	N/A	N/A	N/A	N/A	N/A	N/A	N/A	Pot burial. Left nasal looks possibly burnt due to discolouration.
23	P. Porosity/new growth on left & right maxilla, specifically very porous in the palate areas.	Crazing on 6-2, 6-4 which is normal indication of growth. P. Shovelling on 5-2, 5-1. Possible enamel defect on 7-1.	N/A	N/A	P. Healed left clavicular fracture; lot of growth & texture to it; looks like has a bony callus. Odd shape to both clavicles. Right clavicle not as thick & has less growth.	N/A	P. A lot of new growth patterning on left fibula, which is concentrated on the diaphysis, very slight bend. The left fibula is smaller than the right.	N/A	N/A	N/A	Pot burial. Notes indicate possible 2nd individual due to presence of 2 left pubises. Some growth on misc. frag.s. A lot of blood vessel impressions on the ectocranial surfaces of the cranial bones.
24	N/A	N/A	N/A	Signs of growth on ribs but falls in line with what is seen on other individuals in population.	N/A	N/A	N/A	N/A	N/A	N/A	Very fragmentary.
25	P. Spongey new growth & porosity on right orbit.	Teeth normal; crazing on 8-5, 7-3, 8-3, 7-4, and 8-4.	N/A	N/A	N/A	N/A	Third trochanter right & left femur (not path but a non-metric trait).	N/A	Taphonomic changes to distal phalanges (box 62).	N/A	PMD on x-rays. Grave highly disturbed, lots of frag.s.
26	P. Slight amount of new growth mandible fragment; double socket appearance to tooth sockets.	N/A	N/A	N/A	P. New growth/porosity left scapula, specifically growth in the supraspinous fossa and slight porosity on the infraspinous.	N/A	N/A	N/A	N/A	N/A	B/14 (distal end of unspecified long bone) missing all cortical bone.

Individual #	*Cranium*	*Teeth*	*Vertebral Column*	*Rib Cage*	*Shoulder Girdle*	*Arms*	*Legs*	*Pelvic Girdle*	*Hands*	*Feet*	*Notes*
27	P. Porosity in left orbital socket which looks like new bone deposit that doesn't look like it goes into the diploë.	Crazing on 8-5 & 5-5. P. Enamel defect on 8-3.	Some porosity lateral mass of sacrum; some larger holes may be taphonomy related. Porosity on sacral vertebrae neural arches which may be part of normal development.	N/A	N/A	N/A	N/A	N/A	N/A	N/A	No x-rays for this individual.
28	P. Porosity/new growth in left orbit.	Teeth normal; crazing on 4-1, 3-1. Lower right & left M1 has normal outward growth (prisms).	N/A	N/A	N/A	N/A	N/A	N/A	N/A	N/A	Fair amount of PMD over whole skeleton. Pot burial.
29	N/A	P. Localized hypoplasia primary canines. LEH 4-3, 3-1, 3-3, 4-6, 3-6, 2-1, 2-3.	N/A	N/A	N/A	P. Possible Harris lines (x-ray) distal left & right radii.	N/A	N/A	N/A	N/A	Harris lines, LEH, LHPC noted in paperwork. Harris lines potentially visible via x-rays of long bones. Possible 2nd individual due to smaller size of a second right maxilla. Widespread PMD. Simple inhumation, not a pot burial.
30	N/A	Crazing on non-erupted teeth. P. LHPC in mandibular canines.	N/A	N/A	P. Bit of new growth side of right clavicle.	N/A	N/A	PMD pelvis.	N/A	N/A	Note of LHPC. Fair amount of associated faunal remains w/ this individual.
31	N/A	N/A	N/A	N/A	N/A	N/A	N/A	N/A	N/A	N/A	A lot of faunal remains - perhaps not a full burial but a midden. PMD on frag.s

Individual #	*Cranium*	*Teeth*	*Vertebral Column*	*Rib Cage*	*Shoulder Girdle*	*Arms*	*Legs*	*Pelvic Girdle*	*Hands*	*Feet*	*Notes*
32	P. Porosity around nasal hole & teeth in maxillae; porosity in the sockets & on palate area as well.	Notable wear on incisors. Wear on lower left P3, lower left I2, lower right I1. In situ teeth (maxillae & mandible) have a good amount of wear. P. Caries lower right M3.	N/A	N/A	N/A	N/A	N/A	N/A	N/A	N/A	PMD 177 (not indicated on inventory what bone this is). Burial in a thick deposit of ashy trash.

Table A.1. Legend
PMD = post-mortem damage
NBF = new bone formation
SPNB = subperiosteal new bone formation
SPH = subperiosteal haemorrhage
P = pathology, with list of lesions following.

Appendix B: Metabolic Bone Disease Pathology Tables & Brief Discussion
SG1

Macroscopic Indicators

	Scurvy	Rickets	Anaemia	Fluorosis	Hyperostosis	OI
General Skeleton	○ Irregular & spongy new bone formation	○ General porosity ○ Abnormal growth plates	○ Porosity ○ Osteopenia (Thal.) ○ Large bony masses (Thal.)	○ Diffuse osteosclerosis of the appendicular & axial skeleton ○ Increased cortical & trabecular thickness ○ Periosteal thickening ○ Calcified ligaments, tendons, cartilage, & inter-osseous membrane-s ○ Bony exostoses at ligament & muscle attachment zones	○ Increased weight of bones ○ Increased thickness of cortical bone ○ A lot of subperiosteal new bone formation	○ Lightness/fragility to bones ○ Fractures ○ Osteoporosis
Orbits	○ Cribra orbitalia ○ Porosity	○ Orbital roof porosity	○ Cribra orbitalia ○ Thinning of trabecular & cortical bone ○ Widening interorbital space (Thal.)			○ Elongated orbits
Cranium	Porosity on: ○ the greater sphenoid wing ○ cranial bones ○ facial bones ○ palate ○ basiocciput	○ Frontal bone bossing ○ Deformed mandibular ramus	○ Cranial vault porosity ○ Thickening of the sphenoid, maxillae, & zygomatics (Thal.) ○ Obliterated sutures in the cranium (Thal.)		○ A lot of subperiosteal new bone formation, most commonly on facial bones (Caffey's) ○ Osteal bulges ○ Irregular thickening of internal surface of frontal bone while external surface looks normal (IFH)	○ Expanded cranial vault
Dentition			○ Protruding upper incisors & overbite (Thal.)	○ Linear enamel hypoplasia ○ Brown, dis-coloured teeth, & mottled enamel		○ Dentinogenesis imperfecta
Vertebral Column			○ Perforations in the cortical bone of vertebrae			
Thorax		○ Rib flaring	○ Slight expansion of the ribs ○ Perforated cortical bone in ribs (Thal.) ○ Linear striations on the ribs (Thal.)		○ A lot of subperiosteal new bone formation, most commonly on ribs	
Arms	Porosity on: ○ the scapulae ○ metaphyses of long bones	○ Porosity in concave curvature of long bones ○ Long bone thickening & bowing	○ Long bone porosity ○ Thinning of trabecular & cortical bone ○ Perforated cortical bone in long bones (Thal.)			○ Long bone bowing with cortical thickening ○ Narrowing of long bone diaphyses in comparison to their length

	Scurvy	Rickets	Anaemia	Fluorosis	Hyperostosis	OI
		○ Long bone metaphyseal flaring	○ Necrosis of the humeral head (SCA)			
Hands						
Pelvis		○ Ilium concavity				
Legs	Porosity on: ○ Metaphyses of long bones	○ Porosity in concave curvature of long bones ○ Long bone thickening & bowing ○ Long bone metaphyseal flaring	○ Long bone porosity ○ Thinning of trabecular & cortical bone ○ Perforated cortical bone in long bones (Thal.) ○ Exaggerated sulci on femora & tibiae (Thal.) ○ Necrosis of the femoral head (SCA)			○ Long bone bowing with cortical thickening ○ Narrowing of long bone diaphyses in comparison to their length
Feet			○ Hyper-trophic meta-carpals & phalanges (Thal.)			

Radiographic Indicators

	Scurvy	Rickets	Anaemia	Fluorosis	Hyperostosis	OI
General Skeleton	○ Generalized osteopenia	○ Generalized osteopenia ○ Thick cortex ○ Sharp cortical outline	○ Thinning of cortical bone			
Cranium			○ Hair-on-end appearance cranium ○ Undeveloped sinuses			
Dentition						
Vertebral Column			○ Reduced number of trabeculae in vertebrae			
Thorax		○ Loss of integrity in sternal rib ends				

	Scurvy	Rickets	Anaemia	Fluorosis	Hyperostosis	OI
Arms	○ Long bone cortical thinning ○ Metaphyseal fractures ○ White line of Fraenkel ○ Wimberger's ring ○ Pelkan's spurs	○ Long bone cortical thinning ○ Metaphyseal fractures ○ Metaphyseal trabecular coarsening ○ Fraying of epiphyses ○ Distinction at the end of the epiphysis	○ Infarcts in long bones ○ Reduced number of trabeculae in long bones			○ Zebra stripe
Hands						
Pelvis						
Legs	○ Long bone cortical thinning ○ Metaphyseal fractures ○ White line of Fraenkel ○ Wimberger's ring ○ Pelkan's spurs	○ Long bone cortical thinning ○ Metaphyseal fractures ○ Fraying of epiphyses ○ Distinction at the end of the epiphysis	○ Infarcts in long bones ○ Reduced number of trabeculae in long bones			○ Zebra stripe
Feet						

SG1's lesions that could be associated with scurvy are the porosity seen on the right orbit, the cranial vault fragments, facial bones, and basiocciput. Additionally, the NBF on the zygomatics, right temporal squamous portion, right alisphenoid, maxillae, and the left mandible could also be associated with scurvy. This NBF could be associated due to its shelf-like and spongey appearance as well as its irregular-like patterning.

The cranial vault porosity and slight porosity in the right orbit could also be associated with anaemia. The orbital roof porosity could also be associated with rickets, but this is a non-diagnostic feature of the illness. Additionally, only one criterion is not enough for a diagnosis.

SG2

Macroscopic Indicators

	Scurvy	Rickets	Anaemia	Fluorosis	Hyperostosis	OI
General Skeleton	○ Irregular & spongy new bone formation	○ General porosity ○ Abnormal growth plates	○ Porosity ○ Osteopenia (Thal.) ○ Large bony masses (Thal.)	○ Diffuse osteosclerosis of the appendicular & axial skeleton ○ Increased cortical & trabecular thickness ○ Periosteal thickening ○ Calcified ligaments, tendons, cartilage, & inter-osseous membrane-s ○ Bony exostoses at ligament & muscle attachment zones	○ Increased weight of bones ○ Increased thickness of cortical bone ○ A lot of subperiosteal new bone formation	○ Lightness/fragility to bones ○ Fractures ○ Osteoporosis
Orbits	○ Cribra orbitalia ○ Porosity	○ Orbital roof porosity	○ Cribra orbitalia ○ Thinning of trabecular & cortical bone ○ Widening interorbital space (Thal.)			○ Elongated orbits
Cranium	Porosity on: ○ the greater sphenoid wing ○ cranial bones ○ facial bones ○ palate ○ basiocciput	○ Frontal bone bossing ○ Deformed mandibular ramus	○ Cranial vault porosity ○ Thickening of the sphenoid, maxillae, & zygomatics (Thal.) ○ Obliterated sutures in the cranium (Thal.)		○ A lot of subperiosteal new bone formation, most commonly on facial bones (Caffey's) ○ Osteal bulges ○ Irregular thickening of internal surface of frontal bone while external surface looks normal (IFH)	○ Expanded cranial vault
Dentition			○ Protruding upper incisors & overbite (Thal.)	○ Linear enamel hypoplasia ○ Brown, dis-coloured teeth, & mottled enamel		○ Dentinogenesis imperfecta
Vertebral Column			○ Perforations in the cortical bone of vertebrae			
Thorax		○ Rib flaring	○ Slight expansion of the ribs ○ Perforated cortical bone in ribs (Thal.) ○ Linear striations on the ribs (Thal.)		○ A lot of subperiosteal new bone formation, most commonly on ribs	
Arms	Porosity on: ○ the scapulae ○ metaphyses of long bones	○ Porosity in concave curvature of long bones ○ Long bone thickening & bowing	○ Long bone porosity ○ Thinning of trabecular & cortical bone ○ Perforated cortical bone in long bones (Thal.)			○ Long bone bowing with cortical thickening ○ Narrowing of long bone diaphyses in comparison to their length

	Scurvy	Rickets	Anaemia	Fluorosis	Hyperostosis	OI
		○ Long bone metaphyseal flaring	○ Necrosis of the humeral head (SCA)			
Hands						
Pelvis		○ Ilium concavity				
Legs	Porosity on: ○ Metaphyses of long bones	○ Porosity in concave curvature of long bones ○ Long bone thickening & bowing ○ Long bone metaphyseal flaring	○ Long bone porosity ○ Thinning of trabecular & cortical bone ○ Perforated cortical bone in long bones (Thal.) ○ Exaggerated sulci on femora & tibiae (Thal.) ○ Necrosis of the femoral head (SCA)			○ Long bone bowing with cortical thickening ○ Narrowing of long bone diaphyses in comparison to their length
Feet			○ Hyper-trophic meta-carpals & phalanges (Thal.)			

Radiographic Indicators

	Scurvy	Rickets	Anaemia	Fluorosis	Hyperostosis	OI
General Skeleton	○ Generalized osteopenia	○ Generalized osteopenia ○ Thick cortex ○ Sharp cortical outline	○ Thinning of cortical bone			
Cranium			○ Hair-on-end appearance cranium ○ Undeveloped sinuses			
Dentition						
Vertebral Column			○ Reduced number of trabeculae in vertebrae			
Thorax		○ Loss of integrity in sternal rib ends				

	Scurvy	Rickets	Anaemia	Fluorosis	Hyperostosis	OI
Arms	○ Long bone cortical thinning ○ Metaphyseal fractures ○ White line of Fraenkel ○ Wimberger's ring ○ Pelkan's spurs	○ Long bone cortical thinning ○ Metaphyseal fractures ○ Metaphyseal trabecular coarsening ○ Fraying of epiphyses ○ Distinction at the end of the epiphysis	○ Infarcts in long bones ○ Reduced number of trabeculae in long bones			○ Zebra stripe
Hands						
Pelvis						
Legs	○ Long bone cortical thinning ○ Metaphyseal fractures ○ White line of Fraenkel ○ Wimberger's ring ○ Pelkan's spurs	○ Long bone cortical thinning ○ Metaphyseal fractures ○ Fraying of epiphyses ○ Distinction at the end of the epiphysis	○ Infarcts in long bones ○ Reduced number of trabeculae in long bones			○ Zebra stripe
Feet						

SG2 demonstrates very faint White Lines of Fraenkel in their left radial and tibial radiographs. However, this indicator is not diagnostic or probable. It is possible that SG2 died prior to any changes associated with MBD could be made to the skeleton.

SG3

Macroscopic Indicators

	Scurvy	Rickets	Anaemia	Fluorosis	Hyperostosis	OI
General Skeleton	○ Irregular & spongy new bone formation	○ General porosity ○ Abnormal growth plates	○ Porosity ○ Osteopenia (Thal.) ○ Large bony masses (Thal.)	○ Diffuse osteosclerosis of the appendicular & axial skeleton ○ Increased cortical & trabecular thickness ○ Periosteal thickening ○ Calcified ligaments, tendons, cartilage, & inter-osseous membrane-s ○ Bony exostoses at ligament & muscle attachment zones	○ Increased weight of bones ○ Increased thickness of cortical bone ○ A lot of subperiosteal new bone formation	○ Lightness/fragility to bones ○ Fractures ○ Osteoporosis
Orbits	○ Cribra orbitalia ○ Porosity	○ Orbital roof porosity	○ Cribra orbitalia ○ Thinning of trabecular & cortical bone ○ Widening interorbital space (Thal.)			○ Elongated orbits
Cranium	Porosity on: ○ the greater sphenoid wing ○ cranial bones ○ facial bones ○ palate ○ basiocciput	○ Frontal bone bossing ○ Deformed mandibular ramus	○ Cranial vault porosity ○ Thickening of the sphenoid, maxillae, & zygomatics (Thal.) ○ Obliterated sutures in the cranium (Thal.)		○ A lot of subperiosteal new bone formation, most commonly on facial bones (Caffey's) ○ Osteal bulges ○ Irregular thickening of internal surface of frontal bone while external surface looks normal (IFH)	○ Expanded cranial vault
Dentition			○ Protruding upper incisors & overbite (Thal.)	○ Linear enamel hypoplasia ○ Brown, dis-coloured teeth, & mottled enamel		○ Dentinogenesis imperfecta
Vertebral Column			○ Perforations in the cortical bone of vertebrae			
Thorax		○ Rib flaring	○ Slight expansion of the ribs ○ Perforated cortical bone in ribs (Thal.) ○ Linear striations on the ribs (Thal.)		○ A lot of subperiosteal new bone formation, most commonly on ribs	
Arms	Porosity on: ○ the scapulae ○ metaphyses of long bones	○ Porosity in concave curvature of long bones ○ Long bone thickening & bowing	○ Long bone porosity ○ Thinning of trabecular & cortical bone ○ Perforated cortical bone in long bones (Thal.)			○ Long bone bowing with cortical thickening ○ Narrowing of long bone diaphyses in comparison to their length

	Scurvy	Rickets	Anaemia	Fluorosis	Hyperostosis	OI
		○ Long bone metaphyseal flaring	○ Necrosis of the humeral head (SCA)			
Hands						
Pelvis		○ Ilium concavity				
Legs	Porosity on: ○ Metaphyses of long bones	○ Porosity in concave curvature of long bones ○ Long bone thickening & bowing ○ Long bone metaphyseal flaring	○ Long bone porosity ○ Thinning of trabecular & cortical bone ○ Perforated cortical bone in long bones (Thal.) ○ Exaggerated sulci on femora & tibiae (Thal.) ○ Necrosis of the femoral head (SCA)			○ Long bone bowing with cortical thickening ○ Narrowing of long bone diaphyses in comparison to their length
Feet			○ Hyper-trophic meta-carpals & phalanges (Thal.)			

Radiographic Indicators

	Scurvy	Rickets	Anaemia	Fluorosis	Hyperostosis	OI
General Skeleton	○ Generalized osteopenia	○ Generalized osteopenia ○ Thick cortex ○ Sharp cortical outline	○ Thinning of cortical bone			
Cranium			○ Hair-on-end appearance cranium ○ Undeveloped sinuses			
Dentition						
Vertebral Column			○ Reduced number of trabeculae in vertebrae			
Thorax		○ Loss of integrity in sternal rib ends				

	Scurvy	Rickets	Anaemia	Fluorosis	Hyperostosis	OI
Arms	○ Long bone cortical thinning ○ Metaphyseal fractures ○ White line of Fraenkel ○ Wimberger's ring ○ Pelkan's spurs	○ Long bone cortical thinning ○ Metaphyseal fractures ○ Metaphyseal trabecular coarsening ○ Fraying of epiphyses ○ Distinction at the end of the epiphysis	○ Infarcts in long bones ○ Reduced number of trabeculae in long bones			○ Zebra stripe
Hands						
Pelvis						
Legs	○ Long bone cortical thinning ○ Metaphyseal fractures ○ White line of Fraenkel ○ Wimberger's ring ○ Pelkan's spurs	○ Long bone cortical thinning ○ Metaphyseal fractures ○ Fraying of epiphyses ○ Distinction at the end of the epiphysis	○ Infarcts in long bones ○ Reduced number of trabeculae in long bones			○ Zebra stripe
Feet						

SG3 has lesions which could be related to MBD. The left temporal exhibits NBF on the ectocranial surface. The right parietal of SG3 also has new growth which looks like that seen in the temporals. However, the new growth on the right parietal is not across the entire ectocranial surface, rather it occurs mostly adjacent to the suture lines. SG3 also exhibits some porosity, although not in the orbits. There is clumped porosity on the posterior surface of the basiocciput. On SG3's left maxillary palatine process, porosity is present. On SG3's lower left DC there is an enamel defect on the buccal surface. There are no radiographic indicators in SG3.

The porosity and SPNB on the cranial bones, palate, and basiocciput seen in SG3 could be related to scurvy. SG3 demonstrates a few lesions which are either suggestive or diagnostic of MBD. For one, the left palate porosity is suggestive of scurvy. Additionally, the cranial vault porosity/SPNB is a non-diagnostic feature of scurvy. As there is only one suggestive lesion and only one non-diagnostic lesion type, a diagnosis of scurvy cannot be made but it is possible given other lesions are present. The cranial vault porosity that SG3 demonstrates could also be a non-diagnostic feature of rickets. This one lesion type is again not enough evidence for

a diagnosis though. It is possible that SG3 lived with a type of MBD, but we do not have sufficient skeletal evidence to give a diagnosis.

SG4

Macroscopic Indicators

	Scurvy	Rickets	Anaemia	Fluorosis	Hyperostosis	OI
General Skeleton	○ Irregular & spongy new bone formation	○ General porosity ○ Abnormal growth plates	○ Porosity ○ Osteopenia (Thal.) ○ Large bony masses (Thal.)	○ Diffuse osteosclerosis of the appendicular & axial skeleton ○ Increased cortical & trabecular thickness ○ Periosteal thickening ○ Calcified ligaments, tendons, cartilage, & inter-osseous membrane-s ○ Bony exostoses at ligament & muscle attachment zones	○ Increased weight of bones ○ Increased thickness of cortical bone ○ A lot of subperiosteal new bone formation	○ Lightness/fragility to bones ○ Fractures ○ Osteoporosis
Orbits	○ Cribra orbitalia ○ Porosity	○ Orbital roof porosity	○ Cribra orbitalia ○ Thinning of trabecular & cortical bone ○ Widening interorbital space (Thal.)			○ Elongated orbits
Cranium	Porosity on: ○ the greater sphenoid wing ○ cranial bones ○ facial bones ○ palate ○ basiocciput	○ Frontal bone bossing ○ Deformed mandibular ramus	○ Cranial vault porosity ○ Thickening of the sphenoid, maxillae, & zygomatics (Thal.) ○ Obliterated sutures in the cranium (Thal.)		○ A lot of subperiosteal new bone formation, most commonly on facial bones (Caffey's) ○ Osteal bulges ○ Irregular thickening of internal surface of frontal bone while external surface looks normal (IFH)	○ Expanded cranial vault
Dentition			○ Protruding upper incisors & overbite (Thal.)	○ Linear enamel hypoplasia ○ Brown, dis-coloured teeth, & mottled enamel		○ Dentinogenesis imperfecta
Vertebral Column			○ Perforations in the cortical bone of vertebrae			
Thorax		○ Rib flaring	○ Slight expansion of the ribs ○ Perforated cortical bone in ribs (Thal.) ○ Linear striations on the ribs (Thal.)		○ A lot of subperiosteal new bone formation, most commonly on ribs	

	Scurvy	Rickets	Anaemia	Fluorosis	Hyperostosis	OI
Arms	Porosity on: ○ the scapulae ○ metaphyses of long bones	○ Porosity in concave curvature of long bones ○ Long bone thickening & bowing ○ Long bone metaphyseal flaring	○ Long bone porosity ○ Thinning of trabecular & cortical bone ○ Perforated cortical bone in long bones (Thal.) ○ Necrosis of the humeral head (SCA)			○ Long bone bowing with cortical thickening ○ Narrowing of long bone diaphyses in comparison to their length
Hands						
Pelvis		○ Ilium concavity				
Legs	Porosity on: ○ Metaphyses of long bones	○ Porosity in concave curvature of long bones ○ Long bone thickening & bowing ○ Long bone metaphyseal flaring	○ Long bone porosity ○ Thinning of trabecular & cortical bone ○ Perforated cortical bone in long bones (Thal.) ○ Exaggerated sulci on femora & tibiae (Thal.) ○ Necrosis of the femoral head (SCA)			○ Long bone bowing with cortical thickening ○ Narrowing of long bone diaphyses in comparison to their length
Feet			○ Hyper-trophic meta-carpals & phalanges (Thal.)			

Radiographic Indicators

	Scurvy	Rickets	Anaemia	Fluorosis	Hyperostosis	OI
General Skeleton	○ Generalized osteopenia	○ Generalized osteopenia ○ Thick cortex ○ Sharp cortical outline	○ Thinning of cortical bone			
Cranium			○ Hair-on-end appearance cranium ○ Undeveloped sinuses			
Dentition						
Vertebral Column			○ Reduced number of trabeculae in vertebrae			
Thorax		○ Loss of integrity in sternal rib ends				

	Scurvy	Rickets	Anaemia	Fluorosis	Hyperostosis	OI
Arms	○ Long bone cortical thinning ○ Metaphyseal fractures ○ White line of Fraenkel ○ Wimberger's ring ○ Pelkan's spurs	○ Long bone cortical thinning ○ Metaphyseal fractures ○ Metaphyseal trabecular coarsening ○ Fraying of epiphyses ○ Distinction at the end of the epiphysis	○ Infarcts in long bones ○ Reduced number of trabeculae in long bones			○ Zebra stripe
Hands						
Pelvis						
Legs	○ Long bone cortical thinning ○ Metaphyseal fractures ○ White line of Fraenkel ○ Wimberger's ring ○ Pelkan's spurs	○ Long bone cortical thinning ○ Metaphyseal fractures ○ Fraying of epiphyses ○ Distinction at the end of the epiphysis	○ Infarcts in long bones ○ Reduced number of trabeculae in long bones			○ Zebra stripe
Feet						

SG4 is an individual with widespread post-mortem damage (PMD). SG4 has general porosity throughout their skeleton. The lower right deciduous incisor (DI)4 has a lot of wear, which is not necessarily pathological but interesting to note given this population's method of subsistence and the temporal range of the site. The upper left DI1 has a line across of it but does not have the same appearance as a tooth with linear enamel hypoplasia. Rather this seems to be a demarcation of discolouration. SG4's left clavicle has an extreme curvature to it but only a partial right clavicle is present, so a complete comparison of clavicles in this individual is not possible to determine if this is purely individual variation. The left humerus appears to be displaying some bowing, but the right humerus is not present for comparison. SG4's left femur demonstrates metaphyseal flaring on the distal end and a white line of Fraenkel. Additionally, the left radius seems to also display a white line of Fraenkel on its distal end. It is also interesting to note that SG4 had one Wormian bone.

With SG4's lesions there are a couple of MBDs possible. SG4 has lesions which align with rickets: general porosity and the bowing of left humerus. However, it is more likely if this is a bilateral change, and there is no right humerus present with SG4's remains. It is also important to note that this becomes more probable when there are multiple bones affected, and in this case, there is only one. As well, the metaphyseal flaring of the left femur is consistent with rickety lesions. This can also be suggestive of scurvy.

Another possibility is that of anaemia due to SG4's porosity, however this is the only lesion they demonstrate which is in line with anaemia skeletal indicators. The limb bowing that SG4 demonstrates could be associated with hypophosphatasia, as that is an indicator with that disease. Long bone limb bowing is also associated with OI, but SG4 does not appear to have the associated cortical thickening that would be demonstrated in an individual with OI. Additionally, the metaphyseal flaring in SG4's distal left femur could be associated with osteopetrosis, but the other features of this disease are not present, and this does not occur at the proximal tibia.

SG4's radiographic indicators could point to a different disease as well. The white line of Fraenkel that SG4 exhibits in both their left radius and left femur could be related to scurvy as this is a specific scorbutic indicator, which is not associated with any other MBD. The metaphyseal flaring of the femur could also be associated with scurvy as a suggestive indicator.

SG4 lesions seem to mostly fall in line with rickets as the most likely cause here, as SG4 has the most lesions in common with rickets. It is unclear how to order hypophosphatasia anaemia, and OI as SG4 has one lesion which aligns with each of these MBD. The radiographic indicators are specific to scurvy, and it is possible that this individual had more than one disease afflicting them. SG4 does not have enough suggestive or probable indicators to provide a probable diagnosis. It is possible that this individual did have MBD, but there is not enough macroscopic evidence to support this on their remains.

SG5

Macroscopic Indicators

	Scurvy	Rickets	Anaemia	Fluorosis	Hyperostosis	OI
General Skeleton	○ Irregular & spongy new bone formation	○ General porosity ○ Abnormal growth plates	○ Porosity ○ Osteopenia (Thal.) ○ Large bony masses (Thal.)	○ Diffuse osteosclerosis of the appendicular & axial skeleton ○ Increased cortical & trabecular thickness ○ Periosteal thickening ○ Calcified ligaments, tendons, cartilage, & inter-osseous membrane-s ○ Bony exostoses at ligament & muscle attachment zones	○ Increased weight of bones ○ Increased thickness of cortical bone ○ A lot of subperiosteal new bone formation	○ Lightness/fragility to bones ○ Fractures ○ Osteoporosis
Orbits	○ Cribra orbitalia ○ Porosity	○ Orbital roof porosity	○ Cribra orbitalia ○ Thinning of trabecular & cortical bone ○ Widening interorbital space (Thal.)			○ Elongated orbits
Cranium	Porosity on: ○ the greater sphenoid wing ○ cranial bones ○ facial bones ○ palate ○ basiocciput	○ Frontal bone bossing ○ Deformed mandibular ramus	○ Cranial vault porosity ○ Thickening of the sphenoid, maxillae, & zygomatics (Thal.) ○ Obliterated sutures in the cranium (Thal.)		○ A lot of subperiosteal new bone formation, most commonly on facial bones (Caffey's) ○ Osteal bulges ○ Irregular thickening of internal surface of frontal bone while external surface looks normal (IFH)	○ Expanded cranial vault
Dentition			○ Protruding upper incisors & overbite (Thal.)	○ Linear enamel hypoplasia ○ Brown, dis-coloured teeth, & mottled enamel		○ Dentinogenesis imperfecta
Vertebral Column			○ Perforations in the cortical bone of vertebrae			
Thorax		○ Rib flaring	○ Slight expansion of the ribs ○ Perforated cortical bone in ribs (Thal.) ○ Linear striations on the ribs (Thal.)		○ A lot of subperiosteal new bone formation, most commonly on ribs	
Arms	Porosity on: ○ the scapulae ○ metaphyses of long bones	○ Porosity in concave curvature of long bones ○ Long bone thickening & bowing	○ Long bone porosity ○ Thinning of trabecular & cortical bone ○ Perforated cortical bone in long bones (Thal.)			○ Long bone bowing with cortical thickening ○ Narrowing of long bone diaphyses in comparison to their length

	Scurvy	Rickets	Anaemia	Fluorosis	Hyperostosis	OI
		○ Long bone metaphyseal flaring	○ Necrosis of the humeral head (SCA)			
Hands						
Pelvis		○ Ilium concavity				
Legs	Porosity on: ○ Metaphyses of long bones	○ Porosity in concave curvature of long bones ○ Long bone thickening & bowing ○ Long bone metaphyseal flaring	○ Long bone porosity ○ Thinning of trabecular & cortical bone ○ Perforated cortical bone in long bones (Thal.) ○ Exaggerated sulci on femora & tibiae (Thal.) ○ Necrosis of the femoral head (SCA)			○ Long bone bowing with cortical thickening ○ Narrowing of long bone diaphyses in comparison to their length
Feet			○ Hyper-trophic meta-carpals & phalanges (Thal.)			

Radiographic Indicators

	Scurvy	Rickets	Anaemia	Fluorosis	Hyperostosis	OI
General Skeleton	○ Generalized osteopenia	○ Generalized osteopenia ○ Thick cortex ○ Sharp cortical outline	○ Thinning of cortical bone			
Cranium			○ Hair-on-end appearance cranium ○ Undeveloped sinuses			
Dentition						
Vertebral Column			○ Reduced number of trabeculae in vertebrae			
Thorax		○ Loss of integrity in sternal rib ends				

	Scurvy	Rickets	Anaemia	Fluorosis	Hyperostosis	OI
Arms	○ Long bone cortical thinning ○ Metaphyseal fractures ○ White line of Fraenkel ○ Wimberger's ring ○ Pelkan's spurs	○ Long bone cortical thinning ○ Metaphyseal fractures ○ Metaphyseal trabecular coarsening ○ Fraying of epiphyses ○ Distinction at the end of the epiphysis	○ Infarcts in long bones ○ Reduced number of trabeculae in long bones			○ Zebra stripe
Hands						
Pelvis						
Legs	○ Long bone cortical thinning ○ Metaphyseal fractures ○ White line of Fraenkel ○ Wimberger's ring ○ Pelkan's spurs	○ Long bone cortical thinning ○ Metaphyseal fractures ○ Fraying of epiphyses ○ Distinction at the end of the epiphysis	○ Infarcts in long bones ○ Reduced number of trabeculae in long bones			○ Zebra stripe
Feet						

SG5 is an individual with very few lesions. The lesions that SG5 does have are restricted to the cranium. SG5 has porosity and new bone formation on their right temporal and new bone formation on the left exoccipital. The endocranial surface of the right temporal has NBF and some porosity across the entire cortical surface. This is repeated on the ectocranial surface as well. This NBF appears to be restricted to the outer edges of the bone and does not go across the entire cortical surface. There is a cranial vault fragment which shows slight porosity.

The lesions seen in SG5 could be associated with two different MBDs. One, is scurvy. The porosity on the right temporal could be associated with scurvy. However, this cranial vault porosity is a non-diagnostic indicator. This is also the case for rickets. On the other hand, the porosity seen on the cranial vault fragment could be associated with anaemia. However, having only one lesion for each of these MBDs is not enough to provide evidence for a diagnosis, especially given that it is non-diagnostic. Given that the rest of

SG5's remains demonstrate only normative growth and development indicators, it seems to be more likely that MBD was not present in this individual.

SG6

Macroscopic Indicators

	Scurvy	Rickets	Anaemia	Fluorosis	Hyperostosis	OI
General Skeleton	○ Irregular & spongy new bone formation	○ General porosity ○ Abnormal growth plates	○ Porosity ○ Osteopenia (Thal.) ○ Large bony masses (Thal.)	○ Diffuse osteosclerosis of the appendicular & axial skeleton ○ Increased cortical & trabecular thickness ○ Periosteal thickening ○ Calcified ligaments, tendons, cartilage, & inter-osseous membrane-s ○ Bony exostoses at ligament & muscle attachment zones	○ Increased weight of bones ○ Increased thickness of cortical bone ○ A lot of subperiosteal new bone formation	○ Lightness/fragility to bones ○ Fractures ○ Osteoporosis
Orbits	○ Cribra orbitalia ○ Porosity	○ Orbital roof porosity	○ Cribra orbitalia ○ Thinning of trabecular & cortical bone ○ Widening interorbital space (Thal.)			○ Elongated orbits
Cranium	Porosity on: ○ the greater sphenoid wing ○ cranial bones ○ facial bones ○ palate ○ basiocciput	○ Frontal bone bossing ○ Deformed mandibular ramus	○ Cranial vault porosity ○ Thickening of the sphenoid, maxillae, & zygomatics (Thal.) ○ Obliterated sutures in the cranium (Thal.)		○ A lot of subperiosteal new bone formation, most commonly on facial bones (Caffey's) ○ Osteal bulges ○ Irregular thickening of internal surface of frontal bone while external surface looks normal (IFH)	○ Expanded cranial vault
Dentition			○ Protruding upper incisors & overbite (Thal.)	○ Linear enamel hypoplasia ○ Brown, dis-coloured teeth, & mottled enamel		○ Dentinogenesis imperfecta
Vertebral Column			○ Perforations in the cortical bone of vertebrae			
Thorax		○ Rib flaring	○ Slight expansion of the ribs ○ Perforated cortical bone in ribs (Thal.) ○ Linear striations on the ribs (Thal.)		○ A lot of subperiosteal new bone formation, most commonly on ribs	

	Scurvy	Rickets	Anaemia	Fluorosis	Hyperostosis	OI
Arms	Porosity on: ○ the scapulae ○ metaphyses of long bones	○ Porosity in concave curvature of long bones ○ Long bone thickening & bowing ○ Long bone metaphyseal flaring	○ Long bone porosity ○ Thinning of trabecular & cortical bone ○ Perforated cortical bone in long bones (Thal.) ○ Necrosis of the humeral head (SCA)			○ Long bone bowing with cortical thickening ○ Narrowing of long bone diaphyses in comparison to their length
Hands						
Pelvis		○ Ilium concavity				
Legs	Porosity on: ○ Metaphyses of long bones	○ Porosity in concave curvature of long bones ○ Long bone thickening & bowing ○ Long bone metaphyseal flaring	○ Long bone porosity ○ Thinning of trabecular & cortical bone ○ Perforated cortical bone in long bones (Thal.) ○ Exaggerated sulci on femora & tibiae (Thal.) ○ Necrosis of the femoral head (SCA)			○ Long bone bowing with cortical thickening ○ Narrowing of long bone diaphyses in comparison to their length
Feet			○ Hyper-trophic meta-carpals & phalanges (Thal.)			

Radiographic Indicators

	Scurvy	Rickets	Anaemia	Fluorosis	Hyperostosis	OI
General Skeleton	○ Generalized osteopenia	○ Generalized osteopenia ○ Thick cortex ○ Sharp cortical outline	○ Thinning of cortical bone			
Cranium			○ Hair-on-end appearance cranium ○ Undeveloped sinuses			
Dentition						
Vertebral Column			○ Reduced number of trabeculae in vertebrae			
Thorax		○ Loss of integrity in sternal rib ends				

	Scurvy	Rickets	Anaemia	Fluorosis	Hyperostosis	OI
Arms	○ Long bone cortical thinning ○ Metaphyseal fractures ○ White line of Fraenkel ○ Wimberger's ring ○ Pelkan's spurs	○ Long bone cortical thinning ○ Metaphyseal fractures ○ Metaphyseal trabecular coarsening ○ Fraying of epiphyses ○ Distinction at the end of the epiphysis	○ Infarcts in long bones ○ Reduced number of trabeculae in long bones			○ Zebra stripe
Hands						
Pelvis						
Legs	○ Long bone cortical thinning ○ Metaphyseal fractures ○ White line of Fraenkel ○ Wimberger's ring ○ Pelkan's spurs	○ Long bone cortical thinning ○ Metaphyseal fractures ○ Fraying of epiphyses ○ Distinction at the end of the epiphysis	○ Infarcts in long bones ○ Reduced number of trabeculae in long bones			○ Zebra stripe
Feet						

SG6 is an individual who mostly exhibits NBF, which is not necessarily pathological. For example, the frontal and facial bones of SG6 have new growth but it is not pathological. There is NBF on their right maxillary palate process, and on the lesser wings of the sphenoid. But again, given this individual's age this is not necessarily pathological. There is also new bone formation on the right ulna which is mostly concentrated on the proximal end of the diaphysis. However, this again could be normative given the individual's age. The left radius and ulna both show NBF as well, but again this appears to be normative. In the left radius the NBF is across the diaphysis but concentrated at the proximal end. In the left ulna this patterning is repeated. The left ischium also shows new growth as well which is believed to be normative given the rest of the NBF and new growth patterning displayed in SG6's remains. In the right ilium the growth is outward across the whole bone. There is porosity on the lumbar neural arches, but it is also believed to be normative given SG6's age. Most of SG6's skeleton is covered in new growth but given their young age, none of it is deemed to strictly be pathological or align with any MBD indicators. Due to this, no diagnosis is given.

SG7

Macroscopic Indicators

	Scurvy	Rickets	Anaemia	Fluorosis	Hyperostosis	OI
General Skeleton	○ Irregular & spongy new bone formation	○ General porosity ○ Abnormal growth plates	○ Porosity ○ Osteopenia (Thal.) ○ Large bony masses (Thal.)	○ Diffuse osteosclerosis of the appendicular & axial skeleton ○ Increased cortical & trabecular thickness ○ Periosteal thickening ○ Calcified ligaments, tendons, cartilage, & inter-osseous membrane-s ○ Bony exostoses at ligament & muscle attachment zones	○ Increased weight of bones ○ Increased thickness of cortical bone ○ A lot of subperiosteal new bone formation	○ Lightness/fragility to bones ○ Fractures ○ Osteoporosis
Orbits	○ Cribra orbitalia ○ Porosity	○ Orbital roof porosity	○ Cribra orbitalia ○ Thinning of trabecular & cortical bone ○ Widening interorbital space (Thal.)			○ Elongated orbits
Cranium	Porosity on: ○ the greater sphenoid wing ○ cranial bones ○ facial bones ○ palate ○ basiocciput	○ Frontal bone bossing ○ Deformed mandibular ramus	○ Cranial vault porosity ○ Thickening of the sphenoid, maxillae, & zygomatics (Thal.) ○ Obliterated sutures in the cranium (Thal.)		○ A lot of subperiosteal new bone formation, most commonly on facial bones (Caffey's) ○ Osteal bulges ○ Irregular thickening of internal surface of frontal bone while external surface looks normal (IFH)	○ Expanded cranial vault
Dentition			○ Protruding upper incisors & overbite (Thal.)	○ Linear enamel hypoplasia ○ Brown, dis-coloured teeth, & mottled enamel		○ Dentinogenesis imperfecta
Vertebral Column			○ Perforations in the cortical bone of vertebrae			
Thorax		○ Rib flaring	○ Slight expansion of the ribs ○ Perforated cortical bone in ribs (Thal.) ○ Linear striations on the ribs (Thal.)		○ A lot of subperiosteal new bone formation, most commonly on ribs	
Arms	Porosity on: ○ the scapulae ○ metaphyses of long bones	○ Porosity in concave curvature of long bones ○ Long bone thickening & bowing	○ Long bone porosity ○ Thinning of trabecular & cortical bone ○ Perforated cortical bone in long bones (Thal.)			○ Long bone bowing with cortical thickening ○ Narrowing of long bone diaphyses in comparison to their length

	Scurvy	Rickets	Anaemia	Fluorosis	Hyperostosis	OI
		○ Long bone metaphyseal flaring	○ Necrosis of the humeral head (SCA)			
Hands						
Pelvis		○ Ilium concavity				
Legs	Porosity on: ○ Metaphyses of long bones	○ Porosity in concave curvature of long bones ○ Long bone thickening & bowing ○ Long bone metaphyseal flaring	○ Long bone porosity ○ Thinning of trabecular & cortical bone ○ Perforated cortical bone in long bones (Thal.) ○ Exaggerated sulci on femora & tibiae (Thal.) ○ Necrosis of the femoral head (SCA)			○ Long bone bowing with cortical thickening ○ Narrowing of long bone diaphyses in comparison to their length
Feet			○ Hyper-trophic meta-carpals & phalanges (Thal.)			

Radiographic Indicators

	Scurvy	Rickets	Anaemia	Fluorosis	Hyperostosis	OI
General Skeleton	○ Generalized osteopenia	○ Generalized osteopenia ○ Thick cortex ○ Sharp cortical outline	○ Thinning of cortical bone			
Cranium			○ Hair-on-end appearance cranium ○ Undeveloped sinuses			
Dentition						
Vertebral Column			○ Reduced number of trabeculae in vertebrae			
Thorax		○ Loss of integrity in sternal rib ends				

	Scurvy	Rickets	Anaemia	Fluorosis	Hyperostosis	OI
Arms	○ Long bone cortical thinning ○ Metaphyseal fractures ○ White line of Fraenkel ○ Wimberger's ring ○ Pelkan's spurs	○ Long bone cortical thinning ○ Metaphyseal fractures ○ Metaphyseal trabecular coarsening ○ Fraying of epiphyses ○ Distinction at the end of the epiphysis	○ Infarcts in long bones ○ Reduced number of trabeculae in long bones			○ Zebra stripe
Hands						
Pelvis						
Legs	○ Long bone cortical thinning ○ Metaphyseal fractures ○ White line of Fraenkel ○ Wimberger's ring ○ Pelkan's spurs	○ Long bone cortical thinning ○ Metaphyseal fractures ○ Fraying of epiphyses ○ Distinction at the end of the epiphysis	○ Infarcts in long bones ○ Reduced number of trabeculae in long bones			○ Zebra stripe
Feet						

SG7 demonstrates some PMD and taphonomic changes throughout their skeleton. SG7 has lesions associated with new growth and bone formation, as well as ones which demonstrate porosity. There are a few lesions on their cranium. For one, they have new growth patterning on their left exoccipital and temporal. In the left exoccipital this new growth is around the edges of the bones. There is also new growth on the right exoccipital accompanied by porosity. This new growth and porosity occurs across both the internal and external surface of the bone. On their basiocciput, there is clumped porosity on the posterior surface. Additionally, there is porosity and new growth on the left and right alisphenoid. The new growth on the left alisphenoid takes place across the entire external surface of the bone while on the right alisphenoid the new growth covers about half of the outer cortical surface. Both of SG7's orbits show shelf-like new growth across the orbital roof but there is no porosity. In SG7's shoulder girdle, the left scapula is quite thin. Additionally, their right clavicle has new growth across the diaphysis accompanied by a bump in the middle of the diaphysis. The left clavicle is only partial and has PMD, so a complete comparison cannot be made. However, there is new growth on the left's diaphysis

but does not appear to be to the same extent as the right. Additionally, there does not appear to be or to have been a bump in the diaphysis of the left clavicle. In SG7, both of their ulnae show signs of new growth, but neither is pathological. In SG7's pelvis, the right ilium demonstrates pathological new growth while the right ilium displays outward new growth on the external surface. This is repeated on the inner surface, and the new bone formation appears shelf-like in places. On their upper right DI1, there is an enamel defect on the lingual surface as shown. The upper right DC has a hypoplastic defect on the tip and a line across the centre of the tooth. In the lower right DP3 the enamel formation is poor on the tip of the hypoconid. There are no pathological indicators on SG7's radiographs.

While SG7 has pathological NBF and new growth, these lesions do not necessarily fit into a MBD framework. Their NBF is not sponge-like and irregular, so these areas are not scorbutic lesions. However, some of SG7's lesions could be scorbutic like the porosity seen on the cranial bones and basiocciput. The porosity seen on the left and right alisphenoid is a diagnostic indicator of scurvy though (as the alisphenoid make up the greater wings). The new growth/SPNB seen on the orbital roofs is also a diagnostic indicator of scurvy. The presence of these two diagnostic lesions would indicate a probable case of scurvy. None of SG7's other lesions line up with MBD indicators.

SG8

Macroscopic Indicators

	Scurvy	Rickets	Anaemia	Fluorosis	Hyperostosis	OI
General Skeleton	○ Irregular & spongy new bone formation	○ General porosity ○ Abnormal growth plates	○ Porosity ○ Osteopenia (Thal.) ○ Large bony masses (Thal.)	○ Diffuse osteosclerosis of the appendicular & axial skeleton ○ Increased cortical & trabecular thickness ○ Periosteal thickening ○ Calcified ligaments, tendons, cartilage, & inter-osseous membrane-s ○ Bony exostoses at ligament & muscle attachment zones	○ Increased weight of bones ○ Increased thickness of cortical bone ○ A lot of subperiosteal new bone formation	○ Lightness/fragility to bones ○ Fractures ○ Osteoporosis
Orbits	○ Cribra orbitalia ○ Porosity	○ Orbital roof porosity	○ Cribra orbitalia ○ Thinning of trabecular & cortical bone ○ Widening interorbital space (Thal.)			○ Elongated orbits
Cranium	Porosity on: ○ the greater sphenoid wing ○ cranial bones ○ facial bones ○ palate ○ basiocciput	○ Frontal bone bossing ○ Deformed mandibular ramus	○ Cranial vault porosity ○ Thickening of the sphenoid, maxillae, & zygomatics (Thal.) ○ Obliterated sutures in the cranium (Thal.)		○ A lot of subperiosteal new bone formation, most commonly on facial bones (Caffey's) ○ Osteal bulges ○ Irregular thickening of internal surface of frontal bone while external surface looks normal (IFH)	○ Expanded cranial vault
Dentition			○ Protruding upper incisors & overbite (Thal.)	○ Linear enamel hypoplasia ○ Brown, dis-coloured teeth, & mottled enamel		○ Dentinogenesis imperfecta
Vertebral Column			○ Perforations in the cortical bone of vertebrae			
Thorax		○ Rib flaring	○ Slight expansion of the ribs ○ Perforated cortical bone in ribs (Thal.) ○ Linear striations on the ribs (Thal.)		○ A lot of subperiosteal new bone formation, most commonly on ribs	
Arms	Porosity on: ○ the scapulae ○ metaphyses of long bones	○ Porosity in concave curvature of long bones ○ Long bone thickening & bowing	○ Long bone porosity ○ Thinning of trabecular & cortical bone ○ Perforated cortical bone in long bones (Thal.)			○ Long bone bowing with cortical thickening ○ Narrowing of long bone diaphyses in comparison to their length

	Scurvy	Rickets	Anaemia	Fluorosis	Hyperostosis	OI
		○ Long bone metaphyseal flaring	○ Necrosis of the humeral head (SCA)			
Hands						
Pelvis		○ Ilium concavity				
Legs	Porosity on: ○ Metaphyses of long bones	○ Porosity in concave curvature of long bones ○ Long bone thickening & bowing ○ Long bone metaphyseal flaring	○ Long bone porosity ○ Thinning of trabecular & cortical bone ○ Perforated cortical bone in long bones (Thal.) ○ Exaggerated sulci on femora & tibiae (Thal.) ○ Necrosis of the femoral head (SCA)			○ Long bone bowing with cortical thickening ○ Narrowing of long bone diaphyses in comparison to their length
Feet			○ Hyper-trophic meta-carpals & phalanges (Thal.)			

Radiographic Indicators

	Scurvy	Rickets	Anaemia	Fluorosis	Hyperostosis	OI
General Skeleton	○ Generalized osteopenia	○ Generalized osteopenia ○ Thick cortex ○ Sharp cortical outline	○ Thinning of cortical bone			
Cranium			○ Hair-on-end appearance cranium ○ Undeveloped sinuses			
Dentition						
Vertebral Column			○ Reduced number of trabeculae in vertebrae			
Thorax		○ Loss of integrity in sternal rib ends				

	Scurvy	Rickets	Anaemia	Fluorosis	Hyperostosis	OI
Arms	○ Long bone cortical thinning ○ Metaphyseal fractures ○ White line of Fraenkel ○ Wimberger's ring ○ Pelkan's spurs	○ Long bone cortical thinning ○ Metaphyseal fractures ○ Metaphyseal trabecular coarsening ○ Fraying of epiphyses ○ Distinction at the end of the epiphysis	○ Infarcts in long bones ○ Reduced number of trabeculae in long bones			○ Zebra stripe
Hands						
Pelvis						
Legs	○ Long bone cortical thinning ○ Metaphyseal fractures ○ White line of Fraenkel ○ Wimberger's ring ○ Pelkan's spurs	○ Long bone cortical thinning ○ Metaphyseal fractures ○ Fraying of epiphyses ○ Distinction at the end of the epiphysis	○ Infarcts in long bones ○ Reduced number of trabeculae in long bones			○ Zebra stripe
Feet						

SG8 has a few lesions. The basioccput shows widespread porosity on the external surface, except for in the centre. On the left maxilla, there is porosity accompanied by NBF on the superior surface has porosity and the inferior surface has some new growth. Additionally, on the various cranial fragments there is porosity and new growth as shown in but most of these fragments display what would be in the normative range of change though. In the shoulder girdle, the left scapula has porosity around the edges, and NBF across the posterior surface. This new bone growth almost has a shelf-like appearance. This may be a within normal range outward growth example. There are no clear indicators of pathology on SG8's radiographs.

Some of the lesions in which their provenience is clear, could be tied to scurvy. For one, the porosity seen on the cranial and facial bones could be related. Additionally, the basioccipital porosity could also be related to scurvy. The lesions seen on SG8's remains are not associated with any other kind of MBD. The porosity seen on the maxilla is a diagnostic feature of scurvy. But as the other features are not diagnostic or suggestive of scurvy a probable diagnosis is not made.

SG9

Macroscopic Indicators

	Scurvy	Rickets	Anaemia	Fluorosis	Hyperostosis	OI
General Skeleton	○ Irregular & spongy new bone formation	○ General porosity ○ Abnormal growth plates	○ Porosity ○ Osteopenia (Thal.) ○ Large bony masses (Thal.)	○ Diffuse osteosclerosis of the appendicular & axial skeleton ○ Increased cortical & trabecular thickness ○ Periosteal thickening ○ Calcified ligaments, tendons, cartilage, & inter-osseous membrane-s ○ Bony exostoses at ligament & muscle attachment zones	○ Increased weight of bones ○ Increased thickness of cortical bone ○ A lot of subperiosteal new bone formation	○ Lightness/fragility to bones ○ Fractures ○ Osteoporosis
Orbits	○ Cribra orbitalia ○ Porosity	○ Orbital roof porosity	○ Cribra orbitalia ○ Thinning of trabecular & cortical bone ○ Widening interorbital space (Thal.)			○ Elongated orbits
Cranium	Porosity on: ○ the greater sphenoid wing ○ cranial bones ○ facial bones ○ palate ○ basiocciput	○ Frontal bone bossing ○ Deformed mandibular ramus	○ Cranial vault porosity ○ Thickening of the sphenoid, maxillae, & zygomatics (Thal.) ○ Obliterated sutures in the cranium (Thal.)		○ A lot of subperiosteal new bone formation, most commonly on facial bones (Caffey's) ○ Osteal bulges ○ Irregular thickening of internal surface of frontal bone while external surface looks normal (IFH)	○ Expanded cranial vault
Dentition			○ Protruding upper incisors & overbite (Thal.)	○ Linear enamel hypoplasia ○ Brown, dis-coloured teeth, & mottled enamel		○ Dentinogenesis imperfecta
Vertebral Column			○ Perforations in the cortical bone of vertebrae			
Thorax		○ Rib flaring	○ Slight expansion of the ribs ○ Perforated cortical bone in ribs (Thal.) ○ Linear striations on the ribs (Thal.)		○ A lot of subperiosteal new bone formation, most commonly on ribs	
Arms	Porosity on: ○ the scapulae ○ metaphyses of long bones	○ Porosity in concave curvature of long bones ○ Long bone thickening & bowing	○ Long bone porosity ○ Thinning of trabecular & cortical bone ○ Perforated cortical bone in long bones (Thal.)			○ Long bone bowing with cortical thickening ○ Narrowing of long bone diaphyses in comparison to their length

	Scurvy	Rickets	Anaemia	Fluorosis	Hyperostosis	OI
		○ Long bone metaphyseal flaring	○ Necrosis of the humeral head (SCA)			
Hands						
Pelvis		○ Ilium concavity				
Legs	Porosity on: ○ Metaphyses of long bones	○ Porosity in concave curvature of long bones ○ Long bone thickening & bowing ○ Long bone metaphyseal flaring	○ Long bone porosity ○ Thinning of trabecular & cortical bone ○ Perforated cortical bone in long bones (Thal.) ○ Exaggerated sulci on femora & tibiae (Thal.) ○ Necrosis of the femoral head (SCA)			○ Long bone bowing with cortical thickening ○ Narrowing of long bone diaphyses in comparison to their length
Feet			○ Hyper-trophic meta-carpals & phalanges (Thal.)			

Radiographic Indicators

	Scurvy	Rickets	Anaemia	Fluorosis	Hyperostosis	OI
General Skeleton	○ Generalized osteopenia	○ Generalized osteopenia ○ Thick cortex ○ Sharp cortical outline	○ Thinning of cortical bone			
Cranium			○ Hair-on-end appearance cranium ○ Undeveloped sinuses			
Dentition						
Vertebral Column			○ Reduced number of trabeculae in vertebrae			
Thorax		○ Loss of integrity in sternal rib ends				

	Scurvy	Rickets	Anaemia	Fluorosis	Hyperostosis	OI
Arms	○ Long bone cortical thinning ○ Metaphyseal fractures ○ White line of Fraenkel ○ Wimberger's ring ○ Pelkan's spurs	○ Long bone cortical thinning ○ Metaphyseal fractures ○ Metaphyseal trabecular coarsening ○ Fraying of epiphyses ○ Distinction at the end of the epiphysis	○ Infarcts in long bones ○ Reduced number of trabeculae in long bones			○ Zebra stripe
Hands						
Pelvis						
Legs	○ Long bone cortical thinning ○ Metaphyseal fractures ○ White line of Fraenkel ○ Wimberger's ring ○ Pelkan's spurs	○ Long bone cortical thinning ○ Metaphyseal fractures ○ Fraying of epiphyses ○ Distinction at the end of the epiphysis	○ Infarcts in long bones ○ Reduced number of trabeculae in long bones			○ Zebra stripe
Feet						

SG9 has lesions on their cranium. There is subperiosteal new bone formation and porosity in the right orbit. The hole present in the right orbit would have been from a bubble of new bone formation, which is since missing. This indicates subperiosteal new bone formation as it would have been expanding outwards, and not into the diploë. There is also porosity on the left orbit but not to the same extent as the right. The endocranial surface of both the right and left frontals appears to be normal. There are a few areas of the cranium which exhibit NBF. NBF occurs on the superior and inferior maxillae and is accompanied by porosity. This extends across the palate portion of the bone. SG9's shoulder girdle also demonstrates pathology. The left scapula has porosity along and inside the scapular ridge, accompanied by new growth on the entire bone. While the new growth in this scapula could be normative, the porosity inside the scapular ridge is not. There are no lesions present in SG9's radiographs.

Some of the pathology present in SG9 aligns with MBD. The porosity, and cribra orbitalia, present in SG9 align with scurvy. The porosity present on some of SG9's bones (maxillae and left scapular ridge) are all consistent with how scorbutic lesions can

present in skeletal remains. The lesions SG9 displays also fall into the diagnostic category for scorbutic lesions: maxillary posterior aspect SPNB/porosity, scapular supraspinous fossa porosity, the orbital roof SPNB, and the maxillary palate porosity. However, scurvy is not the only MBD in which SG9's lesions are consistent with. The orbital roof porosity that SG9 has is a non-diagnostic feature of rickets. SG9's cribra orbitalia does not align with anaemia as it came outwards of the bone rather than burrowing into the diploë. Given that SG9's lesions align more concretely with scurvy in the number of diagnostic lesions, that seems to be the most likely MBD that SG9 lived with.

SG10

Macroscopic Indicators

	Scurvy	Rickets	Anaemia	Fluorosis	Hyperostosis	OI
General Skeleton	○ Irregular & spongy new bone formation	○ General porosity ○ Abnormal growth plates	○ Porosity ○ Osteopenia (Thal.) ○ Large bony masses (Thal.)	○ Diffuse osteosclerosis of the appendicular & axial skeleton ○ Increased cortical & trabecular thickness ○ Periosteal thickening ○ Calcified ligaments, tendons, cartilage, & inter-osseous membrane-s ○ Bony exostoses at ligament & muscle attachment zones	○ Increased weight of bones ○ Increased thickness of cortical bone ○ A lot of subperiosteal new bone formation	○ Lightness/fragility to bones ○ Fractures ○ Osteoporosis
Orbits	○ Cribra orbitalia ○ Porosity	○ Orbital roof porosity	○ Cribra orbitalia ○ Thinning of trabecular & cortical bone ○ Widening interorbital space (Thal.)			○ Elongated orbits
Cranium	Porosity on: ○ the greater sphenoid wing ○ cranial bones ○ facial bones ○ palate ○ basiocciput	○ Frontal bone bossing ○ Deformed mandibular ramus	○ Cranial vault porosity ○ Thickening of the sphenoid, maxillae, & zygomatics (Thal.) ○ Obliterated sutures in the cranium (Thal.)		○ A lot of subperiosteal new bone formation, most commonly on facial bones (Caffey's) ○ Osteal bulges ○ Irregular thickening of internal surface of frontal bone while external surface looks normal (IFH)	○ Expanded cranial vault
Dentition			○ Protruding upper incisors & overbite (Thal.)	○ Linear enamel hypoplasia ○ Brown, dis-coloured teeth, & mottled enamel		○ Dentinogenesis imperfecta
Vertebral Column			○ Perforations in the cortical bone of vertebrae			
Thorax		○ Rib flaring	○ Slight expansion of the ribs ○ Perforated cortical bone in ribs (Thal.) ○ Linear striations on the ribs (Thal.)		○ A lot of subperiosteal new bone formation, most commonly on ribs	
Arms	Porosity on: ○ the scapulae ○ metaphyses of long bones	○ Porosity in concave curvature of long bones ○ Long bone thickening & bowing	○ Long bone porosity ○ Thinning of trabecular & cortical bone ○ Perforated cortical bone in long bones (Thal.)			○ Long bone bowing with cortical thickening ○ Narrowing of long bone diaphyses in comparison to their length

	Scurvy	Rickets	Anaemia	Fluorosis	Hyperostosis	OI
		○ Long bone metaphyseal flaring	○ Necrosis of the humeral head (SCA)			
Hands						
Pelvis		○ Ilium concavity				
Legs	Porosity on: ○ Metaphyses of long bones	○ Porosity in concave curvature of long bones ○ Long bone thickening & bowing ○ Long bone metaphyseal flaring	○ Long bone porosity ○ Thinning of trabecular & cortical bone ○ Perforated cortical bone in long bones (Thal.) ○ Exaggerated sulci on femora & tibiae (Thal.) ○ Necrosis of the femoral head (SCA)			○ Long bone bowing with cortical thickening ○ Narrowing of long bone diaphyses in comparison to their length
Feet			○ Hyper-trophic meta-carpals & phalanges (Thal.)			

Radiographic Indicators

	Scurvy	Rickets	Anaemia	Fluorosis	Hyperostosis	OI
General Skeleton	○ Generalized osteopenia	○ Generalized osteopenia ○ Thick cortex ○ Sharp cortical outline	○ Thinning of cortical bone			
Cranium			○ Hair-on-end appearance cranium ○ Undeveloped sinuses			
Dentition						
Vertebral Column			○ Reduced number of trabeculae in vertebrae			
Thorax		○ Loss of integrity in sternal rib ends				

	Scurvy	Rickets	Anaemia	Fluorosis	Hyperostosis	OI
Arms	○ Long bone cortical thinning ○ Metaphyseal fractures ○ White line of Fraenkel ○ Wimberger's ring ○ Pelkan's spurs	○ Long bone cortical thinning ○ Metaphyseal fractures ○ Metaphyseal trabecular coarsening ○ Fraying of epiphyses ○ Distinction at the end of the epiphysis	○ Infarcts in long bones ○ Reduced number of trabeculae in long bones			○ Zebra stripe
Hands						
Pelvis						
Legs	○ Long bone cortical thinning ○ Metaphyseal fractures ○ White line of Fraenkel ○ Wimberger's ring ○ Pelkan's spurs	○ Long bone cortical thinning ○ Metaphyseal fractures ○ Fraying of epiphyses ○ Distinction at the end of the epiphysis	○ Infarcts in long bones ○ Reduced number of trabeculae in long bones			○ Zebra stripe
Feet						

SG10 is an individual whose lesions are mostly contained to the cranium. One of their lesions is NBF and porosity in their left orbit along with orbital roof resorption. There are also these changes in the right orbit, but they are not to the same extent as the left. NBF is present on both temporals. On the left temporal, the NBF occurs around the perimeter of the ectocranial surface and is repeated in the right temporal. Porosity occurs around the perimeter of the ectocranial surface of the left and right parietal. The occipital exhibits this pattern as well. None of this NBF on the cranial vault looks out of the range of normal. However, it should be noted that this individual has possible cranial modification and that could be what is causing the new growth on the cranial vault. This possible cranial deformation would have to be confirmed by 3D modelling as the bones are warped from time and drying so an accurate physical reconstruction is not possible. Another lesion of note is that there is a possible infection in the pituitary fossa of the basisphenoid. There are no radiographic indicators of pathology associated with SG10.

SG10 has two types of lesions: the changes in their orbits, and the possible infection in their basisphenoid. One disease in which these lesions align is that of scurvy as the porosity and cribra orbitalia seen in both orbits could be associated. However, these same lesions could also align with anaemia and pellagra as cribra orbitalia. As well, this orbital roof porosity is a non-diagnostic feature of rickets. However, as SG10 has one lesion type associated with each of these MBDs, there is no way to know which would be the most accurate diagnosis. Additionally, one lesion is not enough support for a diagnosis, especially when they are not diagnostic or suggestive. Given this, no diagnosis is given.

SG11

Macroscopic Indicators

	Scurvy	**Rickets**	**Anaemia**	**Fluorosis**	**Hyperostosis**	**OI**
General Skeleton	○ Irregular & spongy new bone formation	○ General porosity ○ Abnormal growth plates	○ Porosity ○ Osteopenia (Thal.) ○ Large bony masses (Thal.)	○ Diffuse osteosclerosis of the appendicular & axial skeleton ○ Increased cortical & trabecular thickness ○ Periosteal thickening ○ Calcified ligaments, tendons, cartilage, & inter-osseous membrane-s ○ Bony exostoses at ligament & muscle attachment zones	○ Increased weight of bones ○ Increased thickness of cortical bone ○ A lot of subperiosteal new bone formation	○ Lightness/fragility to bones ○ Fractures ○ Osteoporosis
Orbits	○ Cribra orbitalia ○ Porosity	○ Orbital roof porosity	○ Cribra orbitalia ○ Thinning of trabecular & cortical bone ○ Widening interorbital space (Thal.)			○ Elongated orbits
Cranium	Porosity on: ○ the greater sphenoid wing ○ cranial bones ○ facial bones ○ palate ○ basiocciput	○ Frontal bone bossing ○ Deformed mandibular ramus	○ Cranial vault porosity ○ Thickening of the sphenoid, maxillae, & zygomatics (Thal.) ○ Obliterated sutures in the cranium (Thal.)		○ A lot of subperiosteal new bone formation, most commonly on facial bones (Caffey's) ○ Osteal bulges ○ Irregular thickening of internal surface of frontal bone while external surface looks normal (IFH)	○ Expanded cranial vault
Dentition			○ Protruding upper incisors & overbite (Thal.)	○ Linear enamel hypoplasia ○ Brown, dis-coloured teeth, & mottled enamel		○ Dentinogenesis imperfecta

	Scurvy	Rickets	Anaemia	Fluorosis	Hyperostosis	OI
Vertebral Column			○ Perforations in the cortical bone of vertebrae			
Thorax		○ Rib flaring	○ Slight expansion of the ribs ○ Perforated cortical bone in ribs (Thal.) ○ Linear striations on the ribs (Thal.)		○ A lot of subperiosteal new bone formation, most commonly on ribs	
Arms	Porosity on: ○ the scapulae ○ metaphyses of long bones	○ Porosity in concave curvature of long bones ○ Long bone thickening & bowing ○ Long bone metaphyseal flaring	○ Long bone porosity ○ Thinning of trabecular & cortical bone ○ Perforated cortical bone in long bones (Thal.) ○ Necrosis of the humeral head (SCA)			○ Long bone bowing with cortical thickening ○ Narrowing of long bone diaphyses in comparison to their length
Hands						
Pelvis		○ Ilium concavity				
Legs	Porosity on: ○ Metaphyses of long bones	○ Porosity in concave curvature of long bones ○ Long bone thickening & bowing ○ Long bone metaphyseal flaring	○ Long bone porosity ○ Thinning of trabecular & cortical bone ○ Perforated cortical bone in long bones (Thal.) ○ Exaggerated sulci on femora & tibiae (Thal.) ○ Necrosis of the femoral head (SCA)			○ Long bone bowing with cortical thickening ○ Narrowing of long bone diaphyses in comparison to their length
Feet			○ Hyper-trophic meta-carpals & phalanges (Thal.)			

Radiographic Indicators

	Scurvy	Rickets	Anaemia	Fluorosis	Hyperostosis	OI
General Skeleton	○ Generalized osteopenia	○ Generalized osteopenia ○ Thick cortex ○ Sharp cortical outline	○ Thinning of cortical bone			
Cranium			○ Hair-on-end appearance cranium ○ Undeveloped sinuses			

	Scurvy	Rickets	Anaemia	Fluorosis	Hyperostosis	OI
Dentition						
Vertebral Column			○ Reduced number of trabeculae in vertebrae			
Thorax		○ Loss of integrity in sternal rib ends				
Arms	○ Long bone cortical thinning ○ Metaphyseal fractures ○ White line of Fraenkel ○ Wimberger's ring ○ Pelkan's spurs	○ Long bone cortical thinning ○ Metaphyseal fractures ○ Metaphyseal trabecular coarsening ○ Fraying of epiphyses ○ Distinction at the end of the epiphysis	○ Infarcts in long bones ○ Reduced number of trabeculae in long bones			○ Zebra stripe
Hands						
Pelvis						
Legs	○ Long bone cortical thinning ○ Metaphyseal fractures ○ White line of Fraenkel ○ Wimberger's ring ○ Pelkan's spurs	○ Long bone cortical thinning ○ Metaphyseal fractures ○ Fraying of epiphyses ○ Distinction at the end of the epiphysis	○ Infarcts in long bones ○ Reduced number of trabeculae in long bones			○ Zebra stripe
Feet						

SG11 is an individual whose remains are affected widely by PMD. SG11 also has lesions on their cranium. The left petrous and partial squamous portions of the left temporal demonstrate SPNB that is sheet-like on the ectocranial surface. The right temporal petrous and partial squamous portions also demonstrate SPNB across the entire ectocranial surface. The NBF also continues across the endocranial surface, but mostly around the perimeter of the bone. There is also NBF and porosity on the foramen magnum (basiocciput and the exoccipitals) which appears to have been widespread. However, PMD obscures a lot of the skeletal elements which could have had lesions present. Cranial fragments also have widespread NBF, but it is not inherently pathological. The orbits of SG11 demonstrate NBF around their perimeter, there is also NBF on the frontals. The NBF seems to be contained to the perimeter of

the ectocranial surface for the most part with the frontals. Due to the extent of the PMD it is not possible to tell whether this NBF in the orbits was pathological or not. It also appears that there may have been trephination on the left and right frontal bosses, as around these holes there appears to be new growth which may indicate healing. The endocranial surface echoes this. In terms of the shoulder girdle, the left clavicle has an odd curvature and NBF at both the proximal and distal ends. This odd curvature is also visible in the radiographs. The right clavicle also has NBF along with a swollen diaphyseal shaft. However, only a partial right clavicle is present so not many interpretations can be made from it. Moving on to the arms, the right ulna has evidence of NBF along the diaphysis and post-mortem damage. The NBF associated with the right ulna is concentrated at the distal and proximal ends and is reflective of subperiosteal haemorrhage. Previous researchers have noted that there is evidence for subperiosteal haemorrhage on all SG11's long bones. There is NBF and PMD on both the right and left humerus. The NBF occurs all over the right humerus but is concentrated around the proximal end. The left humerus also has NBF, but it is more concentrated on the distal end. Additionally, the radiograph of the left humerus seems to display a new layer of bone growth. Both radii have widespread NBF with the left radius also presenting with PMD. The left tibia has NBF and PMD both anteriorly and posteriorly on the diaphysis, while the left femur has NBF. On the left tibia the NBF is widespread across the diaphysis but is concentrated on the distal end on the posterior surface and concentrated on the proximal end on the anterior surface. The left and right femora have widespread NBF on the diaphysis, with the right having a concentration on the proximal end. The right femoral proximal end seems to indicate slight subperiosteal haemorrhage as well. Finally, the metacarpals or metatarsals (it is unclear which they are) have NBF across their diaphyses.

SG11's lesions only correspond with one MBD, and not all the lesions necessarily fit. The widespread abnormal NBF could be related to scurvy. Additionally, the bones which demonstrate NBF, which looks subperiosteal haemorrhage-like, could be related. The widespread SPNB could be related to another MBD, such as hyperostosis, but in those instances, it is most associated with specific areas of the skeleton in which SG11 does not display SPNB. The SPNB that SG11 demonstrates on the diaphyses of their long bones is suggestive of scurvy, as is the SPNB in their cranial vault, specifically the temporals. As such, the most likely diagnosis is scurvy.

However, the indicators of trephination could be suggestive of a different condition affecting this person in life, as no other individuals with a possible diagnosis of scurvy display markers of trephination.

SG12

Macroscopic Indicators

	Scurvy	Rickets	Anaemia	Fluorosis	Hyperostosis	OI
General Skeleton	○ Irregular & spongy new bone formation	○ General porosity ○ Abnormal growth plates	○ Porosity ○ Osteopenia (Thal.) ○ Large bony masses (Thal.)	○ Diffuse osteosclerosis of the appendicular & axial skeleton ○ Increased cortical & trabecular thickness ○ Periosteal thickening ○ Calcified ligaments, tendons, cartilage, & inter-osseous membrane-s ○ Bony exostoses at ligament & muscle attachment zones	○ Increased weight of bones ○ Increased thickness of cortical bone ○ A lot of subperiosteal new bone formation	○ Lightness/fragility to bones ○ Fractures ○ Osteoporosis
Orbits	○ Cribra orbitalia ○ Porosity	○ Orbital roof porosity	○ Cribra orbitalia ○ Thinning of trabecular & cortical bone ○ Widening interorbital space (Thal.)			○ Elongated orbits
Cranium	Porosity on: ○ the greater sphenoid wing ○ cranial bones ○ facial bones ○ palate ○ basiocciput	○ Frontal bone bossing ○ Deformed mandibular ramus	○ Cranial vault porosity ○ Thickening of the sphenoid, maxillae, & zygomatics (Thal.) ○ Obliterated sutures in the cranium (Thal.)		○ A lot of subperiosteal new bone formation, most commonly on facial bones (Caffey's) ○ Osteal bulges ○ Irregular thickening of internal surface of frontal bone while external surface looks normal (IFH)	○ Expanded cranial vault
Dentition			○ Protruding upper incisors & overbite (Thal.)	○ Linear enamel hypoplasia ○ Brown, dis-coloured teeth, & mottled enamel		○ Dentinogenesis imperfecta
Vertebral Column			○ Perforations in the cortical bone of vertebrae			
Thorax		○ Rib flaring	○ Slight expansion of the ribs ○ Perforated cortical bone in ribs (Thal.) ○ Linear striations on the ribs (Thal.)		○ A lot of subperiosteal new bone formation, most commonly on ribs	

	Scurvy	Rickets	Anaemia	Fluorosis	Hyperostosis	OI
Arms	Porosity on: ○ the scapulae ○ metaphyses of long bones	○ Porosity in concave curvature of long bones ○ Long bone thickening & bowing ○ Long bone metaphyseal flaring	○ Long bone porosity ○ Thinning of trabecular & cortical bone ○ Perforated cortical bone in long bones (Thal.) ○ Necrosis of the humeral head (SCA)			○ Long bone bowing with cortical thickening ○ Narrowing of long bone diaphyses in comparison to their length
Hands						
Pelvis		○ Ilium concavity				
Legs	Porosity on: ○ Metaphyses of long bones	○ Porosity in concave curvature of long bones ○ Long bone thickening & bowing ○ Long bone metaphyseal flaring	○ Long bone porosity ○ Thinning of trabecular & cortical bone ○ Perforated cortical bone in long bones (Thal.) ○ Exaggerated sulci on femora & tibiae (Thal.) ○ Necrosis of the femoral head (SCA)			○ Long bone bowing with cortical thickening ○ Narrowing of long bone diaphyses in comparison to their length
Feet			○ Hyper-trophic meta-carpals & phalanges (Thal.)			

Radiographic Indicators

	Scurvy	Rickets	Anaemia	Fluorosis	Hyperostosis	OI
General Skeleton	○ Generalized osteopenia	○ Generalized osteopenia ○ Thick cortex ○ Sharp cortical outline	○ Thinning of cortical bone			
Cranium			○ Hair-on-end appearance cranium ○ Undeveloped sinuses			
Dentition						
Vertebral Column			○ Reduced number of trabeculae in vertebrae			
Thorax		○ Loss of integrity in sternal rib ends				

	Scurvy	Rickets	Anaemia	Fluorosis	Hyperostosis	OI
Arms	○ Long bone cortical thinning ○ Metaphyseal fractures ○ White line of Fraenkel ○ Wimberger's ring ○ Pelkan's spurs	○ Long bone cortical thinning ○ Metaphyseal fractures ○ Metaphyseal trabecular coarsening ○ Fraying of epiphyses ○ Distinction at the end of the epiphysis	○ Infarcts in long bones ○ Reduced number of trabeculae in long bones			○ Zebra stripe
Hands						
Pelvis						
Legs	○ Long bone cortical thinning ○ Metaphyseal fractures ○ White line of Fraenkel ○ Wimberger's ring ○ Pelkan's spurs	○ Long bone cortical thinning ○ Metaphyseal fractures ○ Fraying of epiphyses ○ Distinction at the end of the epiphysis	○ Infarcts in long bones ○ Reduced number of trabeculae in long bones			○ Zebra stripe
Feet						

There are a few skeletal regions of SG12 which display pathology. The cranium demonstrated widespread PMD but there are still distinguishable lesions. Both orbits demonstrate porosity, but this is more extensive in the right than the left. Some of the cortical bone of the left orbit has been removed via PMD. In the should girdle, the right clavicle has an odd bend to the diaphysis accompanied by a healing fracture indicated by bowing dorsally at the sternal end. The radiograph of the right clavicle also shows this odd bend. In the pelvis, the left ischium has both porosity and NBF across the entire bone.

The orbital changes that SG12 has could be related to scurvy but could also be associated with anaemia, pellagra, or rickets.

SG13

Macroscopic Indicators

	Scurvy	Rickets	Anaemia	Fluorosis	Hyperostosis	OI
General Skeleton	○ Irregular & spongy new bone formation	○ General porosity ○ Abnormal growth plates	○ Porosity ○ Osteopenia (Thal.) ○ Large bony masses (Thal.)	○ Diffuse osteosclerosis of the appendicular & axial skeleton ○ Increased cortical & trabecular thickness ○ Periosteal thickening ○ Calcified ligaments, tendons, cartilage, & inter-osseous membrane-s ○ Bony exostoses at ligament & muscle attachment zones	○ Increased weight of bones ○ Increased thickness of cortical bone ○ A lot of subperiosteal new bone formation	○ Lightness/fragility to bones ○ Fractures ○ Osteoporosis
Orbits	○ Cribra orbitalia ○ Porosity	○ Orbital roof porosity	○ Cribra orbitalia ○ Thinning of trabecular & cortical bone ○ Widening interorbital space (Thal.)			○ Elongated orbits
Cranium	Porosity on: ○ the greater sphenoid wing ○ cranial bones ○ facial bones ○ palate ○ basiocciput	○ Frontal bone bossing ○ Deformed mandibular ramus	○ Cranial vault porosity ○ Thickening of the sphenoid, maxillae, & zygomatics (Thal.) ○ Obliterated sutures in the cranium (Thal.)		○ A lot of subperiosteal new bone formation, most commonly on facial bones (Caffey's) ○ Osteal bulges ○ Irregular thickening of internal surface of frontal bone while external surface looks normal (IFH)	○ Expanded cranial vault
Dentition			○ Protruding upper incisors & overbite (Thal.)	○ Linear enamel hypoplasia ○ Brown, dis-coloured teeth, & mottled enamel		○ Dentinogenesis imperfecta
Vertebral Column			○ Perforations in the cortical bone of vertebrae			
Thorax		○ Rib flaring	○ Slight expansion of the ribs ○ Perforated cortical bone in ribs (Thal.) ○ Linear striations on the ribs (Thal.)		○ A lot of subperiosteal new bone formation, most commonly on ribs	
Arms	Porosity on: ○ the scapulae ○ metaphyses of long bones	○ Porosity in concave curvature of long bones ○ Long bone thickening & bowing	○ Long bone porosity ○ Thinning of trabecular & cortical bone ○ Perforated cortical bone in long bones (Thal.)			○ Long bone bowing with cortical thickening ○ Narrowing of long bone diaphyses in comparison to their length

	Scurvy	Rickets	Anaemia	Fluorosis	Hyperostosis	OI
		○ Long bone metaphyseal flaring	○ Necrosis of the humeral head (SCA)			
Hands						
Pelvis		○ Ilium concavity				
Legs	Porosity on: ○ Metaphyses of long bones	○ Porosity in concave curvature of long bones ○ Long bone thickening & bowing ○ Long bone metaphyseal flaring	○ Long bone porosity ○ Thinning of trabecular & cortical bone ○ Perforated cortical bone in long bones (Thal.) ○ Exaggerated sulci on femora & tibiae (Thal.) ○ Necrosis of the femoral head (SCA)			○ Long bone bowing with cortical thickening ○ Narrowing of long bone diaphyses in comparison to their length
Feet			○ Hyper-trophic meta-carpals & phalanges (Thal.)			

Radiographic Indicators

	Scurvy	Rickets	Anaemia	Fluorosis	Hyperostosis	OI
General Skeleton	○ Generalized osteopenia	○ Generalized osteopenia ○ Thick cortex ○ Sharp cortical outline	○ Thinning of cortical bone			
Cranium			○ Hair-on-end appearance cranium ○ Undeveloped sinuses			
Dentition						
Vertebral Column			○ Reduced number of trabeculae in vertebrae			
Thorax		○ Loss of integrity in sternal rib ends				

	Scurvy	Rickets	Anaemia	Fluorosis	Hyperostosis	OI
Arms	○ Long bone cortical thinning ○ Metaphyseal fractures ○ White line of Fraenkel ○ Wimberger's ring ○ Pelkan's spurs	○ Long bone cortical thinning ○ Metaphyseal fractures ○ Metaphyseal trabecular coarsening ○ Fraying of epiphyses ○ Distinction at the end of the epiphysis	○ Infarcts in long bones ○ Reduced number of trabeculae in long bones			○ Zebra stripe
Hands						
Pelvis						
Legs	○ Long bone cortical thinning ○ Metaphyseal fractures ○ White line of Fraenkel ○ Wimberger's ring ○ Pelkan's spurs	○ Long bone cortical thinning ○ Metaphyseal fractures ○ Fraying of epiphyses ○ Distinction at the end of the epiphysis	○ Infarcts in long bones ○ Reduced number of trabeculae in long bones			○ Zebra stripe
Feet						

In SG13's remains, the left tibia presents with widespread NBF, which is concentrated at the proximal end. But this NBF is not inherently pathological and is insufficient evidence for a diagnosis of any kind.

SG14

Macroscopic Indicators

	Scurvy	Rickets	Anaemia	Fluorosis	Hyperostosis	OI
General Skeleton	○ Irregular & spongy new bone formation	○ General porosity ○ Abnormal growth plates	○ Porosity ○ Osteopenia (Thal.) ○ Large bony masses (Thal.)	○ Diffuse osteosclerosis of the appendicular & axial skeleton ○ Increased cortical & trabecular thickness ○ Periosteal thickening ○ Calcified ligaments, tendons, cartilage, & inter-osseous membrane-s ○ Bony exostoses at ligament & muscle attachment zones	○ Increased weight of bones ○ Increased thickness of cortical bone ○ A lot of subperiosteal new bone formation	○ Lightness/fragility to bones ○ Fractures ○ Osteoporosis
Orbits	○ Cribra orbitalia ○ Porosity	○ Orbital roof porosity	○ Cribra orbitalia ○ Thinning of trabecular & cortical bone ○ Widening interorbital space (Thal.)			○ Elongated orbits
Cranium	Porosity on: ○ the greater sphenoid wing ○ cranial bones ○ facial bones ○ palate ○ basiocciput	○ Frontal bone bossing ○ Deformed mandibular ramus	○ Cranial vault porosity ○ Thickening of the sphenoid, maxillae, & zygomatics (Thal.) ○ Obliterated sutures in the cranium (Thal.)		○ A lot of subperiosteal new bone formation, most commonly on facial bones (Caffey's) ○ Osteal bulges ○ Irregular thickening of internal surface of frontal bone while external surface looks normal (IFH)	○ Expanded cranial vault
Dentition			○ Protruding upper incisors & overbite (Thal.)	○ Linear enamel hypoplasia ○ Brown, dis-coloured teeth, & mottled enamel		○ Dentinogenesis imperfecta
Vertebral Column			○ Perforations in the cortical bone of vertebrae			
Thorax		○ Rib flaring	○ Slight expansion of the ribs ○ Perforated cortical bone in ribs (Thal.) ○ Linear striations on the ribs (Thal.)		○ A lot of subperiosteal new bone formation, most commonly on ribs	
Arms	Porosity on: ○ the scapulae ○ metaphyses of long bones	○ Porosity in concave curvature of long bones ○ Long bone thickening & bowing	○ Long bone porosity ○ Thinning of trabecular & cortical bone ○ Perforated cortical bone in long bones (Thal.)			○ Long bone bowing with cortical thickening ○ Narrowing of long bone diaphyses in comparison to their length

	Scurvy	Rickets	Anaemia	Fluorosis	Hyperostosis	OI
		○ Long bone metaphyseal flaring	○ Necrosis of the humeral head (SCA)			
Hands						
Pelvis		○ Ilium concavity				
Legs	Porosity on: ○ Metaphyses of long bones	○ Porosity in concave curvature of long bones ○ Long bone thickening & bowing ○ Long bone metaphyseal flaring	○ Long bone porosity ○ Thinning of trabecular & cortical bone ○ Perforated cortical bone in long bones (Thal.) ○ Exaggerated sulci on femora & tibiae (Thal.) ○ Necrosis of the femoral head (SCA)			○ Long bone bowing with cortical thickening ○ Narrowing of long bone diaphyses in comparison to their length
Feet			○ Hyper-trophic meta-carpals & phalanges (Thal.)			

Radiographic Indicators

	Scurvy	Rickets	Anaemia	Fluorosis	Hyperostosis	OI
General Skeleton	○ Generalized osteopenia	○ Generalized osteopenia ○ Thick cortex ○ Sharp cortical outline	○ Thinning of cortical bone			
Cranium			○ Hair-on-end appearance cranium ○ Undeveloped sinuses			
Dentition						
Vertebral Column			○ Reduced number of trabeculae in vertebrae			
Thorax		○ Loss of integrity in sternal rib ends				

	Scurvy	Rickets	Anaemia	Fluorosis	Hyperostosis	OI
Arms	○ Long bone cortical thinning ○ Metaphyseal fractures ○ White line of Fraenkel ○ Wimberger's ring ○ Pelkan's spurs	○ Long bone cortical thinning ○ Metaphyseal fractures ○ Metaphyseal trabecular coarsening ○ Fraying of epiphyses ○ Distinction at the end of the epiphysis	○ Infarcts in long bones ○ Reduced number of trabeculae in long bones			○ Zebra stripe
Hands						
Pelvis						
Legs	○ Long bone cortical thinning ○ Metaphyseal fractures ○ White line of Fraenkel ○ Wimberger's ring ○ Pelkan's spurs	○ Long bone cortical thinning ○ Metaphyseal fractures ○ Fraying of epiphyses ○ Distinction at the end of the epiphysis	○ Infarcts in long bones ○ Reduced number of trabeculae in long bones			○ Zebra stripe
Feet						

SG14 is an individual who displays cranial pathology. For one, the inner surface of their left orbit has NBF, and porosity and all cranial fragments associated display NBF and porosity. Additionally, there is porosity on the maxillae. This porosity is widespread across the entire inferior surface. It is more porous on the right maxilla on the palatine process. In terms of SG14's teeth, there is an enamel defect on the upper right DP4 The radiographs of SG14 do not indicate any pathology.

A few of SG14's lesions are consistent with MBD. The porosity on their left orbit (or cribra orbitalia) is consistent with scorbutic lesions. Their other lesions which are consistent with scurvy are the porosity seen on both their cranial bones (fragments) and facial bones (maxillae). The palate porosity is suggestive of scurvy, and the cranial vault fragment porosity is a non-diagnostic feature of scurvy. The cranial vault porosity and orbital porosity are also non-diagnostic features of rickets. However, there is not sufficient evidence of either scurvy or rickets to make a diagnosis, instead this could be a possible case of both.

SG15

Macroscopic Indicators

	Scurvy	Rickets	Anaemia	Fluorosis	Hyperostosis	OI
General Skeleton	○ Irregular & spongy new bone formation	○ General porosity ○ Abnormal growth plates	○ Porosity ○ Osteopenia (Thal.) ○ Large bony masses (Thal.)	○ Diffuse osteosclerosis of the appendicular & axial skeleton ○ Increased cortical & trabecular thickness ○ Periosteal thickening ○ Calcified ligaments, tendons, cartilage, & inter-osseous membrane-s ○ Bony exostoses at ligament & muscle attachment zones	○ Increased weight of bones ○ Increased thickness of cortical bone ○ A lot of subperiosteal new bone formation	○ Lightness/fragility to bones ○ Fractures ○ Osteoporosis
Orbits	○ Cribra orbitalia ○ Porosity	○ Orbital roof porosity	○ Cribra orbitalia ○ Thinning of trabecular & cortical bone ○ Widening interorbital space (Thal.)			○ Elongated orbits
Cranium	Porosity on: ○ the greater sphenoid wing ○ cranial bones ○ facial bones ○ palate ○ basiocciput	○ Frontal bone bossing ○ Deformed mandibular ramus	○ Cranial vault porosity ○ Thickening of the sphenoid, maxillae, & zygomatics (Thal.) ○ Obliterated sutures in the cranium (Thal.)		○ A lot of subperiosteal new bone formation, most commonly on facial bones (Caffey's) ○ Osteal bulges ○ Irregular thickening of internal surface of frontal bone while external surface looks normal (IFH)	○ Expanded cranial vault
Dentition			○ Protruding upper incisors & overbite (Thal.)	○ Linear enamel hypoplasia ○ Brown, dis-coloured teeth, & mottled enamel		○ Dentinogenesis imperfecta
Vertebral Column			○ Perforations in the cortical bone of vertebrae			
Thorax		○ Rib flaring	○ Slight expansion of the ribs ○ Perforated cortical bone in ribs (Thal.) ○ Linear striations on the ribs (Thal.)		○ A lot of subperiosteal new bone formation, most commonly on ribs	
Arms	Porosity on: ○ the scapulae ○ metaphyses of long bones	○ Porosity in concave curvature of long bones ○ Long bone thickening & bowing	○ Long bone porosity ○ Thinning of trabecular & cortical bone ○ Perforated cortical bone in long bones (Thal.)			○ Long bone bowing with cortical thickening ○ Narrowing of long bone diaphyses in comparison to their length

	Scurvy	Rickets	Anaemia	Fluorosis	Hyperostosis	OI
		○ Long bone metaphyseal flaring	○ Necrosis of the humeral head (SCA)			
Hands						
Pelvis		○ Ilium concavity				
Legs	Porosity on: ○ Metaphyses of long bones	○ Porosity in concave curvature of long bones ○ Long bone thickening & bowing ○ Long bone metaphyseal flaring	○ Long bone porosity ○ Thinning of trabecular & cortical bone ○ Perforated cortical bone in long bones (Thal.) ○ Exaggerated sulci on femora & tibiae (Thal.) ○ Necrosis of the femoral head (SCA)			○ Long bone bowing with cortical thickening ○ Narrowing of long bone diaphyses in comparison to their length
Feet			○ Hyper-trophic meta-carpals & phalanges (Thal.)			

Radiographic Indicators

	Scurvy	Rickets	Anaemia	Fluorosis	Hyperostosis	OI
General Skeleton	○ Generalized osteopenia	○ Generalized osteopenia ○ Thick cortex ○ Sharp cortical outline	○ Thinning of cortical bone			
Cranium			○ Hair-on-end appearance cranium ○ Undeveloped sinuses			
Dentition						
Vertebral Column			○ Reduced number of trabeculae in vertebrae			
Thorax		○ Loss of integrity in sternal rib ends				

	Scurvy	Rickets	Anaemia	Fluorosis	Hyperostosis	OI
Arms	○ Long bone cortical thinning ○ Metaphyseal fractures ○ White line of Fraenkel ○ Wimberger's ring ○ Pelkan's spurs	○ Long bone cortical thinning ○ Metaphyseal fractures ○ Metaphyseal trabecular coarsening ○ Fraying of epiphyses ○ Distinction at the end of the epiphysis	○ Infarcts in long bones ○ Reduced number of trabeculae in long bones			○ Zebra stripe
Hands						
Pelvis						
Legs	○ Long bone cortical thinning ○ Metaphyseal fractures ○ White line of Fraenkel ○ Wimberger's ring ○ Pelkan's spurs	○ Long bone cortical thinning ○ Metaphyseal fractures ○ Fraying of epiphyses ○ Distinction at the end of the epiphysis	○ Infarcts in long bones ○ Reduced number of trabeculae in long bones			○ Zebra stripe
Feet						

SG15 is an individual who has fairly non-specific lesions. On SG15's teeth there is a pit on the buccal surface of the lower left DC (deciduous canine) and a hypoplastic defect on the upper left DC crown. The left clavicle is larger than the right and has a different shape. The clavicular radiograph displays these abnormalities as well. In the legs, there are possible Harris lines in the left femur visible due to PMD. Additionally, this individual is another possible case of cranial deformation, but as with the other individual highlighted, this would need to be confirmed with 3D modelling for accurate reconstruction. This can be seen in the profile of SG15's frontals and occipital. If cranial modification occurred it could have triggered the NBF that is seen on the temporals, which is not necessarily pathological new growth.

The Harris lines on the left femur are a non-specific indicator of stress which could be related with a disease like anaemia or scurvy or could be due to other stress in this individual's life. This individual does not display any lesions that are indicative of MBD or any specific disease, and as such no diagnosis is given.

SG16

Macroscopic Indicators

	Scurvy	Rickets	Anaemia	Fluorosis	Hyperostosis	OI
General Skeleton	○ Irregular & spongy new bone formation	○ General porosity ○ Abnormal growth plates	○ Porosity ○ Osteopenia (Thal.) ○ Large bony masses (Thal.)	○ Diffuse osteosclerosis of the appendicular & axial skeleton ○ Increased cortical & trabecular thickness ○ Periosteal thickening ○ Calcified ligaments, tendons, cartilage, & inter-osseous membrane-s ○ Bony exostoses at ligament & muscle attachment zones	○ Increased weight of bones ○ Increased thickness of cortical bone ○ A lot of subperiosteal new bone formation	○ Lightness/fragility to bones ○ Fractures ○ Osteoporosis
Orbits	○ Cribra orbitalia ○ Porosity	○ Orbital roof porosity	○ Cribra orbitalia ○ Thinning of trabecular & cortical bone ○ Widening interorbital space (Thal.)			○ Elongated orbits
Cranium	Porosity on: ○ the greater sphenoid wing ○ cranial bones ○ facial bones ○ palate ○ basiocciput	○ Frontal bone bossing ○ Deformed mandibular ramus	○ Cranial vault porosity ○ Thickening of the sphenoid, maxillae, & zygomatics (Thal.) ○ Obliterated sutures in the cranium (Thal.)		○ A lot of subperiosteal new bone formation, most commonly on facial bones (Caffey's) ○ Osteal bulges ○ Irregular thickening of internal surface of frontal bone while external surface looks normal (IFH)	○ Expanded cranial vault
Dentition			○ Protruding upper incisors & overbite (Thal.)	○ Linear enamel hypoplasia ○ Brown, dis-coloured teeth, & mottled enamel		○ Dentinogenesis imperfecta
Vertebral Column			○ Perforations in the cortical bone of vertebrae			
Thorax		○ Rib flaring	○ Slight expansion of the ribs ○ Perforated cortical bone in ribs (Thal.) ○ Linear striations on the ribs (Thal.)		○ A lot of subperiosteal new bone formation, most commonly on ribs	
Arms	Porosity on: ○ the scapulae ○ metaphyses of long bones	○ Porosity in concave curvature of long bones ○ Long bone thickening & bowing	○ Long bone porosity ○ Thinning of trabecular & cortical bone ○ Perforated cortical bone in long bones (Thal.)			○ Long bone bowing with cortical thickening ○ Narrowing of long bone diaphyses in comparison to their length

	Scurvy	Rickets	Anaemia	Fluorosis	Hyperostosis	OI
		○ Long bone metaphyseal flaring	○ Necrosis of the humeral head (SCA)			
Hands						
Pelvis		○ Ilium concavity				
Legs	Porosity on: ○ Metaphyses of long bones	○ Porosity in concave curvature of long bones ○ Long bone thickening & bowing ○ Long bone metaphyseal flaring	○ Long bone porosity ○ Thinning of trabecular & cortical bone ○ Perforated cortical bone in long bones (Thal.) ○ Exaggerated sulci on femora & tibiae (Thal.) ○ Necrosis of the femoral head (SCA)			○ Long bone bowing with cortical thickening ○ Narrowing of long bone diaphyses in comparison to their length
Feet			○ Hyper-trophic meta-carpals & phalanges (Thal.)			

Radiographic Indicators

	Scurvy	Rickets	Anaemia	Fluorosis	Hyperostosis	OI
General Skeleton	○ Generalized osteopenia	○ Generalized osteopenia ○ Thick cortex ○ Sharp cortical outline	○ Thinning of cortical bone			
Cranium			○ Hair-on-end appearance cranium ○ Undeveloped sinuses			
Dentition						
Vertebral Column			○ Reduced number of trabeculae in vertebrae			
Thorax		○ Loss of integrity in sternal rib ends				

	Scurvy	Rickets	Anaemia	Fluorosis	Hyperostosis	OI
Arms	○ Long bone cortical thinning ○ Metaphyseal fractures ○ White line of Fraenkel ○ Wimberger's ring ○ Pelkan's spurs	○ Long bone cortical thinning ○ Metaphyseal fractures ○ Metaphyseal trabecular coarsening ○ Fraying of epiphyses ○ Distinction at the end of the epiphysis	○ Infarcts in long bones ○ Reduced number of trabeculae in long bones			○ Zebra stripe
Hands						
Pelvis						
Legs	○ Long bone cortical thinning ○ Metaphyseal fractures ○ White line of Fraenkel ○ Wimberger's ring ○ Pelkan's spurs	○ Long bone cortical thinning ○ Metaphyseal fractures ○ Fraying of epiphyses ○ Distinction at the end of the epiphysis	○ Infarcts in long bones ○ Reduced number of trabeculae in long bones			○ Zebra stripe
Feet						

SG16 has quite a few lesions on their remains. Porosity occurs on the inferior surface of the right zygomatic and slight porosity occurs on the right orbit. Porosity and NBF is consistent across the entire cranium. There is also new growth along with porosity on the left exoccipital which occurs across the entire ectocranial surface. Additionally, porosity is present, along with new growth, on the inferior surface of the left maxilla, near where the palatine. Porosity also occurs on the frontals, on the ectocranial surface. This is also true for the right parietal fragments and the parietals in general. Porosity is widespread on both the ecto and endocranial surface of the occipital. Porosity occurs across the associated cranial fragments. The cranium of this individual is oddly elongated and bulbous with at least two Wormian bones (the Wormian bones being a non-metric trait rather than pathology). Moving on to the shoulder girdles, both of SG16's clavicles are rather robust for their age. Additionally, there may be a healed fracture due to a dent being present 1/3 acromially on the left clavicle.

It is important to note that the odd shape to SG16's cranium may be reflective of hydrocephalus, due to the enlargement of the cranium and the resulting oblong expanded shape. An elongated cranial shape also occurs in hypophosphatasia, but there are no other skeletal indicators to support that diagnosis. As well, an expanded cranial vault is associated with OI but again there are no other skeletal indicators to support that diagnosis. Other MBD may be indicated in this individual though. The porosity on the cranial bones (all over cranium, left exoccipital, parietals, occipital), porotic facial bones (inferior right zygomatic, left maxillary fragment, frontals), and the porosity on the basiocciput could be associated with scurvy. The porosity seen on their inferior maxilla in what would have been the palatine process area is a feature which is suggestive of scurvy, while the cranial vault porosity is a non-diagnostic feature. This is not sufficient evidence for a probable diagnosis of scurvy though. The porosity seen in SG16's orbit could be a non-diagnostic feature of rickets, but there is no other evidence for a diagnosis of rickets. Anaemia does have some support: cribra orbitalia, and cranial vault porosity. Cribra orbitalia could also be indicative of pellagra but there is again no other support for this diagnosis. There is not sufficient skeletal evidence for a probable diagnosis of any MBD.

SG17

Macroscopic Indicators

	Scurvy	Rickets	Anaemia	Fluorosis	Hyperostosis	OI
General Skeleton	○ Irregular & spongy new bone formation	○ General porosity ○ Abnormal growth plates	○ Porosity ○ Osteopenia (Thal.) ○ Large bony masses (Thal.)	○ Diffuse osteosclerosis of the appendicular & axial skeleton ○ Increased cortical & trabecular thickness ○ Periosteal thickening ○ Calcified ligaments, tendons, cartilage, & inter-osseous membrane-s ○ Bony exostoses at ligament & muscle attachment zones	○ Increased weight of bones ○ Increased thickness of cortical bone ○ A lot of subperiosteal new bone formation	○ Lightness/fragility to bones ○ Fractures ○ Osteoporosis
Orbits	○ Cribra orbitalia ○ Porosity	○ Orbital roof porosity	○ Cribra orbitalia ○ Thinning of trabecular & cortical bone ○ Widening interorbital space (Thal.)			○ Elongated orbits
Cranium	Porosity on: ○ the greater sphenoid wing ○ cranial bones ○ facial bones ○ palate ○ basiocciput	○ Frontal bone bossing ○ Deformed mandibular ramus	○ Cranial vault porosity ○ Thickening of the sphenoid, maxillae, & zygomatics (Thal.) ○ Obliterated sutures in the cranium (Thal.)		○ A lot of subperiosteal new bone formation, most commonly on facial bones (Caffey's) ○ Osteal bulges ○ Irregular thickening of internal surface of frontal bone while external surface looks normal (IFH)	○ Expanded cranial vault
Dentition			○ Protruding upper incisors & overbite (Thal.)	○ Linear enamel hypoplasia ○ Brown, dis-coloured teeth, & mottled enamel		○ Dentinogenesis imperfecta
Vertebral Column			○ Perforations in the cortical bone of vertebrae			
Thorax		○ Rib flaring	○ Slight expansion of the ribs ○ Perforated cortical bone in ribs (Thal.) ○ Linear striations on the ribs (Thal.)		○ A lot of subperiosteal new bone formation, most commonly on ribs	
Arms	Porosity on: ○ the scapulae ○ metaphyses of long bones	○ Porosity in concave curvature of long bones ○ Long bone thickening & bowing	○ Long bone porosity ○ Thinning of trabecular & cortical bone ○ Perforated cortical bone in long bones (Thal.)			○ Long bone bowing with cortical thickening ○ Narrowing of long bone diaphyses in comparison to their length

	Scurvy	Rickets	Anaemia	Fluorosis	Hyperostosis	OI
		○ Long bone metaphyseal flaring	○ Necrosis of the humeral head (SCA)			
Hands						
Pelvis		○ Ilium concavity				
Legs	Porosity on: ○ Metaphyses of long bones	○ Porosity in concave curvature of long bones ○ Long bone thickening & bowing ○ Long bone metaphyseal flaring	○ Long bone porosity ○ Thinning of trabecular & cortical bone ○ Perforated cortical bone in long bones (Thal.) ○ Exaggerated sulci on femora & tibiae (Thal.) ○ Necrosis of the femoral head (SCA)			○ Long bone bowing with cortical thickening ○ Narrowing of long bone diaphyses in comparison to their length
Feet			○ Hyper-trophic meta-carpals & phalanges (Thal.)			

Radiographic Indicators

	Scurvy	Rickets	Anaemia	Fluorosis	Hyperostosis	OI
General Skeleton	○ Generalized osteopenia	○ Generalized osteopenia ○ Thick cortex ○ Sharp cortical outline	○ Thinning of cortical bone			
Cranium			○ Hair-on-end appearance cranium ○ Undeveloped sinuses			
Dentition						
Vertebral Column			○ Reduced number of trabeculae in vertebrae			
Thorax		○ Loss of integrity in sternal rib ends				

	Scurvy	Rickets	Anaemia	Fluorosis	Hyperostosis	OI
Arms	○ Long bone cortical thinning ○ Metaphyseal fractures ○ White line of Fraenkel ○ Wimberger's ring ○ Pelkan's spurs	○ Long bone cortical thinning ○ Metaphyseal fractures ○ Metaphyseal trabecular coarsening ○ Fraying of epiphyses ○ Distinction at the end of the epiphysis	○ Infarcts in long bones ○ Reduced number of trabeculae in long bones			○ Zebra stripe
Hands						
Pelvis						
Legs	○ Long bone cortical thinning ○ Metaphyseal fractures ○ White line of Fraenkel ○ Wimberger's ring ○ Pelkan's spurs	○ Long bone cortical thinning ○ Metaphyseal fractures ○ Fraying of epiphyses ○ Distinction at the end of the epiphysis	○ Infarcts in long bones ○ Reduced number of trabeculae in long bones			○ Zebra stripe
Feet						

SG17 is an individual with no lesions associated with their remains. There is, however, widespread PMD on their remains and not many remains are present.

SG18

Macroscopic Indicators

	Scurvy	Rickets	Anaemia	Fluorosis	Hyperostosis	OI
General Skeleton	○ Irregular & spongy new bone formation	○ General porosity ○ Abnormal growth plates	○ Porosity ○ Osteopenia (Thal.) ○ Large bony masses (Thal.)	○ Diffuse osteosclerosis of the appendicular & axial skeleton ○ Increased cortical & trabecular thickness ○ Periosteal thickening ○ Calcified ligaments, tendons, cartilage, & inter-osseous membrane-s ○ Bony exostoses at ligament & muscle attachment zones	○ Increased weight of bones ○ Increased thickness of cortical bone ○ A lot of subperiosteal new bone formation	○ Lightness/fragility to bones ○ Fractures ○ Osteoporosis
Orbits	○ Cribra orbitalia ○ Porosity	○ Orbital roof porosity	○ Cribra orbitalia ○ Thinning of trabecular & cortical bone ○ Widening interorbital space (Thal.)			○ Elongated orbits
Cranium	Porosity on: ○ the greater sphenoid wing ○ cranial bones ○ facial bones ○ palate ○ basiocciput	○ Frontal bone bossing ○ Deformed mandibular ramus	○ Cranial vault porosity ○ Thickening of the sphenoid, maxillae, & zygomatics (Thal.) ○ Obliterated sutures in the cranium (Thal.)		○ A lot of subperiosteal new bone formation, most commonly on facial bones (Caffey's) ○ Osteal bulges ○ Irregular thickening of internal surface of frontal bone while external surface looks normal (IFH)	○ Expanded cranial vault
Dentition			○ Protruding upper incisors & overbite (Thal.)	○ Linear enamel hypoplasia ○ Brown, dis-coloured teeth, & mottled enamel		○ Dentinogenesis imperfecta
Vertebral Column			○ Perforations in the cortical bone of vertebrae			
Thorax		○ Rib flaring	○ Slight expansion of the ribs ○ Perforated cortical bone in ribs (Thal.) ○ Linear striations on the ribs (Thal.)		○ A lot of subperiosteal new bone formation, most commonly on ribs	
Arms	Porosity on: ○ the scapulae ○ metaphyses of long bones	○ Porosity in concave curvature of long bones ○ Long bone thickening & bowing	○ Long bone porosity ○ Thinning of trabecular & cortical bone ○ Perforated cortical bone in long bones (Thal.)			○ Long bone bowing with cortical thickening ○ Narrowing of long bone diaphyses in comparison to their length

	Scurvy	Rickets	Anaemia	Fluorosis	Hyperostosis	OI
		○ Long bone metaphyseal flaring	○ Necrosis of the humeral head (SCA)			
Hands						
Pelvis		○ Ilium concavity				
Legs	Porosity on: ○ Metaphyses of long bones	○ Porosity in concave curvature of long bones ○ Long bone thickening & bowing ○ Long bone metaphyseal flaring	○ Long bone porosity ○ Thinning of trabecular & cortical bone ○ Perforated cortical bone in long bones (Thal.) ○ Exaggerated sulci on femora & tibiae (Thal.) ○ Necrosis of the femoral head (SCA)			○ Long bone bowing with cortical thickening ○ Narrowing of long bone diaphyses in comparison to their length
Feet			○ Hyper-trophic meta-carpals & phalanges (Thal.)			

Radiographic Indicators

	Scurvy	Rickets	Anaemia	Fluorosis	Hyperostosis	OI
General Skeleton	○ Generalized osteopenia	○ Generalized osteopenia ○ Thick cortex ○ Sharp cortical outline	○ Thinning of cortical bone			
Cranium			○ Hair-on-end appearance cranium ○ Undeveloped sinuses			
Dentition						
Vertebral Column			○ Reduced number of trabeculae in vertebrae			
Thorax		○ Loss of integrity in sternal rib ends				

	Scurvy	Rickets	Anaemia	Fluorosis	Hyperostosis	OI
Arms	○ Long bone cortical thinning ○ Metaphyseal fractures ○ White line of Fraenkel ○ Wimberger's ring ○ Pelkan's spurs	○ Long bone cortical thinning ○ Metaphyseal fractures ○ Metaphyseal trabecular coarsening ○ Fraying of epiphyses ○ Distinction at the end of the epiphysis	○ Infarcts in long bones ○ Reduced number of trabeculae in long bones			○ Zebra stripe
Hands						
Pelvis						
Legs	○ Long bone cortical thinning ○ Metaphyseal fractures ○ White line of Fraenkel ○ Wimberger's ring ○ Pelkan's spurs	○ Long bone cortical thinning ○ Metaphyseal fractures ○ Fraying of epiphyses ○ Distinction at the end of the epiphysis	○ Infarcts in long bones ○ Reduced number of trabeculae in long bones			○ Zebra stripe
Feet						

SG18's ribs demonstrate a lot of striations, but this is not necessarily pathological. Rather, this could be normative growth patterning. However, there is pathology in their shoulder girdle. The right scapula is very thin with NBF along the ridge and anterior surface. There is also new growth on the posterior surface. An interesting characteristic is that the medullary cavity of both their femora is nearly non-existent in their radiographs. The lesions associated with SG18 are not indicative of any MBD or associated with any MBD.

SG19

Macroscopic Indicators

	Scurvy	Rickets	Anaemia	Fluorosis	Hyperostosis	OI
General Skeleton	○ Irregular & spongy new bone formation	○ General porosity ○ Abnormal growth plates	○ Porosity ○ Osteopenia (Thal.) ○ Large bony masses (Thal.)	○ Diffuse osteosclerosis of the appendicular & axial skeleton ○ Increased cortical & trabecular thickness ○ Periosteal thickening ○ Calcified ligaments, tendons, cartilage, & inter-osseous membrane-s ○ Bony exostoses at ligament & muscle attachment zones	○ Increased weight of bones ○ Increased thickness of cortical bone ○ A lot of subperiosteal new bone formation	○ Lightness/fragility to bones ○ Fractures ○ Osteoporosis
Orbits	○ Cribra orbitalia ○ Porosity	○ Orbital roof porosity	○ Cribra orbitalia ○ Thinning of trabecular & cortical bone ○ Widening interorbital space (Thal.)			○ Elongated orbits
Cranium	Porosity on: ○ the greater sphenoid wing ○ cranial bones ○ facial bones ○ palate ○ basiocciput	○ Frontal bone bossing ○ Deformed mandibular ramus	○ Cranial vault porosity ○ Thickening of the sphenoid, maxillae, & zygomatics (Thal.) ○ Obliterated sutures in the cranium (Thal.)		○ A lot of subperiosteal new bone formation, most commonly on facial bones (Caffey's) ○ Osteal bulges ○ Irregular thickening of internal surface of frontal bone while external surface looks normal (IFH)	○ Expanded cranial vault
Dentition			○ Protruding upper incisors & overbite (Thal.)	○ Linear enamel hypoplasia ○ Brown, dis-coloured teeth, & mottled enamel		○ Dentinogenesis imperfecta
Vertebral Column			○ Perforations in the cortical bone of vertebrae			
Thorax		○ Rib flaring	○ Slight expansion of the ribs ○ Perforated cortical bone in ribs (Thal.) ○ Linear striations on the ribs (Thal.)		○ A lot of subperiosteal new bone formation, most commonly on ribs	
Arms	Porosity on: ○ the scapulae ○ metaphyses of long bones	○ Porosity in concave curvature of long bones ○ Long bone thickening & bowing	○ Long bone porosity ○ Thinning of trabecular & cortical bone ○ Perforated cortical bone in long bones (Thal.)			○ Long bone bowing with cortical thickening ○ Narrowing of long bone diaphyses in comparison to their length

	Scurvy	Rickets	Anaemia	Fluorosis	Hyperostosis	OI
		○ Long bone metaphyseal flaring	○ Necrosis of the humeral head (SCA)			
Hands						
Pelvis		○ Ilium concavity				
Legs	Porosity on: ○ Metaphyses of long bones	○ Porosity in concave curvature of long bones ○ Long bone thickening & bowing ○ Long bone metaphyseal flaring	○ Long bone porosity ○ Thinning of trabecular & cortical bone ○ Perforated cortical bone in long bones (Thal.) ○ Exaggerated sulci on femora & tibiae (Thal.) ○ Necrosis of the femoral head (SCA)			○ Long bone bowing with cortical thickening ○ Narrowing of long bone diaphyses in comparison to their length
Feet			○ Hyper-trophic meta-carpals & phalanges (Thal.)			

Radiographic Indicators

	Scurvy	Rickets	Anaemia	Fluorosis	Hyperostosis	OI
General Skeleton	○ Generalized osteopenia	○ Generalized osteopenia ○ Thick cortex ○ Sharp cortical outline	○ Thinning of cortical bone			
Cranium			○ Hair-on-end appearance cranium ○ Undeveloped sinuses			
Dentition						
Vertebral Column			○ Reduced number of trabeculae in vertebrae			
Thorax		○ Loss of integrity in sternal rib ends				

	Scurvy	Rickets	Anaemia	Fluorosis	Hyperostosis	OI
Arms	○ Long bone cortical thinning ○ Metaphyseal fractures ○ White line of Fraenkel ○ Wimberger's ring ○ Pelkan's spurs	○ Long bone cortical thinning ○ Metaphyseal fractures ○ Metaphyseal trabecular coarsening ○ Fraying of epiphyses ○ Distinction at the end of the epiphysis	○ Infarcts in long bones ○ Reduced number of trabeculae in long bones			○ Zebra stripe
Hands						
Pelvis						
Legs	○ Long bone cortical thinning ○ Metaphyseal fractures ○ White line of Fraenkel ○ Wimberger's ring ○ Pelkan's spurs	○ Long bone cortical thinning ○ Metaphyseal fractures ○ Fraying of epiphyses ○ Distinction at the end of the epiphysis	○ Infarcts in long bones ○ Reduced number of trabeculae in long bones			○ Zebra stripe
Feet						

In SG19's ribs there are a lot of striations, but these may be indicative of normative growth rather than a lesion. There is an odd bend to the radii accompanied by a lack of a medullary cavity in the radiographs. The femora echo what is seen in the radii – there is an odd bend to them along with a lack of medullary cavity in the radiographs. The humeri are also very thick at the epiphyseal ends and have new growth. In SG19 there is widespread new growth along with curvature of the long bones which is thought to be due to this individual's age rather than being lesions. SG19's remains also display warping which is due to drying out and age. None of SG19's remains display pathological changes, or lesions associated with MBD. As such, a diagnosis is not given as there does not appear to be anything to diagnose.

SG20

Macroscopic Indicators

	Scurvy	Rickets	Anaemia	Fluorosis	Hyperostosis	OI
General Skeleton	○ Irregular & spongy new bone formation	○ General porosity ○ Abnormal growth plates	○ Porosity ○ Osteopenia (Thal.) ○ Large bony masses (Thal.)	○ Diffuse osteosclerosis of the appendicular & axial skeleton ○ Increased cortical & trabecular thickness ○ Periosteal thickening ○ Calcified ligaments, tendons, cartilage, & inter-osseous membrane-s ○ Bony exostoses at ligament & muscle attachment zones	○ Increased weight of bones ○ Increased thickness of cortical bone ○ A lot of subperiosteal new bone formation	○ Lightness/fragility to bones ○ Fractures ○ Osteoporosis
Orbits	○ Cribra orbitalia ○ Porosity	○ Orbital roof porosity	○ Cribra orbitalia ○ Thinning of trabecular & cortical bone ○ Widening interorbital space (Thal.)			○ Elongated orbits
Cranium	Porosity on: ○ the greater sphenoid wing ○ cranial bones ○ facial bones ○ palate ○ basiocciput	○ Frontal bone bossing ○ Deformed mandibular ramus	○ Cranial vault porosity ○ Thickening of the sphenoid, maxillae, & zygomatics (Thal.) ○ Obliterated sutures in the cranium (Thal.)		○ A lot of subperiosteal new bone formation, most commonly on facial bones (Caffey's) ○ Osteal bulges ○ Irregular thickening of internal surface of frontal bone while external surface looks normal (IFH)	○ Expanded cranial vault
Dentition			○ Protruding upper incisors & overbite (Thal.)	○ Linear enamel hypoplasia ○ Brown, dis-coloured teeth, & mottled enamel		○ Dentinogenesis imperfecta
Vertebral Column			○ Perforations in the cortical bone of vertebrae			
Thorax		○ Rib flaring	○ Slight expansion of the ribs ○ Perforated cortical bone in ribs (Thal.) ○ Linear striations on the ribs (Thal.)		○ A lot of subperiosteal new bone formation, most commonly on ribs	
Arms	Porosity on: ○ the scapulae ○ metaphyses of long bones	○ Porosity in concave curvature of long bones ○ Long bone thickening & bowing	○ Long bone porosity ○ Thinning of trabecular & cortical bone ○ Perforated cortical bone in long bones (Thal.)			○ Long bone bowing with cortical thickening ○ Narrowing of long bone diaphyses in comparison to their length

	Scurvy	Rickets	Anaemia	Fluorosis	Hyperostosis	OI
		○ Long bone metaphyseal flaring	○ Necrosis of the humeral head (SCA)			
Hands						
Pelvis		○ Ilium concavity				
Legs	Porosity on: ○ Metaphyses of long bones	○ Porosity in concave curvature of long bones ○ Long bone thickening & bowing ○ Long bone metaphyseal flaring	○ Long bone porosity ○ Thinning of trabecular & cortical bone ○ Perforated cortical bone in long bones (Thal.) ○ Exaggerated sulci on femora & tibiae (Thal.) ○ Necrosis of the femoral head (SCA)			○ Long bone bowing with cortical thickening ○ Narrowing of long bone diaphyses in comparison to their length
Feet			○ Hyper-trophic meta-carpals & phalanges (Thal.)			

Radiographic Indicators

	Scurvy	Rickets	Anaemia	Fluorosis	Hyperostosis	OI
General Skeleton	○ Generalized osteopenia	○ Generalized osteopenia ○ Thick cortex ○ Sharp cortical outline	○ Thinning of cortical bone			
Cranium			○ Hair-on-end appearance cranium ○ Undeveloped sinuses			
Dentition						
Vertebral Column			○ Reduced number of trabeculae in vertebrae			
Thorax		○ Loss of integrity in sternal rib ends				

	Scurvy	Rickets	Anaemia	Fluorosis	Hyperostosis	OI
Arms	○ Long bone cortical thinning ○ Metaphyseal fractures ○ White line of Fraenkel ○ Wimberger's ring ○ Pelkan's spurs	○ Long bone cortical thinning ○ Metaphyseal fractures ○ Metaphyseal trabecular coarsening ○ Fraying of epiphyses ○ Distinction at the end of the epiphysis	○ Infarcts in long bones ○ Reduced number of trabeculae in long bones			○ Zebra stripe
Hands						
Pelvis						
Legs	○ Long bone cortical thinning ○ Metaphyseal fractures ○ White line of Fraenkel ○ Wimberger's ring ○ Pelkan's spurs	○ Long bone cortical thinning ○ Metaphyseal fractures ○ Fraying of epiphyses ○ Distinction at the end of the epiphysis	○ Infarcts in long bones ○ Reduced number of trabeculae in long bones			○ Zebra stripe
Feet						

SG20 has lesions in their remains, especially in their cranium. SG20's basiocciput has porosity and new growth on the ectocranial surface while the endocranial surface has new growth. There is also new growth and porosity on the basisphenoid which is sheet-like in appearance and seems to be SPNB. Additionally, unidentified cranial fragments demonstrate outward new growth. In SG20's legs, their tibia has new growth along the diaphysis, but this may fall in the normative range.

Some of SG20's lesions align with MBD. The porosity seen on the basisphenoid along with the basiocciput would align with scurvy. But these features are neither suggestive nor diagnostic. However, no other lesions align with scurvy or any other MBD. These two lesions are not a strong enough support for a diagnosis of scurvy. So, SG20 may have had MBD or some other disease but there is not enough evidence.

SG21

Macroscopic Indicators

	Scurvy	Rickets	Anaemia	Fluorosis	Hyperostosis	OI
General Skeleton	○ Irregular & spongy new bone formation	○ General porosity ○ Abnormal growth plates	○ Porosity ○ Osteopenia (Thal.) ○ Large bony masses (Thal.)	○ Diffuse osteosclerosis of the appendicular & axial skeleton ○ Increased cortical & trabecular thickness ○ Periosteal thickening ○ Calcified ligaments, tendons, cartilage, & inter-osseous membrane-s ○ Bony exostoses at ligament & muscle attachment zones	○ Increased weight of bones ○ Increased thickness of cortical bone ○ A lot of subperiosteal new bone formation	○ Lightness/fragility to bones ○ Fractures ○ Osteoporosis
Orbits	○ Cribra orbitalia ○ Porosity	○ Orbital roof porosity	○ Cribra orbitalia ○ Thinning of trabecular & cortical bone ○ Widening interorbital space (Thal.)			○ Elongated orbits
Cranium	Porosity on: ○ the greater sphenoid wing ○ cranial bones ○ facial bones ○ palate ○ basiocciput	○ Frontal bone bossing ○ Deformed mandibular ramus	○ Cranial vault porosity ○ Thickening of the sphenoid, maxillae, & zygomatics (Thal.) ○ Obliterated sutures in the cranium (Thal.)		○ A lot of subperiosteal new bone formation, most commonly on facial bones (Caffey's) ○ Osteal bulges ○ Irregular thickening of internal surface of frontal bone while external surface looks normal (IFH)	○ Expanded cranial vault
Dentition			○ Protruding upper incisors & overbite (Thal.)	○ Linear enamel hypoplasia ○ Brown, dis-coloured teeth, & mottled enamel		○ Dentinogenesis imperfecta
Vertebral Column			○ Perforations in the cortical bone of vertebrae			
Thorax		○ Rib flaring	○ Slight expansion of the ribs ○ Perforated cortical bone in ribs (Thal.) ○ Linear striations on the ribs (Thal.)		○ A lot of subperiosteal new bone formation, most commonly on ribs	
Arms	Porosity on: ○ the scapulae ○ metaphyses of long bones	○ Porosity in concave curvature of long bones ○ Long bone thickening & bowing	○ Long bone porosity ○ Thinning of trabecular & cortical bone ○ Perforated cortical bone in long bones (Thal.)			○ Long bone bowing with cortical thickening ○ Narrowing of long bone diaphyses in comparison to their length

	Scurvy	Rickets	Anaemia	Fluorosis	Hyperostosis	OI
		○ Long bone metaphyseal flaring	○ Necrosis of the humeral head (SCA)			
Hands						
Pelvis		○ Ilium concavity				
Legs	Porosity on: ○ Metaphyses of long bones	○ Porosity in concave curvature of long bones ○ Long bone thickening & bowing ○ Long bone metaphyseal flaring	○ Long bone porosity ○ Thinning of trabecular & cortical bone ○ Perforated cortical bone in long bones (Thal.) ○ Exaggerated sulci on femora & tibiae (Thal.) ○ Necrosis of the femoral head (SCA)			○ Long bone bowing with cortical thickening ○ Narrowing of long bone diaphyses in comparison to their length
Feet			○ Hyper-trophic meta-carpals & phalanges (Thal.)			

Radiographic Indicators

	Scurvy	Rickets	Anaemia	Fluorosis	Hyperostosis	OI
General Skeleton	○ Generalized osteopenia	○ Generalized osteopenia ○ Thick cortex ○ Sharp cortical outline	○ Thinning of cortical bone			
Cranium			○ Hair-on-end appearance cranium ○ Undeveloped sinuses			
Dentition						
Vertebral Column			○ Reduced number of trabeculae in vertebrae			
Thorax		○ Loss of integrity in sternal rib ends				

	Scurvy	Rickets	Anaemia	Fluorosis	Hyperostosis	OI
Arms	○ Long bone cortical thinning ○ Metaphyseal fractures ○ White line of Fraenkel ○ Wimberger's ring ○ Pelkan's spurs	○ Long bone cortical thinning ○ Metaphyseal fractures ○ Metaphyseal trabecular coarsening ○ Fraying of epiphyses ○ Distinction at the end of the epiphysis	○ Infarcts in long bones ○ Reduced number of trabeculae in long bones			○ Zebra stripe
Hands						
Pelvis						
Legs	○ Long bone cortical thinning ○ Metaphyseal fractures ○ White line of Fraenkel ○ Wimberger's ring ○ Pelkan's spurs	○ Long bone cortical thinning ○ Metaphyseal fractures ○ Fraying of epiphyses ○ Distinction at the end of the epiphysis	○ Infarcts in long bones ○ Reduced number of trabeculae in long bones			○ Zebra stripe
Feet						

SG21's remains contain a variety of lesions. There is porosity on the right alisphenoid on the ectocranial surface. New growth and porosity occur on the ectocranial surface of the partial maxilla. New growth also occurs on the scapulae but is more extensive on the left than the right. The left scapular NBF is sheet-like in appearance, which would suggest that it is SPNB. The right also has extensive PMD. The radiographs associated with SG21 do not display any indicators.

While SG21 demonstrates pathological changes, not all those lesions fit into MBD. Those that do are the porosity seen on the sphenoid, and facial bones (left maxilla). The porosity seen on the alisphenoid would be classified as a diagnostic scorbutic lesion, as would the SPNB seen on the left scapular infraspinous fossa. Additionally, the porosity seen on the left maxillary piece around the infraorbital foramen would be a suggestive scorbutic lesion. These two diagnostic lesions together would support a probable diagnosis of scurvy. The additional suggestive lesion would add support to such a diagnosis.

SG22

Macroscopic Indicators

	Scurvy	Rickets	Anaemia	Fluorosis	Hyperostosis	OI
General Skeleton	○ Irregular & spongy new bone formation	○ General porosity ○ Abnormal growth plates	○ Porosity ○ Osteopenia (Thal.) ○ Large bony masses (Thal.)	○ Diffuse osteosclerosis of the appendicular & axial skeleton ○ Increased cortical & trabecular thickness ○ Periosteal thickening ○ Calcified ligaments, tendons, cartilage, & inter-osseous membrane-s ○ Bony exostoses at ligament & muscle attachment zones	○ Increased weight of bones ○ Increased thickness of cortical bone ○ A lot of subperiosteal new bone formation	○ Lightness/fragility to bones ○ Fractures ○ Osteoporosis
Orbits	○ Cribra orbitalia ○ Porosity	○ Orbital roof porosity	○ Cribra orbitalia ○ Thinning of trabecular & cortical bone ○ Widening interorbital space (Thal.)			○ Elongated orbits
Cranium	Porosity on: ○ the greater sphenoid wing ○ cranial bones ○ facial bones ○ palate ○ basiocciput	○ Frontal bone bossing ○ Deformed mandibular ramus	○ Cranial vault porosity ○ Thickening of the sphenoid, maxillae, & zygomatics (Thal.) ○ Obliterated sutures in the cranium (Thal.)		○ A lot of subperiosteal new bone formation, most commonly on facial bones (Caffey's) ○ Osteal bulges ○ Irregular thickening of internal surface of frontal bone while external surface looks normal (IFH)	○ Expanded cranial vault
Dentition			○ Protruding upper incisors & overbite (Thal.)	○ Linear enamel hypoplasia ○ Brown, dis-coloured teeth, & mottled enamel		○ Dentinogenesis imperfecta
Vertebral Column			○ Perforations in the cortical bone of vertebrae			
Thorax		○ Rib flaring	○ Slight expansion of the ribs ○ Perforated cortical bone in ribs (Thal.) ○ Linear striations on the ribs (Thal.)		○ A lot of subperiosteal new bone formation, most commonly on ribs	
Arms	Porosity on: ○ the scapulae ○ metaphyses of long bones	○ Porosity in concave curvature of long bones ○ Long bone thickening & bowing	○ Long bone porosity ○ Thinning of trabecular & cortical bone ○ Perforated cortical bone in long bones (Thal.)			○ Long bone bowing with cortical thickening ○ Narrowing of long bone diaphyses in comparison to their length

	Scurvy	Rickets	Anaemia	Fluorosis	Hyperostosis	OI
		○ Long bone metaphyseal flaring	○ Necrosis of the humeral head (SCA)			
Hands						
Pelvis		○ Ilium concavity				
Legs	Porosity on: ○ Metaphyses of long bones	○ Porosity in concave curvature of long bones ○ Long bone thickening & bowing ○ Long bone metaphyseal flaring	○ Long bone porosity ○ Thinning of trabecular & cortical bone ○ Perforated cortical bone in long bones (Thal.) ○ Exaggerated sulci on femora & tibiae (Thal.) ○ Necrosis of the femoral head (SCA)			○ Long bone bowing with cortical thickening ○ Narrowing of long bone diaphyses in comparison to their length
Feet			○ Hyper-trophic meta-carpals & phalanges (Thal.)			

Radiographic Indicators

	Scurvy	Rickets	Anaemia	Fluorosis	Hyperostosis	OI
General Skeleton	○ Generalized osteopenia	○ Generalized osteopenia ○ Thick cortex ○ Sharp cortical outline	○ Thinning of cortical bone			
Cranium			○ Hair-on-end appearance cranium ○ Undeveloped sinuses			
Dentition						
Vertebral Column			○ Reduced number of trabeculae in vertebrae			
Thorax		○ Loss of integrity in sternal rib ends				

	Scurvy	Rickets	Anaemia	Fluorosis	Hyperostosis	OI
Arms	○ Long bone cortical thinning ○ Metaphyseal fractures ○ White line of Fraenkel ○ Wimberger's ring ○ Pelkan's spurs	○ Long bone cortical thinning ○ Metaphyseal fractures ○ Metaphyseal trabecular coarsening ○ Fraying of epiphyses ○ Distinction at the end of the epiphysis	○ Infarcts in long bones ○ Reduced number of trabeculae in long bones			○ Zebra stripe
Hands						
Pelvis						
Legs	○ Long bone cortical thinning ○ Metaphyseal fractures ○ White line of Fraenkel ○ Wimberger's ring ○ Pelkan's spurs	○ Long bone cortical thinning ○ Metaphyseal fractures ○ Fraying of epiphyses ○ Distinction at the end of the epiphysis	○ Infarcts in long bones ○ Reduced number of trabeculae in long bones			○ Zebra stripe
Feet						

SG22 has a few lesions on their cranium. The inferior surface of the left maxilla has new bone growth which is shelf-like and outward expanding, along with porosity. The right and left temporal both have new growth. On the left temporal, this NBF is widespread across the entire ectocranial surface, and appears shelf-like in areas. It also occurs on the endocranial surface. The right temporal shows the same pattern. SG22's teeth present with enamel defects on the distal surface of the lower right DI1, labial surface of the upper left DI1, upper right DI1, and upper left DI2. SG22's radiographs do not display any abnormalities.

Some of SG22's lesions fall within those associated with MBD. The SPNB seen on the temporals would be considered a non-diagnostic indicator of scurvy while the porosity on the palate area of the left mandible would be seen as a suggestive scorbutic lesion. However, only one non-diagnostic feature and one suggestive is not enough skeletal evidence for a probable diagnosis of scurvy. The lesions seen on SG22 do not align with any other MBD.

SG23

Macroscopic Indicators

	Scurvy	Rickets	Anaemia	Fluorosis	Hyperostosis	OI
General Skeleton	○ Irregular & spongy new bone formation	○ General porosity ○ Abnormal growth plates	○ Porosity ○ Osteopenia (Thal.) ○ Large bony masses (Thal.)	○ Diffuse osteosclerosis of the appendicular & axial skeleton ○ Increased cortical & trabecular thickness ○ Periosteal thickening ○ Calcified ligaments, tendons, cartilage, & inter-osseous membrane-s ○ Bony exostoses at ligament & muscle attachment zones	○ Increased weight of bones ○ Increased thickness of cortical bone ○ A lot of subperiosteal new bone formation	○ Lightness/fragility to bones ○ Fractures ○ Osteoporosis
Orbits	○ Cribra orbitalia ○ Porosity	○ Orbital roof porosity	○ Cribra orbitalia ○ Thinning of trabecular & cortical bone ○ Widening interorbital space (Thal.)			○ Elongated orbits
Cranium	Porosity on: ○ the greater sphenoid wing ○ cranial bones ○ facial bones ○ palate ○ basiocciput	○ Frontal bone bossing ○ Deformed mandibular ramus	○ Cranial vault porosity ○ Thickening of the sphenoid, maxillae, & zygomatics (Thal.) ○ Obliterated sutures in the cranium (Thal.)		○ A lot of subperiosteal new bone formation, most commonly on facial bones (Caffey's) ○ Osteal bulges ○ Irregular thickening of internal surface of frontal bone while external surface looks normal (IFH)	○ Expanded cranial vault
Dentition			○ Protruding upper incisors & overbite (Thal.)	○ Linear enamel hypoplasia ○ Brown, dis-coloured teeth, & mottled enamel		○ Dentinogenesis imperfecta
Vertebral Column			○ Perforations in the cortical bone of vertebrae			
Thorax		○ Rib flaring	○ Slight expansion of the ribs ○ Perforated cortical bone in ribs (Thal.) ○ Linear striations on the ribs (Thal.)		○ A lot of subperiosteal new bone formation, most commonly on ribs	
Arms	Porosity on: ○ the scapulae ○ metaphyses of long bones	○ Porosity in concave curvature of long bones ○ Long bone thickening & bowing	○ Long bone porosity ○ Thinning of trabecular & cortical bone ○ Perforated cortical bone in long bones (Thal.)			○ Long bone bowing with cortical thickening ○ Narrowing of long bone diaphyses in comparison to their length

	Scurvy	Rickets	Anaemia	Fluorosis	Hyperostosis	OI
		○ Long bone metaphyseal flaring	○ Necrosis of the humeral head (SCA)			
Hands						
Pelvis		○ Ilium concavity				
Legs	Porosity on: ○ Metaphyses of long bones	○ Porosity in concave curvature of long bones ○ Long bone thickening & bowing ○ Long bone metaphyseal flaring	○ Long bone porosity ○ Thinning of trabecular & cortical bone ○ Perforated cortical bone in long bones (Thal.) ○ Exaggerated sulci on femora & tibiae (Thal.) ○ Necrosis of the femoral head (SCA)			○ Long bone bowing with cortical thickening ○ Narrowing of long bone diaphyses in comparison to their length
Feet			○ Hyper-trophic meta-carpals & phalanges (Thal.)			

Radiographic Indicators

	Scurvy	Rickets	Anaemia	Fluorosis	Hyperostosis	OI
General Skeleton	○ Generalized osteopenia	○ Generalized osteopenia ○ Thick cortex ○ Sharp cortical outline	○ Thinning of cortical bone			
Cranium			○ Hair-on-end appearance cranium ○ Undeveloped sinuses			
Dentition						
Vertebral Column			○ Reduced number of trabeculae in vertebrae			
Thorax		○ Loss of integrity in sternal rib ends				

	Scurvy	Rickets	Anaemia	Fluorosis	Hyperostosis	OI
Arms	○ Long bone cortical thinning ○ Metaphyseal fractures ○ White line of Fraenkel ○ Wimberger's ring ○ Pelkan's spurs	○ Long bone cortical thinning ○ Metaphyseal fractures ○ Metaphyseal trabecular coarsening ○ Fraying of epiphyses ○ Distinction at the end of the epiphysis	○ Infarcts in long bones ○ Reduced number of trabeculae in long bones			○ Zebra stripe
Hands						
Pelvis						
Legs	○ Long bone cortical thinning ○ Metaphyseal fractures ○ White line of Fraenkel ○ Wimberger's ring ○ Pelkan's spurs	○ Long bone cortical thinning ○ Metaphyseal fractures ○ Fraying of epiphyses ○ Distinction at the end of the epiphysis	○ Infarcts in long bones ○ Reduced number of trabeculae in long bones			○ Zebra stripe
Feet						

SG23 is an individual who presents with many lesions upon their remains. Both the right and left inferior maxillary surfaces have porosity is visible on the palate. SG23 also has a possible enamel defect on the lower left DI1. There is a healed left clavicular fracture which has a lot of new growth and texture to it which may be the remains of a callus. The right clavicle is not as thick as the left and exhibits less new growth. The left fibula also has a lot of new growth which is concentrated on its diaphysis, with a slight bend to the bone. This is different than the right, which has less new growth, and is slightly larger. SG23's radiographs do show any pathological indicators.

SG23 only has one lesion which aligns with any MBD indicators. This would be the palate porosity seen on their maxillae. Palate porosity is a suggestive scorbutic lesion. Additionally, this porosity is not associated with any other MBD. However, only one suggestive lesion is not sufficient evidence for probable scurvy. As such, no probable MBD diagnosis is given for SG23.

SG24

Macroscopic Indicators

	Scurvy	Rickets	Anaemia	Fluorosis	Hyperostosis	OI
General Skeleton	○ Irregular & spongy new bone formation	○ General porosity ○ Abnormal growth plates	○ Porosity ○ Osteopenia (Thal.) ○ Large bony masses (Thal.)	○ Diffuse osteosclerosis of the appendicular & axial skeleton ○ Increased cortical & trabecular thickness ○ Periosteal thickening ○ Calcified ligaments, tendons, cartilage, & inter-osseous membrane-s ○ Bony exostoses at ligament & muscle attachment zones	○ Increased weight of bones ○ Increased thickness of cortical bone ○ A lot of subperiosteal new bone formation	○ Lightness/fragility to bones ○ Fractures ○ Osteoporosis
Orbits	○ Cribra orbitalia ○ Porosity	○ Orbital roof porosity	○ Cribra orbitalia ○ Thinning of trabecular & cortical bone ○ Widening interorbital space (Thal.)			○ Elongated orbits
Cranium	Porosity on: ○ the greater sphenoid wing ○ cranial bones ○ facial bones ○ palate ○ basiocciput	○ Frontal bone bossing ○ Deformed mandibular ramus	○ Cranial vault porosity ○ Thickening of the sphenoid, maxillae, & zygomatics (Thal.) ○ Obliterated sutures in the cranium (Thal.)		○ A lot of subperiosteal new bone formation, most commonly on facial bones (Caffey's) ○ Osteal bulges ○ Irregular thickening of internal surface of frontal bone while external surface looks normal (IFH)	○ Expanded cranial vault
Dentition			○ Protruding upper incisors & overbite (Thal.)	○ Linear enamel hypoplasia ○ Brown, dis-coloured teeth, & mottled enamel		○ Dentinogenesis imperfecta
Vertebral Column			○ Perforations in the cortical bone of vertebrae			
Thorax		○ Rib flaring	○ Slight expansion of the ribs ○ Perforated cortical bone in ribs (Thal.) ○ Linear striations on the ribs (Thal.)		○ A lot of subperiosteal new bone formation, most commonly on ribs	
Arms	Porosity on: ○ the scapulae ○ metaphyses of long bones	○ Porosity in concave curvature of long bones	○ Long bone porosity ○ Thinning of trabecular & cortical bone			○ Long bone bowing with cortical thickening ○ Narrowing of long bone diaphyses in comparison to their length

	Scurvy	Rickets	Anaemia	Fluorosis	Hyperostosis	OI
		○ Long bone thickening & bowing ○ Long bone metaphyseal flaring	○ Perforated cortical bone in long bones (Thal.) ○ Necrosis of the humeral head (SCA)			
Hands						
Pelvis		○ Ilium concavity				
Legs	Porosity on: ○ Metaphyses of long bones	○ Porosity in concave curvature of long bones ○ Long bone thickening & bowing ○ Long bone metaphyseal flaring	○ Long bone porosity ○ Thinning of trabecular & cortical bone ○ Perforated cortical bone in long bones (Thal.) ○ Exaggerated sulci on femora & tibiae (Thal.) ○ Necrosis of the femoral head (SCA)			○ Long bone bowing with cortical thickening ○ Narrowing of long bone diaphyses in comparison to their length
Feet			○ Hyper-trophic meta-carpals & phalanges (Thal.)			

Radiographic Indicators

	Scurvy	Rickets	Anaemia	Fluorosis	Hyperostosis	OI
General Skeleton	○ Generalized osteopenia	○ Generalized osteopenia ○ Thick cortex ○ Sharp cortical outline	○ Thinning of cortical bone			
Cranium			○ Hair-on-end appearance cranium ○ Undeveloped sinuses			
Dentition						
Vertebral Column			○ Reduced number of trabeculae in vertebrae			
Thorax		○ Loss of integrity in sternal rib ends				

	Scurvy	Rickets	Anaemia	Fluorosis	Hyperostosis	OI
Arms	○ Long bone cortical thinning ○ Metaphyseal fractures ○ White line of Fraenkel ○ Wimberger's ring ○ Pelkan's spurs	○ Long bone cortical thinning ○ Metaphyseal fractures ○ Metaphyseal trabecular coarsening ○ Fraying of epiphyses ○ Distinction at the end of the epiphysis	○ Infarcts in long bones ○ Reduced number of trabeculae in long bones			○ Zebra stripe
Hands						
Pelvis						
Legs	○ Long bone cortical thinning ○ Metaphyseal fractures ○ White line of Fraenkel ○ Wimberger's ring ○ Pelkan's spurs	○ Long bone cortical thinning ○ Metaphyseal fractures ○ Fraying of epiphyses ○ Distinction at the end of the epiphysis	○ Infarcts in long bones ○ Reduced number of trabeculae in long bones			○ Zebra stripe
Feet						

SG24 is an individual with no lesions, and their remains are very fragmentary.

SG25

Macroscopic Indicators

	Scurvy	Rickets	Anaemia	Fluorosis	Hyperostosis	OI
General Skeleton	○ Irregular & spongy new bone formation	○ General porosity ○ Abnormal growth plates	○ Porosity ○ Osteopenia (Thal.) ○ Large bony masses (Thal.)	○ Diffuse osteosclerosis of the appendicular & axial skeleton ○ Increased cortical & trabecular thickness ○ Periosteal thickening ○ Calcified ligaments, tendons, cartilage, & inter-osseous membrane-s ○ Bony exostoses at ligament & muscle attachment zones	○ Increased weight of bones ○ Increased thickness of cortical bone ○ A lot of subperiosteal new bone formation	○ Lightness/fragility to bones ○ Fractures ○ Osteoporosis
Orbits	○ Cribra orbitalia ○ Porosity	○ Orbital roof porosity	○ Cribra orbitalia ○ Thinning of trabecular & cortical bone ○ Widening interorbital space (Thal.)			○ Elongated orbits
Cranium	Porosity on: ○ the greater sphenoid wing ○ cranial bones ○ facial bones ○ palate ○ basiocciput	○ Frontal bone bossing ○ Deformed mandibular ramus	○ Cranial vault porosity ○ Thickening of the sphenoid, maxillae, & zygomatics (Thal.) ○ Obliterated sutures in the cranium (Thal.)		○ A lot of subperiosteal new bone formation, most commonly on facial bones (Caffey's) ○ Osteal bulges ○ Irregular thickening of internal surface of frontal bone while external surface looks normal (IFH)	○ Expanded cranial vault
Dentition			○ Protruding upper incisors & overbite (Thal.)	○ Linear enamel hypoplasia ○ Brown, dis-coloured teeth, & mottled enamel		○ Dentinogenesis imperfecta
Vertebral Column			○ Perforations in the cortical bone of vertebrae			
Thorax		○ Rib flaring	○ Slight expansion of the ribs ○ Perforated cortical bone in ribs (Thal.) ○ Linear striations on the ribs (Thal.)		○ A lot of subperiosteal new bone formation, most commonly on ribs	
Arms	Porosity on: ○ the scapulae ○ metaphyses of long bones	○ Porosity in concave curvature of long bones ○ Long bone thickening & bowing	○ Long bone porosity ○ Thinning of trabecular & cortical bone ○ Perforated cortical bone in long bones (Thal.)			○ Long bone bowing with cortical thickening ○ Narrowing of long bone diaphyses in comparison to their length

	Scurvy	Rickets	Anaemia	Fluorosis	Hyperostosis	OI
		○ Long bone metaphyseal flaring	○ Necrosis of the humeral head (SCA)			
Hands						
Pelvis		○ Ilium concavity				
Legs	Porosity on: ○ Metaphyses of long bones	○ Porosity in concave curvature of long bones ○ Long bone thickening & bowing ○ Long bone metaphyseal flaring	○ Long bone porosity ○ Thinning of trabecular & cortical bone ○ Perforated cortical bone in long bones (Thal.) ○ Exaggerated sulci on femora & tibiae (Thal.) ○ Necrosis of the femoral head (SCA)			○ Long bone bowing with cortical thickening ○ Narrowing of long bone diaphyses in comparison to their length
Feet			○ Hyper-trophic meta-carpals & phalanges (Thal.)			

Radiographic Indicators

	Scurvy	Rickets	Anaemia	Fluorosis	Hyperostosis	OI
General Skeleton	○ Generalized osteopenia	○ Generalized osteopenia ○ Thick cortex ○ Sharp cortical outline	○ Thinning of cortical bone			
Cranium			○ Hair-on-end appearance cranium ○ Undeveloped sinuses			
Dentition						
Vertebral Column			○ Reduced number of trabeculae in vertebrae			
Thorax		○ Loss of integrity in sternal rib ends				

	Scurvy	Rickets	Anaemia	Fluorosis	Hyperostosis	OI
Arms	○ Long bone cortical thinning ○ Metaphyseal fractures ○ White line of Fraenkel ○ Wimberger's ring ○ Pelkan's spurs	○ Long bone cortical thinning ○ Metaphyseal fractures ○ Metaphyseal trabecular coarsening ○ Fraying of epiphyses ○ Distinction at the end of the epiphysis	○ Infarcts in long bones ○ Reduced number of trabeculae in long bones			○ Zebra stripe
Hands						
Pelvis						
Legs	○ Long bone cortical thinning ○ Metaphyseal fractures ○ White line of Fraenkel ○ Wimberger's ring ○ Pelkan's spurs	○ Long bone cortical thinning ○ Metaphyseal fractures ○ Fraying of epiphyses ○ Distinction at the end of the epiphysis	○ Infarcts in long bones ○ Reduced number of trabeculae in long bones			○ Zebra stripe
Feet						

SG25 presents with one type of lesion upon their remains which is spongey new growth and porosity in their right orbital roof. Radiography does not indicate any lesions. SG25's lesion are consistent with MBD. The irregular and spongey new bone formation is consistent with scorbutic lesions but is not a diagnostic feature. The porosity seen in the orbit could also be associated with anaemia, pellagra, and rickets. Given that there are no other lesions on SG25's remains, related to MBD or otherwise, there is not sufficient evidence for any diagnosis.

SG26

Macroscopic Indicators

	Scurvy	Rickets	Anaemia	Fluorosis	Hyperostosis	OI
General Skeleton	○ Irregular & spongy new bone formation	○ General porosity ○ Abnormal growth plates	○ Porosity ○ Osteopenia (Thal.) ○ Large bony masses (Thal.)	○ Diffuse osteosclerosis of the appendicular & axial skeleton ○ Increased cortical & trabecular thickness ○ Periosteal thickening ○ Calcified ligaments, tendons, cartilage, & inter-osseous membrane-s ○ Bony exostoses at ligament & muscle attachment zones	○ Increased weight of bones ○ Increased thickness of cortical bone ○ A lot of subperiosteal new bone formation	○ Lightness/fragility to bones ○ Fractures ○ Osteoporosis
Orbits	○ Cribra orbitalia ○ Porosity	○ Orbital roof porosity	○ Cribra orbitalia ○ Thinning of trabecular & cortical bone ○ Widening interorbital space (Thal.)			○ Elongated orbits
Cranium	Porosity on: ○ the greater sphenoid wing ○ cranial bones ○ facial bones ○ palate ○ basiocciput	○ Frontal bone bossing ○ Deformed mandibular ramus	○ Cranial vault porosity ○ Thickening of the sphenoid, maxillae, & zygomatics (Thal.) ○ Obliterated sutures in the cranium (Thal.)		○ A lot of subperiosteal new bone formation, most commonly on facial bones (Caffey's) ○ Osteal bulges ○ Irregular thickening of internal surface of frontal bone while external surface looks normal (IFH)	○ Expanded cranial vault
Dentition			○ Protruding upper incisors & overbite (Thal.)	○ Linear enamel hypoplasia ○ Brown, dis-coloured teeth, & mottled enamel		○ Dentinogenesis imperfecta
Vertebral Column			○ Perforations in the cortical bone of vertebrae			
Thorax		○ Rib flaring	○ Slight expansion of the ribs ○ Perforated cortical bone in ribs (Thal.) ○ Linear striations on the ribs (Thal.)		○ A lot of subperiosteal new bone formation, most commonly on ribs	
Arms	Porosity on: ○ the scapulae ○ metaphyses of long bones	○ Porosity in concave curvature of long bones ○ Long bone thickening & bowing	○ Long bone porosity ○ Thinning of trabecular & cortical bone ○ Perforated cortical bone in long bones (Thal.)			○ Long bone bowing with cortical thickening ○ Narrowing of long bone diaphyses in comparison to their length

	Scurvy	Rickets	Anaemia	Fluorosis	Hyperostosis	OI
		○ Long bone metaphyseal flaring	○ Necrosis of the humeral head (SCA)			
Hands						
Pelvis		○ Ilium concavity				
Legs	Porosity on: ○ Metaphyses of long bones	○ Porosity in concave curvature of long bones ○ Long bone thickening & bowing ○ Long bone metaphyseal flaring	○ Long bone porosity ○ Thinning of trabecular & cortical bone ○ Perforated cortical bone in long bones (Thal.) ○ Exaggerated sulci on femora & tibiae (Thal.) ○ Necrosis of the femoral head (SCA)			○ Long bone bowing with cortical thickening ○ Narrowing of long bone diaphyses in comparison to their length
Feet			○ Hyper-trophic meta-carpals & phalanges (Thal.)			

Radiographic Indicators

	Scurvy	Rickets	Anaemia	Fluorosis	Hyperostosis	OI
General Skeleton	○ Generalized osteopenia	○ Generalized osteopenia ○ Thick cortex ○ Sharp cortical outline	○ Thinning of cortical bone			
Cranium			○ Hair-on-end appearance cranium ○ Undeveloped sinuses			
Dentition						
Vertebral Column			○ Reduced number of trabeculae in vertebrae			
Thorax		○ Loss of integrity in sternal rib ends				

	Scurvy	Rickets	Anaemia	Fluorosis	Hyperostosis	OI
Arms	○ Long bone cortical thinning ○ Metaphyseal fractures ○ White line of Fraenkel ○ Wimberger's ring ○ Pelkan's spurs	○ Long bone cortical thinning ○ Metaphyseal fractures ○ Metaphyseal trabecular coarsening ○ Fraying of epiphyses ○ Distinction at the end of the epiphysis	○ Infarcts in long bones ○ Reduced number of trabeculae in long bones			○ Zebra stripe
Hands						
Pelvis						
Legs	○ Long bone cortical thinning ○ Metaphyseal fractures ○ White line of Fraenkel ○ Wimberger's ring ○ Pelkan's spurs	○ Long bone cortical thinning ○ Metaphyseal fractures ○ Fraying of epiphyses ○ Distinction at the end of the epiphysis	○ Infarcts in long bones ○ Reduced number of trabeculae in long bones			○ Zebra stripe
Feet						

SG26 presents with a slight amount of new growth on their mandible fragment, which is accompanied by a double alveolar socket appearance. New growth is also present on the left scapula, concentrated around the scapular ridge. The new growth is concentrated on the supraspinous fossa while there is slight porosity across the infraspinous fossa. Radiography associated with SG26 indicates no lesions or radiographic indicators of disease.

While there are not many remains present for SG26, or associated lesions, there are still some consistencies with MBD. The porosity present on the left scapula is consistent with scurvy and is a diagnostic feature. However, this is not sufficient evidence for probable diagnosis.

SG27

Macroscopic Indicators

	Scurvy	Rickets	Anaemia	Fluorosis	Hyperostosis	OI
General Skeleton	○ Irregular & spongy new bone formation	○ General porosity ○ Abnormal growth plates	○ Porosity ○ Osteopenia (Thal.) ○ Large bony masses (Thal.)	○ Diffuse osteosclerosis of the appendicular & axial skeleton ○ Increased cortical & trabecular thickness ○ Periosteal thickening ○ Calcified ligaments, tendons, cartilage, & inter-osseous membrane-s ○ Bony exostoses at ligament & muscle attachment zones	○ Increased weight of bones ○ Increased thickness of cortical bone ○ A lot of subperiosteal new bone formation	○ Lightness/fragility to bones ○ Fractures ○ Osteoporosis
Orbits	○ Cribra orbitalia ○ Porosity	○ Orbital roof porosity	○ Cribra orbitalia ○ Thinning of trabecular & cortical bone ○ Widening interorbital space (Thal.)			○ Elongated orbits
Cranium	Porosity on: ○ the greater sphenoid wing ○ cranial bones ○ facial bones ○ palate ○ basiocciput	○ Frontal bone bossing ○ Deformed mandibular ramus	○ Cranial vault porosity ○ Thickening of the sphenoid, maxillae, & zygomatics (Thal.) ○ Obliterated sutures in the cranium (Thal.)		○ A lot of subperiosteal new bone formation, most commonly on facial bones (Caffey's) ○ Osteal bulges ○ Irregular thickening of internal surface of frontal bone while external surface looks normal (IFH)	○ Expanded cranial vault
Dentition			○ Protruding upper incisors & overbite (Thal.)	○ Linear enamel hypoplasia ○ Brown, dis-coloured teeth, & mottled enamel		○ Dentinogenesis imperfecta
Vertebral Column			○ Perforations in the cortical bone of vertebrae			
Thorax		○ Rib flaring	○ Slight expansion of the ribs ○ Perforated cortical bone in ribs (Thal.) ○ Linear striations on the ribs (Thal.)		○ A lot of subperiosteal new bone formation, most commonly on ribs	
Arms	Porosity on: ○ the scapulae ○ metaphyses of long bones	○ Porosity in concave curvature of long bones ○ Long bone thickening & bowing	○ Long bone porosity ○ Thinning of trabecular & cortical bone ○ Perforated cortical bone in long bones (Thal.)			○ Long bone bowing with cortical thickening ○ Narrowing of long bone diaphyses in comparison to their length

	Scurvy	Rickets	Anaemia	Fluorosis	Hyperostosis	OI
		○ Long bone metaphyseal flaring	○ Necrosis of the humeral head (SCA)			
Hands						
Pelvis		○ Ilium concavity				
Legs	Porosity on: ○ Metaphyses of long bones	○ Porosity in concave curvature of long bones ○ Long bone thickening & bowing ○ Long bone metaphyseal flaring	○ Long bone porosity ○ Thinning of trabecular & cortical bone ○ Perforated cortical bone in long bones (Thal.) ○ Exaggerated sulci on femora & tibiae (Thal.) ○ Necrosis of the femoral head (SCA)			○ Long bone bowing with cortical thickening ○ Narrowing of long bone diaphyses in comparison to their length
Feet			○ Hyper-trophic meta-carpals & phalanges (Thal.)			

Radiographic Indicators

	Scurvy	Rickets	Anaemia	Fluorosis	Hyperostosis	OI
General Skeleton	○ Generalized osteopenia	○ Generalized osteopenia ○ Thick cortex ○ Sharp cortical outline	○ Thinning of cortical bone			
Cranium			○ Hair-on-end appearance cranium ○ Undeveloped sinuses			
Dentition						
Vertebral Column			○ Reduced number of trabeculae in vertebrae			
Thorax		○ Loss of integrity in sternal rib ends				

	Scurvy	Rickets	Anaemia	Fluorosis	Hyperostosis	OI
Arms	○ Long bone cortical thinning ○ Metaphyseal fractures ○ White line of Fraenkel ○ Wimberger's ring ○ Pelkan's spurs	○ Long bone cortical thinning ○ Metaphyseal fractures ○ Metaphyseal trabecular coarsening ○ Fraying of epiphyses ○ Distinction at the end of the epiphysis	○ Infarcts in long bones ○ Reduced number of trabeculae in long bones			○ Zebra stripe
Hands						
Pelvis						
Legs	○ Long bone cortical thinning ○ Metaphyseal fractures ○ White line of Fraenkel ○ Wimberger's ring ○ Pelkan's spurs	○ Long bone cortical thinning ○ Metaphyseal fractures ○ Fraying of epiphyses ○ Distinction at the end of the epiphysis	○ Infarcts in long bones ○ Reduced number of trabeculae in long bones			○ Zebra stripe
Feet						

SG27 presents with porosity in their left orbit which has the appearance of a new bone deposit which does not burrow into the diploë, rather that it grows outwards. In terms of their teeth, there is an enamel defect on the lower right DC. There is no radiography available for this individual.

Some of SG27's lesions are consistent with MBD. For one, the changes seen in the left orbit could be associated with scurvy or pellagra but there are no other lesions which would support diagnosis of either of these MBD. Additionally, the orbital roof porosity can be a non-diagnostic feature of rickets. Given that the orbital porosity and changes appear to grow outwards, rather than tunneling inwards, anaemia seems less likely. However, one lesion is not enough skeletal evidence to support a diagnosis of any of MBD.

SG28

Macroscopic Indicators

	Scurvy	Rickets	Anaemia	Fluorosis	Hyperostosis	OI
General Skeleton	○ Irregular & spongy new bone formation	○ General porosity ○ Abnormal growth plates	○ Porosity ○ Osteopenia (Thal.) ○ Large bony masses (Thal.)	○ Diffuse osteosclerosis of the appendicular & axial skeleton ○ Increased cortical & trabecular thickness ○ Periosteal thickening ○ Calcified ligaments, tendons, cartilage, & inter-osseous membrane-s ○ Bony exostoses at ligament & muscle attachment zones	○ Increased weight of bones ○ Increased thickness of cortical bone ○ A lot of subperiosteal new bone formation	○ Lightness/fragility to bones ○ Fractures ○ Osteoporosis
Orbits	○ Cribra orbitalia ○ Porosity	○ Orbital roof porosity	○ Cribra orbitalia ○ Thinning of trabecular & cortical bone ○ Widening interorbital space (Thal.)			○ Elongated orbits
Cranium	Porosity on: ○ the greater sphenoid wing ○ cranial bones ○ facial bones ○ palate ○ basiocciput	○ Frontal bone bossing ○ Deformed mandibular ramus	○ Cranial vault porosity ○ Thickening of the sphenoid, maxillae, & zygomatics (Thal.) ○ Obliterated sutures in the cranium (Thal.)		○ A lot of subperiosteal new bone formation, most commonly on facial bones (Caffey's) ○ Osteal bulges ○ Irregular thickening of internal surface of frontal bone while external surface looks normal (IFH)	○ Expanded cranial vault
Dentition			○ Protruding upper incisors & overbite (Thal.)	○ Linear enamel hypoplasia ○ Brown, dis-coloured teeth, & mottled enamel		○ Dentinogenesis imperfecta
Vertebral Column			○ Perforations in the cortical bone of vertebrae			
Thorax		○ Rib flaring	○ Slight expansion of the ribs ○ Perforated cortical bone in ribs (Thal.) ○ Linear striations on the ribs (Thal.)		○ A lot of subperiosteal new bone formation, most commonly on ribs	
Arms	Porosity on: ○ the scapulae ○ metaphyses of long bones	○ Porosity in concave curvature of long bones ○ Long bone thickening & bowing	○ Long bone porosity ○ Thinning of trabecular & cortical bone ○ Perforated cortical bone in long bones (Thal.)			○ Long bone bowing with cortical thickening ○ Narrowing of long bone diaphyses in comparison to their length

	Scurvy	Rickets	Anaemia	Fluorosis	Hyperostosis	OI
		○ Long bone metaphyseal flaring	○ Necrosis of the humeral head (SCA)			
Hands						
Pelvis		○ Ilium concavity				
Legs	Porosity on: ○ Metaphyses of long bones	○ Porosity in concave curvature of long bones ○ Long bone thickening & bowing ○ Long bone metaphyseal flaring	○ Long bone porosity ○ Thinning of trabecular & cortical bone ○ Perforated cortical bone in long bones (Thal.) ○ Exaggerated sulci on femora & tibiae (Thal.) ○ Necrosis of the femoral head (SCA)			○ Long bone bowing with cortical thickening ○ Narrowing of long bone diaphyses in comparison to their length
Feet			○ Hyper-trophic meta-carpals & phalanges (Thal.)			

Radiographic Indicators

	Scurvy	Rickets	Anaemia	Fluorosis	Hyperostosis	OI
General Skeleton	○ Generalized osteopenia	○ Generalized osteopenia ○ Thick cortex ○ Sharp cortical outline	○ Thinning of cortical bone			
Cranium			○ Hair-on-end appearance cranium ○ Undeveloped sinuses			
Dentition						
Vertebral Column			○ Reduced number of trabeculae in vertebrae			
Thorax		○ Loss of integrity in sternal rib ends				

	Scurvy	Rickets	Anaemia	Fluorosis	Hyperostosis	OI
Arms	○ Long bone cortical thinning ○ Metaphyseal fractures ○ White line of Fraenkel ○ Wimberger's ring ○ Pelkan's spurs	○ Long bone cortical thinning ○ Metaphyseal fractures ○ Metaphyseal trabecular coarsening ○ Fraying of epiphyses ○ Distinction at the end of the epiphysis	○ Infarcts in long bones ○ Reduced number of trabeculae in long bones			○ Zebra stripe
Hands						
Pelvis						
Legs	○ Long bone cortical thinning ○ Metaphyseal fractures ○ White line of Fraenkel ○ Wimberger's ring ○ Pelkan's spurs	○ Long bone cortical thinning ○ Metaphyseal fractures ○ Fraying of epiphyses ○ Distinction at the end of the epiphysis	○ Infarcts in long bones ○ Reduced number of trabeculae in long bones			○ Zebra stripe
Feet						

SG28 demonstrates very slight porosity occurs in the left orbit. While SG28 does not present with a lot of lesions, there are consistencies with MBD indicators. The orbital porosity seen in their left orbit could be associated with scurvy, but this is not a diagnostic feature of the disease. It is also a non-diagnostic criterion for rickets. As this is their only lesion, there is insufficient evidence for any probable MBD diagnosis.

SG29

Macroscopic Indicators

	Scurvy	Rickets	Anaemia	Fluorosis	Hyperostosis	OI
General Skeleton	○ Irregular & spongy new bone formation	○ General porosity ○ Abnormal growth plates	○ Porosity ○ Osteopenia (Thal.) ○ Large bony masses (Thal.)	○ Diffuse osteosclerosis of the appendicular & axial skeleton ○ Increased cortical & trabecular thickness ○ Periosteal thickening ○ Calcified ligaments, tendons, cartilage, & inter-osseous membrane-s ○ Bony exostoses at ligament & muscle attachment zones	○ Increased weight of bones ○ Increased thickness of cortical bone ○ A lot of subperiosteal new bone formation	○ Lightness/fragility to bones ○ Fractures ○ Osteoporosis
Orbits	○ Cribra orbitalia ○ Porosity	○ Orbital roof porosity	○ Cribra orbitalia ○ Thinning of trabecular & cortical bone ○ Widening interorbital space (Thal.)			○ Elongated orbits
Cranium	Porosity on: ○ the greater sphenoid wing ○ cranial bones ○ facial bones ○ palate ○ basiocciput	○ Frontal bone bossing ○ Deformed mandibular ramus	○ Cranial vault porosity ○ Thickening of the sphenoid, maxillae, & zygomatics (Thal.) ○ Obliterated sutures in the cranium (Thal.)		○ A lot of subperiosteal new bone formation, most commonly on facial bones (Caffey's) ○ Osteal bulges ○ Irregular thickening of internal surface of frontal bone while external surface looks normal (IFH)	○ Expanded cranial vault
Dentition			○ Protruding upper incisors & overbite (Thal.)	○ Linear enamel hypoplasia ○ Brown, dis-coloured teeth, & mottled enamel		○ Dentinogenesis imperfecta
Vertebral Column			○ Perforations in the cortical bone of vertebrae			
Thorax		○ Rib flaring	○ Slight expansion of the ribs ○ Perforated cortical bone in ribs (Thal.) ○ Linear striations on the ribs (Thal.)		○ A lot of subperiosteal new bone formation, most commonly on ribs	
Arms	Porosity on: ○ the scapulae ○ metaphyses of long bones	○ Porosity in concave curvature of long bones ○ Long bone thickening & bowing	○ Long bone porosity ○ Thinning of trabecular & cortical bone ○ Perforated cortical bone in long bones (Thal.)			○ Long bone bowing with cortical thickening ○ Narrowing of long bone diaphyses in comparison to their length

	Scurvy	Rickets	Anaemia	Fluorosis	Hyperostosis	OI
		○ Long bone metaphyseal flaring	○ Necrosis of the humeral head (SCA)			
Hands						
Pelvis		○ Ilium concavity				
Legs	Porosity on: ○ Metaphyses of long bones	○ Porosity in concave curvature of long bones ○ Long bone thickening & bowing ○ Long bone metaphyseal flaring	○ Long bone porosity ○ Thinning of trabecular & cortical bone ○ Perforated cortical bone in long bones (Thal.) ○ Exaggerated sulci on femora & tibiae (Thal.) ○ Necrosis of the femoral head (SCA)			○ Long bone bowing with cortical thickening ○ Narrowing of long bone diaphyses in comparison to their length
Feet			○ Hyper-trophic meta-carpals & phalanges (Thal.)			

Radiographic Indicators

	Scurvy	Rickets	Anaemia	Fluorosis	Hyperostosis	OI
General Skeleton	○ Generalized osteopenia	○ Generalized osteopenia ○ Thick cortex ○ Sharp cortical outline	○ Thinning of cortical bone			
Cranium			○ Hair-on-end appearance cranium ○ Undeveloped sinuses			
Dentition						
Vertebral Column			○ Reduced number of trabeculae in vertebrae			
Thorax		○ Loss of integrity in sternal rib ends				

	Scurvy	Rickets	Anaemia	Fluorosis	Hyperostosis	OI
Arms	○ Long bone cortical thinning ○ Metaphyseal fractures ○ White line of Fraenkel ○ Wimberger's ring ○ Pelkan's spurs	○ Long bone cortical thinning ○ Metaphyseal fractures ○ Metaphyseal trabecular coarsening ○ Fraying of epiphyses ○ Distinction at the end of the epiphysis	○ Infarcts in long bones ○ Reduced number of trabeculae in long bones			○ Zebra stripe
Hands						
Pelvis						
Legs	○ Long bone cortical thinning ○ Metaphyseal fractures ○ White line of Fraenkel ○ Wimberger's ring ○ Pelkan's spurs	○ Long bone cortical thinning ○ Metaphyseal fractures ○ Fraying of epiphyses ○ Distinction at the end of the epiphysis	○ Infarcts in long bones ○ Reduced number of trabeculae in long bones			○ Zebra stripe
Feet						

SG29 presents with lesions in their cranium. On their teeth, there is localized hypoplasia of the primary canines (LHPC). As well, linear enamel hypoplasia (LEH) occurs on the lower right canine, lower left I1, lower left canine, lower right M1, lower left M1, upper left I1, and upper left canine. In their arms, there are possible Harris lines indicated on the x-rays of the radii on the distal ends.

SG29's lesions are non-specific. But pellagra is something to consider due to the enamel hypoplasias present. Fluorosis should also be considered due to the LEH. But one lesion type is again insufficient evidence for a MBD diagnosis. Thus, no diagnosis is made. However, the Harris lines and enamel hypoplasias would indicate that this child lived through some periods of stress in their life.

SG30

Macroscopic Indicators

	Scurvy	Rickets	Anaemia	Fluorosis	Hyperostosis	OI
General Skeleton	○ Irregular & spongy new bone formation	○ General porosity ○ Abnormal growth plates	○ Porosity ○ Osteopenia (Thal.) ○ Large bony masses (Thal.)	○ Diffuse osteosclerosis of the appendicular & axial skeleton ○ Increased cortical & trabecular thickness ○ Periosteal thickening ○ Calcified ligaments, tendons, cartilage, & inter-osseous membrane-s ○ Bony exostoses at ligament & muscle attachment zones	○ Increased weight of bones ○ Increased thickness of cortical bone ○ A lot of subperiosteal new bone formation	○ Lightness/fragility to bones ○ Fractures ○ Osteoporosis
Orbits	○ Cribra orbitalia ○ Porosity	○ Orbital roof porosity	○ Cribra orbitalia ○ Thinning of trabecular & cortical bone ○ Widening interorbital space (Thal.)			○ Elongated orbits
Cranium	Porosity on: ○ the greater sphenoid wing ○ cranial bones ○ facial bones ○ palate ○ basiocciput	○ Frontal bone bossing ○ Deformed mandibular ramus	○ Cranial vault porosity ○ Thickening of the sphenoid, maxillae, & zygomatics (Thal.) ○ Obliterated sutures in the cranium (Thal.)		○ A lot of subperiosteal new bone formation, most commonly on facial bones (Caffey's) ○ Osteal bulges ○ Irregular thickening of internal surface of frontal bone while external surface looks normal (IFH)	○ Expanded cranial vault
Dentition			○ Protruding upper incisors & overbite (Thal.)	○ Linear enamel hypoplasia ○ Brown, dis-coloured teeth, & mottled enamel		○ Dentinogenesis imperfecta
Vertebral Column			○ Perforations in the cortical bone of vertebrae			
Thorax		○ Rib flaring	○ Slight expansion of the ribs ○ Perforated cortical bone in ribs (Thal.) ○ Linear striations on the ribs (Thal.)		○ A lot of subperiosteal new bone formation, most commonly on ribs	
Arms	Porosity on: ○ the scapulae ○ metaphyses of long bones	○ Porosity in concave curvature of long bones ○ Long bone thickening & bowing	○ Long bone porosity ○ Thinning of trabecular & cortical bone ○ Perforated cortical bone in long bones (Thal.)			○ Long bone bowing with cortical thickening ○ Narrowing of long bone diaphyses in comparison to their length

	Scurvy	Rickets	Anaemia	Fluorosis	Hyperostosis	OI
		○ Long bone metaphyseal flaring	○ Necrosis of the humeral head (SCA)			
Hands						
Pelvis		○ Ilium concavity				
Legs	Porosity on: ○ Metaphyses of long bones	○ Porosity in concave curvature of long bones ○ Long bone thickening & bowing ○ Long bone metaphyseal flaring	○ Long bone porosity ○ Thinning of trabecular & cortical bone ○ Perforated cortical bone in long bones (Thal.) ○ Exaggerated sulci on femora & tibiae (Thal.) ○ Necrosis of the femoral head (SCA)			○ Long bone bowing with cortical thickening ○ Narrowing of long bone diaphyses in comparison to their length
Feet			○ Hyper-trophic meta-carpals & phalanges (Thal.)			

Radiographic Indicators

	Scurvy	Rickets	Anaemia	Fluorosis	Hyperostosis	OI
General Skeleton	○ Generalized osteopenia	○ Generalized osteopenia ○ Thick cortex ○ Sharp cortical outline	○ Thinning of cortical bone			
Cranium			○ Hair-on-end appearance cranium ○ Undeveloped sinuses			
Dentition						
Vertebral Column			○ Reduced number of trabeculae in vertebrae			
Thorax		○ Loss of integrity in sternal rib ends				

	Scurvy	Rickets	Anaemia	Fluorosis	Hyperostosis	OI
Arms	○ Long bone cortical thinning ○ Metaphyseal fractures ○ White line of Fraenkel ○ Wimberger's ring ○ Pelkan's spurs	○ Long bone cortical thinning ○ Metaphyseal fractures ○ Metaphyseal trabecular coarsening ○ Fraying of epiphyses ○ Distinction at the end of the epiphysis	○ Infarcts in long bones ○ Reduced number of trabeculae in long bones			○ Zebra stripe
Hands						
Pelvis						
Legs	○ Long bone cortical thinning ○ Metaphyseal fractures ○ White line of Fraenkel ○ Wimberger's ring ○ Pelkan's spurs	○ Long bone cortical thinning ○ Metaphyseal fractures ○ Fraying of epiphyses ○ Distinction at the end of the epiphysis	○ Infarcts in long bones ○ Reduced number of trabeculae in long bones			○ Zebra stripe
Feet						

SG30 is an individual with not a lot of lesions present on their remains. Their first pathological indicator is localized hypoplasia of the primary canines (LHPC)in their mandibular canines, and their right clavicle demonstrates a little bit of new growth towards the distal end. No pathological signs were found on any of the associated radiography for SG30.

None of the lesions present on SG30's remains appear to be related to MBD. The LPHC could be thought to be associated with pellagra, as pellagra can result in enamel hypoplasias. One lesion is insufficient evidence for a diagnosis but, given the LHPC it is possible that SG30 lived through a period of stress in their life.

SG31

Macroscopic Indicators

	Scurvy	Rickets	Anaemia	Fluorosis	Hyperostosis	OI
General Skeleton	○ Irregular & spongy new bone formation	○ General porosity ○ Abnormal growth plates	○ Porosity ○ Osteopenia (Thal.) ○ Large bony masses (Thal.)	○ Diffuse osteosclerosis of the appendicular & axial skeleton ○ Increased cortical & trabecular thickness ○ Periosteal thickening ○ Calcified ligaments, tendons, cartilage, & inter-osseous membrane-s ○ Bony exostoses at ligament & muscle attachment zones	○ Increased weight of bones ○ Increased thickness of cortical bone ○ A lot of subperiosteal new bone formation	○ Lightness/fragility to bones ○ Fractures ○ Osteoporosis
Orbits	○ Cribra orbitalia ○ Porosity	○ Orbital roof porosity	○ Cribra orbitalia ○ Thinning of trabecular & cortical bone ○ Widening interorbital space (Thal.)			○ Elongated orbits
Cranium	Porosity on: ○ the greater sphenoid wing ○ cranial bones ○ facial bones ○ palate ○ basiocciput	○ Frontal bone bossing ○ Deformed mandibular ramus	○ Cranial vault porosity ○ Thickening of the sphenoid, maxillae, & zygomatics (Thal.) ○ Obliterated sutures in the cranium (Thal.)		○ A lot of subperiosteal new bone formation, most commonly on facial bones (Caffey's) ○ Osteal bulges ○ Irregular thickening of internal surface of frontal bone while external surface looks normal (IFH)	○ Expanded cranial vault
Dentition			○ Protruding upper incisors & overbite (Thal.)	○ Linear enamel hypoplasia ○ Brown, dis-coloured teeth, & mottled enamel		○ Dentinogenesis imperfecta
Vertebral Column			○ Perforations in the cortical bone of vertebrae			
Thorax		○ Rib flaring	○ Slight expansion of the ribs ○ Perforated cortical bone in ribs (Thal.) ○ Linear striations on the ribs (Thal.)		○ A lot of subperiosteal new bone formation, most commonly on ribs	
Arms	Porosity on: ○ the scapulae ○ metaphyses of long bones	○ Porosity in concave curvature of long bones ○ Long bone thickening & bowing	○ Long bone porosity ○ Thinning of trabecular & cortical bone ○ Perforated cortical bone in long bones (Thal.)			○ Long bone bowing with cortical thickening ○ Narrowing of long bone diaphyses in comparison to their length

	Scurvy	Rickets	Anaemia	Fluorosis	Hyperostosis	OI
		○ Long bone metaphyseal flaring	○ Necrosis of the humeral head (SCA)			
Hands						
Pelvis		○ Ilium concavity				
Legs	Porosity on: ○ Metaphyses of long bones	○ Porosity in concave curvature of long bones ○ Long bone thickening & bowing ○ Long bone metaphyseal flaring	○ Long bone porosity ○ Thinning of trabecular & cortical bone ○ Perforated cortical bone in long bones (Thal.) ○ Exaggerated sulci on femora & tibiae (Thal.) ○ Necrosis of the femoral head (SCA)			○ Long bone bowing with cortical thickening ○ Narrowing of long bone diaphyses in comparison to their length
Feet			○ Hyper-trophic meta-carpals & phalanges (Thal.)			

Radiographic Indicators

	Scurvy	Rickets	Anaemia	Fluorosis	Hyperostosis	OI
General Skeleton	○ Generalized osteopenia	○ Generalized osteopenia ○ Thick cortex ○ Sharp cortical outline	○ Thinning of cortical bone			
Cranium			○ Hair-on-end appearance cranium ○ Undeveloped sinuses			
Dentition						
Vertebral Column			○ Reduced number of trabeculae in vertebrae			
Thorax		○ Loss of integrity in sternal rib ends				

	Scurvy	Rickets	Anaemia	Fluorosis	Hyperostosis	OI
Arms	○ Long bone cortical thinning ○ Metaphyseal fractures ○ White line of Fraenkel ○ Wimberger's ring ○ Pelkan's spurs	○ Long bone cortical thinning ○ Metaphyseal fractures ○ Metaphyseal trabecular coarsening ○ Fraying of epiphyses ○ Distinction at the end of the epiphysis	○ Infarcts in long bones ○ Reduced number of trabeculae in long bones			○ Zebra stripe
Hands						
Pelvis						
Legs	○ Long bone cortical thinning ○ Metaphyseal fractures ○ White line of Fraenkel ○ Wimberger's ring ○ Pelkan's spurs	○ Long bone cortical thinning ○ Metaphyseal fractures ○ Fraying of epiphyses ○ Distinction at the end of the epiphysis	○ Infarcts in long bones ○ Reduced number of trabeculae in long bones			○ Zebra stripe
Feet						

SG31 is represented by a singular human bone, and the rest of the burial is made up of faunal remains. The one bone present is a right clavicle which shows a bit of new growth, but this is thought to be normal. Also, PMD has obscured most of this new growth spot. It is unknown whether this individual lived with MBD as there are not enough skeletal remains present to make an accurate diagnosis.

SG32

Macroscopic Indicators

	Scurvy	Rickets	Anaemia	Fluorosis	Hyperostosis	OI
General Skeleton	○ Irregular & spongy new bone formation	○ General porosity ○ Abnormal growth plates	○ Porosity ○ Osteopenia (Thal.) ○ Large bony masses (Thal.)	○ Diffuse osteosclerosis of the appendicular & axial skeleton ○ Increased cortical & trabecular thickness ○ Periosteal thickening ○ Calcified ligaments, tendons, cartilage, & inter-osseous membrane-s ○ Bony exostoses at ligament & muscle attachment zones	○ Increased weight of bones ○ Increased thickness of cortical bone ○ A lot of subperiosteal new bone formation	○ Lightness/fragility to bones ○ Fractures ○ Osteoporosis
Orbits	○ Cribra orbitalia ○ Porosity	○ Orbital roof porosity	○ Cribra orbitalia ○ Thinning of trabecular & cortical bone ○ Widening interorbital space (Thal.)			○ Elongated orbits
Cranium	Porosity on: ○ the greater sphenoid wing ○ cranial bones ○ facial bones ○ palate ○ basiocciput	○ Frontal bone bossing ○ Deformed mandibular ramus	○ Cranial vault porosity ○ Thickening of the sphenoid, maxillae, & zygomatics (Thal.) ○ Obliterated sutures in the cranium (Thal.)		○ A lot of subperiosteal new bone formation, most commonly on facial bones (Caffey's) ○ Osteal bulges ○ Irregular thickening of internal surface of frontal bone while external surface looks normal (IFH)	○ Expanded cranial vault
Dentition			○ Protruding upper incisors & overbite (Thal.)	○ Linear enamel hypoplasia ○ Brown, dis-coloured teeth, & mottled enamel		○ Dentinogenesis imperfecta
Vertebral Column			○ Perforations in the cortical bone of vertebrae			
Thorax		○ Rib flaring	○ Slight expansion of the ribs ○ Perforated cortical bone in ribs (Thal.) ○ Linear striations on the ribs (Thal.)		○ A lot of subperiosteal new bone formation, most commonly on ribs	
Arms	Porosity on: ○ the scapulae ○ metaphyses of long bones	○ Porosity in concave curvature of long bones ○ Long bone thickening & bowing	○ Long bone porosity ○ Thinning of trabecular & cortical bone ○ Perforated cortical bone in long bones (Thal.)			○ Long bone bowing with cortical thickening ○ Narrowing of long bone diaphyses in comparison to their length

	Scurvy	Rickets	Anaemia	Fluorosis	Hyperostosis	OI
		○ Long bone metaphyseal flaring	○ Necrosis of the humeral head (SCA)			
Hands						
Pelvis		○ Ilium concavity				
Legs	Porosity on: ○ Metaphyses of long bones	○ Porosity in concave curvature of long bones ○ Long bone thickening & bowing ○ Long bone metaphyseal flaring	○ Long bone porosity ○ Thinning of trabecular & cortical bone ○ Perforated cortical bone in long bones (Thal.) ○ Exaggerated sulci on femora & tibiae (Thal.) ○ Necrosis of the femoral head (SCA)			○ Long bone bowing with cortical thickening ○ Narrowing of long bone diaphyses in comparison to their length
Feet			○ Hyper-trophic meta-carpals & phalanges (Thal.)			

Radiographic Indicators

	Scurvy	Rickets	Anaemia	Fluorosis	Hyperostosis	OI
General Skeleton	○ Generalized osteopenia	○ Generalized osteopenia ○ Thick cortex ○ Sharp cortical outline	○ Thinning of cortical bone			
Cranium			○ Hair-on-end appearance cranium ○ Undeveloped sinuses			
Dentition						
Vertebral Column			○ Reduced number of trabeculae in vertebrae			
Thorax		○ Loss of integrity in sternal rib ends				

	Scurvy	Rickets	Anaemia	Fluorosis	Hyperostosis	OI
Arms	○ Long bone cortical thinning ○ Metaphyseal fractures ○ White line of Fraenkel ○ Wimberger's ring ○ Pelkan's spurs	○ Long bone cortical thinning ○ Metaphyseal fractures ○ Metaphyseal trabecular coarsening ○ Fraying of epiphyses ○ Distinction at the end of the epiphysis	○ Infarcts in long bones ○ Reduced number of trabeculae in long bones			○ Zebra stripe
Hands						
Pelvis						
Legs	○ Long bone cortical thinning ○ Metaphyseal fractures ○ White line of Fraenkel ○ Wimberger's ring ○ Pelkan's spurs	○ Long bone cortical thinning ○ Metaphyseal fractures ○ Fraying of epiphyses ○ Distinction at the end of the epiphysis	○ Infarcts in long bones ○ Reduced number of trabeculae in long bones			○ Zebra stripe
Feet						

SG32 is the oldest individual within this population. Overall, their skeleton appears to be fairly normative with some lesions present. Porosity is visible on the anterior surface of the maxillae as well as on the inferior surface of the palate and around the alveolar processes. SG32's teeth have a lot of wear as well as caries on the lower right M3. Notable wear is present on the incisors as well as the lower left PM3, lower left I2, and lower right I1. There is no associated radiography for SG32.

The porosity on the facial bones (maxillae) is slight. However, the slight palate porosity and slight porosity around the alveolar processes are suggestive features of scurvy. However, two suggestive lesions are insufficient skeletal evidence for a probable diagnosis. The caries seen in the lower right M3 could be associated with pellagra, but there are no other lesions that would align with that diagnosis. As such, no probable diagnosis is given.

Appendix C: Observations of Scorbutic and Rachitic Lesions

Table C.1. *Observations of Scorbutic Lesions within the Seh Gabi Population*

	Sphenoid Greater Wing SPNB/ Porosity (d)	Maxilla: posterior aspect SPNB/ Porosity (d)	Scapula: Supra-spinous fossa Porosity (d)	Scapula: Infra-spinous fossa SPNB/ Porosity (d)	Frontal: orbital roof SPNB (d)	Sphenoid: lesser wings SPNB (s)	Mandible: mental coronoid process SPNB/ Porosity (s)	Zygo-matic: orbital surface Porosity (s)	Maxilla: infra orbital foramen SPNB/ Porosity (s)	Upper/ Lower limbs: diaphysis SPNB (s)	Upper/ Lower limbs: metaphys eal flaring (s)	Maxilla: palate Porosity (s)	Maxilla/ Mandible: alveolar process SPNB/ Porosity (s)	Rib flaring/cu pping (s)	Cranial Vault SPNB/ Porosity (n-d)	Ilium porosity (n-d)
SG1	No	No	No	No	No	N/A	No	No	No	No	No	No	No	No	**Yes**	No
SG2	N/A	N/A	No	No	N/A	N/A	N/A	N/A	N/A	No	No	N/A	N/A	No	No	No
SG3	No	No	No	No	No	No	No	No	No	No	No	**Yes**	No	No	**Yes**	No
SG4	N/A	N/A	No	No	No	N/A	No	No	No	No	**Yes**	N/A	No	No	No	No
SG5	N/A	N/A	N/A	N/A	N/A	N/A	N/A	N/A	N/A	No	No	N/A	N/A	No	**Yes**	No
SG6	No	No	No	No	No	No	No	No	No	No	No	No	No	No	No	No
SG7	**Yes**	No	No	No	**Yes**	No	No	No	No	No	No	No	No	No	No	No
SG8	No	**Yes**	No	No	N/A	No	No	No	No	N/A	N/A	No	No	No	N/A	N/A
SG9	No	**Yes**	**Yes**	No	**Yes**	No	No	No	No	No	No	**Yes**	No	No	No	No
SG10	No	No	No	No	No	No	No	No	No	No	No	No	No	No	No	No
SG11	N/A	N/A	No	No	No	N/A	N/A	N/A	N/A	**Yes**	No	N/A	No	No	**Yes**	N/A
SG12	No	N/A	No	No	No	N/A	N/A	N/A	N/A	No	No	N/A	No	No	No	N/A
SG13	N/A	N/A	N/A	N/A	No	N/A	N/A	N/A	N/A	No	No	N/A	N/A	No	N/A	No
SG14	No	No	No	No	No	No	No	No	No	No	No	**Yes**	No	No	**Yes**	No
SG15	No	N/A	No	No	No	No	No	No	No	No	No	N/A	No	No	No	No
SG16	No	N/A	No	No	No	No	No	No	N/A	No	No	**Yes**	No	No	**Yes**	No
SG17	N/A	N/A	N/A	N/A	N/A	N/A	N/A	N/A	N/A	N/A	N/A	N/A	N/A	N/A	N/A	No
SG18	N/A	N/A	No	No	N/A	N/A	N/A	N/A	N/A	N/A	N/A	N/A	N/A	No	N/A	N/A
SG19	No	N/A	No	No	No	No	No	No	N/A	No	No	N/A	No	No	No	No
SG20	No	N/A	N/A	N/A	N/A	No	N/A	No	N/A	No	No	N/A	No	No	N/A	No

	Sphenoid Greater Wing SPNB/ Porosity (d)	Maxilla: posterior aspect SPNB/ Porosity (d)	Scapula: Supra-spinous fossa Porosity (d)	Scapula: Infra-spinous fossa SPNB/ Porosity (d)	Frontal: orbital roof SPNB (d)	Sphenoid: lesser wings SPNB (s)	Mandible: mental coronoid process SPNB/ Porosity (s)	Zygo-matic: orbital surface Porosity (s)	Maxilla: infra orbital foramen SPNB/ Porosity (s)	Upper/ Lower limbs: diaphysis SPNB (s)	Upper/ Lower limbs: metaphys eal flaring (s)	Maxilla: palate Porosity (s)	Maxilla/ Mandible: alveolar process SPNB/ Porosity (s)	Rib flaring/cu pping (s)	Cranial Vault SPNB/ Porosity (n-d)	Ilium porosity (n-d)
SG21	**Yes**	No	No	**Yes**	No	No	No	No	**Yes**	No	No	No	No	No	No	No
SG22	No	No	No	No	No	No	No	No	No	No	No	**Yes**	No	No	**Yes**	No
SG23	No	No	No	No	No	No	No	No	No	No	No	**Yes**	No	No	No	No
SG24	N/A	N/A	N/A	No	No	N/A	N/A	No	N/A	No	No	N/A	N/A	No	No	N/A
SG25	N/A	N/A	No	No	**Yes**	N/A	No	No	N/A	No	No	N/A	No	No	No	No
SG26	N/A	N/A	No	**Yes**	N/A	N/A	N/A	N/A	N/A	No	No	N/A	No	N/A	No	N/A
SG27	N/A	No	No	No	**Yes**	N/A	No	No	No	No	No	No	No	No	No	No
SG28	No	No	No	No	No	N/A	N/A	No	No	No	No	No	No	No	No	No
SG29	N/A	No	N/A	N/A	N/A	N/A	N/A	No	No	No	No	No	No	No	No	No
SG30	N/A	N/A	N/A	N/A	N/A	N/A	No	N/A	N/A	N/A	N/A	N/A	No	No	N/A	No
SG31	N/A	N/A	N/A	N/A	N/A	N/A	N/A	N/A	N/A	N/A	N/A	N/A	N/A	N/A	N/A	N/A
SG32	No	No	No	No	No	N/A	No	No	No	No	No	**Yes**	**Yes**	No	No	No
PREVALENCE	**2/18**	**2/15**	**1/24**	**2/24**	**4/22**	**0/14**	**0/19**	**0/22**	**1/17**	**1/27**	**1/27**	**7/16**	**1/25**	**0/29**	**7/25**	**0/25**

Table C.1 Legend
d = diagnostic
s = suggestive
n-d = non-diagnostic
N/A = that portion of element not present for assessment.

Table C.2. *Observations of Rachitic Lesions within the Seh Gabi Population*

	Deformed arm & leg long bones when multiple bones affected & clear bend, radiography rules out trauma (d)	Abnormal growth plate distally (d)	Flattening of femoral metaphysis & coxa vara (d)	Thickened long bones bilaterally & confirmed radiographically (d)	Sternal rib end flaring if cupped (d)	Sternal rib end porosity (s)	Rib deformity with a sharp angle if multiple bones affected (s)	Deformed mandibular ramus (s)	Ilium concavity (s)	Long bone meta-physeal flaring; arms & legs (s)	Long bone concave curvature porosity (s; d if there is curvature along w/ porosity)	Cranial vault porosity ectocranial(n-d)	Cranial vault porosity endocranial (n-d)	Frontal bone bossing (n-d)	Orbital roof porosity (n-d)	Irregular & porous metaphyseal cortex of long bones (n-d)
SG1	No	No	No	No	No	No	No	No	No	No	No	No	No	No	**Yes**	No
SG2	No	No	No	No	No	No	No	N/A	No	No	No	No	No	N/A	N/A	No
SG3	No	No	No	No	No	No	No	No	No	No	No	**Yes**	No	No	No	No
SG4	No	No	No	No	No	No	No	No	No	**Yes**	No	No	No	No	No	No
SG5	No	No	No	No	No	No	No	N/A	No	No	No	**Yes**	**Yes**	N/A	N/A	No
SG6	No	No	No	No	No	No	No	No	No	No	No	No	No	No	No	No
SG7	No	No	No	No	No	No	No	No	No	No	No	No	No	N/A	No	No
SG8	N/A	No	N/A	N/A	No	No	No	No	N/A	N/A	N/A	N/A	No	N/A	N/A	No
SG9	No	No	No	No	No	No	No	No	No	No	No	No	No	No	**Yes**	No
SG10	No	No	No	No	No	No	No	No	No	No	No	No	No	No	**Yes**	No
SG11	No	No	No	No	No	No	No	No	N/A	No	No	No	No	No	No	No
SG12	No	No	No	No	No	No	No	N/A	N/A	No	No	No	No	No	**Yes**	No
SG13	No	N/A	No	No	No	No	No	N/A	No	No	No	N/A	No	N/A	No	No
SG14	No	No	No	No	No	No	No	No	No	No	No	**Yes**	No	No	**Yes**	No
SG15	No	No	No	No	No	No	No	No	No	No	No	No	No	No	No	No
SG16	No	No	No	No	No	No	No	N/A	No	No	No	No	No	No	**Yes**	No
SG17	N/A	N/A	N/A	N/A	N/A	N/A	N/A	N/A	No	N/A	N/A	N/A	No	N/A	N/A	No
SG18	N/A	No	N/A	N/A	No	No	No	N/A	N/A	N/A	N/A	N/A	No	N/A	N/A	No
SG19	No	No	No	No	No	No	No	No	No	No	No	No	No	No	No	No
SG20	No	No	No	No	No	No	No	No	No	No	No	N/A	No	N/A	N/A	No
SG21	No	No	No	No	No	No	No	No	No	No	No	No	No	No	No	No
SG22	No	No	No	No	No	No	No	No	No	No	No	No	No	No	No	No
SG23	No	No	No	No	No	No	No	No	No	No	No	No	No	No	No	No
SG24	No	No	No	No	No	No	No	N/A	N/A	No	No	No	No	N/A	No	No
SG25	No	No	No	No	No	No	No	No	No	No	No	No	No	No	**Yes**	No
SG26	No	No	N/A	N/A	N/A	N/A	N/A	N/A	N/A	No	No	No	No	N/A	N/A	No

	Deformed arm & leg long bones when multiple bones affected & clear bend, radiography rules out trauma (d)	Abnormal growth plate distally (d)	Flattening of femoral metaphysis & coxa vara (d)	Thickened long bones bilaterally & confirmed radiographically (d)	Sternal rib end flaring if cupped (d)	Sternal rib end porosity (s)	Rib deformity with a sharp angle if multiple bones affected (s)	Deformed mandibular ramus (s)	Ilium concavity (s)	Long bone meta-physeal flaring; arms & legs (s)	Long bone concave curvature porosity (s; d if there is curvature along w/ porosity)	Cranial vault porosity ectocranial(n-d)	Cranial vault porosity endocranial (n-d)	Frontal bone bossing (n-d)	Orbital roof porosity (n-d)	Irregular & porous metaphyseal cortex of long bones (n-d)
SG27	No	No	No	No	No	No	No	No	No	No	No	No	No	No	**Yes**	No
SG28	No	No	No	No	No	No	No	N/A	No	No	No	No	No	No	**Yes**	No
SG29	No	No	No	No	No	No	No	No	No	No	No	No	No	No	N/A	No
SG30	N/A	N/A	N/A	N/A	N/A	N/A	No	No	No	N/A	No	N/A	No	N/A	N/A	No
SG31	N/A	N/A	N/A	N/A	N/A	N/A	N/A	N/A	N/A	N/A	N/A	N/A	No	N/A	N/A	N/A
SG32	No	No	No	No	No	No	No	No	No	No	No	No	No	No	No	No
Prevalence	**0/27**	**0/28**	**0/26**	**0/26**	**0/28**	**0/28**	**0/29**	**0/21**	**0/25**	**1/27**	**0/28**	**3/25**	**1/25**	**0/20**	**9/22**	**0/31**

Table C.2 Legend
d = diagnostic
s = suggestive
n-d = non-diagnostic
N/A = that portion of element not present for assessment.